STUDIES TO UNDERSTAND THE PATHOLOGICAL MECHANISMS IN PREECLAMPSIA VIA EXTRACELLULAR VESICLES

Maria Carolina Motta Mejia

Division of Biosciences
College of Health and Life Sciences
BRUNEL UNIVERSITY LONDON

Thesis submitted for the Degree of Doctor of Philosophy

2018

DECLARATION

This thesis is submitted to Brunel University London, in fulfilment of the requirements for the degree of Doctor of Philosophy.

I, (Maria) Carolina Motta-Mejia, thereby state that this thesis is entirely my work, and except where otherwise indicated, describes the research performed by me.

_____   _____

Signature   Date

Now onto Him

Who can do exceeding abundantly all that we may ask or imagine

According to His power at work within us

To Him be the Glory

In the Church and Christ Jesus throughout all generations

Forever and ever.

Ephesians 3.20 (NIV)

I dedicate this thesis to **Dr Janez Ferluga**, *my guardian angel.*

Whose contagious passion for science, young and vibrant spirit and extraordinary kindness and support has significantly impacted my life, and has permitted me to complete this challenging yet rewarding PhD journey.

Forever thankful for you.

ACKNOWLEDGEMENTS

SUMMARY OF THESIS

Preeclampsia (PE) is a pregnancy-specific disorder, affecting 3-5% of pregnancies worldwide. There is no current cure for PE apart from the removal of the placenta and the fetus, irrespective of gestation. Thus, PE does not only severely affect the mother but also causes a significant impact on the fetus development. The exact mechanisms by which PE occurs remains unclear. Extracellular vesicles (EV) are membrane-encapsulated particles carrying cargo originating from their parental cells; they have been shown to have an essential role in mediating intercellular communication. Here, syncytiotrophoblast derived EV (STBEV) were isolated from PE and normal pregnancies (NP) by dual-lobe *ex vivo* placental perfusion and differential ultracentrifugation. We show that STBEV carry functional endothelial nitric oxide synthase (eNOS), and its expression and activity were reduced in STBEV isolated from PE placentae. eNOS is an enzyme essential for the synthesis of nitric oxide (NO), which is a potent vasodilator. The reduced NO generated by STBEV-bound eNOS in PE may contribute to an overall decreased NO bioavailability associated with the endothelial dysfunction previously reported in PE. PE has been described as early- (≤34 weeks gestation) and late- (≥34 weeks gestation) onset. We also demonstrated that late-onset PE-derived STBEV do not exacerbate a pro-inflammatory profile on a macrophage/monocytic cell line, THP-1. Instead, a suppressed inflammatory response is being reported, which is distinct from maternal systemic inflammation associated with early-onset PE. Thus, early- and late-onset PE are different pathophysiological entities. We also report, for the first time, the characterisation, protein cargo and possible functions of placental capillary pericytes (PLVP) derived exosomes (PLVPex) cultured under normal (20% O_2) and hypoxic (8% and 1% O_2) conditions. We show that PLVPex can induce a pro-angiogenic effect on primary human umbilical vein endothelial cells (HUVEC), irrespective of oxygen stimulus, carrying bound molecules needed for angiogenesis. Hypoxia does not alter the function of PLVPex on HUVEC, but stimulates the increased production of PLVPex and growth factors, indicating a potential survival mechanism by PLVP in response to oxygen deprivation, which is common in PE placentae.

PUBLICATIONS

Original Articles Published

1. Gill, M., **Motta-Mejia, C.,** Kandzija, N., White, K., Thammasate, B., Ri, R., Cooke, W., Cerdeira, A.S., Zhang, W., Redman, C.W., and Vatish M. **2019**. Neprilysin is active in placental vesicles, and its expression is upregulated in PE. *Hypertension.*
2. Kandzija, N., Zhang, W., **Motta-Mejia, C.,** Mhlomi, V., McGowan-Downey, J., Cerdeira, A.S., Tannetta, D., Sargent, I.L., Redman, C.W., Bastie C., and Vatish M. **2019**. Maternal circulating levels of STB vesicles expressing Dipeptidyl Peptidase IV (DPPIV) are increased in Gestational Diabetes Mellitus pregnancy. *Journal of Extracellular Vesicles.*
3. Ferlaino, M., Glastonbury, C.A., **Motta-Mejia, C.,** Vatish, M., Granne, I., Kennedy, S., Lindgren, C.M. and Nellåker, C., **2018**. Towards Deep Cellular Phenotyping in Placental Histology. *arXiv* preprint arXiv:1804.0327
4. **Motta-Mejia, C.,** Kandzija, N., Zhang, W., Mhlomi, V., Cerdeira, A.S., Burdujan, A., Tannetta, D., Dragovic, R., Sargent, I.L., Redman, C.W., Kishore, U., and Vatish M. **2017**. Placental vesicles carry active endothelial nitric oxide synthase, and their activity is reduced in PE. *Hypertension.*

Under Review

5. **Motta-Mejia, C.,** Kouser, L., White, K., Zhang, W., Kandzija, N., Kaur, A., Tannetta, D., Alhamlan, F., Redman, C.W., Kishore, U., and Vatish M. **2019**. Syncytiotrophoblast Extracellular Vesicles from Late-Onset Preeclampsia Placentae do not induce a Pro-Inflammatory immune response in THP-1 Macrophages. *Placenta.*

In Progress

6. **Motta-Mejia, C.,** Bari, M.F., Zhang, W., Couch, Y., Neuhaus, A.A., Cooke, W., Kandzija, N., Kishore, U., Shamji, MH., Kenney, S., Buchan, A.M., Sutherland, B.O., Redman, C.W., and Vatish, M. **2019**. Hypoxia induces Exosome release with a Pro-angiogenic profile from Placental Pericytes. *Atherosclerosis, Thrombosis and Vascular Biology.*
7. **Motta-Mejia, C.,** Neuhaus, A.A., Bari, M.F., Couch, Y., Kandzija, N., Zhang, W., Redman, C.W., Sutherland, B.O., Kishore, U., and Vatish, M. Novel marker for placental capillary pericytes. *Placenta.*
8. Zhang, W., Kandzija, N., **Motta-Mejia, C.,** Mhlomi, V., Burdujan, A., McGowan-Downey, J., Cerdeira, A.S., Ferguson, D., Sargent, I.L., Redman, C.W., and Vatish M. High throughput multi-parameter interrogation of syncytial trophoblast microvesicles in the complex biological fluid. *Journal of Extracellular Vesicles.*

TABLE OF CONTENTS

LIST OF ABBREVIATIONS

ADP	Adenosine diphosphatase
ADMA	Asymmetric dimethylarginine
ALIX	ALG-2-interacting protein X
ALK5	Activin-like kinase receptor
Ang	Angiopoietin
APC	Allophycocyanin
ATP	Adenosine triphosphate
BCA	Bicinchoninic acid
BGN	Biglycan
BH$_4$	Tetrahydrobiopterin
BMI	Body mass index
BSA	Bovine albumin serum
CaM	Calmodulin
cGMP	Cyclic guanosine monophosphate
cDNA	Complementary DNA
COOH	C-terminal reductase module
CO$_2$	Carbon dioxide
CoCl$_2$	Cobalt chloride
COL2A1	Collagen type II alpha chain 1
CXCL	C-X-C motif chemokine
DCs	Dendritic cells
DAB	3,3'-diaminobenzidine
DAMPs	Damage-associated molecular patterns
DNA	Deoxyribonucleic acid
EC	Endothelial cells
ECL	Enhanced chemiluminescence
EDTA	Ethylenediaminetetraacetic acid
EDHF	Endothelium-derived hyperpolarising factor
ELISA	Enzyme-linked immunosorbent assay
EM	Electron Microscopy
eNOS	Endothelial nitric oxide synthase
ENG	Endoglin
ESCRT	Endosomal sorting complex required for transport
ET$_B$	Endothelial receptors
EV	Extracellular vesicles
FAD	Flavin adenine dinucleotide
FBS	Fetal bovine serum
FcR	Fc Receptor
FCS	Fetal calf serum
FGF-2	Fibroblast growth factor 2
FITC	Fluorescein Isothiocyanate
FLT-1	Vascular endothelial growth factor receptor 1 precursor

FMO	Fluorescence minus one
FMN	Flavin mononucleotide
FSC	Forward scatter
GC	Guanylate cyclase
G-CSF	Granulocyte-colony stimulating factor
GM-CSF	Granulocyte-macrophage colony-stimulating factor
HIF	Hypoxia-inducible factor
HLA	Human Leukocyte Antigen
HMEC	Human microvascular endothelial cells
HMGB1	High motility group box 1
HMOX-1	Heme oxygenase 1
HRP	Horseradish peroxidase
HUVEC	Human umbilical endothelial vein cells
IDO	Indoleamine 2,3-dioxygenase
IFN	Interferon
IHC	Immunohistochemistry
IL	Interleukin
ILT-2	Ig-like transcript 2
iNOS	Inducible nitric oxide synthase
ISSHP	International Society for the study of hypertension in pregnancy
JAK	Janus kinase
KIR	Inhibitory killer-immunoglobulin
LAMβ1	Laminin subunit beta 1
L-NAME	N-Nitroarginine methyl ester
LPS	Lipopolysaccharide
MHC	Major histocompatibility complex
MMP	Matric metallopeptidase
mRNA	Messenger ribonucleic acid
mirRNA	Micro ribonucleic acid
MIP-1α	Macrophage inflammatory protein 1alpha
MCP-1	Monocyte chemoattractant protein 1
M-CSF	Macrophage colony-stimulating factor
MSC	Mesenchymal stem cell
MV	Microvesicles
MVB	Multivesicular bodies
NADPH	Nicotinamide adenine dinucleotide phosphatase
NF-κB	Nuclear factor κB
NG2	Nerve-glial antigen-2
NK	Natural killer cells
NLRs	NOD-like receptors
NO	Nitric oxide
NOS	Nitric oxide synthase
NP	Normal pregnancy
NRP1	Neuropilin 1
NTA	Nanoparticle Tracking Analysis

O$_2$	Oxygen
PAMPs	Pathogen associated molecular patterns
PB	Peripheral vein blood
PBMCs	Peripheral blood mononuclear cells
PBS	Phosphate Buffered Saline
PBS-T	Phosphate Buffered Saline-Tween
PC	Capillary pericytes
PDGFRβ	Platelet-derived growth factor receptor -beta
PE	Preeclampsia
PE	Phycoerythrin
PE-CY5	Phycoerythrin Cyanine 5
PE-CY7	Phycoerythrin Cyanine 7
PFA	Paraformaldehyde
PFP	Platelet-free plasma
PKG	cGMP-dependent protein kinase
PKH26	Yellow-orange fluorescent dye with long aliphatic tails
PLAP	Placental alkaline phosphatase
PLGF	Placental growth factor
PLVP	Placental capillary pericytes
PLVPev	PLVP extracellular vesicles
PLVPex	PLVP exosomes
PLVPmv	PLVP microvesicles
PMA	Phorbol 12-Myristate 13-Acetate
PPP	Platelet-poor plasma
PRRs	Pattern recognition receptors
PVDF	Polyvinylidene difluoride
qPCR	Quantitative Polymerase Chain Reaction
RBC	Red Blood Cells
REA	REAffinity recombinant antibodies
RNA	Ribonucleic acid
rRNA	Ribosomal ribonucleic acid
RIPA	Radioimmunoprecipitation buffer
SDS	Sodium dodecyl sulfate
SSC	Side scatter
SEM	Standard error mean
sGC	Soluble guanynyl cyclase
STBEV	STB extracellular vesicles
STBEX	STB exosomes
STBMV	STB microvesicles
TBS	Tris-buffered saline
TBS-T	Tris-buffered saline Tween 20
TEM	Transmission Electron Microscopy
TGF-β	Transforming growth factor -beta
THP-1	Human monocyte leukaemia cell line
TLR	Toll-like receptor
TNF-α	Tumour necrosis factor- alpha

T$_{reg}$	T regulatory cells
UV	Uterine vein blood
VEGF	Vascular endothelial growth factor
VEGFR1/FLT-1	VEGF receptor 1
VEGFR2/KDR	VEGF receptor 2
WGA	Wheat germ agglutinin
αSMA	α-Smooth muscle cell

LIST OF FIGURES

CHAPTER 5

LIST OF TABLES

CHAPTER 1

General Introduction

1. Introduction

Hypertensive disorders affect nearly 10% of pregnant women around the world (Duley 2009; Steegers *et al.* 2010), causing severe morbidity, long-term disability, and death among both mothers and their babies. Among the hypertensive disorders that complicate pregnancy, Preeclampsia (PE) and eclampsia remain the leading causes of maternal and perinatal morbidity and mortality (World Health Organization 2011). Considerable advances in research have helped understand the pathology of this disease. This thesis examines the role of extracellular vesicles in healthy pregnancy and PE as a potential link between the placental pathology, the maternal syndrome and the effects on the fetus' development.

1.1. Preeclampsia

1.1.1. Definition and symptoms

PE is a pregnancy-specific disorder characterised by new-onset hypertension and proteinuria at ≥ 20 weeks of gestation (Redman & Sargent 2005; Romero *et al.* 1988; Steegers *et al.* 2010). In the absence of proteinuria, the diagnosis of PE requires the presence of hypertension, together with other systemic disturbances, such as thrombocytopenia, elevated levels of liver transaminases, renal insufficiency, pulmonary oedema, and visual and cerebral disturbances (National Institute for Health and Clinical Excellence 2011). There are two different classification entities for this syndrome: early-onset PE, which develops before 34 weeks of gestation, and late-onset PE, which occurs after 34 weeks gestation (Von Dadelszen *et al.* 2003). Nevertheless, it remains unclear whether early- and late-onset PE have different pathogenic mechanisms, or it is merely stages of the same underlying disorder (Ogge *et al.* 2011).

PE affects up to 5% of pregnancies worldwide with the potential to kill either the mother and the baby or both, even in the Western World (World Health Organization 2011). Pregnant women suffering from PE might progress to eclampsia, which is the final stage of this disorder, characterised by the occurrence of new-onset grand mal seizures, affecting 2.7 - 8.2 women per 10,000 deliveries (Thornton *et al.* 2013). Other complications include liver rupture, stroke, pulmonary oedema, or kidney failure, which

all can result in maternal death (Souza *et al.* 2013). Currently, there is no cure for PE but the delivery of the placenta, irrespective of gestation and new-born development (Redman 2005). PE is one of the commonest causes of fetal growth restriction and preterm birth, either spontaneous or through induced delivery (Redman 2005). It has also been revealed that babies born to mothers with PE have a high risk of bronchopulmonary dysplasia (Hansen *et al.* 2010), cerebral palsy (Strand *et al.* 2013) and cardiovascular risk factors, including high blood pressure and body mass index (BMI) (Davis *et al.* 2012).

1.1.2. Risk factors

Both maternal and paternal risk factors can cause the development of PE. Strong maternal risk factors include: previous PE or hypertension in pregnancy, chronic kidney disease, hypertension, diabetes (type 1 and 2), and autoimmune disorders such as systemic lupus erythematosus or antiphospholipid syndrome (Mol *et al.* 2016; National Institute for Health and Clinical Excellence 2011). Other moderate risks factors include primiparity, age 40 or above, obesity, family history of PE, multiple pregnancies, polycystic ovarian syndrome, pregnancy interval of greater than ten years, and BMI of 35 kg/m2 or above (Duckitt & Harrington 2005; Roos *et al.* 2011). Young primiparous women suffering from PE might be due to a relative failure to induce maternal tolerance to paternal alloantigens following exposure to semen (Redman & Sargent 2010a). Prolonged contact with the same-partner semen seems to reduce the risks of developing PE. Women that receive artificial insemination with a sperm donor, barrier methods of contraception and multiparous women who have changed partner since the previous pregnancy, have been found to have a high risk for PE (Dekker 2002). Interestingly, men who have fathered a prior pregnancy involving PE can also pass this disorder to the new partner's pregnancy (Dekker *et al.* 2011).

1.1.3. Origin and development of PE

Placenta is the principal cause of PE. After delivery, the disease symptoms disappeared rapidly (Redman & Sargent 2005). The fetus is also not required for the development of this disease as PE can develop in trophoblast tumours (Acosta-Sison

1956), and extrauterine pregnancies (excluding the uterus as a contributor) (Hailu *et al.* 2017).

During human placentation, numerous changes occur in the uterus. Foremost, the stromal compartment of the endometrium differentiates into the decidua. The placental villous trophoblast of fetal origin transverses the uterine epithelium and occupies the decidua and the inner third of the myometrium. The gestational sac exists in a low-oxygen environment with low oxygen tension (~2%; 25.6mmHG O_2) (Jauniaux *et al.* 2001), maintaining an environment that supports trophoblast in an immature and proliferative state via the action of TGF-β (Lyall *et al.* 2001). Trophoblast anchors the blastocyst to maternal tissues by unplugging the tips of the spiral arteries within the decidua and forming the intervillous space. The stimulation of invading trophoblast through the uterine wall assists in developing the placental villi, the structural unit of the placenta. The placental villi encompass an inner layer of mononuclear cytotrophoblast cells, and an outer layer of continuous multinucleated cytoplasm denoted as the syncytiotrophoblast (STB). The STB layer is the multinucleated, terminally differentiated, polarised epithelium that covers the entire surface of the human placental villi (Askelund & Chamley 2011). STB is essential for the feto-maternal interface as it is responsible for the nutrient uptake, gaseous exchange, waste removal, protein and steroid hormone production and modulation of maternal physiology (Askelund & Chamley 2011).

Rapid differentiation and proliferation of trophoblast lead to branching of the villi into villous tree ramifications referred as the chorionic villi. The cytotrophoblast invades and plugs the spiral arteries' myometrial segment, remodelling the spiral arteries from narrow-diameter to large-diameter vessels with a low-velocity, high-flow chamber (**Figure 1.1A**; Redman, 2005). This opening of the spiral arteries increases the oxygen tension, generating oxidative stress on the trophoblast, which in turn induces a trophoblastic significant invasive phenotype in related hypoxic conditions (Genbacev *et al.* 1996). As a result, uterine blood flow increases, allowing the perfusion of the placental intervillous space and sustenance of the fetal development.

The exact pathogenesis of PE remains to be fully understood, but it is generally thought to be characterised by poor placentation during early gestation (weeks 8-18,

Figure 1.1B). Poor placentation is believed to be caused by failure to supply the uteroplacental circulation due to early trophoblast unplugging, constrained spiral artery invasion, and compromised remodelling, causing malperfusion characterised by intermittent high-velocity blood flow to the intervillous space (Hung & Burton 2006; Redman 2005). These have two main impacts on placentation. Primarily, the increase in oxygen tension causes an ischemia-reperfusion or hypoxia-reperfusion type of injury, which it is known to generate high quantities of reactive oxygen species leading to oxidative stress (Hung *et al.* 2001). Secondly, factors including cellular debris and extracellular vesicles are shed in increasing numbers from the STB cells of the syncytium into the maternal bloodstream (Hutchinson *et al.* 2009).
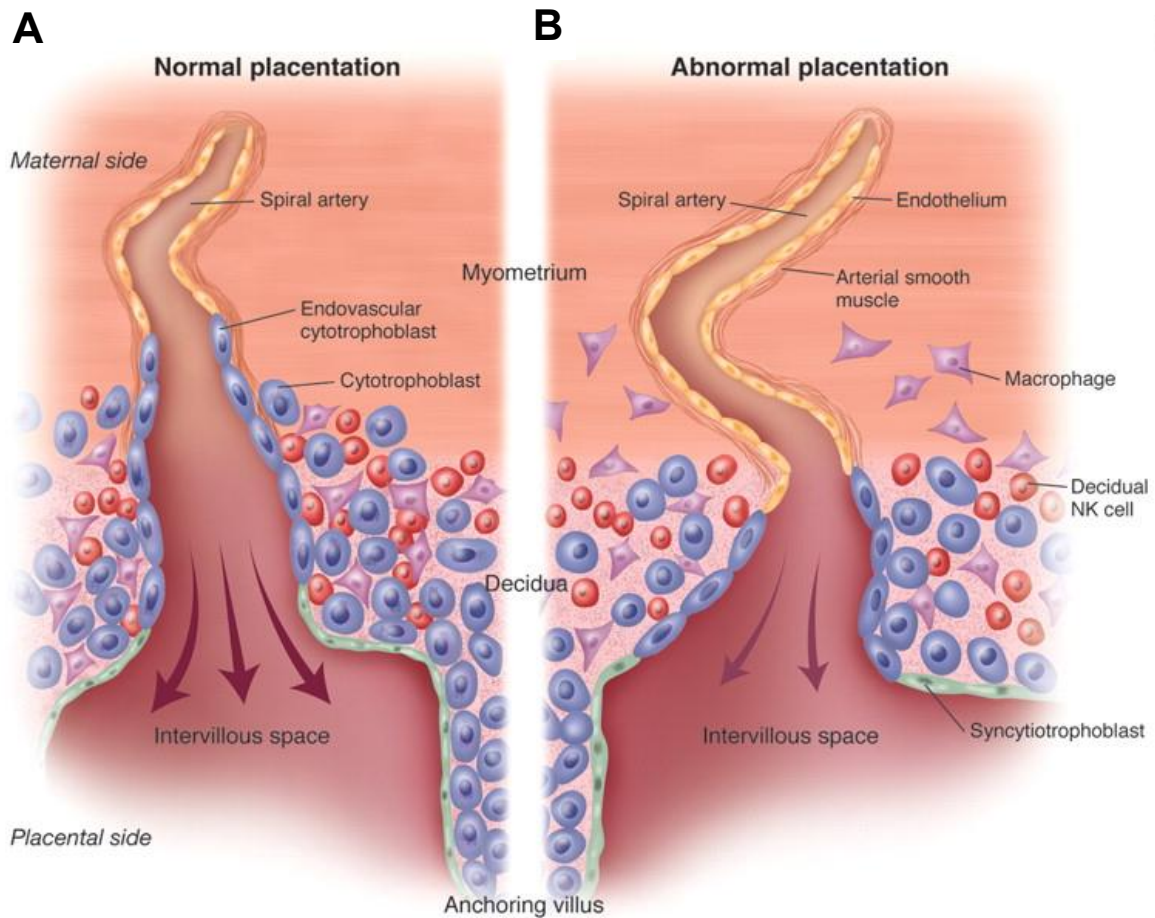
Figure 1. 1. Spiral artery-remodeling model leading to normal and abnormal placentation. During the second trimester, the placenta links the maternal decidua by anchoring the villi. A, In normal placentation, cytotrophoblast (blue) invade the maternal decidua and adjacent spiral arteries, penetrating the walls of the arteries and replacing part of the maternal endothelium (yellow). The cytotrophoblast invasion leads to the remodelling of the arterial wall resulting in the loss of smooth muscle and arterial dilation, assisted by natural killer cells (red) and some macrophages (purple) in the decidua. B, In PE's first stage model, the deep cytotrophoblast invasion and arterial remodelling are restricted and altered, correspondingly. Image take from (Redman 2005).

For more than a decade, the secretion of these factors into the maternal circulation has been believed to be responsible for the clinical manifestations of PE causing endothelial cell dysfunction (Rodgers *et al.* 1988; Roberts *et al.* 1992), intravascular inflammation (Sacks *et al.* 1998; Redman *et al.* 1999; Gervasi *et al.* 2001) and activation of the haemostatic system (Kenny et al, 2009). Consequently, PE is considered to be primarily a vascular disorder (Roberts *et al.* 1990). Other pathogenic mechanisms associated with PE also include autoantibodies to Type-1 angiotensin II receptor, platelet and thrombin activation, and the presence of an antiangiogenic state; an imbalance between angiogenic and antiangiogenic factors seemed to be the most important (Chaiworapongsa *et al.* 2014).

This thesis discusses the normal and pathogenic mechanisms that affect both the mother and the fetus. For the mother, we focus on the maternal vascular and immune systems in regards to endothelial dysfunction and maternal systemic inflammation characterised in PE. On the fetal side, we examine the fetal vascular system and address a relatively disregarded cell type in placenta biology, the capillary pericyte.

1.2. Endothelial dysfunction

A healthy pregnancy is characterised by adaptations of the maternal cardiovascular system to ensure adequate oxygenation to the feto-maternal unit. Circulating blood volume increases by approximately 1.5 L, 50% above non-pregnant values, and red blood cell mass increases by 15 to 20% (Chesley 1972; Pritchard 1965). In addition, there is a significant increase in stroke volume and heart rate which results in a 30% rise in the cardiac output above non-pregnant levels. As a result, systemic maternal arteries display diminished vascular tone, which contributes to the reduced peripheral vascular resistance (Sibai & Frangieh 1995). The maternal endothelium maintains the homeostatic balance by participating in the regulation of blood flow and structure through the production of vasoactive molecules such as nitric oxide, prostacyclin and endothelium-derived hyperpolarizing factor (EDHF), as well as contracting factors such as endothelin-1 and thromboxane A2 (Possomato-Vieira & Khalil 2016).

Endothelial dysfunction is a significant phenotype of PE, which results in generalised vasoconstriction and reduced blood to multiple organs. Endothelial dysfunction is considered the result of an increased ET-1 secretion by endothelial cells and lack of

appropriate vascular responses to endothelial-mediated vasodilators. While the exact mechanisms accountable for the systemic maternal vascular dysfunction remain unknown, intermediaries of endothelial dysfunction such as decreased nitric oxide have been shown to play a role in the development of hypertension in PE women (Matsubara *et al.* 2010; Roberts & Von Versen-Hoeynck 2007).

1.2.1. Nitric oxide

Nitric oxide (NO) is a soluble gas with a half-life of ~ 6 to 30 seconds, synthesised from the amino acid L-arginine by nitric oxide synthases (NOS). US scientists Robert F. Furchgott, Luis J. Ignarro and Ferid Murad, who established NO as a signalling molecule in the cardiovascular system, were conferred the 1998's Nobel Prize for Physiology and Medicine (SoRelle 1998). NO plays essential roles in the control of blood pressure, immune system functioning, and central nervous system's activation mechanisms (SoRelle 1998; Tousoulis *et al.* 2012). Nitric oxide synthase (NOS) is the enzyme responsible for the conversion of substrate L-arginine to L-citrulline and the synthesis of NO.

There are three known isoforms of NOS:

a) Type I NOS or neuronal NOS (nNOS)
b) Type II NOS or cytokine-inducible NOS (iNOS)
c) Type III NOS or endothelial NOS (eNOS)

nNOS and eNOS are entirely dependent on augmented intracellular Ca^{2+} to synthesize NO, while iNOS possess a Ca^{2+} independent intracellular activity. Typically, nNOS is found in the blood vessels, iNOS is present in macrophages stimulated by inflammatory cytokines and lipopolysaccharides, and eNOS is one of the main sources of endothelium-derived NO (Ignarro 1990). We will focus on eNOS as this NOS isoform is of our research interest.

1.2.2. Endothelial nitric oxide synthase (eNOS)

All NOS isoforms, including eNOS, share the same modular organisation (Stuehr 1999): (i) the N-terminal catalytic oxygenase module (N_2H) binds Fe-protoporphyrin IX (heme), substrate L-arginine and (6R)-5,6,7,8-tetrahydrobiopterin; (ii) the C-terminal reductase module (COOH) contains binding sites for nicotinamide adenine dinucleotide phosphate (NADPH), flavin adenine dinucleotide (FAD) and flavin mononucleotide (FMN); and (iii) the intervening region interacts with calmodulin (CaM) (**Figure 1.2A**).

NOS is a homodimer, each monomer containing a C-terminal reductase domain and an N-terminal oxygenase domain (Andrew & Mayer 1999). NOS requires heme to dimerise; otherwise it stays monomeric, incapable of catalysing NO production (Klatt *et al.* 1996). This heme-containing oxygenase domain catalyses five-electron oxidation from one of the simple guanidine nitrogen atoms of L-arginine in the presence of several co-factors and oxygen (Stuehr 1997). In the case of iNOS, both haem and pteridine tetrahydrobiopterin (BH4) are essential for NO synthesis (Baek *et al.* 1993). **Figure 1.2B** highlights the importance of haem.
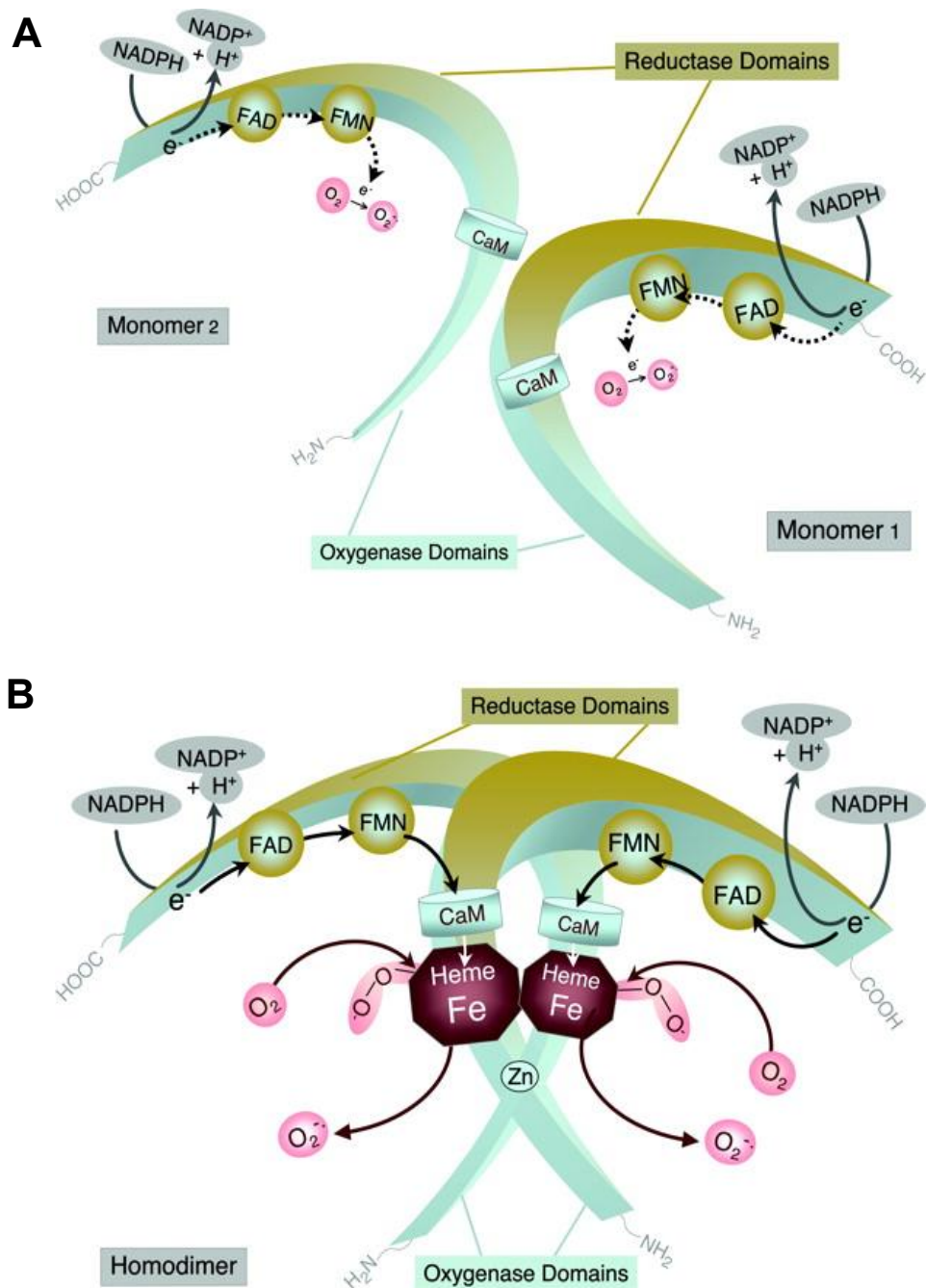
Figure 1. 2. Structure of eNOS and key mechanism of NOS catalysis. A, Basic structure of eNOS. Each subunit consists of a reductase domain (green) and an oxygenase domain (seafoam green). Monomers allow the transfer of electrons from NADPH to the flavins FAD and FMN, which it is stimulated by the binding of CaM within the reductase domain. However, monomers are unable to bind to cofactor BH4 or substrate L-arginine to catalyse NO production. B, Presence of heme in eNOS structure. Heme is the essential requisite for the formation of NOS dimers, allowing the interaction of the reductase and oxygenase domains and the interdomain electron

transfer from the flavins to the heme of the opposite monomer. Image taken from (Förstermann & Münzel 2006).

1.2.3. Mechanism of nitric oxide production

Calcium-calmodulin-dependent eNOS allows NO to be synthesised continuously from the amino acid L-arginine into L-citrulline in the endothelial cell (Palmer *et al.* 1988; **Figure 1.3**). A variety of agonists (such as acetylcholine, histamine, thrombin, serotonin, adenosine diphosphatase (ADP), bradykinin, norepinephrine and isoproterenol) bind to specific receptors or open ion channels of the endothelial cell membrane to increase influx of Ca^{2+}, activating its formation from intracellular stores and mitochondria (Tousoulis *et al.* 2012). The calcium ions bind to calmodulin (CaM) to enable the CaM-domain of eNOS to produce NO. Conversely, increased hemodynamic shear stress and agonists, such as certain hormones (i.e., adiponectin and insulin) or growth factors [i.e., vascular endothelial growth factor (VEGF)], trigger the phosphorylation of eNOS via the activation of the phosphoinositide 3-kinase (Pl3K)-phosphoinositide-dependent kinase II (PDK1/2) pathway (Vanhoutte *et al.* 2016).

Once formed, NO stimulates the soluble guanylyl cyclase (sGC), which in turn, produces increased concentrations of cyclic guanosine monophosphate (cGMP) in the vascular smooth muscle cell. cGMP interacts with the intracellular receptor protein, cGMP-dependent protein kinase (PKG), which inhibits both the release of intracellular Ca^{2+} as well as its influx from the extracellular space. At the vascular smooth muscle membrane, PKG also stimulates the Ca^{2+}-ATPase accelerating calcium-extrusion (Vanhoutte *et al.* 2016). These actions reduce the intracellular concentration of the activator ion, so calcium-dependent myosin light-chain kinase can no longer phosphorylate myosin, preventing the contractile process and resulting in the relaxation of the vascular smooth muscle cells (Tousoulis *et al.* 2012).

The eNOS isoform is expressed constitutively in the vascular endothelium. It sustains vascular tone through the intrinsic synthesis of NO while inhibiting the adhesion of leukocytes and platelets to the endothelium, preventing a proinflammatory state from occurring (Matsubara *et al.* 2015). Likewise, it also plays a crucial role in the management of the biogenesis of mitochondria in vascular cells, adipocytes, and

monocytes (Vanhoutte *et al.* 2016). Apart from its powerful vasodilator effect, it also carries a gatekeeper role by controlling EDH-mediated hyperpolarisations (Godo *et al.* 2016), and inhibiting the production and action of both endothelium-derived contracting factors and ET-1 (Vanhoutte 2000).
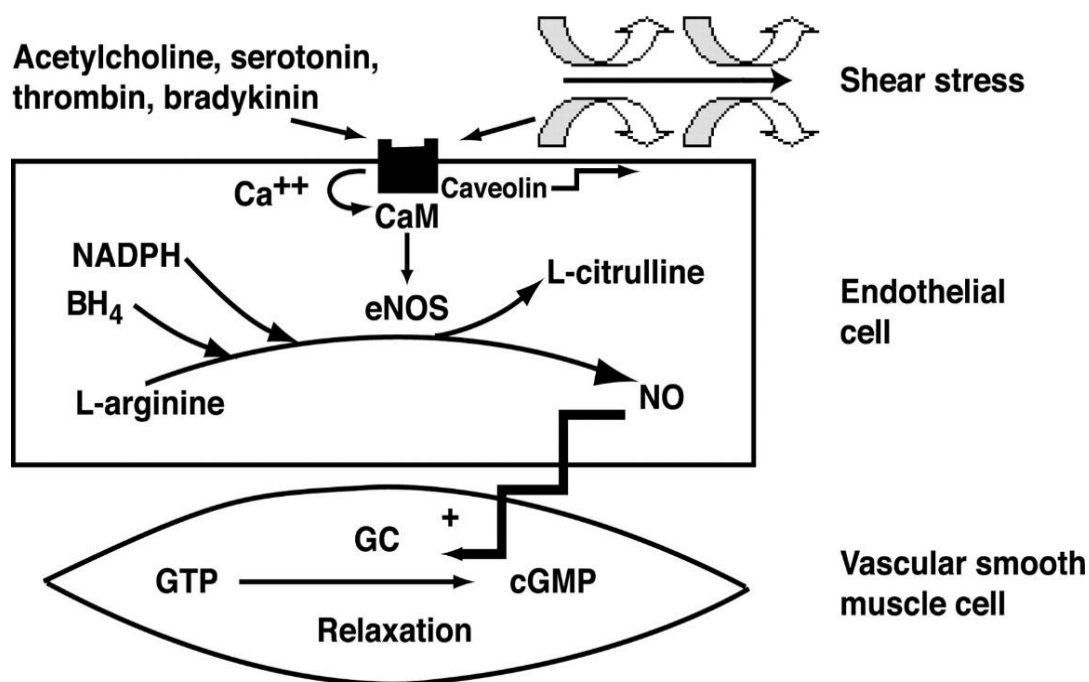
Figure 1. 3. Mechanism of NO production by endothelial cells. The conversion of L-arginine makes NO to L-citrulline in the presence of co-factors, including BH4 and NADPH. Vasodilator agonists or shear stress increases intercellular Ca^{2+} and dislocates the inhibitor caveolin from CaM, activating eNOS. NO diffuses to vascular smooth muscle resulting in relaxation by activating guanylate cyclase (GC), thereby increasing intracellular cyclic guanosine monophosphate (cGMP). Taken from (Davignon & Ganz 2004).

1.2.4. Nitric oxide in normal and PE pregnancies

During normal pregnancy, NO is considered to participate in the maternal systemic vasodilation, regulation of the uterine and fetoplacental blood flow, and the uterine quiescence prior to parturition (Sladek *et al.* 1997). For example, increased oestrogen level during pregnancy allows up-regulation and endothelium-dependent vasodilation to be mediated in part by NO (Hayashi *et al.* 1995). Raised cGMP levels have been

shown in plasma during the first trimester of pregnancy (Conrad *et al.* 1999). On the other hand, NO is also a key player in maternal uterine vascular remodelling. Vasculogenesis and angiogenesis depend on signalling molecules such as VEGF, Flt-1, TGF-β1, angiopoietin 1 and 2 (Burton *et al.* 2009), which in part, exert their effects through NO synthesis. Therefore, VEGF-Flt-1 interactions during the placental bed arteries remodelling induce the release of NO (Papapetropoulos *et al.* 1997), which results in the activation and expression of pro-invasive matrix metallopeptidase (MMP) 2 and 9 (Novaro *et al.* 2001). Nevertheless, most of the circulating NO is generally considered to originate from the maternal endothelium. However, we believe that the placenta may also contribute.

In the placenta, eNOS and iNOS have been found present in diverse species since the early stages of placental development (Krause *et al.* 2011). iNOS is expressed mainly at the feto-maternal interface during the first stages of pregnancy (Marinoni *et al.* 2004). Conversely, in human first trimester placenta, eNOS is expressed in the STB (STB), villous endothelium intermediate and extravillous trophoblast (Conrad *et al.* 1993; K Buttery *et al.* 1994; Myatt *et al.* 1993a) contributing to the total NO production in this gestational stage (Al-Hijji *et al.* 2003). As pregnancy progresses, there is a rise and redistribution of eNOS expression, mainly to the STB layer and endothelial cells (Dötsch *et al.* 2001; Myatt *et al.* 1997; Rossmanith *et al.* 1999; Schiessl *et al.* 2005). Nevertheless, NOS expression on extracellular vesicles derived from STB has not been investigated.

Roberts *et al.* proposed endothelial cell activation and dysfunction to be a central feature of PE (Roberts *et al.* 1990). The dysfunctional endothelium is depicted by endothelial injury, reduced vasodilatory responses, as well as a bioavailability imbalance of endothelium-derived vasoactive substances (Possomato-Vieira & Khalil 2016). PE women have been reported to suffer glomerular endotheliosis, characterised by glomerular endothelial swelling with loss of endothelial fenestrae and occlusion of the capillary lumens (Stillman & Karumanchi 2007). These aberrations cause renal injury and microalbuminuria, which could prolong for up to 2 to 4 months after delivery.

NO synthesis deficiency has been proposed to cause vasoconstriction and inadequate perfusion in the feto-maternal unit (Noris *et al.* 2005), which could partly elucidate the pathogenesis of PE. Unfortunately, studies investigating circulating levels of NO in PE have reported conflicting results. Circulating levels and urinary excretion of NO are challenging to interpret as these can involve all three isoforms, and be influenced by dietary intakes of nitrites and nitrates. As a result, total NO production in plasma during hypertensive pregnancy and/or PE have been shown to either decrease (Choi, Im & Pai 2002; Mutlu-Türkoglu *et al.* 1999; Seligman *et al.* 1994), increase (Baker *et al.* 1995; Pathak *et al.* 1999) or remain unchanged (Conrad & Davis 1995; Silver *et al.* 1996).

Overall, the placenta and its secreted factors contributing to the overall NO bioavailability in PE have not been taken into consideration. We attempt to explore this link further in **Chapter 3**.

1.3. Maternal inflammatory response

Pregnancy is a unique biological process which presents a significant challenge to the maternal immune system. The mother and the semi-allogeneic fetus coexist throughout the 40 weeks of gestation via maternal tolerance. Nobel Prize winner, Peter Medawar, recognised this remarkable phenomenon after his investigations with skin graft rejection in genetically different individuals (Medawar 1961). Successful pregnancy implicates complex interactions between the fetal trophoblast and maternal decidual immune cells, allowing the fetus to develop in the uterus while the maternal immune system remains unaltered yet operative to fight infections (Mor *et al.* 2017).

1.3.1. Immunological stages in normal pregnancy

Pregnancy consists of several development processes with different immunological stages, each step requiring a unique immune environment (**Figure 1.4**). Pregnancy commences in a pro-inflammatory environment that enables implantation and placentation to occur. At the implantation site, both endometrial stromal cells and infiltrating immune cells secrete molecules to create a pro-inflammatory environment (Gnainsky *et al.* 2015; Zenclussen & Hämmerling 2015). Likewise, uterine dendritic

cells are essential in this stage as these regulate tissue remodelling and angiogenesis, as well as promoting tolerance to paternal antigens (Plaks *et al.* 2008).

The fetus and the placenta develop rapidly during the second trimester. The mother, the placenta and the fetus become symbiotic coexisting in a T_H2 type or an anti-inflammatory environment (Saito *et al.* 2010). At this stage, any continuous pro-inflammatory signals can lead to miscarriage (Christiansen *et al.* 2006), and any ensuing pro-inflammatory insult, such as infection, can precede to pre-term birth (Agrawal & Hirsch 2012). Numerous immune cells types, including macrophages, decidual natural killer cells, and T regulatory (T_{reg}) cells, contribute to the anti-inflammatory microenvironment during the second trimester (Faas & de Vos 2017).

Lastly, once the fetus is fully developed, a switch to a pro-inflammatory environment is initiated and continued for labour and delivery during the third trimester. The switch is effectively done via the nuclear factor κB (NF- κB) signalling pathway activation and regulation (Lindström & Bennett 2005). This signalling pathway is induced as a result of toll-like receptor 4 (TLR4) activation by ligands such as surfactant protein A, which it is a protein secreted by fetal lungs (Condon *et al.* 2004), and endogenous damage-associated molecular patterns (DAMPs), such as high motility group box 1 (HMGB1) which are present in high levels at the end of pregnancy (Plazyo *et al.* 2016).
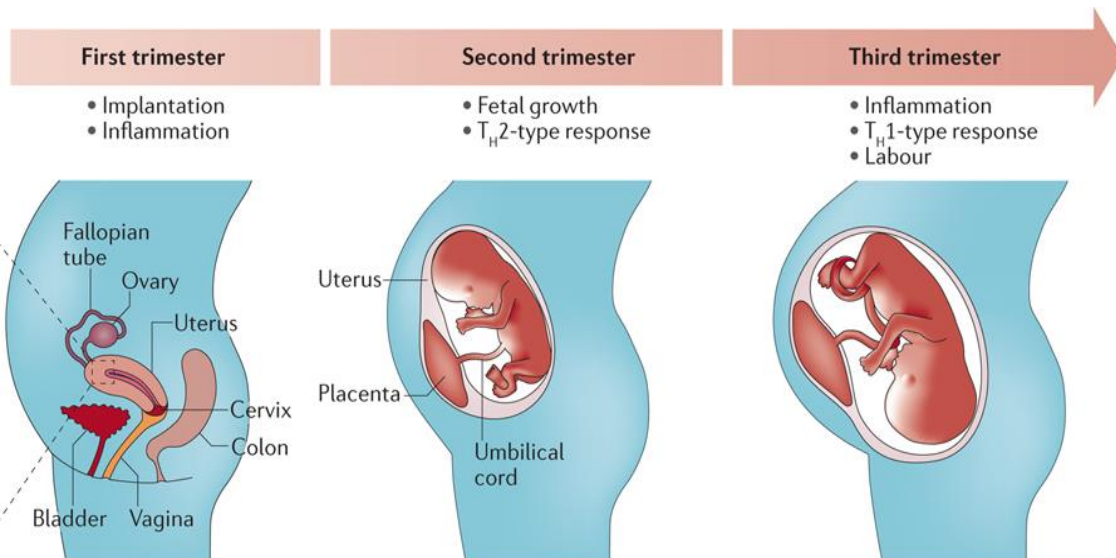
Figure 1. 4. The different immunological stages of pregnancy per trimester. The first trimester of pregnancy is connected with inflammation to allow blastocyst implantation. Fetal growth during the second trimester requires an anti-inflammatory response and T_H2 immune microenvironment. Lastly, during the third trimester, a pro-inflammatory switch and T_H1 state are necessary for labour and delivery of the newborn and the placenta. Image taken from (Mor *et al.* 2017).

1.3.2. Trophoblast-mediated immune regulation

At implantation, the blastocyst and the maternal decidua interact through the trophoblast cell layer. Trophoblast cells secrete cytokines and chemokines, such as C-X-C motif chemokine (CXCL) 12 [or stromal cell-derived factor 1], CXCL8 (also known as IL-8), transforming growth factor-β (TGF-β), and monocyte chemoattractant protein 1 (MCP-1), to stimulate the recruitment of peripheral monocytes, neutrophils, NK cells, T cells and T_{reg} cells at the implantation site (**Figure 1.5A**; Ramhorst *et al.* 2012). This immune cell trafficking is central for a healthy pregnancy as studies have shown that reduced immune cell infiltration has harmful effects on pregnancy outcomes (Romero *et al.* 2006).

In addition, trophoblast cells also release cytokines that act on immune cells after their recruitment (**Figure 1.5B**). These cytokines stimulate the differentiation of individual immature immune cells present in the endometrium by attaining a unique phenotype shown to be crucial for a successful pregnancy (Manaster *et al.* 2008). For example, decidual NK cells are distinctly different from peripheral NK cells as these as less

cytotoxic, and their unique receptor repertoire is believed to be induced by trophoblast-derived IL-15 and perhaps by additional stimulants such as TGF-β (Hanna *et al.* 2006). Thus, specialised NK cells have been shown to play an essential role in decidual vascular remodelling as these contribute to the physiological modification of the mesometrial endometrium into a particular stromal environment called decidua basalis (Zhang *et al.* 2011). Similarly, upon recruitment to the maternal-fetal interface, trophoblast-derived macrophage colony-stimulating factor (M-CSF) and IL-10 seem to stimulate CD14+ monocytes to acquire a unique M2-like macrophage phenotype essential for tissue remodelling as they phagocytose degraded extracellular matrix and clear apoptotic cells (Mills *et al.* 2000). Unlike other tissue-resident macrophages, these M2-like macrophages retain their CD14 expression and are capable of secreting TGF-β and type-1 interferons (IFNs), such as IFN-α and IFN-β (Houser *et al.* 2011). Also, TGF-β derived from trophoblast can induce the differentiation of $CD4^+$ cells into $FOXP3^+$ T_{reg} cells (Oettel *et al.* 2016; Poloski *et al.* 2016), which are believed to be crucial for maternal tolerance.

Trophoblast cells express cell-surface receptors such as TLRs, which can recognise specific molecular patterns in the microenvironment (**Figure 1.5C**; Abrahams & Mor 2005; Costello *et al.* 2007). DAMPs released by dying cells and damaged tissues, as well as pathogen-associated molecular patterns (PAMPs) from invading pathogens, can be recognised and responded to by trophoblast cells. Trophoblast cells have the potential to recruit and instruct immune cells, responding to signals from the microenvironment to sustain decidual differentiation, trophoblast migration and invasion, angiogenesis and spiral artery remodelling, as well as placental and fetal development (Mor *et al.* 2017).
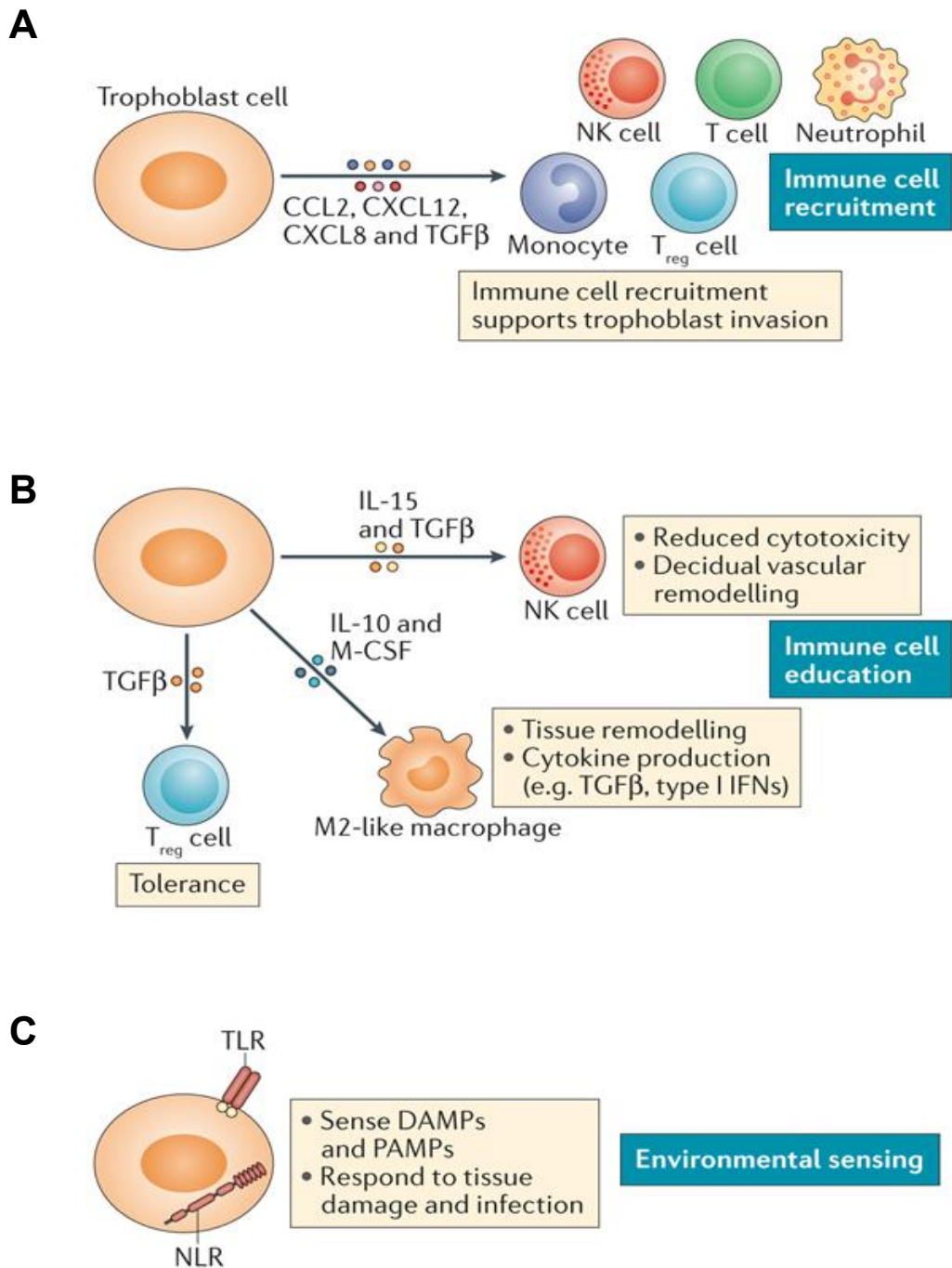
Figure 1. 5. Trophoblast cells as immune regulators. A, The secretion of cytokines by trophoblast cells stimulates the recruitment of immune cells to the maternal-fetal interface and for the immune cells to support the trophoblast invasion. B, Trophoblast-derived cytokines can also promote the instruction of NK cells and M2-like macrophages which in turn support vascular and tissue remodelling required for decidual invasion and differentiation into cytotrophoblast an STB. C, Trophoblast cells can express PRRs, such as TLRs and NOD-like recpetors (NLRs), which permits them to respond to DAMPs an PAMPs formed during infection or tissue damage. Image taken from (Mor *et al.* 2017).

Most importantly, trophoblast highly regulates the expression of human leukocyte antigen (HLA) family from the major histocompatibility complex (MHC). The mother should generally produce graft-attacking antibodies and cytotoxic T lymphocytes to different or paternal HLA or other antigens expressed by fetal cells. Extravillous trophoblast cells express a vast repertoire of MHC class I non-classical HLA-G and small amounts of MHC class I HLA-C, HLA-E and HLA-F antigens. However, the MHC class I antigens (HLA-A and HLA-B), and MHC Class II molecules (HLA-DR, HLA-DQ, and HLA-DP) are absent (Apps *et al.* 2009; Arck & Hecher 2013). This absence of polymorphic MHC Class I expression prevents trophoblast to present antigenic fetal peptides to specific CD8$^+$ T cells, which are potentially present in the maternal blood and the decidua basalis or decidua parietalis. In contrast, MHC Class I HLA-C, HLA-E, and HLA-G interact, correspondingly, with the inhibitory killer-immunoglobulin-like (KIR), CD 94/NKGs and Ig-like transcript 2 (ILT-2) receptors on NK cells (Le Bouteiller & Sargent 2000) to prevent the cytotoxic attack on the placental and fetal tissues. In particular, HLA-G is a key player involved in dampening maternal immune response in the context of vascular remodelling during placentation, thus, protecting the semi-allogeneic fetus (Djurisic & Hviid 2014).

STB, the multinucleated layer at the maternal-fetal interface, is also immunologically inert to prevent recognition and rejection by maternal T cells due to the lack of HLA expression. While maternal NK cells could potentially target the STB as their programmed function, this does not occur (Redman & Sargent 2010b).

1.3.3. Maternal systemic inflammation in PE

An abnormal trophoblastic invasion early in pregnancy has been considered to be associated with PE. It might be trigerred by an altered maternal immune response or a defective development of maternal tolerance to the foetal antigens (Redman *et al.* 1999; Saito & Sakai, 2003; Redman, 2005; Redman & Sargent, 2010c; Yoshinaga, 2012). Substantial evidence exist to support the notion that the maternal immune system does contribute to the pathogenesis of PE (Borzychowski *et al.* 2006; Schiessl, 2007; Redman & Sargent, 2008).

Excessive activation of neutrophils and monocytes in PE patients, circulating and present in the decidua, has been described by several research groups (Laresgoiti-Servitje 2013; Miko *et al.* 2009; Mishra *et al.* 2011; Saito *et al.* 2007). For example, monocytes have been found to spontaneously synthesize considerable higher amounts of pro-inflammatory cytokines such as IL-1β, IL-6 and IL-8 (Weiss *et al.* 2009). CD4^{+} and CD8^{+} T, along with NK cells and dendritic cells (DCs), have also been found to be over pro-inflammatory in PE women compared to healthy pregnancies (Santner-Nanan *et al.* 2009).

Another important immune aspect of PE development is the $T_H1/T_H2/T_H17$ imbalance. T_H17 subpopulation has been described to be up-regulated in PE, hence, increased IL-17-producing lymphocytes in the peripheral blood of PE patients compared to control group was reported in the third trimester (Darmochwal-Kolarz *et al.* 2012). Also, they described a significant association between T_H17, IL-2 and IFN-γ-producing T-cells, and PE development. Similarly, low levels of indoleamine 2,3-dioxygenase (IDO) and diminished numbers of Treg cells have been reported in the PE placentae (Santillan *et al.* 2015). IDO acts like a switch: when present, T_{reg} cells are promoted; and in its absence, T_{reg} cells are reprogrammed to acquire T_H17 phenotype with more proinflammatory activity (Baban *et al.* 2009).

Furthermore, studies have shown that TLRs and other pattern recognition receptors (PRRs) may be linked to the chronic inflammation seen in PE through PAMPs and DAMPs associated inflammatory processes (Bouças *et al.* 2017). Consequently, clinical studies have shown a connection between intrauterine bacterial or viral infections and pregnancy specific disorders such as PE, miscarriage, preterm labour, and intrauterine growth restriction (Koga & Mor 2010). Extreme necrosis and apoptosis caused by aberrant implantation, placentation, placental hypoxia, and trophoblast invasion can generate DAMPs, which can increase placental expressions of various TLRs (Chatterjee *et al.* 2011). Both TLR-3 and TLR-4 have been associated with PE, but other TLR members might also generate a local inflammatory reaction in placenta (Bouças *et al.* 2017; Chatterjee *et al.* 2012; Pineda *et al.* 2011). Mediated through the MyD88- or TRIF-mediated pathways to converge to NF-kB activation, TLRs can upregulate the expression of pro-inflammatory cytokines such as IL-6, TNF-α, IL-1-β,

IFN-γ by trophoblast (Takeuchi & Akira 2010), which in excess can lead to the manifestations of PE.

The placenta releases soluble factors into the maternal circulation throughout pregnancy and abnormally increased when the placenta is oxidatively stressed. These include growth factors, their soluble receptors or inflammatory cytokines, and, placental oxidative stress' products comprising placental debris and associated factors (Borzychowski *et al.* 2006). STB secretes the soluble receptor for VEGF, known as sFlt-1, which neutralises the angiogenic activities of VEGF and placental growth factor (PlGF). PE women have increased circulating sFlt-1 levels and placental sFlt-1 mRNA compared to women who have normal pregnancies (Maynard *et al.* 2003). Reduced levels of VEGF and PlGF are associated with high levels of sFlt-1 during PE (Maynard *et al.* 2003). The roles of pro-angiogenic VEGF and PlGF are important for maintaining vascular endothelium, which can be antagonised by sFlt-1, resulting in endothelial dysfunction (Clark *et al.* 1998). STB also secretes activin-A, corticotrophin-releasing hormone, leptin and free-heme into the mother's bloodstream which are of pro-inflammatory consequences (Redman & Sargent 2010a). Most importantly, STB also secretes extracellular vesicles into the mother's bloodstream which have been proposed to contribute to the severe maternal inflammatory response commonly seen in PE (Redman and Sargent, 2007; **Section 1.5**).

Generally, how the factors released by the PE placenta, specifically STBEV, interact with maternal immune cells have not been thoroughly investigated. We aim to examine these interactions in **Chapter 4**.

1.4. Capillary pericytes

1.4.1. Description, morphology and characterisation

Capillary pericytes (PC) are mural cells that wrap around endothelial cells in capillaries and postcapillaries venules. Carl Joseph Eberth and Charles-Marie Benjamin Rouget first described these cells as 'Rouget cells' (Rouget 1874); they were given their current name by Karl Wilhelm Zimmermann due to their location at the abluminal side of blood vessels (Zimmermann 1923). Compared to the vastly characterised

endothelial cells (EC), these cells remain elusive despite progressively interesting research recently.

PC have a distinctive morphology. It has a pronounced round nucleus, which it is distinct from the elongated cigar-shaped core of EC (**Figure 1.6**). PC also extends long processes that spread as finger-like projections, wrapping around the capillary and spanning over a large continuous surface of the vessel (Dore-Duffy & Cleary 2011). During angiogenesis or injury, the typical pattern of PC orientation in the microvessel involves the retraction of projections or the extension along the extended axis of the capillary known as longitudinal migration (Dore-Duffy & Cleary 2011). PC are separated from EC by a single basement membrane synthesised by both EC and PC, also identified as basal lamina. In the central nervous system, the basal lamina has been shown to thicken or thin in response to stress stimuli (Hughes *et al.* 2004; Wiley *et al.* 2005). These changes have been linked directly to pericyte expression of proteases (Du *et al.* 2008), and eventual migration from its vascular location (Dore-Duffy *et al.* 2000). Basal lamina provides anchoring and structural integrity to the capillary, as well as having a possible role in the regulation of pericyte function to vascular adaptability and pericyte signalling mechanisms (Hayden *et al.* 2005). Thus, PC communicate with EC by tight and gap junctions in the basal lamina which contacts directly and by paracrine signalling (Bergers & Song 2005).

PC are heterogenous in regards to phenotype, distribution and embryonic origin (Attwell *et al.* 2016). Initially, PC were visualised via light and electron microscopy (Navarro *et al.* 2016). However, it became increasingly difficult to differentiate them from other perivascular cells. Thus, several markers such as platelet-derived growth factor receptor β (PDGFRβ), nerve-glial antigen-2 (NG2), α smooth muscle actin (αSMA), endoglin and adhesion molecule CD146 among others have been used to characterise PC (Dore-Duffy & Cleary 2011). All PC do not express every single marker because their expression is dynamic and differs between organs, developmental phases, activation/maturation state, and specific microvascular systems (Armulik *et al.* 2011; Attwell *et al.* 2016). Therefore, isolating pure PC populations has been a challenge.
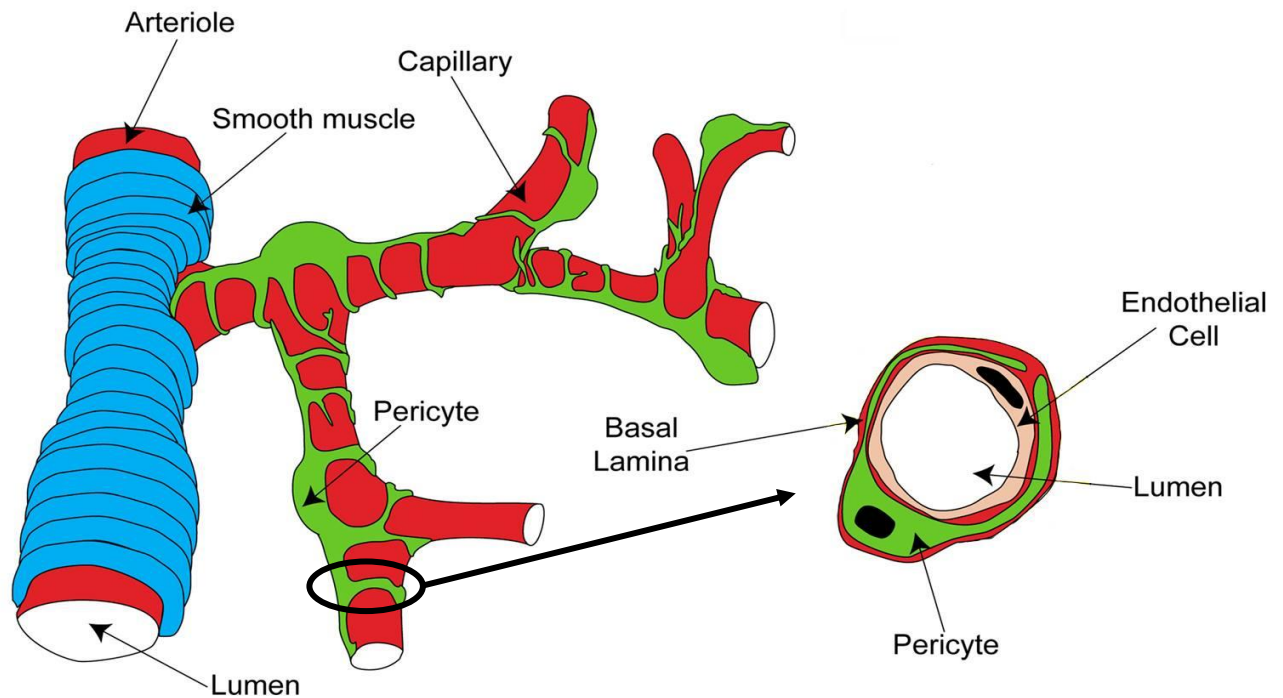
Figure 1. 6. Capillary pericytes diagram. Smooth muscle cells circle the arterioles like rings, while capillary pericytes direct processes along and around capillaries without entirely masking the vessels. Capillary pericytes are located outside the endothelial cells and are separated from them by the basal lamina. Image modified from (Hamilton, Attwell & Hall 2010).

1.4.2. Properties and functions of PC

In the brain, PC have a role in the regulation of blood flow (Hall *et al.* 2014). Hall *et al.* demonstrated that pericytes may be involved in brain damage mechanism. Functional imaging revealed PC being the first vascular component to dilate during neuronal activity followed by death due to ischemia (Hall *et al.* 2014). However, lack of characterisation of PC subpopulation has made such claims controversial (Attwell *et al.* 2016). PC have mesenchymal stem cell (MSC)-like abilities because PC can express MSC markers and behave like them both *in vitro* and *in vivo* (Tian *et al.* 2017). MSC have also been found to originate from the perivascular unit (Crisan *et al.* 2008) and exhibit a PC-like behaviour (Bexell *et al.* 2009). In addition, PC have been considered associated to contribute to tumour angiogenesis and metastasis (Barlow *et al.* 2013). PC coverage in the tumour microvasculature has suggested a tumour-

homing ability and participation in the tumour microenvironment (TME), implying PC may play a role in anti-tumour immune response (Ribeiro & Okamoto 2015).

PC have been shown to have immunomodulatory properties beyond their structural role in the microvasculature (Navarro *et al.* 2016). PC contribute to the onset of innate and adaptive immune responses. PC can react to pro-inflammatory stimuli upon PAMPs engagement and identify danger due to their surface expression of functional PRRs (Navarro *et al.* 2016). PC appear to have macrophage-like and antigen-presenting cells (APC) characteristics (Balabanov *et al.* 1996). Moreover, PC have been suggested to exert an immunosuppressive role; retinal PC decreased T cell proliferation and IFN-γ and TNF-α production in a co-culture system (Tu *et al.* 2011).

PC act as vessels stabiliser but can also differentiate into other cells types, such as adipocytes, chondrocytes, osteocytes, myocytes, and neural cells (*in vitro*) (Birbrair *et al.* 2013). This supports a role for PC in regenerative mechanisms following tissue injury. It is thought that their ability to differentiate into various lineages is the result of their mesenchymal origin (Corselli *et al.* 2013).

PC have a role to play in angiogenesis and vascular homeostasis, contributing in the management of the endothelial tips cells and vessel maturation and stabilisation (Jain, 2003; Sweeney *et al.* 2016). The detachment of PC-EC and basement membrane degradation is the initial step in angiogenesis, followed by EC migration, proliferation and resultant EC tube formation and vessel stabilisation by newly recruited PC (Potente *et al.* 2011). The growth phase of angiogenesis might require PC-mediated signalling, where the presence of PC tubes may be central to the angiogenic sprout, generating pathways for directing migrating EC (Ozerdem & Stallcup 2003).

Platelet-derived growth factor B (PDGF-B), and PDGF receptor β (PDGFRβ) signalling pathway are essential for extension and movement of PC along with the vessel during angiogenesis. PDGF-B is released by sprouting EC during angiogenesis, and it interacts with PDGFRβ on the PC (Hoch *et al.* 2003). TGF-β/ Activin-like kinase receptor (ALK5) pathway allows latent TGF-β to be synthesised by EC and become activated by direct contact of EC and PC. Once activated, TGF-β affects the proliferation of EC through the TGF-β receptor (TβR)/ALK-1/Smad5 pathway), which

in turn supports the differentiation of both PC and EC (Goumans *et al.* 2002). The Angiopoietin (Ang) 1/receptor tyrosine kinase of the Tie family (Tie2) and Ang2/Tie2 signalling pathways also contribute to the PC-EC communication. PC express Ang1 and the interaction with Tie2 on them stimulate EC, ensuing vessel stabilisation and maturation. The antagonist ligand of Tie2 is Ang2, which is mainly expressed on EC; thus, Ang2/Tie2 signalling results in the detachment and loss of PC, leading to vessel destabilisation (Maisonpierre *et al.* 1997; Sato *et al.* 1995). Other pathways involved include Jag1/Notch3 and the S1P/SIP$_1$ signalling pathways (Gaengel *et al.* 2009), which are essential for vessel maturation as well as stable PC-EC contact.

1.4.3. Placental capillary pericytes

Few studies have connected placental altered vascular morphology and function with placental capillary pericytes (PLVP). Placentae of PDGF-B or PDGFRβ gene deficient mice, exhibited diluted embryonic blood vessels and reduced number of both PLVP and trophoblasts (Ohlsson *et al.* 1999), which emphasised the importance of PDGF-B/PDGFRβ signalling in the development of the labyrinthine layer of the fetal placenta. Placental capillaries in women from high altitude communities showed an increased in vessel profile diameter and a reduced PC association compared to those pregnancies from lowland (Zhang *et al.* 2002), suggesting that reduction of local oxygen tension leads to vascular remodelling. Another study quantified the pericyte coverage in microvessels of placentae of pregnancies complicated by Type 1 diabetes mellitus and normal pregnancies (Kučera *et al.* 2010). However, no significant difference was found. Similarly, semi-quantitative analysis of placental ultrastructural micrographs indicated that PLVP were present in placentae from normal, term pregnancies but increasingly observed in abnormal capillaries such as those from complicated pregnancies by diabetes, postmaturity and rhesus incompatibility and PE (Jones & Desoye 2011).

A group of researchers were able to isolate and culture human pericytes expressing NG2, CD90, CD146, α-SMA, and PDGFRβ without contamination from smooth muscle cells, EC and leukocytes from the human placenta (Maier *et al.* 2010). They also co-cultured PLVP with human EC into mice, demonstrating investment and stabilisation of developing human EC cell-lined microvessels by the PLVP (Maier *et al.* 2010).

PLVP can support cytomegalovirus replication, promoting pro-inflammatory cytokines and angiogenic factors, which could potentially lead to viral dissemination, placental inflammation, and dysregulation of placental angiogenesis (Aronoff *et al.* 2017).

PLVP are distinctively associated with the fetal circulatory system of the placenta, which can significantly affect the fetus' growth and placental development. There is limited evidence regarding the factors released by the PLVP in response to a stimulus, such as hypoxia, and how these can affect the neighbouring cells, EC. We aim to decipher this secretome further in **Chapter 5**.

1.5. Extracellular Vesicles

1.5.1. Properties and biogenesis of extracellular vesicles

Extracellular vesicles (EV) are membrane-bound spherical particles enclosed in phospholipid-bilayer structures that are secreted from cells under physiological as well as pathological conditions. In the past decade, EV have been recognised as potent messengers of intercellular communication and signalling (Harrison *et al.* 2014). EV carry cargo of transmembrane and enclosed proteins, lipids and nucleic acids from their parental cells to other distant cells (Colombo *et al.* 2014). Recent research on the role of EV have primarily focused on pathological conditions; however, EV-mediated homeostasis under physiological conditions have not been extensively investigated (reviewed in Yáñez-Mó *et al.* 2015). Furthermore, there is an increased interest in the possible uses of EV as biomarkers for disease as well as potential targets for disease therapy.

EV were first reported as pro-coagulant platelet-derived particles in normal plasma (Chargaff & West 1946), and referred as 'platelet-dust' by Wolf in 1967 (Wolf 1967). Consequently, antigen-presenting vesicles isolated from Epstein-Barr virus-transformed B lymphocytes were shown to induce T cell responses (Raposo *et al.* 1996a). Subsequently, EV were shown to contain RNA, including microRNA, suggesting a likely role in cell-to-cell communication (Ratajczak *et al.* 2006; Valadi *et al.* 2007). EV have been shown to be present in most biological fluids including breastmilk, blood, urine and saliva (Pisitkun *et al.* 2004; Caby *et al.* 2005; Keller *et al.* 2011). EV can be produced by various cells including red blood cells (Simpson *et al.*

2008), fibroblasts (Stadtman & Levine 2006), endothelial cells (Winyard *et al.* 2011), and trophoblasts (Tannetta *et al.* 2017a). EV carry proteins, lipids, RNAs including mRNA, miRNA, vault RNA and tRNAs (Raposo & Stoorvogel 2013). EV are believed to signal to their target cells via surface interactions consisting of (1) protein or lipid ligand-receptor binding, (2) cell-membrane via fusing and releasing their contents into the cytosol of the target cell, and (3) via endocytosis and subsequent fusion with endosomes (Raposo & Stoorvogel 2013; Tannetta *et al.* 2017a).

EV are classified according to size, function, morphology and biogenesis (Cocucci *et al.* 2009; Mathivanan *et al.* 2010). The term EV encompasses apoptotic bodies, microvesicles and exosomes (**Figure 1.7**), and in pathological conditions, necrotic debris (Raposo & Stoorvogel 2013). Apoptotic bodies (800 - 5,000 nm) are the largest vesicles and are released by blebbing cells undergoing apoptosis. Microvesicles (50 - 1,000 nm) are formed through the direct budding or shedding of the plasma membrane of living cells in response to cellular activation or stress. Exosomes (30 - 200 nm) are the smallest vesicle type, formed as intraluminal vesicles by an inward budding of early endosomes.

Microvesicles are a heterogeneous population of EV. Although it is challenging to differentiate microvesicles from exosomes as their sizes technically overlap, microvesicles lack endosomal features found in exosomes (Cocucci *et al.* 2009). The mechanisms by which microvesicles are formed remain unclear. However, it has been shown that the budding process is regulated and stimulated by the remodelling of the plasma membrane and an increase in intracellular calcium (Pasquet *et al.* 1996). Subsequently, biomolecules move towards the cell surface, resulting in membrane protrusion, budding, and detachment of spherical bodies from specific areas of the plasma membrane enriched in lipid rafts (del Conde *et al.* 2005).

Exosomes have a very small, 'cup-shaped' and homogeneous morphology (Cocucci *et al.* 2009). The endocytic pathway constitutively generates exosomes. This pathway recruits proteins and lipids into recycling endosomes or targeted for lysosomal degradation by ubiquitylation and ubiquitin-dependent connections with the endosomal sorting complex required for transport (ESCRT) (Colombo *et al.* 2013). As a result, exosomes are formed by inward budding of the endosomal membranes within

the endosome, which then increase build-up of intraluminal vesicles within the large multivesicular body. These can either be trafficked to lysosomes for removal, or to the plasma membrane, where it fuses with the surface and secrete its contents into the extracellular space. (Raposo & Stoorvogel 2013)
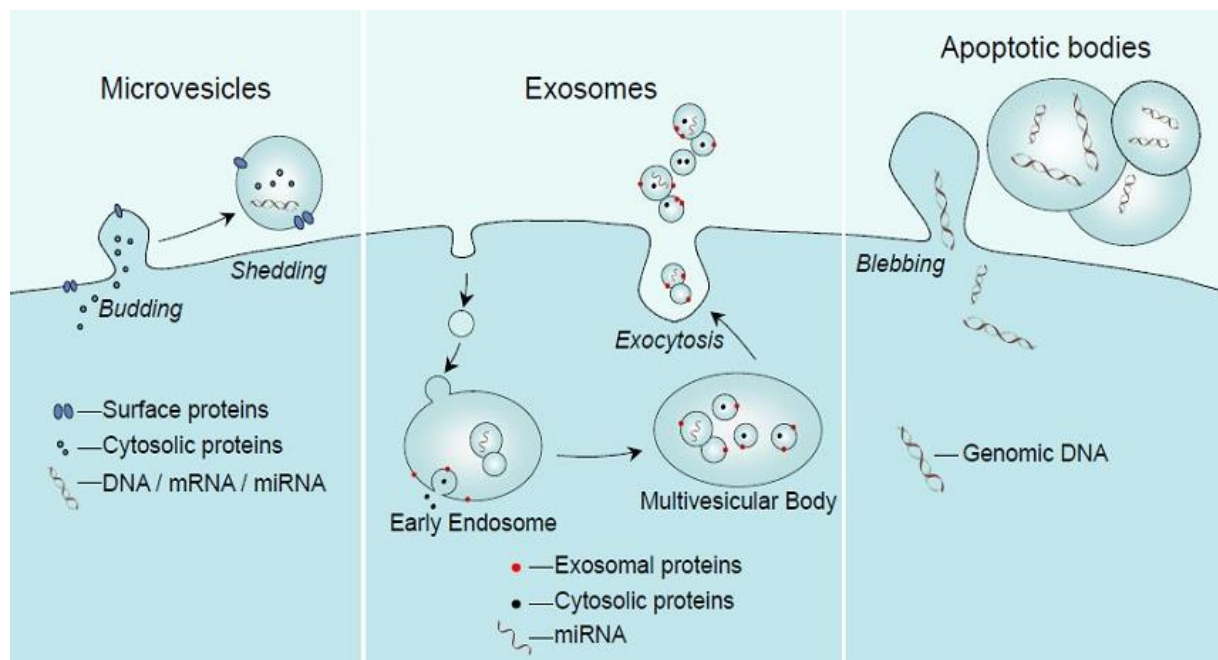
Figure 1. 7. Schematic diagram of extracellular vesicles formation. Microvesicles (50 - 1,000 nm) formed through the direct budding or shedding of the plasma membrane of living cells (left). Exosomes (30 - 200 nm), the smallest vesicle type, formed as intraluminal vesicles by the inward budding of early endosomes (centre). Apoptotic bodies (800 - 5,000 nm), the largest vesicles, formed by blebbing cells undergoing apoptosis (right). Image taken from (Lawson *et al.* 2016).

Currently, it remains a matter of intense debate what different vesicles should be called and how should they be isolated from bodily fluids, cell's supernatant and placenta. Hence, a major challenge in EV research is to advance and standardise methods for EV isolation and analysis (Théry *et al.* 2006). Isolation strategies include density gradient centrifugation, sucrose cushion centrifugation, gel-permeation chromatography, affinity capture, microfluidic devices, synthetic polymer-based precipitation, and membrane filtration (Xu *et al.* 2016). Tong and Chamley have also

reviewed in detail the different methods on isolating placental micro/nanovesicles (Tong & Chamley 2015).

The most widely used method of EV isolation is based on differential ultracentrifugation. This involves the sequential centrifugation of supernatant fluid at increasing rotational velocities, allowing the isolation of both microvesicles and exosomes; differently sized vesicles will sediment at different velocity rates (Raposo *et al.* 1996b). Our laboratory has used a method to isolate EV derived from placenta, specifically the STB layer, using the *ex vivo* dual-lobe placental perfusion model followed by serial ultracentrifugation method is used to isolate STBEV (Dragovic *et al.* 2015). Briefly, microvesicles are isolated from the accumulated placental perfusate after centrifugation at 10,000 x g while centrifugation of the supernatant at 150,000 x g result in a pellet enriched in exosomes (**Chapter 2**; Dragovic *et al.* 2015). However, this isolation method does not result in the complete separation of the two EV types (Witwer *et al.* 2013), as sedimentation is subject to vesicle density as well as possible contaminants having similar sizes, such as lipoproteins and soluble protein complexes. Nevertheless, this method remains the most appropriate for purification of EV at a relatively low cost (Dragovic *et al.* 2015).

After the isolation of EV, further characterisation of both EV groups (microvesicles and exosomes) requires complementary biochemical, immunoblotting, mass spectrometry, and imaging techniques such as electron microscopy (Raposo & Stoorvogel 2013). Due to their endosomal origins, exosomes can be identified by the expression of proteins related to transport and fusion (caveolin-1 and flotillin), tetraspanins (CD63, CD81, CD9), heat shock proteins (Hsp90) and lipid-related proteins (Colombo *et al.* 2014; Zeringer *et al.* 2015). The molecules are not unique to exosomes, but their enrichment in exosomes differentiate them from microvesicles or cell debris. Unfortunately, there are no current potential markers for microvesicles. Instead, our laboratory has developed further characterisation techniques for STBEV, via flow cytometry (Dragovic *et al.* 2013) and nanoparticle tracking analysis (NTA) (Redman *et al.* 2012).

1.5.2. STB derived extracellular vesicles

From gametogenesis through to late gestation, EV have an important role during all reproductive events (Tannetta *et al.* 2014). It is known that the STB layer of the placenta deposits material into the mother's bloodstream (Burton & Jones 2009). STB continually secretes EV directly into the maternal blood circulation during pregnancy where they can engage with the maternal immune and vascular systems (Mincheva-Nilsson & Baranov 2014). The placental origin of these vesicles is confirmed by the expression of the STB specific marker, placental alkaline phosphatase (PLAP) (Germain *et al.* 2007), their large quantity in the uterine vein blood compared to peripheral vein blood (Knight *et al.* 1998), their increase in particle number throughout gestation (Germain *et al.* 2007), and their absence to non-pregnant levels 48 hours post-delivery (Reddy *et al.* 2008). Salomon *et al.* revealed that PLAP and CD63 double positive exosomes were detected as early as 6 weeks of gestation (Salomon *et al.* 2014). Thus, the STB-derived EV (STBEV) can be prepared either through a sampling of maternal blood or by placental perfusion, obtained at term from elective caesarean sections or first trimester terminations.

Circulating STBEV provide a small biopsy of the material released from the placental surface. Our laboratory has shown that these STBEV comprise both microvesicle and exosomes (Tannetta et al. 2013a). Although syncytial nuclear aggregates have been identified in uterine vein and inferior cava blood, these get held-up in the pulmonary capillary bed due to their large size (Johansen *et al.* 1999). As a result, only smaller STBEV can pass through the lung capillaries and enter the peripheral circulation (Knight *et al.* 1998). Both microvesicles and exosomes, derived from STB, are part of the molecular communication channel between the fetus and the mother, dependent on the cargo carried by these vesicles. STBEV carry an abundant number of proteins that differ among EV populations potentially triggering an effect on the maternal cells (Tong *et al.* 2016). These include immunologically related proteins, vasoactive proteins, proteins involved in thrombosis, as well as those that potentially target specific organs or cell types (Tong & Chamley 2015). Similarly, STBEV also carry nucleic acids and lipids which may play an imperative role in mediating their effects on maternal physiology (Tong & Chamley 2015).

During PE, an excessive shedding of STBEV released into the maternal circulation due to placental oxidative and inflammatory stress have been demonstrated (Germain *et al.* 2007; Goswami *et al.* 2006; Reddy *et al.* 2008). STBEV derived from PE plasma differ in both phenotypic composition and number of circulating EV from those obtained from normal pregnancies (Redman and Sargent, 2007; Tannetta *et al.* 2017b). A mass spectrometry analysis of STBEV from normal and PE identified over 2,500 proteins with 538 unique peptides associated with PE (Tanetta *et al. Unpublished*; Redman *et al.* 2012). Additionally, both syncytial nuclear aggregates and microvesicles derived from STB have been reported to carry Flt-1 (Rajakumar et al. 2012; Tannetta et al. 2013a), which has been shown to be significantly expressed on STBEV secreted by the PE placentae compared to the healthy term placentae. Similarly, the soluble form of endoglin (part of the TGF-β receptor) has also been detected in high portions on STB derived microparticles from PE placentae (Guller *et al.* 2011), which might contribute to the pathogenesis of PE due to its impact on the vasculature. STBM express tissue factor and the expression levels are higher on PE vesicles (Gardiner *et al.* 2011), where it is proposed to compromise a considerable intravascular pro-thrombotic stimulus in these patients.

STBEV might interact with and instigate neighbouring cells including lymphocytes, monocytes, neutrophils, platelets and endothelial cells, exerting a wide range of outcomes (Yáñez-Mó *et al.* 2015). For example, STB derived microvesicles stimulate monocytes to release pro-inflammatory cytokines such as TNFα (Germain *et al.* 2007; Messerli *et al.* 2010). Additionally, STBEV have been reported to bind and get internalised by monocytes and B cells directly and have been proposed to have an immunomodulatory role (Southcombe *et al.* 2011). Von Dadelszen *et al.* reported that the microvesicles from healthy term placentae added to the conditioned media of cultured endothelial cells resulted in a pro-inflammatory effect and could activate resting monocytes, granulocytes, and lymphocytes (Von Dadelszen *et al.* 1999). Likewise, it has also been shown that STB derived microvesicles from healthy term placentae can inhibit proliferation and increase apoptosis of EC (Smárason *et al.* 1993a). Most recently, studies have demonstrated that EC bind and internalise STBEV *in vitro* which results in the transfer of placenta-specific functional miRNA from STBEV

into the endoplasmic reticulum and mitochondria of the recipient cells (Cronqvist *et al.* 2017).

1.5.3. Capillary pericytes derived extracellular vesicles

As mentioned before, all cell types are capable of producing and releasing EV. Both microvesicles and micro-RNA have been proposed to play a role in the cross-talk between pericytes and endothelial cells (Caporali *et al.* 2017; Gaceb *et al.* 2018). Recently, upon addition of PDGF-BB, human brain pericytes released several growth factors and a host of cytokines, as well as microvesicles carrying molecules specific for the PDGFRβ signalling and activation of the ERK I/2 pathway (Gaceb *et al.* 2017). This is the first report to show a type of EV secreted by PC in a stimulus-specific manner, containing growth factors that have been implicated in neuroprotection and neurorestoration (Gaceb *et al.* 2017).

Similarly, exosomes derived from pericytes stimulated with cobalt chloride ($CoCl_2$) to activate the hypoxia-inducible factor (HIF) pathway were able to adopt wound healing properties in a scratch assay and promote microvascular sprouting in spinal cord explants (Mayo and Bearden, 2015). MSC derived microparticles have also been found to play a role in vessel destabilisation by interfering with the interactions between endothelial cells and pericytes as well as pericytes and extracellular matrix (Beltramo *et al.* 2014). In addition, it was found that MSC derived microparticles can enter pericytes and cause detachment and migration from the substrate, increase blood-barrier permeability, and promote *in vitro* angiogenesis (Beltramo *et al.* 2014). Nevertheless, PLVP derived EV (PLVPev) have **<u>never</u>** been isolated or characterised before in placental biology.

EV play a role in the communication from the fetus to the mother. Still, the mechanisms by which EV cause changes in the phenotype and behaviour of maternal target cells have to be further investigated. Thus, we aim to explore the cargo and function differences of STBEV derived from normal and PE pregnancies in **Chapter 3** and **4**. We also intend to investigate the potential functions of PLVP derived EV from normal and PE-like conditions in **Chapter 5**.

1.6. Aims of thesis

1. To investigate the protein cargo expression and activity difference of STB derived EV isolated from *ex vivo* dual-lobe placental perfusion and blood plasma in normal and PE patients.
2. To assess the impact of *ex vivo* STB derived EV from normal and PE placentae on a differentiated macrophage cell line, THP-1, to determine if there are any differences in cytokine/chemokine protein profile and secretion.
3. To examine the role of PLVP when exposed to *in vitro* normal and PE-like conditions to consider the possible functions of secreted EV on primary endothelial cells, HUVEC.

CHAPTER 2

Materials and Methods

2. Materials and Methods

2.1. Study research ethical approval

The research ethics committee of the Brunel University London approved this research work under the reference code 2968-TISS-May/2016- 3081-1.

2.2. Human subjects

The human subjects' material used in this project was approved by the Central Oxfordshire Research Ethics Committee C (REFS 07/H0607/74 & 07/H0606/148). All mothers undergoing elective caesarean section without labour were approached by the research midwives who facilitated written informed consent for the use of their blood and placentas. Placentae were collected within 10 minutes of delivery in a clean plastic bucket with warm sterile Hanks solution. Placentae from normal pregnancy (NP) were taken from healthy singleton pregnancies with no current or previous history of PE or hypertensive disorders, and without fetal abnormalities.

Mothers suffering from PE were recruited using the corresponding diagnostic criteria by the International Society for the Study of Hypertension in Pregnancy (ISSHP) (Tranquilli *et al.* 2014). According to ISSHP, PE is defined as de-novo hypertension present after 20 weeks of gestation combined with one or more complications: proteinuria (>300mg/day); or other maternal organ dysfunction such as liver involvement, neurological or haematological complications, renal insufficiency; and/or an uteroplacental dysfunction such as fetal growth restriction. In the new definition, proteinuria is no longer required therefore there are now two separate categories for PE: proteinuric or non-proteinuric. Hypertension includes systolic blood pressure higher than 140 mm Hg or diastolic blood pressure higher than 90 mm Hg on two occasions that are 4 to 6 hours apart (National Institute for Health and Clinical Excellence 2011).

2.3. Isolation and characterisation of STBEV

2.3.1. *Ex vivo* dual-lobe placental perfusion

STBEV were prepared using a dual placental lobe perfusion system from human placenta (**Figure 2.1**) as previously described (Southcombe *et al.* 2011). Firstly, the

maternal-side placenta was examined to identify one peripheral lobule with no signs of postpartum villus breakage. The fetal umbilical artery and vein connected with the isolated lobe were cannulated at the chorionic plate. The 0.1 μm filtered (stericup-VP, Merck Millipore) and modified M-199 tissue culture medium (Medium 199 with L-glutamine and Earle's salts, containing 0.8% w/v Dextran 20, 0.5% w/v BSA, 5000 U/L sodium heparin, and 2.75 g/L sodium bicarbonate, pH 7.4), comprising a 20 mL bolus of 100,000 IU streptokinase (Oxford Hospitals) to prevent clot blockage, was used to perfused the lobe through the fetal circulation at a rate of 5 mL/min. The whole placenta was then turned upside down and placed inside a Perspex water jacket container maintained at 37°C. The maternal surface isolated lobe was then perfused with the corresponding tissue culture medium (Medium 199 with L-glutamine and Earle's salts, containing 0.5% BSA, 5000 U/L sodium heparin, and 2.75 g/L sodium bicarbonate, pH 7.4) through six 1.7 mm fetal feeding tubes (Pennine Healthcare, UK) at a controlled rate of 20 mL/min. Perfusion media was kept warm in a 37°C water bath, and the maternal perfusion medium was continuously oxygenated with 95% v/v O_2 and 5 % v/v CO_2. The lobe was perfused for 20 minutes to equilibrate the system, after which the maternal circuit was closed with a total volume of perfusion medium of 600 mL. The fetal outflow was measured every 20 minutes over the 3-hour perfusion course to monitor the integrity of the lobe's circulation. The maternal perfusate was collected to harvest STBEV.
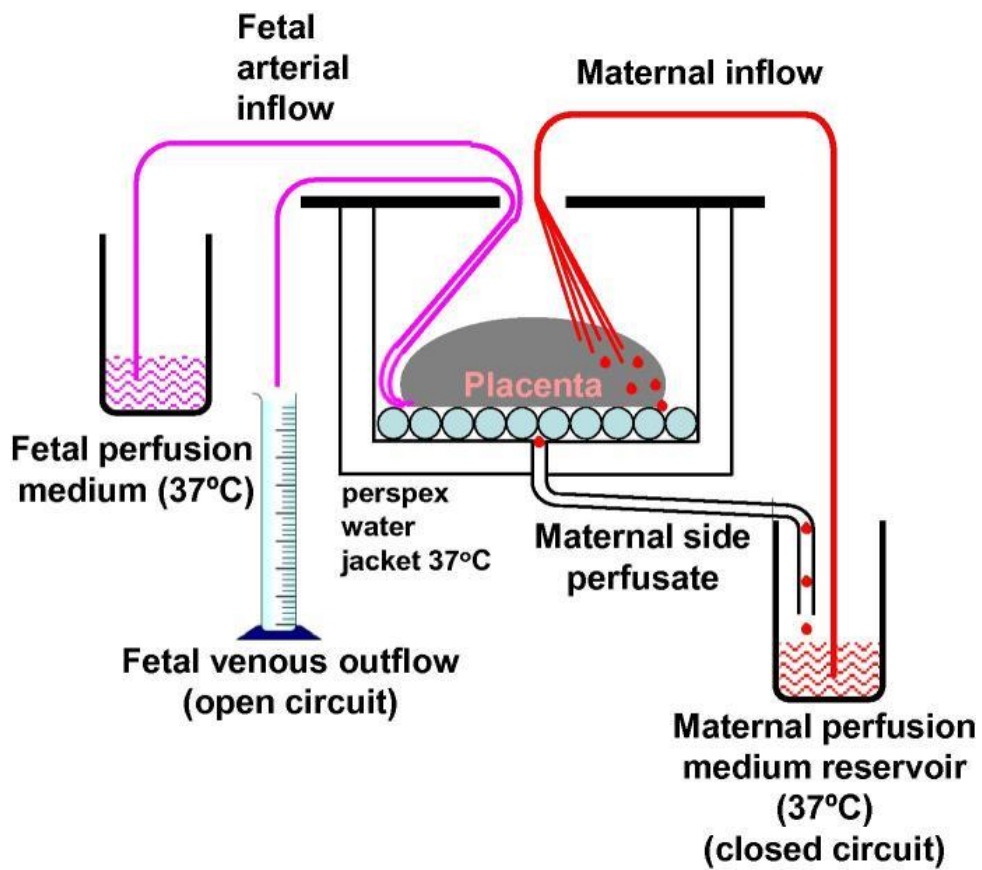
Figure 2. 1. Schematic diagram of *ex vivo* dual placental lobe perfusion system. Diagram taken from (Dragovic *et al.* 2015).

2.3.2. Differential serial ultra-centrifugation and filtration

At the end of the 3-hour perfusion period, the maternal perfusate was centrifuged in a Beckman J6-M centrifuge at 600 x g for 10 minutes at 4°C to remove red blood cells contamination. The supernatant was then centrifuged at 10,000 x g for 35 minutes at 4°C in a Beckman L8-80M ultracentrifuge, and Sorvall TST28.39 swing-out rotor. The supernatant was removed and stored at 4°C for further processing. The resultant pellets were pooled and washed with filtered phosphate buffered saline (PBS) by centrifugation at 10,000 x g for 35 minutes at 4°C. The final pellet was resuspended in filtered PBS according to pellet size. This fraction contained enrichment of STB derived microvesicles (STBMV). The stored supernatant was passed through a 0.22 µm filter stericup-VP device (Merck Millipore). The filtered supernatant was centrifuged again at 150,000 x g for 2 hours at 4°C. The resultant supernatant was discarded, and the pellets were pooled and washed with filtered PBS by ultracentrifugation at 150,000 x g for 2 hours at 4°C. The pellet obtained was resuspended in filtered PBS to give an enriched STB derived exosome (STBEX) fraction. STBMV and STBEX were further characterised by flow cytometry (**Section 2.3.3**), Nanoparticle Tracking Analysis (**Section 2.4**), BCA assay for protein concentration (**Section 2.9**), and Western blotting (**Section 2.10**), before being aliquoted and stored at - 80°C.

2.3.3. STBMV characterisation by flow cytometry

Isolated STBEV characterisation and validation was performed by flow cytometry, using a BD LSRII flow cytometer (BD Biosciences), and conducted before downstream experimentation as previously described (Dragovic et al. 2011, 2013).

At the start of this procedure, all antibodies or markers and the Fc receptor blocker (Miltenye Biotech) were passed through a 0.2 µm Nanosep centrifugal devices with Bio-inert membrane (VWR) before use. PBS was filtered using a 0.1 µm stericup-VP device (Merck Millipore). Flow cytometer performance check was carried out using CST beads (BD Biosciences) to ensure correct laser and cytometer set up. To avoid background contaminating events, filtered PBS was run at low speed through the machine until background event rate reduced to 2,000 events in 2 minutes. TruCount beads (BD Biosciences) were used to accurately achieve flow rate setting of around

11 - 12 µL/minute. Briefly, 500 µL of filtered PBS were added to a BD TruCount tube and data was acquired for 2 minutes. The flow rate was calculated as follows: where events obtained in the 'TruCount beads' gate was divided by the bead number per TruCount tube and multiplied by the volume. Once the flow rate was set, each STBMV sample was diluted accordingly with filtered PBS to achieve 20,000 - 30,000 events in 2 minutes to proceed with the staining.

Fluorochrome compensation was set using BD CompBeads (BD Biosciences), REA CompBeads (Miltenyi Biotech) and a single stain using Bio-Maleimide labelled STBMV, before final staining. The EV pan lipid membrane marker, Bio-maleimide or BODIFY FL N-(2-aminoethyl)-maleimide (505/513 nm) (Molecular Probes) was used to confirm biological material. Bio-maleimide binds to biological membranes via cysteine residues and thiol groups in proteins. Anti-CD41 and anti-CD235a/b antibodies were used to exclude platelet and red blood cell (RBC) EV contamination, respectively. HLA-ABC was used to also discriminate possible contamination by leukocyte derived EV. The STBEV specific marker, placental alkaline phosphatase (PLAP), was used to confirm the placental origin of the vesicles. The corresponding isotype controls were used as Fluorescence minus one (FMO) controls, which contained all the fluorochromes in the panel except for the one to be measured, allowing distinguishing true events from the noise and set control gates. STBMV were first incubated with 10 µL of FcR blocking reagent for 10 minutes at 4°C to avoid non-specific binding, followed by the labelling with antibodies and isotype-matched control antibodies within a volume of 100 µL for 15 minutes at room temperature in the dark. Samples were made up to 300 µL with filtered PBS, prior to running 100,000 events on the flow cytometer. Data were analysed using FACSDiva software (BD Biosciences).

2.3.4. STBEV validation by SDS-PAGE and Western blotting

The phenotype of STBEV were additionally assessed by SDS-PAGE and Western blotting analysis via PLAP positivity combined with the exosome markers ALIX, Syntenin and CD9, to confirm exosomal phenotype. SDS-PAGE and Western blotting methods are described in **Section 2.10**. Details of antibodies are summarised in **Table 2.3**.

2.4.   Nanoparticle Tracking Analysis

Freshly isolated EV (either STBEV or PLVPev) were assessed for particle size and number by Nanoparticle Tracking Analysis (NTA) using a NanoSight NS500 (Malvern UK) and NanoSight 3.1 software (NanoSight Ltd) (**Figure 2.2**). The system is composed of a finely focused laser beam directed to the sample chamber through a glass prism (**Figure 2.2A**). As it enters the chamber sample, the beam refracts at a low angle, resulting in a thin beam of laser light that illuminates particles through the sample. Illuminated particles within the beam are visualised using a conventional optical microscope with an incorporated video camera. The camera is aligned generally to the beam axis, collecting light scattered from all particles in the field of view from the sample chamber. Once the videos are recorded, these are analysed by the NTA software (**Figure 2.2B**). The protocol has been optimised to identify the particles first, and then track the movement of each particle on a frame-to-frame basis. The two-dimensional Stokes-Einstein equation (Filipe *et al.* 2010) is automatically applied to calculate the particle size using the velocity of particle movement.

First, filtered PBS was slowly flushed through the Nanosight, followed by several rapid flushes to remove any air bubbles and dust from the sample chamber. Stage's correct position was checked, and the video camera was maintained at Level 12 (camera shutter at 12 milliseconds and camera gain at 350). Silica 100 nm size beads (PolySciences) were diluted in filtered PBS to give rise to a 1/50,000 dilution, and passed through the NanoSight using a 1 mL syringe device. Camera focus was adjusted using the beads and the script 'PRIME, DELAY 5, CAPTURE 30; REPEAT 4' was loaded onto software to record 5 video-recordings of 30 seconds long with 15 frames per second. The summary file was automatically generated and particle number, mean size and mode were noted. Nanosight set up is completed if data shows silica beads particle number and mode size close to 5×10^8 particles/mL and 100 nm, respectively.
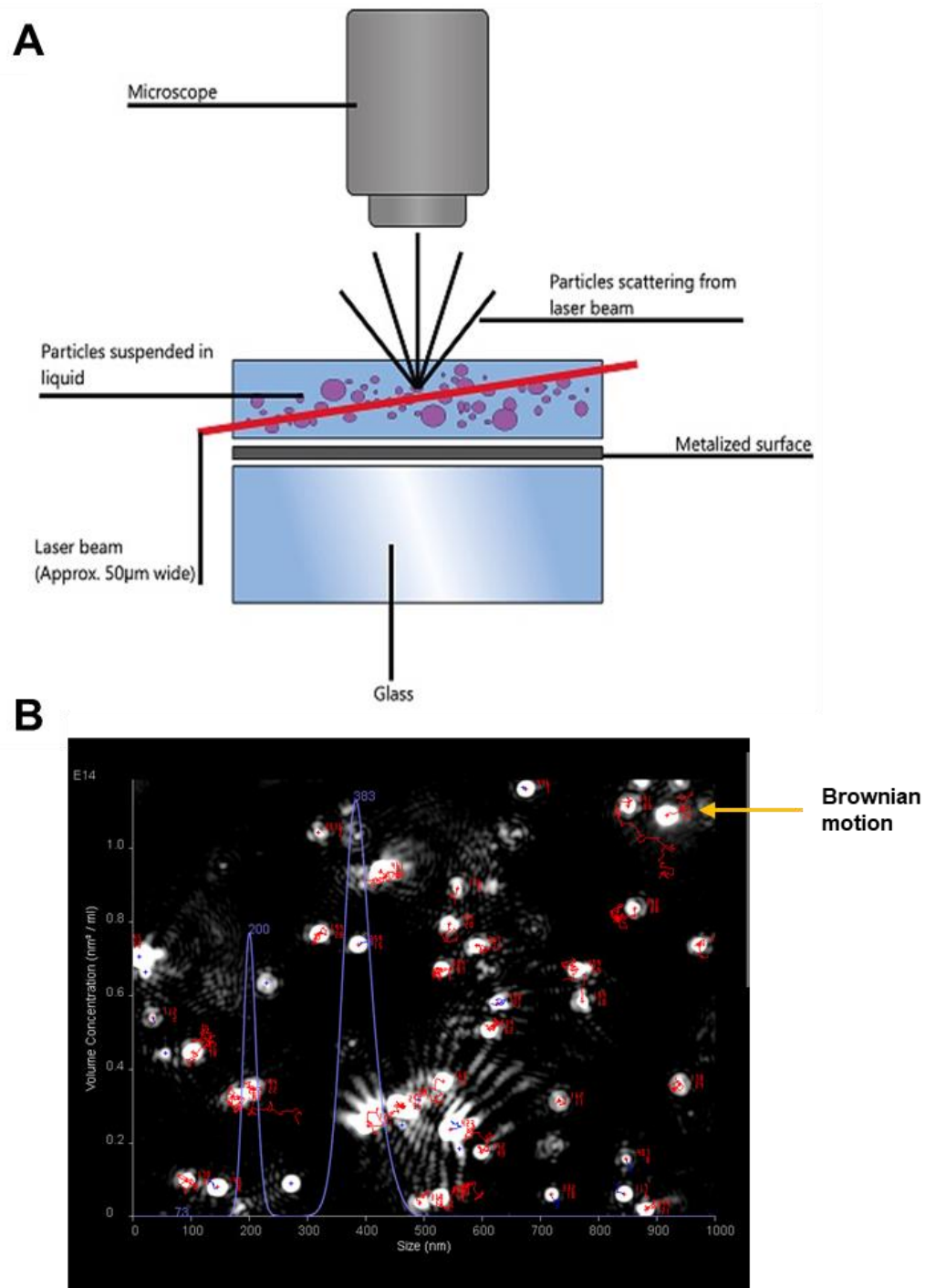
Figure 2. 2. Nanoparticle Tracking Analysis (NTA) performance. A, Diagram of NTA's laser beam passing through the sample chamber where particles in suspension are visualised by the beam scatter light using an x20 magnification microscope mounted onto a video camera. B, Representative image of video file showing how individual moving particles are tracked under the Brownian motion (yellow arrow) by software while calculating their hydrodynamic diameters using the Stokes-Einstein equation to determine the size (nm) and particle number (particle/mL). Image taken from Malvern Panalytical Website (www.malvernpanalytical.com).

2.5. Isolation of STBMV derived from peripheral and uterine blood plasma

2.5.1. Blood collection and processing

Blood samples were collected in four 5 mL EDTA or citrate tubes using a 21-gauge needle. Peripheral blood vein (PB) samples were from the left antecubital fossa while uterine blood vein (UV) samples were taken at caesarean section (after bladder reflection before the uterine incision was made). Samples were centrifuged at 1,500 x g for 15 minutes at room temperature using a Beckman Coulter JS-5.3 centrifuge. The subsequent supernatant was centrifuged again at 13,000 x g for 2 minutes using a centrifuge (Eppendorf 5417R) to produce platelet-free plasma (PFP). Samples were stored in aliquots at -80°C until the following use.

2.6. Human placenta tissue

2.6.1. Immunohistochemistry

Placental tissues were fixed in 4% v/v paraformaldehyde (PFA), embedded in paraffin blocks, cut in 8 μm thick sections and placed on slides. Slides were deparaffinized in Histo-clear (Company), rehydrated in graded ethanol, and antigens were retrieved to enable detection using 0.01M Citrate buffer. Endogenous peroxidase was reduced with 3% v/v hydrogen peroxide. Tissue sections were blocked in 10% v/v fetal calf serum (FCS) for 1 hour. Slides were incubated overnight at 4°C with primary monoclonal antibodies against: eNOS (0.6 μg/mL, NOS3-A9 Santa Cruz), eNOS isotype control IgG2a (0.6 μg/mL, Clone DAK-GO5, Dako), iNOS (1 μg/mL, clone 2D2-B2, R&D) and iNOS isotype control IgG1 (1 μg/mL, IgG1 Clone MOPC-21, BioLegend in 1% v/v FCS in PBS with 0.05% 0.01M Tween 20 (PBS-T) overnight at 4°C. All sections were then incubated with of 0.2 μg/mL anti-mouse IgG secondary antibody conjugated to horseradish peroxidase (HRP) in 10% v/v FCS for 1 hour at room temperature. After washing with PBS-T, Antigen-specific detection was revealed using Horseradish Peroxidase (HRP) Substrate Kit with Nickel 3,3'-diaminobenzidine (DAB; Vector Laboratories) and counterstained with Shandon Gill 2 Haematoxylin (ThermoFisher). The slides were dehydrated in graded ethanol and mounted with Depex (VWR). Sections were viewed under a Leica DM2500 optical microscope (Leica

Microsystems) and photographed using a digital camera linked to a computer hard drive (Micropublisher 5.0 RTV).

2.7. Cell culture

Cells were maintained at 5% v/v CO2 at 37ºC with their corresponding media. The medium was changed every 2 to 3 days and cells were passaged once they reached 80-90% confluence. For passaging, cells were washed with warm PBS and lifted using 1 mL of Trypsin-EDTA and incubated for 5 minutes at the 37ºC incubator.

2.7.1. Trypan blue basic cell viability check and cell counting

Trypan Blue dye is impermeable to healthy cells and enters through the cells' membrane if cells are dying or dead. Cells were checked for viability by visual observation using this dye. To count cells, equal volumes of cell suspension and Trypan Blue (0.4% w/v solution) were mixed and mounted onto a haemocytometer with Neubauer rulings (Superior Marienfled).

2.7.2. HUVEC isolation and cell culture

Human umbilical vein endothelial cells (HUVEC) were isolated from the normal pregnancy human umbilical cord, as previously described (Jaffe *et al.* 1973). Briefly, the umbilical cord was clamped and cut from the placenta delivered within 10 minutes of caesarean section. The umbilical cord was immersed in warm PBS to remove contaminating RBC for 5 minutes. The state of the cord was reviewed for damaged vessels, and 10 cm length of healthy cord was localised for the following steps. The umbilical cord vein was cannulated from one end and flushed slowly with 20 mL of warm PBS before clamping the other end of the vein. The vein was then filled with 5 mL of 1x collagenase type 1a (1mg/mL) and incubated at 37ºC in 5% v/v CO_2 for 15 minutes to achieve maximal digestion of extracellular matrix and detachment of endothelial cells. The cord vein was subsequently flushed with 30 mL of endothelial cell growth medium (EGM-2 SingleQuot Kit CC-4176, Lonza), collecting the cells in a 50 mL falcon tube. The cell suspension was pelleted by centrifugation at 13,000 rpm for 5 minutes before being cultured in a T25 flask. Primary cells were left to grow at

approximate of 2 days before passage. Only passages 2-5 cells were used for functional studies.

2.7.3. THP-1 culture

THP-1 cells, originally derived from human acute monocyte leukaemia cell line (ATCC® TIB-202™), were cultured in RMPI-1640 medium (Gibco) containing 10% v/v FCS, 2 mM L-glutamine, 100U/mL penicillin and 100 µg/mL streptomycin. Cells were left to grow for 3 days before passage.

2.7.3.1. THP-1 differentiation using PMA

FCS was centrifuged at 150,000 x g for 18 hours using a Beckman L8-80M ultracentrifuge, to reduce possible contamination from microvesicles or exosomes derived from serum. After centrifugation, FCS pellets were removed, and the supernatant was pooled and sterilised using a 0.1 µm filter under sceptic conditions before storage at -20ºC until use. THP-1 cells were adjusted to 5 x 10^6 cells/mL per well in a 24-well plate and differentiated into macrophage-like phenotype using 50ng/mL of Phorbol 12-Myristate 13-Acetate (PMA) in RPMI-1640 complete media (including 10% v/v of centrifuged FCS) for 48 hours at the 37ºC.

2.7.3.2. THP-1 treatment with STBEV

THP-1 cells were washed with warm PBS and incubated with serum-free media containing STBMV or STBEX of six patients pooled from NP and PE pregnancies at 50 µg/mL. STBMV and STBEX were passed through the NTA, and further dilution in serum-free media was carried out to accomplish the same particle number among normal and PE STBMV or STBEX (~1 x 10^8 particles/mL). STBEV were incubated with differentiated THP-1 cells for 2, 6, 12 and 24 hours. THP-1 cells with no STBEV were used as a control for each time point. The supernatant was collected, and dead cells and debris were removed by centrifugation at 1,500 x g for 10 minutes at 4 ºC. Next, supernatant from each sample were stored at -80 ºC for subsequent experiments. Cells were washed with warm PBS before RNA extraction (**Section 2.11.1**) for real-time quantitative PCR analysis (**Section 2.11.2**). In addition, for PLAP ELISA (**Section 2.7.3.3**), cells were lifted following Trypsin-EDTA treatment, thoroughly washed with

media and PBS, and then harshly re-suspended using a 21-gauge needle syringe to disrupt the cell membrane.

2.7.3.3. PLAP ELISA assay

A 96-well IgG surface treatment MaxiSorp™ plate (Nunc) was coated with 100 µL of 10 µg/mL of PLAP antibody (NDOG2, in-house), and incubated inside a covered box overnight at room temperature. The plate was washed with PBS-T (PBS 0.05% Tween), and then incubated with 300 µL of blocking buffer (5% w/v BSA in PBS-T) for 3 hours at room temperature. For ELISA standards, NP STBMV derived from 3 patients were pooled together to make 8 quadruple dilutions from 4,000 ng/ml down to 1ng/ml in 1% BSA PBS-T. After washing, standard and samples were incubated in triplicates overnight and were thoroughly cleaned the next day using PBS-T. 1-Step pNPP (p-nitrophenyl phosphate disodium salt) substrate kit (Sigma) was used to detect alkaline phosphatase activity. 100 µL of the substrate was added to the plate sample wells and was left to incubate for 1 and a half hours. 50 µL of 2N NaOH was added to stop the reaction. Absorbance was measured at 405nm using the FluoStar OPTIMA (BMG) plate reader.

2.7.4. Placental capillary pericytes culture

Human placental capillary pericytes (PLVP), isolated from normal placenta, were purchased (C-12980, PromoCell). PLVP were cultured in pericyte growth medium (C-28040, PromoCell), according to manufacturer's instructions, for 3-4 days before passage.

2.7.4.1. Hypoxia

For hypoxic conditions, pericyte growth medium was incubated for 24 hours within a chamber conditioned to 1% or 8% O_2, 5% CO_2 at 37 ºC. Cells were grown in 12-well plates or T175 flasks at normal air conditions. Once cells reached confluency, they were washed with warm PBS, and cultured with a hypoxic or normal medium for 24 hours. After incubation, cells were rewashed with warm PBS and cells were either lysed with radioimmunoprecipitation (RIPA) buffer or processed for RNA isolation

(**Section 2.11.1**). The supernatant was kept for the isolation of PLVP extracellular vesicles (PLVPev).

2.7.4.2. Isolation of PLVPev

After 24-hour incubation at different O_2 % conditions, dead cells and debris were removed from the supernatant by 1,500 x g centrifugation for 10 minutes at room temperature. 5 mL of dead cells and debris-free supernatant samples were stored at -80°C for subsequent experiments. The rest of the supernatant were then ultracentrifuged at 10,000 x g for 35 minutes at 4°C to collect the pellet containing PLVP derived microvesicles (PLVPmv). PLVPmv pellets were washed with filtered PBS, spun again as described above, and then re-suspended in 100 µL filtered PBS. Remaining supernatant were passed through a 0.2 µm filter, followed by ultracentrifugation at 150,000 x g for 2 hours 5 minutes at 4°C. Finally, PLVP derived exosomes (PLVPex) pellet samples were washed with filtered PBS before being resuspended in 100 µL of filtered PBS. 5mL of EV-free supernatant samples were stored -80°C for subsequent experiments. PLVPev samples were assayed for protein content using bicinchoninic acid (BCA) assay kit (Pierce) before storage at -80°C, and particle size and number were analysed using the NTA.

2.7.4.3. Cell cytotoxicity assay with PLVPex

A CellTox^{TM} Green cytotoxicity assay (Promega, G8741) was used using HUVEC to determine the non-toxic particle concentration of PLVPex for subsequent experiments. 2×10^4 cells/mL of HUVEC were grown overnight in a black 96-well plate with clear bottom (Nunc) before being treated with PLVPex. Next day, neat PLVPex were diluted in EV-free media containing 2% FCS without supplement (EV-free media). Using the NTA, different particle concentration (1×10^{10}, 1×10^9 and 1×10^8 particle/mL) were achieved per each PLVPex sample in a 100 µL volume. PLVPex samples were added in triplicates to the plate. Maximum toxicity control was achieved by adding lysis buffer to EV-free media in a 1/25 dilution in triplicate. The negative control was HUVEC in EV-free media without any exosome samples in triplicate. CellTox^{TM} Green reagent stock was diluted in EV-free media for an (x2) final dilution. 50 µL of X2 CellTox^{TM} Green reagent was added to each well. Background control was achieved by adding

50 µL of CellTox™ Green and 100 µL of media to empty cells. The cells were then incubated at 37°C in 5%CO_2 in a FLUOStar Omega (BMG LabTech) plate reader for 21 hours. The fluorescence measured at 485-500 nm excitation wavelength and 520-530 emission wavelength.

2.7.4.4. Tube formation angiogenesis assay

Primary HUVEC were used at passages 3-4 for tube formation angiogenesis assays. Matrigel basement membrane with reduced matrix growth factor 10 mL stock (Scientific Laboratory Supplies Limited, #356231) was distributed into 1 mL aliquots and stored at -20°C until use. Before starting the experiment, filter 200 µL tips, clear 96-well plate, cover, etc were kept at -20°C and matrigel aliquots were kept at 4°C overnight. Next day, neat PLVPex samples were resuspended in EV-free PLVP media and run through the NTA to achieve a concentration of 1 x 10^9 particles/mL. During the evening of the same day, utensils were kept on ice inside the hood, and 50 µL of Matrigel was added to each well of the 96-well plate. The cover was placed on a plate and left at 37°C in 5% CO_2 for 30 minutes to settle. Meanwhile, 80% confluent HUVEC were washed with warm PBS and lifted with Trypsin-EDTA. 1 x 10^4 cells/mL were resuspended in EV-free un-supplemented HUVEC media with 4% FCS. After the 30-minute incubation, 100 µL of cells were added to all wells of the matrigel coated plate and 100 µL of each PLVPex sample to each well. 100 µL of EV-free PLVP supernatant samples collected from **Section 2.7.4.2** were also added to each well. EV-free PLVP stock media alone was used as control. All samples were added in quadruple in the matrigel coated plate. The total volume of each well should be around 200 µL. The matrigel coated plate was left overnight for 16 hours incubation at 37°C in 5% CO_2.

Next day, 150 µL volume was removed from each well of the Matrigel-coated plate. 150 µL of cold filtered PBS was used to wash the matrigel coated plate. After the matrigel coated plate was washed three times, 100 µL of cold 4% PFA (10% formalin) was added to each well and plate was left to incubate for 1 hour at 4°C fridge. After incubation, the plate was washed three times with cold filtered PBS. Microscope at X4 Magnification was used to take pictures of each well of the matrigel coated plate. Image files were converted from 8-bit to RGB before being analysed using 'Batch

Image Treatment Tool' and 'HUVEC phase contrast' angiogenesis analyser on ImageJ software (Fiji).

2.7.5. Cell Immunofluorescence with PKH26 stained EV

50 µg of pooled STBMV or STBEX from three NP or PE mothers, as well as neat PLVPex, were stained using the PKH26 red fluorescent cell linker kit (MINI26, Sigma) according to manufacturer's instructions. Briefly, EV were diluted in 200 µL of Diluent C and mixed with 200 µL of Diluent C and 1.6 µL of PKH26 stock (1 mM). The mix was left to incubate for 5 minutes in the dark, and the reaction was stopped by 1-minute incubation with 400 µL of 1% BSA in PBS in the dark.

Next, stained exosomes were washed thoroughly using the qEV size exclusion columns (Izon Science Ltd). Briefly, columns were washed with 30 mL of filtered PBS before use. Stained exosome sample was carefully added to the column, 12 fractions of 500 µL each were collected, and assessed by NTA to confirm size and particle number per fraction. Fractions 7-10 were pooled together, and STBEV were concentrated in a 50 µL volume using an Amicon ultra-4 centrifugal filter unit with ultracel-100 membrane (Merck Millipore). In contrast, stained STBMV were washed by ultracentrifugation at 10,000 x g for 35 minutes and resuspended in 50 µL filtered PBS.

Stained EV were added to an initial volume (500 µL) of serum-free media, and NTA assessed particle number. Each sample was diluted accordingly to achieve the same particle number among sample groups. 2.5×10^5 cells/mL were grown overnight over autoclaved coverslips in a 24-well plate. The next day, cells were washed with warm PBS and incubated with EV-free media and the corresponding stained EV for 2 and 6 hours. After incubation, cells were carefully and thoroughly washed with warm PBS. Cells were then incubated with 5 µg/mL of wheat germ-like agglutinin (WGA) green (Vector Laboratories) diluted in media for 5 minutes at room temperature in the dark. Cells were washed three times with PBS followed by an incubation of 10 minutes with 2% v/v paraformaldehyde (PFA). Again, cells were thoroughly washed. Next, cells were stained with 1/5,000 Hoechst 33342, Trihydrochloride, Trihydrate (Hoechst) for 5 minutes. Finally, cells were thoroughly washed, and coverslips were carefully moved

with tweezers to slides, cells facing upwards. Slides were mounted with bigger square-like coverslips using the fluorescent mounting medium (Vectashield).

Cells were viewed under a Zeiss confocal microscope with a Yokogawa spinning disk scanning unit and an attached Evolve® 512 Delta EMCCD camera, and images were taken using a Zen Blue software (Zeiss). Z-stacks (11 slices) were taken through a 10 µm width, and pictures were compressed on maximum intensity using ImageJ software (Fiji).

2.8. Flow cytometry

BD LSRII flow cytometer (BD Biosciences) equipped with blue (488nm) and red (633nm) lasers was used and data was analysed with either FACSDiva software (BD Biosciences) or FlowJO version 10 (Tree Star Inc., Ashland, OR).

2.8.1. eNOS-APC antibody titration using HUVEC

HUVEC cells were used for eNOS-APC (Miltenyi Biotech) antibody titration before STBMV analysis by flow cytometry. HUVEC were grown in a T75 flask (see **Section 2.7.2**) until 90% confluency was reached. Media was removed, and cells were washed with warm PBS before being lifted following 1 mL of Trypsin-EDTA treatment and centrifuged at 13,000 RPM for 5 minutes. Cell pellets were fixed with 2% paraformaldehyde and permeabilised using 1/1000 dilution of Triton X100. 2.5×10^5 cells per sample were incubated with 5 µL of Fc receptor blocking reagent for 10 minutes at 4ºC before labelling with antibodies. Cell samples were stained with different concentrations of either REAfinity recombinant antibodies (REA) eNOS-Allophycocyanin (eNOS-APC) or its corresponding isotype control. An un-stained cell sample was used as a control. Samples were incubated in the dark for 30 minutes at room temperature, gently washed with filtered PBS by centrifugation, and volume adjusted to 300 µL with PBS. 5,000 events were recorded per sample using FACSDiva software (BD Biosciences).

2.8.2. Placenta perfusion derived STBMV & eNOS analysis

Perfusion isolated STBMV from NP and PE placentae were analysed by multi-colour flow cytometry panel using the protocol and equipment settings previously described (Dragovic et al. 2013, 2015), and specifically interrogated for eNOS.

Briefly, PLAP positivity combined with CD41 (platelet EV), CD235ab (RBC EV) negativity confirmed enrichment of STBEV. The equipment settings and detailed method used are described in detail in **Section 2.3.3**, where HLA-ABC marker was substituted by our antigen of interest marker, eNOS-APC (Miltenyi Biotech). Using preferred antibody titration determined by HUVEC (described in the previous section), we proceeded to analyse STBMV using the multi-colour panel.

2.8.3. Platelet Free Plasma (PFP) derived STBMV & eNOS analysis

Circulating STBMV from PB and UV were analysed by flow cytometry using a previously described protocol and flow cytometer settings (Inglis et al. 2016), with additional modifications to exclude potential non-placental EV contaminants. Peripheral vein blood (PB) and uterine vein blood (UV) PFP samples were thawed in a water bath at 37 °C. 200 µl from each plasma sample was labelled with the 'Dump Channel' antibodies. 'Dump Channel' includes contaminant markers against Classical HLA class I and II (leukocytes), CD235a/b (RBC) and CD41 (platelet) all conjugated to PEvio770 (Miltenyi Biotec). The sample was also stained against PLAP-PE (STB marker) and eNOS-APC for co-expression analysis. Plasma samples were incubated for staining for 15 min at 4°C in the dark. Samples were passed through a durapore-PVDF 0.22µm filter (Ultrafree-MV-GV, Millipore) by centrifugation at 800g for 3 minutes (5430R, Eppendorf) in order to concentrate the EV > 200 nm on the filter membrane. The filtrate (pass through) was made up to 800 µL with sterile PBS (1/5 dilution). The EV (on the filter membrane) were carefully resuspended using 100 µL filtered PBS and stained in the dark with 10 µL Bio-maleimide for 10 min at room temperature. After staining, the EV sample was made up with filtered PBS up to 500 µL (1/5 dilution), and then analysed for 10-minute of data acquisition on the flow cytometer. EV sample was then incubated with 20 µL (1/25 dilution) of detergent Nonidet P-40 detergent (Sigma) for 20 minutes in the dark (to disrupt the vesicle

membranes). The EV sample-treated with detergent, together with the filtrate, were also analysed for 2-minute data acquisition on the flow cytometer and used to set up the control gates.

Plasma-derived STBMV data was then analysed using the following gating strategy (see Figure 2.2). The filtrate sample (pass through) was used to set up the 'Dump Channel' control gate at 1% cut-off to separate EV population positive for Bio-Maleimide and negative for 'Dump Channel' contaminants. The EV sample-treated with detergent was used to set up the PLAP+ eNOS+ control gates at 1% cut off. Once control gates were set up, plasma-derived STBMV double positive (PLAP+ eNOS+) events/mL was calculated taking into account the dilution factor of EV sample (1/5) and to standardise all samples to 1mL. The following formula we used:

PLAP+ eNOS+ STBMV events/mL= (PLAP+ eNOS+ EV events x 5) x 5

Antibodies	Conc.	Antigen	Specificity	Source
STBMV Analysis				
Bio-maleimide (BODIFY FL N-(-2-aminoethyl)-maleimide	0.25µM	Thiol groups	All EV	Molecular probes
Anti-PLAP-PE (NDOG2)	0.05µg/mL	PLAP	STBEV	In-house antibody
IgG1-PE (clone MOPC-21)	0.05µg/mL	Isotype control	-	Biolegend
Anti-eNOS-APC (clone REA451)	0. 4µg/mL	eNOS	-	Miltenyi Biotech
REA-APC	0.025µg/mL	Isotype control	-	Miltenyi Biotech
Anti-CD41-PECy7 (clone P2)	0.25µg/mL	CD41	Platelet EV	Beckam Coulter
IgG1-PECy7 (clone MOPC-21)	0.25µg/mL	Isotype Control	-	Beckam Coulter
Anti-CD235a/b-PECy5 (clone HIR2)	0.05µg/mL	CD235a/b	RBC EV	Biolegend
IgG2b-PECy5 (clone MPC-11)	0.05µg/mL	Isotype Control	-	Biolegend
Plasma Analysis				
Anti-PLAP-PE (NDOG2)	0.7µg/mL	PLAP	STBEV	In-house antibody
Anti-eNOS-APC (clone REA451)	0.8µg/mL	eNOS	-	Miltenyi Biotech
Anti-CD41-PEvio770	0.33µg/mL	CD41	Platelet EV	Miltenyi Biotech
Anti-CD235a/b-PEvio770	0.11µg/mL	CD235a/b	RBC EV	Miltenyi Biotech
Anti-HLA Class I-PEvio770	2.2mg/mL	HLA Class I	Leukocyte EV	Miltenyi Biotech

Table 2. 1. Antibody details for flow cytometry analysis.

2.8.4. HLA-ABC- PEvio770 antibody titration using THP-1 cells

THP-1 cells were used for HLA-ABC-PEvio770 (Miltenyi Biotech) antibody titration prior to analysis by flow cytometry. Cell samples were stained with different concentrations of either HLA-ABC-PEvio770 or REA-PEvio770 (isotype control) antibodies as described in **Section 2.8.1**.

2.8.5. Placenta perfusion derived STBMV treatment with THP-1 cells

50 μg of pooled STBMV from three NP or PE mothers were pre-stained with 2 μM of Bio-maleimide (previously filtered using a 0.2 μm nanosep centrifugal device VWR) for 30 minutes at room temperature in the dark. Stained STBMV were transferred to ultra-clear centrifuge tubes (Beckman Coulter) and adjusted with filtered PBS. This was followed by centrifugation at 10,000 x g at 4°C in a Beckman L8-80M ultracentrifuge for 35 minutes, and the resultant pellet was re-suspended in 100 μL of filtered PBS.

Stained STBMV were pass through the NTA to confirm size and determine the particle number. Further dilution in serum-free media was set in order to accomplish same particle number among NP and PE STBMV (~1 x 10^8 particles/mL). STBMV were incubated with differentiated THP-1 cells for 2 and 6 hours. THP-1 cells with no STBMV were used as a control for each time point.

After incubation, cells were carefully washed three times with warm PBS and 100 μL Trypsin-EDTA was added to each well to lift up the cells. Cells were moved into a 1 mL Eppendorf tube and made up with serum-free medium and centrifuged at 1,300 rpm for 5 minutes. The supernatant was discarded, and the pellet was resuspended in warm PBS and washed again by centrifugation. Pellet was incubated with 1 mL of 2% v/v PFA for 15 minutes at room temperature. Again, cells were washed with warm PBS by centrifugation. Finally, the pellet was resuspended in 300 μL of filtered PBS. Samples were stored at 4 ºC until applied to the flow cytometer. 5,000 events were recorded per sample using FACSDiva software (BD Biosciences).

2.9. BCA protein estimation assay

Fresh STBMV and STBEX were assayed for their protein content using the Bicinchoninic acid (BCA) protein assay kit (Pierce). Briefly, BSA stock (2 mg/mL) was diluted in filtered PBS to give rise to standards' protein concentrations: 2, 1, 0.5, 0.25, 0.125 and 0.0625 mg/mL. STBEV samples were also diluted in filtered PBS if protein concentration was above the standards' regression line. 12.5 µL of standard and samples were added to a 96-well plate, followed by 100 µL of BCA solution and copper II sulphate solution (previously combined in a 50:1 ratio, respectively). Proteins can reduce Cu^{+2} into Cu^{+1} in an alkaline solution (the biuret reaction), resulting in a purple colour formation by BCA. The plate was covered in foil and put in the shaker for 5 minutes prior to 30 minutes incubation at 37°C. Reactions were measured in duplicate and absorbance was read at 562 nm using a FluoStar OPTIMA (BMG) plate reader. This method was also used when determining the protein concentration of cell lysates.

2.10. SDS-PAGE and Western blotting

Samples were diluted with Laemmli 4x reducing buffer (Bio-Rad, UK), boiled at 96°C and centrifuged at 13,000 RPM for 1 minute before loading. Protein ladder (Bio-Rad) and samples were loaded onto SDS-PAGE Novex ™ 4-12% gel (ThermoFisher) and run at 150 V for 1 hour using an electrophoresis apparatus. To activate the immuno-blot PVDF membrane (Bio-Rad), this was immersed in methanol (5 minutes), followed by tap water (10 minutes) and finally, in Anode 2 (5 minutes). Whatman filter paper pieces were immersed in the following buffers: Anode buffer 1 (4 pieces), Anode buffer 2 (2 pieces), and Cathode buffer (3 pieces). For electrophoretic transfer of the proteins onto the PVDF membrane: Anode buffer 1 immersed filter paper, Anode buffer 2 soaked filter paper, Novex ™ gel, PVDF membrane and Cathode soaked filter paper, were placed onto the transfer machine (arranged as stated from the bottom up) and ran for 1 hour at 50V. Membranes were blocked using 5% w/v dried milk dissolved in tris-buffered saline with 0.05% Tween 20 (TBS-T) and probed overnight at 4°C with primary antibodies in blocking solution. Immunoblots were then washed and incubated with secondary antibody conjugated to horseradish peroxidase (HRP) (New England Biolabs) for 1 hour at room temperature. Membranes were finally washed with PBS-T on a shaker before to 1-minute incubation with HRP substrate enhanced luminescence

(ThermoFisher) and exposed for of 1-5 minutes to Hyperfilm ECL (GE Health Care). Buffers formulation details are shown in **Table 2.2** and antibody details used for Western blotting experiments are shown in **Table 2.3.**

Buffers	Composition
Laemmli 4X reducing buffer **pH 6.8**	90% 4 x Laemmli buffer 10% 2-beta-mercaptoethanol
Laemmli 4X non-reducing buffer	90% 4 x Laemmli buffer
Anode buffer 1 **pH 10.4**	300mM Tris base (36.34 g/L) 20% methanol (20 mL/L) dH$_2$O to 1 L
Anode buffer 2 **pH 10.4**	25mM Tris base (3.0 g/L) 20% methanol (20 mL/L) dH$_2$O to 1 L
Cathode buffer **pH 9.4**	25mM Tris base (3.0 g/L) 40nM 6-aminocaproic acid (5.2 g/L) 20% methanol (20 mL/L) dH$_2$O to 1 L
TBS X10 **pH 8.0**	NaCl (87.6 g) Tris base (12.1 g) 700 mL of dH$_2$O Add HCl to get pH 8.0
TBS-T **pH 8.0**	TBS X10 (100 mL) 0.1% Tween-20 (1 mL) 900 mL of dH$_2$O
5% Milk TBS-T	5 g or 5mL in 100 mL TBS-T

Table 2. 2. The composition of buffers used for Western blotting.

Antibodies	Conc./Dilution	Antigen	Specificity	Source
Anti-eNOS (NOS3-A9)	0.6 µg/mL	eNOS	-	Santa Cruz
Anti-iNOS (clone 2D2-B2)	1 µg/mL	iNOS	-	R&D
Anti-PLAP (NDOG2)	0.6 µg/mL	PLAP	STBEV	In-house antibody
Anti-Alix	1/1000	Alix	Exosomes	Cell Signalling
Anti-Syntenin	1/1000	Syntenin	Exosomes	Abcam
Anti-CD9	1/200	CD9	Exosomes	Santa Cruz
Polyclonal goat-anti-mouse/rabbit immunoglobulin HRP	1/2000	Mouse/rabbit immunoglobulins	-	Cell Signalling
Anti-PDGFRβ	0.1 µg/ml	PDGFRβ	Brain/ placental pericytes	R&D
Anti-Neuropilin 1	1/250	Neuropilin 1		Abcam
Anti-Endoglin	1/400	Endoglin		Novus Biologicals
Anti-VEGFR2	1/250	VEGR2		Abcam

Table 2. 3. Antibody details used for Western blotting.

2.11. Co-immunoprecipitation using magnetic Dynabeads

3.25×10^7 Dynabead (Life Technologies) stocks were initially vortexed for 30 seconds and then washed with PBS-T buffer containing 1% BSA using a magnetic particle concentrator (Dynal MPC-S, ThermoFisher). 50 µl of Dynbeads were separately coated with a saturated concentration of 6 µg/mL of the following antibodies: (a) anti-eNOS (NOS3 A9; Santa Cruz Biotech); (b) eNOS isotype control (IgG2a Clone DAK-GO5, Dako); (c) anti-PLAP antibody (NDOG2); and (d) PLAP isotype control (IgG1 Clone MOPC-21, BioLegend) in an overnight incubation in slow rotation at 4°C. STBMV or STBEX pooled from 4 NP patients (1 mg/mL) were incubated with anti-human Fc receptor blocking reagent (10 µL, Miltenyi Biotec) for 10 min at 4°C to block any non-specific antigen binding (same pool was used at each experiment). Next, antibody-coated Dynabeads were washed thoroughly prior to overnight incubation at 4°C in slow rotation with 25 µg of protein from either STBMV or STBEX pools in 1 mL filtered PBS. After incubation, the supernatant was collected from samples and stored at 4°C, and bound-Dynabeads were subsequently washed with PBS. STBMV or STBEX bound to antibody-coated Dynabeads were placed in magnet and separated using 30 µl of 1 X reducing buffer and centrifuged at 13,000 rpm for 1 minute prior to being processed for Western blotting (**Section 2.10**).

To calculate STBMV or STBEX particle number bound to antibody-coated Dynabeads, STBMV or STBEX without Dynabeads at 25 µg (Total) and nominal unbound STBMV or STBEX fraction left in the supernatant (eNOS and PLAP negative) were analysed using NTA. The percentage of STBMV or STBEX bound eNOS or PLAP was calculated as follows:

eNOS and PLAP positive = (([Total]-(eNOS and PLAP negative)) / [Total]) x 100

2.12. NOS dimerization

To investigate eNOS dimerization in STBMV and STBEX, low-temperature SDS-PAGE was performed, as previously described (Cai, Khoo & Channon 2005). HUVEC were grown in a T75 flask (see **Section 2.5.4**) until 90% confluency was reached. Cell lysates were obtained by re-suspending pellet with cold RIPA buffer (150mM NaCl, 50mM Tris pH 8, 0.1% SDS, 1% Triton X100, 0.5% sodium deoxycholate) subjected

to BCA protein assay and stored at -20°C. NP samples at 15 μg and HUVEC cell lysate were loaded under non-reducing conditions onto a 4-12% SDS PAGE Novex ™ gel, and run at 5 mA overnight at 4°C. Separated proteins were then transferred onto PVDF membranes and blocked with 3% w/v BSA dissolved in TBST for 1 hour prior to overnight incubation at 4°C with 0.6 μg/mL of anti-eNOS (NOS3-A; Santa Cruz) diluted in blocking buffer. Protein visualisation was then performed on Western blot as described in **Section 2.6**.

2.13. NOS activity assay

NOS activity by STBMV and STBEX was determined using an ultrasensitive colourimetric NOS assay kit, which converts all NO metabolites to nitrite using nitrate reductase (NB78 & NB70; Oxford Biomedical Research). We followed the manufacturer's protocol and depicted nitrite accumulation as NOS activity (i.e. production of NO). STBMV and STBEX pools of 4 NP patients (different pools used at each experiment) were first incubated in different concentrations (0, 10, 25, 50 and 100 μg). NOS activity was also measured in NP pools with or without specific eNOS inhibitor, N-Nitroarginine methyl ester (L-NAME) (1mmol/L; Sigma-Aldrich) and the highly specific iNOS inhibitor, 1400W (2μmol/L; Enzo Life Sciences) (Garvey et al. 1997). Inhibitors were incubated with STBMV and STBEX at 25 μg for 1 hour prior to analysis. NP and PE STBMV and STBEX (25 μg) isolated from each individual patient were also analysed for NOS activity. Reactions were measured three times in triplicate and absorbance was read at 540nm using a FluoStar OPTIMA (BMG) plate reader.

2.14. Quantitative real-time PCR

2.14.1. RNA isolation and quality control

Cells were washed with warm PBS prior to RNA extraction using the RNeasy micro kit (Qiagen). Samples were then treated with DNA-free removal kit (ThermoFisher) to remove any contaminating DNA. Briefly, rDNase I and 10X DNase I buffer were incubated with samples at 37°C for 30 minutes. To inactivate both the DNase I and the RNase, samples were incubated with DNase inactivation reagent for 2 minutes before centrifugation at 10,000 x g and subsequently chilled on ice. RNA protein concentration was measured using a NanoDrop ND-1000 Spectrophotometer

(ThermoFisher) at 260 nm absorbance, and RNA purity was assessed using the 260:280 nm absorbance ratio. All samples were diluted with RNase-free water accordingly to obtain a standard 100 ng/µL concentration.

2.14.2. RNA to cDNA conversion synthesis

RNA samples were converted into cDNA using High capacity RNA-cDNA conversion kit (Applied Biosystems). Each RNA sample (9 µL), 2X RT Enzyme (1µL) and 20X Enzyme (10 µL) were mixed and gently vortexed prior to reverse transcription reaction. The reaction was incubated at 37°C for 1 hour, followed by 95°C heating for 5 minutes to stop the reaction, and subsequently, hold at 4°C prior to use.

2.14.3. Quantitative real-time PCR for cytokines expression

The nucleotide Basic Local Alignment Search Tool and Primer-BLAST were used to design and analyse the specificity of the primer sequences.

Gene Targets	Forward Primer	Reverse Primer	Size of Amplicons
18S	ATGGCCGTTCTTAGTTGGTG	CGCTGAGCCAGTCAGTGTAG	75-150 bp
TNF- α	AGCCCATGTTGTAGCAAACC	TGAGGTACAGGCCCTCTGAT	75-150 bp
TGF- β	GTACCTGAACCCGTGTTGCT	GTATCGCCAGGAATTGTTGC	75-150 bp
IL-10	TTACCTGGAGGAGGTGATGC	GGCCTTGCTCTTGTTTTCAC	75-150 bp
IL-12	AACTTGCAGCTGAAGCCATT	GACCTGAACGCAGAATGTCA	75-150 bp
IL-8	CTGTGTGAAGGTGCAGTTTTG	GTGTTGGCGCAGTGTGGTC	75-150 bp
IL-6	GAAAGCAGCAAAGAGGCACT	TTTCACCAGGCAAGTCTCCT	75-150 bp

Table 2. 4. Primer sequences used for qPCR.

qPCR reaction consisted of 3.7 µL of RNase-free water, 5 µL Power SYBR Green Master mix (Applied Biosystems), 75 nM of forwards and reversed primers and 100 ng template cDNA in a final reaction volume using a 7900HT Fast Real-Time PCR system (Applied Biosystems). The qPCR reaction initially included 2 minutes

incubation at 50°C, followed by 10 minutes incubation at 95°C. The template was amplified for 40 cycles under the following conditions: 15 seconds incubation at 95°C and 1-minute incubation at 60°C. Homogenous housekeeping gene 18S was included at each qPCR reaction to normalise the rest of the samples against the expression of human 18S rRNA. Data were acquired using the RQ Manager Version 1.2.1 (Applied Biosystems). Ct (cycle threshold) values from each target gene expression were calculated, and Relative Quantification (RQ) values for each cytokine target gene was subsequently calculated using the formula: RQ= $2^{-\Delta\Delta Ct}$. Assays were completed twice in triplicate.

2.15. Multiplex cytokine analysis

Supernatant samples collected in previous experiments (described in **Section 2.7.3.2** and **Section 2.7.4.2**) were analysed using a Milliplex ® MAP Human cytokine/chemokine magnetic bead panel kit (HCYTOMAG-60K; EMD Millipore). Briefly, in a 96-well plate, 25 µL of assay buffer was added to each well. This was subsequent to the addition of 25 µL of standard, controls and supernatant samples. The 96-well plate was washed with assay buffer, and 25 µL of target antibodies were incubated with the beads for 1 hour at room temperature. 25 µL of Streptavidin-Phycoerythrin conjugate was then added to each well and incubated for 30 minutes in the dark at room temperature. After washing step with assay buffer, 150 µL of sheath fluid was added to each well, and the plate was read using the Luminex Magpix instrument.

2.16. Mass Spectrometry

PLVPex samples were characterised for digestion and mass spectrometry run at the Target Discovery Institute (University of Oxford, Oxford). MASCOT and PROGENESIS analyses were also included in the services' quotation. Muhammad Furqan Bari, the collaborator, affiliated to the Department of Pathology at Dow University of Health Sciences (Karachi, Pakistan), performed general bioinformatic analysis and graphs shown in Chapter 5's results.

2.17. Statistical Analysis

The data were analysed using GraphPad 5 software. Normality testing was performed using the Kolmogorov-Smirnov test and visual observation. The data were analysed using paired, or unpaired t-test with Welch's correction or one-way ANOVA, and data were presented as mean ± SEM.

CHAPTER 3

Characterisation of endothelial nitric oxide synthase on STBEV isolated from normal and PE placentae

3. Characterisation of endothelial nitric oxide synthase on STBEV isolated from normal and PE pregnancies

3.1. Abstract

PE, a pregnancy-specific hypertensive disorder, is associated with augmented systemic vascular resistance. The PE placentae have lower levels of eNOS, and hence, reduced NO. STBEV, including microvesicles (STBMV) and exosomes (STBEX), transport signals the STB to the mother. We hypothesised that STBEV bound eNOS (STBEV-eNOS), are secreted into mother's bloodstream. Dual-lobe *ex vivo* placental perfusion and serial centrifugation were used to isolate STBEV from PE (n=8) and NP (n=11). Plasma samples of gestational age-matched PE and NP (n=6) were used to enrich STBMV. STBEV expressed PLAP, that corroborated placental origin. STBEV co-expressed eNOS, but not iNOS, as established using Western blot, flow cytometry and immuno-depletion. STBEV-eNOS produced NO, which was inhibited by L-NAME significantly (eNOS inhibitor, *p<0.05), but not by 1400W (iNOS inhibitor). STBEV-eNOS catalytic activity was verified by visualising eNOS dimerisation. STBEV-eNOS was significantly more in uterine vein compared to peripheral blood, indicating placental origin. STBEV isolated from PE perfused placentae had lower levels of STBEV-eNOS (STBMV; *p<0.05) and overall reduced NO activity (STBMV, ns; STBEX, *p<0.05) compared to NP. Circulating plasma STBMV from PE women had fewer STBEV-eNOS expression in comparison to NP women (**p<0.01). This is the first report of functional eNOS expressed on STBEV from NP and PE placentae, as well as in plasma. The reduced STBEV-eNOS NO production seen in PE may contribute to the decreased NO bioavailability in this disorder.

3.2. Background

Soon after conception, dramatic changes in the maternal cardiovascular system takes place through gestation to increase blood flow and nutrient delivery to the fetal-placental unit. From 6 to 8 weeks gestation onwards, maternal blood volume expands by 45% to reach an approximate 5 litres at 32 weeks gestation (Pritchard 1965). Both total vascular resistance and systemic arterial pressure decline, while cardiac output and plasma volume rise (Robson *et al.* 1989). Therefore, a combination of adaptive processes to maintain healthy blood pressure in pregnancy include peripheral vasodilation, increased vascular compliance and growth of the uteroplacental circulation. These changes modify significantly in PE, a pregnancy-specific syndrome affecting up to 10% of all pregnancies worldwide (World Health Organization 2011), which is characterised by maternal new-onset hypertension and proteinuria or organ dysfunction, developing after 20 weeks of gestation (Roberts & Redman 1993). PE is believed to originate as a result of poor placentation causing endothelial dysfunction, angiogenic imbalance and subsequent hypertension, glomerular lesions, and hepatic failure (Redman *et al.* 1999).

NO is an effective vasodilator, thought to have important effects on gestational endothelial function (Sladek *et al.* 1997). Studies examining circulating levels of NO in PE have yielded conflicting results (Shah & Khalil 2015). Plasma from women with PE elicits decreased endothelium-dependent vasodilatation in isolated vessels. NO availability may be reduced (Ashworth *et al.* 1998; English *et al.* 2013; Hayman *et al.* 2001), due to oxidative stress, vascular endothelial growth factor deficit or endogenous inhibitors such as asymmetric dimethylarginine (ADMA) (Khalil *et al.* 2015). Most of the circulating NO is thought to originate from maternal endothelium; however, the placenta may also contribute.

In the placenta, NOS is expressed in the STB (STB), villous endothelium and macrophages, particularly the eNOS isoform (Conrad *et al.* 1993; Myatt *et al.* 1993b; Buttery *et al.* 1994). The multinucleated STB layer, lining the chorionic villi, is the border between the maternal and fetal vascular systems (Redman 1991), and could supply circulating NO. Here, we if STB derived NOS could be transferred to the mother via STBEV, with the potential of systemically modulating maternal vascular response.

STBEV encompasses two subgroups: microvesicles (STBMV), which are secreted directly from the plasma membrane as a result of cell activation or death, and exosomes (STBEX), which are released by exocytosis from multi-vesicular bodies of the endosome (Tannetta et al. 2013a). Consequently, STBEV could allow communication between the mother and the fetus via contents of their cargo (Tong & Chamley 2015).

3.3. Hypothesis

We hypothesised whether STBEV might carry eNOS as part of their load. Thus, we investigated whether eNOS was present on STBEV derived from NP and PE perfused placental lobules, as well as circulating STBMV from NP and PE peripheral vein blood (PB) and uterine vein blood (UV). We wanted to evaluate whether STBEV bound eNOS (STBEV-eNOS) was active and generate NO and whether its expression and activity was altered in PE.

3.4. Aims

The research objectives described in this chapter were as follows:

- To isolate and characterise STBEV from human placenta
- To identify whether eNOS or iNOS are expressed on the placenta and STBEV isolated from NP and PE placentae
- To support the idea that STBMV expressing eNOS are derived from the placenta by examining NOS expression on STBMV isolated from peripheral and uterine blood
- To affirm eNOS is co-expressed with STBEV specific marker, PLAP
- To corroborate whether the eNOS isoform is active and can be inhibited
- To explore whether eNOS-bound STBEV activity is different between STBEV isolated from NP and PE placentas

3.5. Materials & Methods

3.5.1. Human Subjects

Clinical characteristics of normal pregnancy (NP) or PE pregnancy (PE) mothers are described in **Table 3.1**. Plasma samples used to isolate STBMV were matched for gestational age.

Patient Characteristics	Placental STBEV		Plasma STBEV		p value
	NP (n=11)	PE (n=8)	NP (n=6)	PE (n=6)	
Age (years)	35.5 ± 1.5	32.4 ± 1.6	31.8 ± 2.4	30.7 ± 2.4	ns, ns
Gestation Age (weeks)	39+4 ± 3	34+4 ± 5.7	35+5 ± 0.3	36+6 ± 0.5	****, ns
Mean no. of pregnancies	2.1 ± 0.4	0.5 ± 0.2	0.5 ± 0.2	1.3 ± 0.6	**, ns
Body Mass Index (kg/m²)	32 ± 2	32.1 ± 3.5	21.8 ± 0.8	28.2 ± 2.3	ns,
Max. Proteinuria PCR (mg/mmol)	5.5 ± 0.2	204.1 ± 77.4	0 ± 0	360.2 ± 162.8	***, ††
Max. Systolic pressure (mm Hg)	127.3 ± 4.3	168.8 ± 8.3	116.7 ± 2.6	161.2 ± 7.7	***, ††
Max. Diastolic pressure (mm Hg)	75.5 ± 2.4	104.4 ± 4	71 ± 3.3	111.5 ± 5.1	****, ††
New-born weight (g)	3999.2 ±152.5	1985 ± 205.1	3641 ± 198	2769 ± 189	****, †
Smoking History	3/11	3/8	0/6	0/6	-

Table 3. 1. Clinical data of human subjects. Data presented as Mean ± SEM, significant difference was presented as $p<0.05$ (*, †), $p<0.01$ (**, ††), $p<0.001$ (***), $p<0.0001$ (****) or non-significant (ns). Statistical evaluation between NP and PE's placental STBEV was shown as * and plasma STBEV is shown as †.

3.6.   Results

3.6.1. Isolated STBEV confirmed the microvesicular and exosomal phenotype

We first re-confirmed the expected microvesicular and exosomal phenotypes and sizes for STBEV (**Figure 3.1**). Western blotting of STBEV demonstrated enrichment of the STBEV marker, PLAP, relative to placental lysates. This enrichment was notable in both STBMV and STBEX (**Figure 3.1A**). STBEX expressed the exosomal markers Alix, Syntenin and CD9 (**Figure 3.1A**). Freshly isolated STBEV were analysed on NTA for size and particle number profiles. STBMV showed a broad size distribution with a modal size of 323.2 ± 7.1 nm, while STBEX showed a narrower size distribution with a modal size of 189.3 ± 9.7 nm (**Figure 3.1B**). Representative Transmission Electron Micrographs (TEM) confirmed the NTA and Western blot data showing STBMV was enriched for different EV >200nm, while STBEX contained a more homogenous population with a range of 30 to 200 nm EV (**Figure 3.1C**). Our data confirmed that STBMV and STBEX had been successfully isolated.
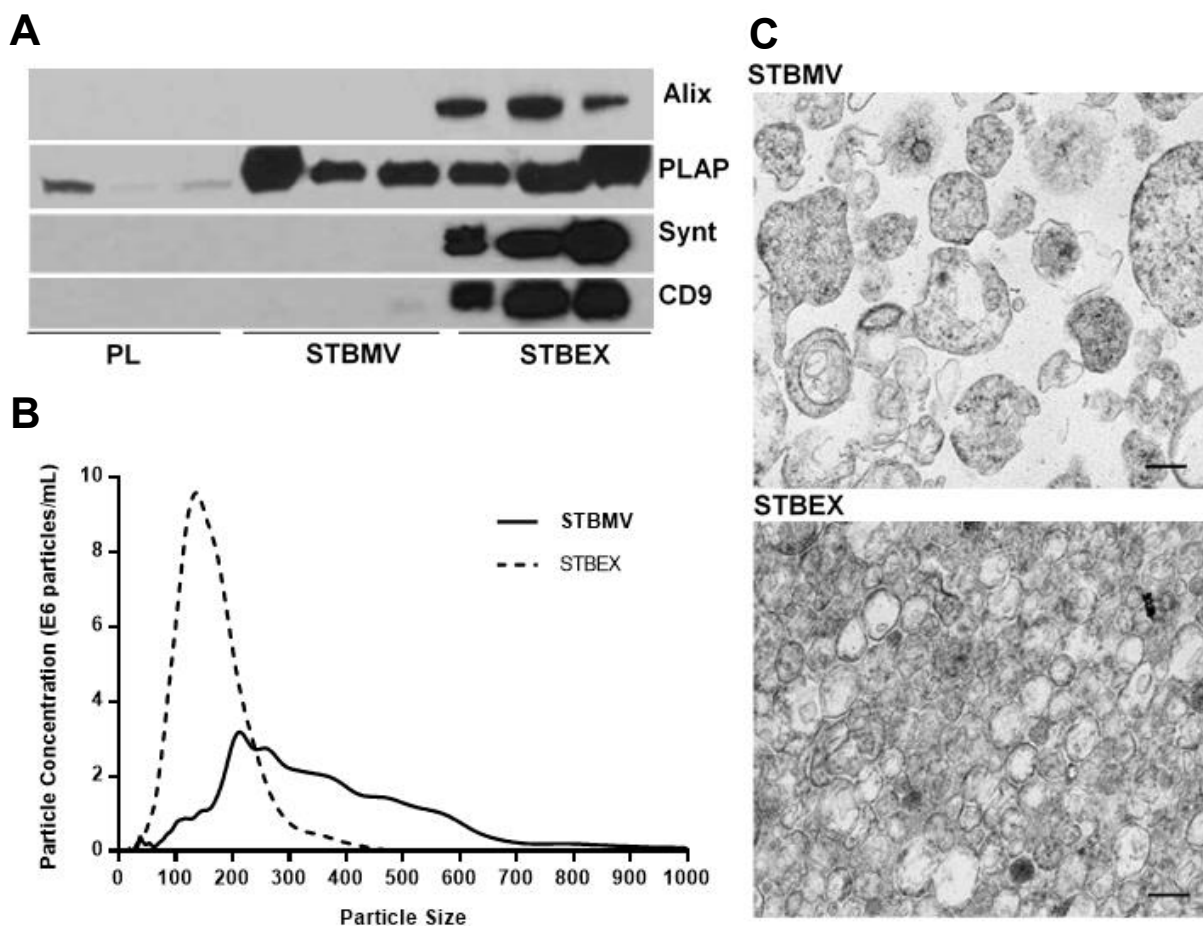
Figure 3. 1. Characterisation of NP derived STBMV and STBEX. A, Representative Immunoblot showing enrichment of STBEV marker, PLAP (60 kDa) on NP placenta lysate (PL), STBMV and TSBEX; and enrichment of exosomal markers Alix (96 KDa), Syntenin (60 kDa) and CD9 (24 kDa) on STBEX. B, Representative NTA size vs particle number distribution profiles of STBMV (323.2 ± 7 nm) and STBEX (189.3 ± 9.7 nm). C, Representative Transmission Electron Micrographs (TEM) of STBMV and STBEX. Scale bars represent 200 nm.

3.6.2. STB and STB-derived EV express eNOS but then not iNOS

Immunohistochemistry revealed that eNOS expression primarily localized in the STB cell layer of NP samples compared to negative staining of isotype control IgG2a (n=3, **Figure 3.2A**), consistent with previous results **X**. Likewise, eNOS expression was also found in the placental lysate samples (PL). We were also able to ascertain eNOS expression in STBMV and STBEX isolated from NP (**Figure 3.2B**) and from PE (**Figure 3.2C**) placentae by Western blotting. Positive control used for eNOS was HUVEC lysate.

Interestingly, iNOS expression was not detectable in the STB cell layer (n=3, **Figure 3.2D**). Moreover, no expression of iNOS in placental lysates, STBMV or STBEX from NP (**Figure 3.2E**) or PE placentas (**Figure 3.2F**) was observed (n=3). However, expression of iNOS was seen in the positive control, murine macrophage cell line (RAW 264.7 cell lysate; Santa Cruz Biotech), reassuring the antibody's quality (**Figure 3.2E and F**). Positive PLAP expression indicated that the EV were derived from STB. iNOS absence led us to perform mass spectrometry.
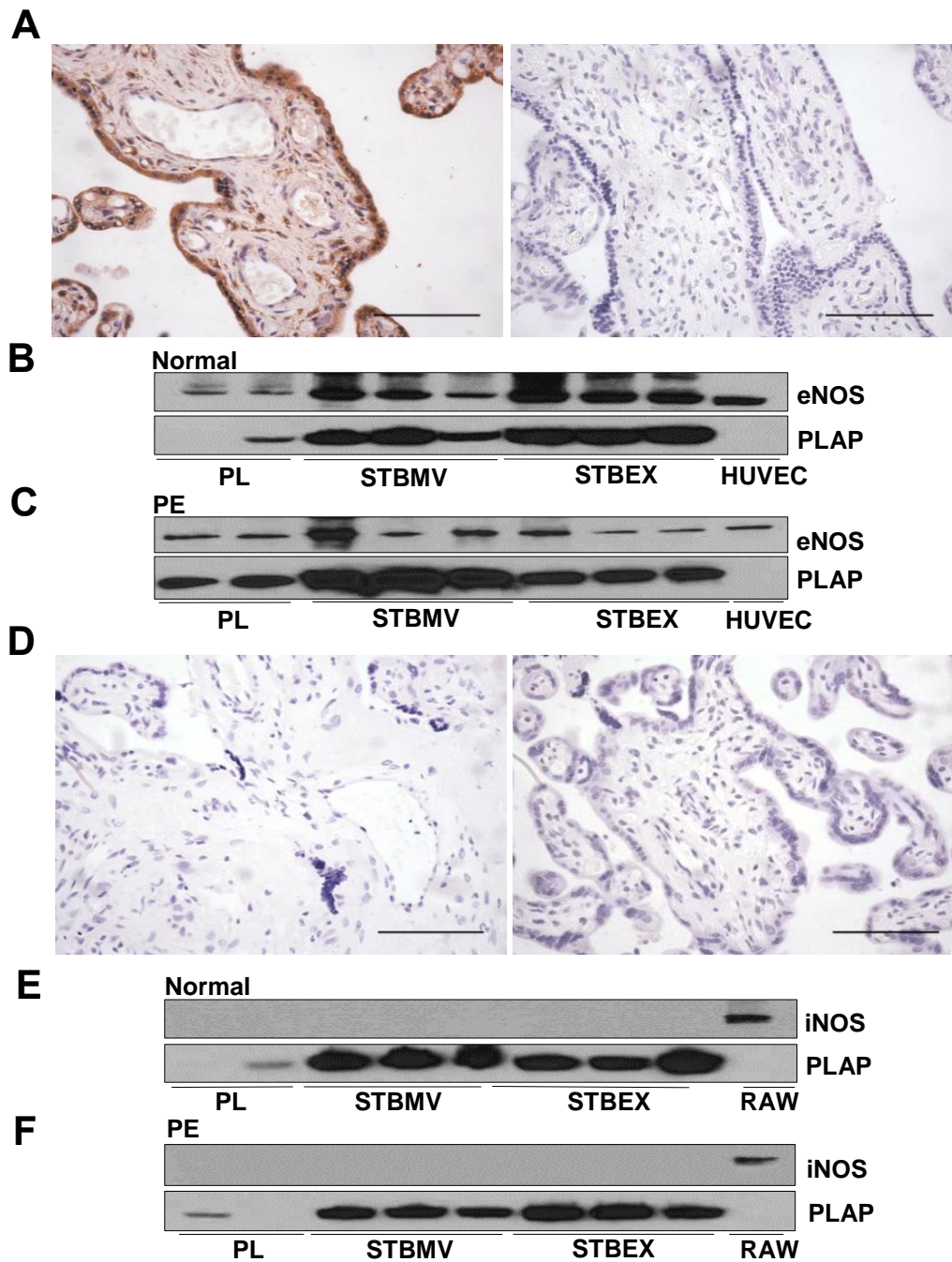
Figure 3. 2. Immunohistochemical staining of NP placenta tissue and Western blot of placenta lysate (PL) of NP and PE placentae, STBMV and STBEX (n=3). A, Placental tissue showing eNOS staining (brown; left) on STB layer and IgG2a negative staining (right). Immunoblot showing eNOS (140 kDa) and PLAP (60 kDa) expression in the placental lysate, STBMV and STBEX derivative from NP (B) and PE (C) similar to the expression of positive control, HUVEC. D, Placental tissue demonstrating lack of iNOS staining (left) and isotype control IgG1 negative staining (right). Western blotting showing no expression for iNOS (131 kDa) yet the positive control, RAW, is expressed as well as PLAP (60 kDa) in PL, STBMV and STBEX derived from NP (E) and PE (F). Scale bar set at 100mm.

To confirm our results, we also assessed a mass spectrometry analysis that was previously performed on PL, STBMV and STBEX from NP (n=6) and PE (n=8) patients (*Tannetta et. al. Unpublished),* and individually interrogated it for the presence of NOS isoforms (see **Table 3.2**). The mass spectrometry was able to reveal eNOS, but not iNOS, at the protein level. We, therefore, focussed on STBEV expressing eNOS.

NOS Isoforms	Samples	Peptide count	Unique peptides	Confidence Score
eNOS	PL	3	3	159.32
	STBMV	42	38	2476.18
	STBEX	46	39	2757.70
nNOS	PL	/	/	/
	STBMV	3	0	102.73
	STBEX	2	0	73.98
iNOS	PL	/	/	/
	STBMV	/	/	/
	STBEX	/	/	/

Table 3. 2. Nitric oxide synthase (NOS) isoforms identified by mass spectrometry. Analysis included placental lysate (PL), microvesicles (STBMV) and exosomes (STBEX) samples from 8 NP and 6 PE patients. eNOS, endothelial nitric oxide synthase; nNOS, neuronal nitric oxide synthase; iNOS, inducible nitric oxide synthase.

3.6.3. Flow cytometry optimisation of eNOS antibody using HUVEC

First, eNOS antibody was titrated using eNOS-expressing cell line, HUVEC, in order to stain the STBMV. Cultured HUVEC (**Section 2.10.3**) were stained with eNOS antibody or its corresponding isotype control at different volumes (5 µL, 2.5 µL, 1.25 µL, 0.625 µL).

Data was collected using FACSDiva software (BD Biosciences) and plotted using side-scattered light (SSC) and forward-scattered light (FSC) plot (**Figure. 3.3A**), where SSC is an estimation of intracellular granularity, and FCS is an estimation of cell size. Unstained cells were used to assist with the voltage set up and to draw a 'gate' of interest after recording 10,000 events at a low flow rate. Our gate of interest was used as a numerical or graphical boundary to define the characteristics of cells for further analysis. Stained samples were passed through the flow cytometer, and events were recorded. Histograms plots were used to study fluorescent intensity of labelled cells. Each isotope control sample was used to draw the '1% cut-off gate' (**Figure 3.3B**) in order to determine the best corresponding eNOS-APC antibody concentration staining (**Figure 3.3C**).

We concluded that volume 1.25 µL (0.4 µg/mL) of eNOS-APC antibody was optimal for STBMV analysis.
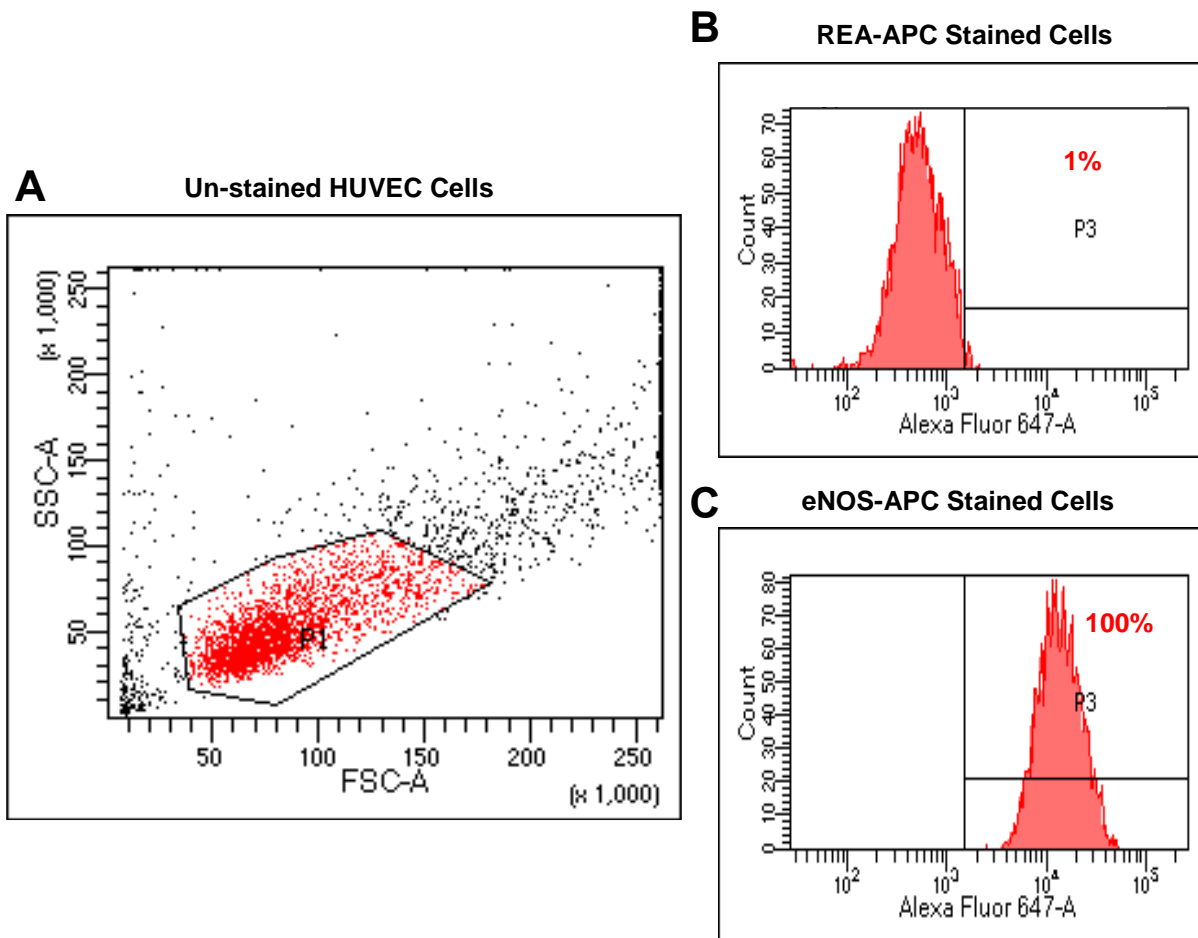
Figure 3. 3. Representative flow cytometric gating strategy used for eNOS-APC antibody titration analysis using HUVEC. A, Side-scattered vs forward-scattered plot showing a gate with chosen HUVEC population (red). B, Histogram event count vs APC channel plot from HUVEC population gate showing cells stained with isotype control REA-APC. The 1% cut-off gate was set using a vertical line. C, eNOS-APC stained HUVEC population events depicted from the set-gate histogram (B).

3.6.4. Flow cytometric analysis of perfused placenta derived STBMV reveal co-expression of eNOS and PLAP

STBMV derived from NP and PE placental perfusions were analysed by flow cytometry for eNOS and PLAP co-expression (n=6). Using the corresponding FMO controls and the appropiate gate strategy (**Figure 3.4**), we found double eNOS and PLAP positivity of 30.3% ± 8.5% in NP derived STBMV and 6.3% ± 3.3% in PE-derived STBMV (*p<0.05; **Figure 3.5**).
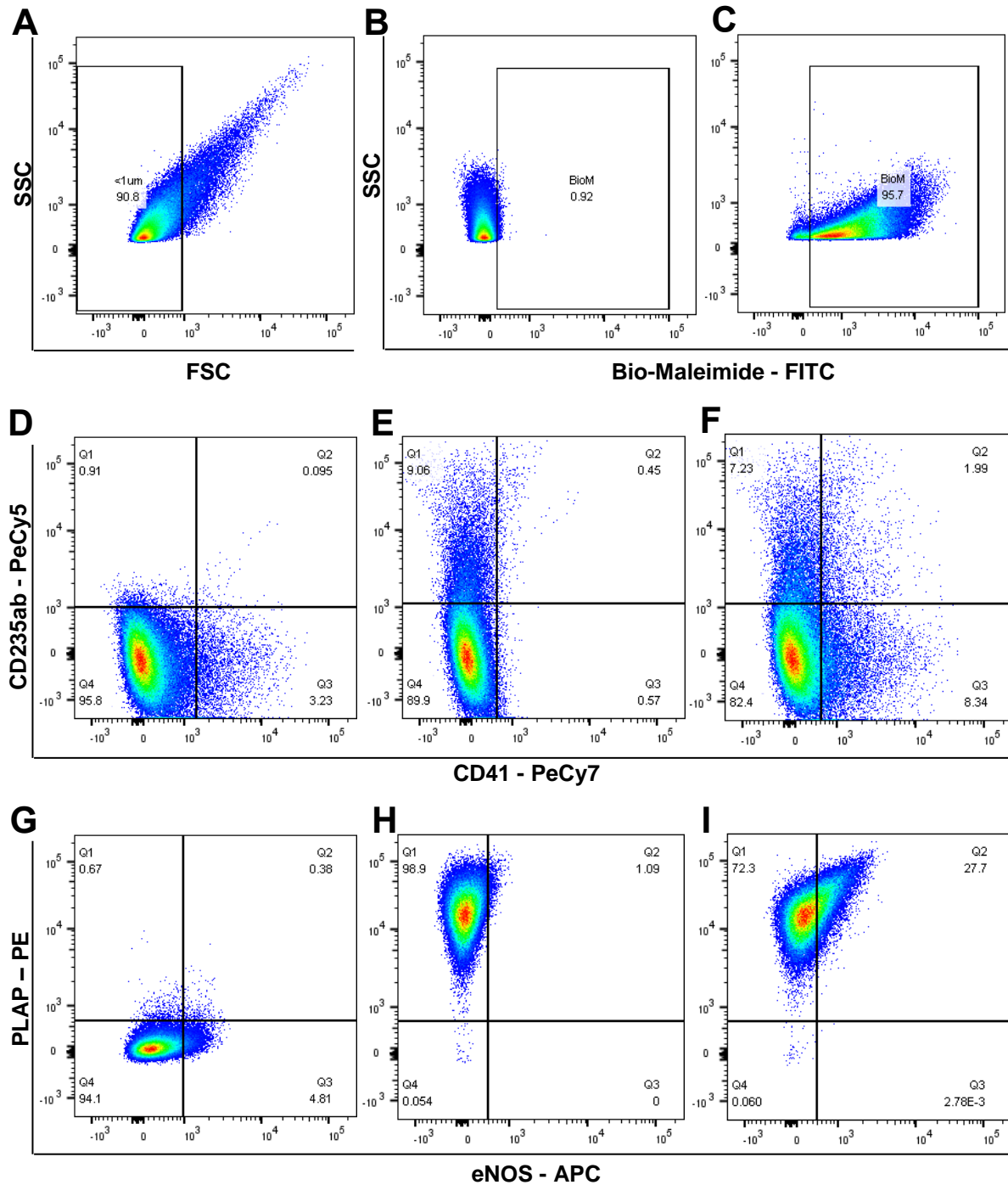
Figure 3. 4. Flow cytometric multicolour gating strategy used to investigate STBMV. A, EV presented on Forward Scatter (FSC) versus Side Scatter (SSC) plot with 1µm cut-off gate., ≤ 1µm EV presented on SSC vs Bio-maleimide (BioM) plot and stained with: (B) BioMaleimie fluorochrome minus one (FMO) gate was used to draw 1 % cut-off gate for BioM positive; and (C), BioM (EV marker) to contain BioM positive EV population. CD235a/b-PECy5 vs CD41-PECy7 plots showing ≤ 1µm BioM positive EV stained with: (D) CD235a/b FMO to draw 1% cut-off gate for CD235a/b positive (Q1 and Q2); (E) CD41 FMO to draw the 1% cut-off gate for CD41 positive (Q2 and Q3) as well as (F) CD235a/b and CD41 markers of contaminants to disregard EV positive

for CD235ab and CD41 (Q1, Q2 and Q3). ≤ 1µm BioM positive and negative for CD235a/b and CD41 EV displayed in a PLAP-PE vs eNOS-APC plot stained with: (G) PLAP FMO to draw 1% cut-off gate for PLAP positive (Q1 and Q2); (H) eNOS FMO to draw 1% cut-off gate for eNOS positive (Q2 and Q3) and (I) PLAP (STBMV maker) and eNOS (antigen of interest marker) to display the final analysis of double positivity for PLAP and eNOS (Q2).
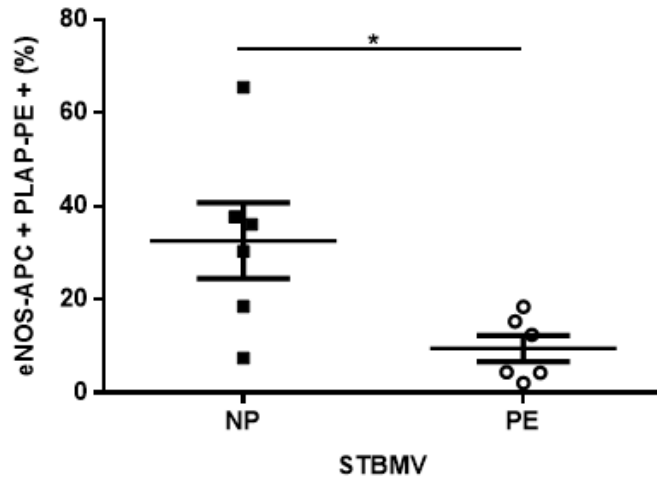
Figure 3. 5. Flow cytometry analysis of *ex vivo* STBMV derived from NP and PE placentae (n=6). STBMV bound eNOS expression was significantly lower in PE compared to NP (*p<0.05).

3.6.5. Flow cytometric analysis of peripheral and uterine blood vein derived STBMV-eNOS confirmed they originate from the placenta

Circulating STBMV were also analysed by flow cytometry in plasma prepared from paired PB and UV samples (n=8), using an appropriate gate strategy (**Figure 3.6**). PLAP and eNOS double positive events per mL were significantly higher in UV (49,686 ± 28,162) compared to PB (7,723 ± 2,823) plasma samples, confirming that STBMV-bound eNOS originated from the placenta (**p<0.01; **Figure 3.7A**). Correspondingly, STBMV bound eNOS was measured in gestational age-matched plasma PB samples from NP and PE patients (n=6). After the omission of EV derived from other cells rather than the STB, the results showed a significant reduction in PLAP and eNOS double positive events per mL of plasma-derived STBMV from PE (12,798 ± 7,121) in comparison to NP (62,838 ± 15,246; **p<0.01; **Figure 3.7B**). Thus, our data propose that there is less plasma-derived STBMV bound eNOS in PE compared to NP.
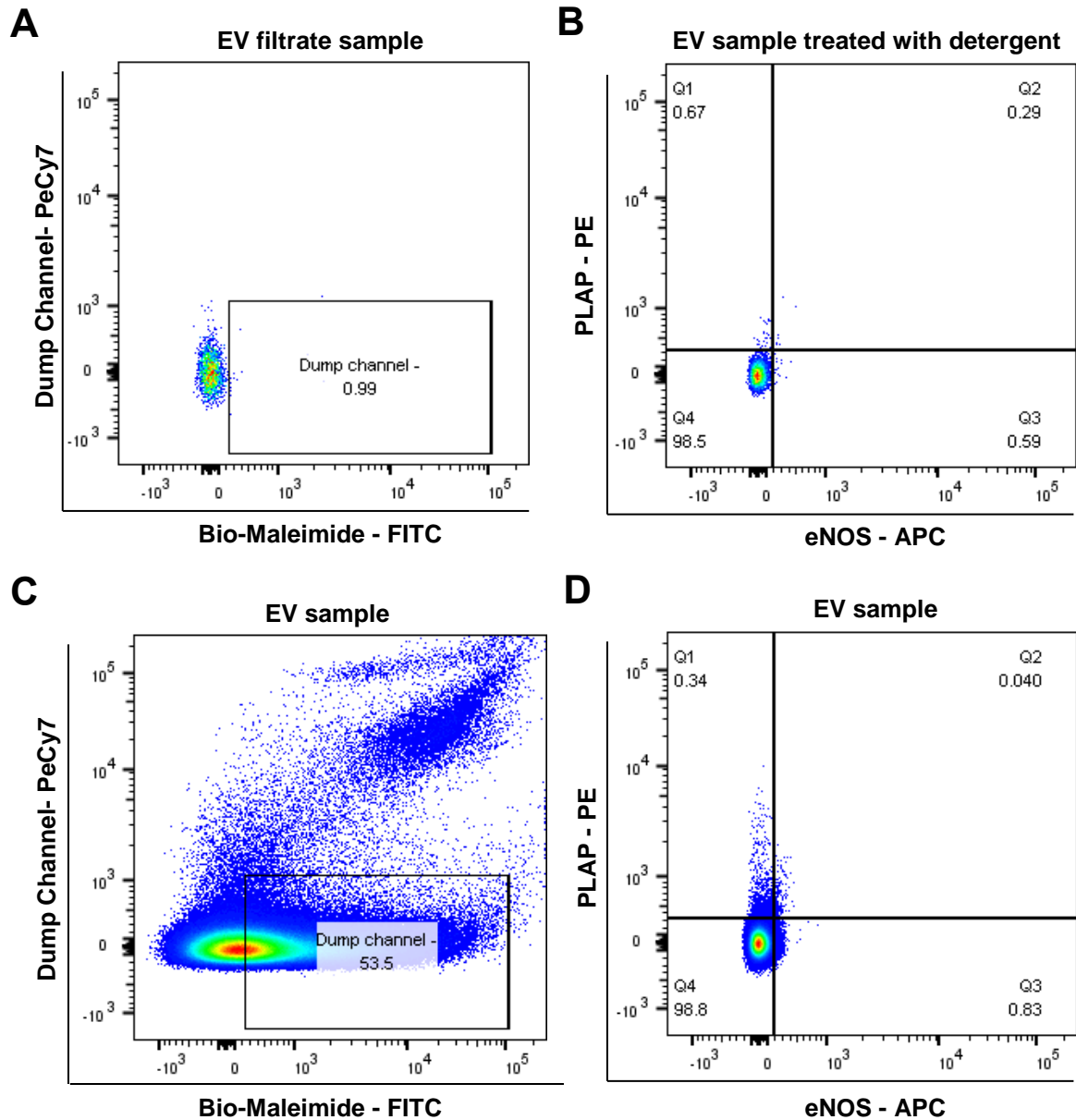
Figure 3. 6. Flow cytometric multicolour gating strategy used to analyse STBMV derived from platelet-free plasma (PFP). A, The filtrate sample (pass through) used to draw the 'Dump Channel' gate at 1% cut off using Dump channel-PeCy7 vs Bio-Maleimide-FITC dot plot. Dump Channel includes contaminant markers such as CD231a/b, CD41, HLA-ABC and HLA Class II; all conjugated with PEvio770 labelling. B, Dump channel negative and Biomaleimide positive STBMV stained sample was treated with detergent to draw the 1% cut off gates for PLAP+ (Q1 and Q2) and eNOS+ (Q2 and Q3), using PLAP-PE vs eNOS-APC dot plot graph. C, Positive population of 'Dump Channel' gate from the STBMV sample was excluded (outside dump channel gate), while 'Dump Channel' negative EV and Bio-Maleimide positive EV was included (inside dump channel gate). D, STBMV population double positive for PLAP and eNOS (Q2) showed circulating plasma-derived STBMV co-expressed PLAP and eNOS. STBMV event number per mL was calculated.

94
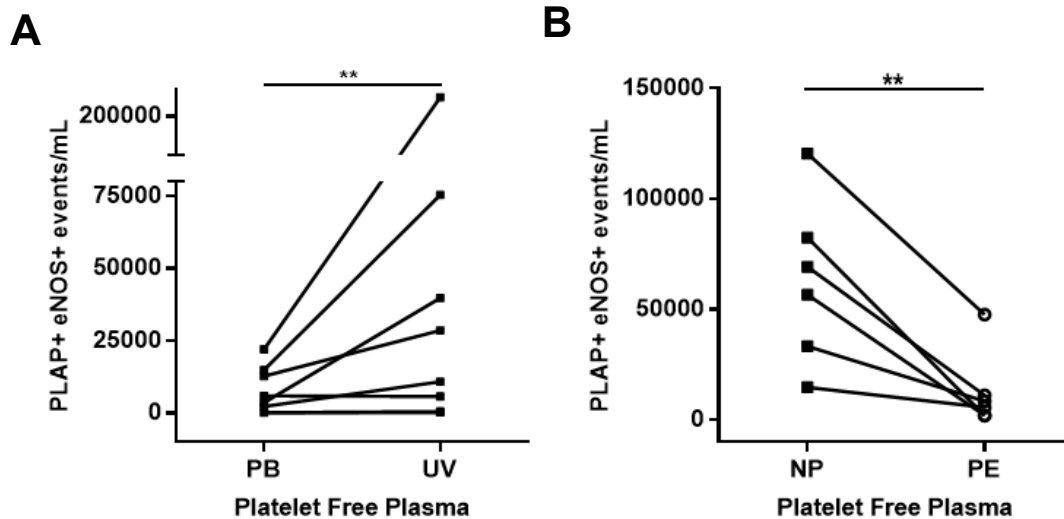
Figure 3. 7. Flow cytometry analysis of circulating STBMV. STBMV derived from paired PB and UV plasma (n=8). A, Double positive eNOS and PLAP events per mL were higher in UV compared to PB (**p<0.01). Flow cytometry analysis of circulating *in vivo* STBEV derived from matched PB plasma of NP and PE patients (n=6). B, PLAP and eNOS double positive STBMV events per mL were significantly lower in plasma from PE compared to NP (**p<0.01).

3.6.6. eNOS and PLAP are present on the same STBEV population

Immunodepletion was used to confirm STBMV and STBEX co-expression of eNOS and PLAP and exclude potential aggregation.

For Western blot analysis, we used anti-eNOS coated beads to immunoprecipitate eNOS positive STBEV, which were interrogated for the presence of PLAP. We also used anti-PLAP coated beads to immunoprecipitate PLAP positive STBEV, which were then interrogated for eNOS. **Figure 3.8A** reveals that anti-eNOS coated magnetic beads could pull-out (PO) STBMV bound eNOS, which was positive for PLAP. The experiment using anti-PLAP coated beads revealed similar results, confirming that both species were bound on the same population of STBMV (Figure 3.4A). Interestingly, PLAP PO yielded a greater signal for eNOS compared to the eNOS PO, which may indicate that some eNOS is intravesicular. To assess the relative quantities of STBMV bound eNOS or PLAP, we used NTA analysis. The total concentration of STBMV was compared to the supernatant samples from the bead depletion experiments. This data displayed that STBMV were 35.5% ± 4.2% of eNOS positivity and 64.3% ± 0.4% of PLAP positivity (n=3; **Figure 3.8B**), whilst IgG2a control was positive for 11.3% ± 5.7%, and IgG1 control was positive for 11.4% ± 3.4% (n=3; **Figure 3.8C**). Analysis of the STBEX fraction (**Figure 3.8D**) revealed similar results. STBEX bound eNOS comprised 36.7% ± 6.6% whilst STBEX bound PLAP was 39.2% ± 5.8% of the initial preparation (n=3; **Figure 3.8E**), whilst IgG2a control was positive for 10.8% ± 4.5%, and IgG1 control was positive for 15.1% ± 5.8% (n=3; **Figure 3.8F**).
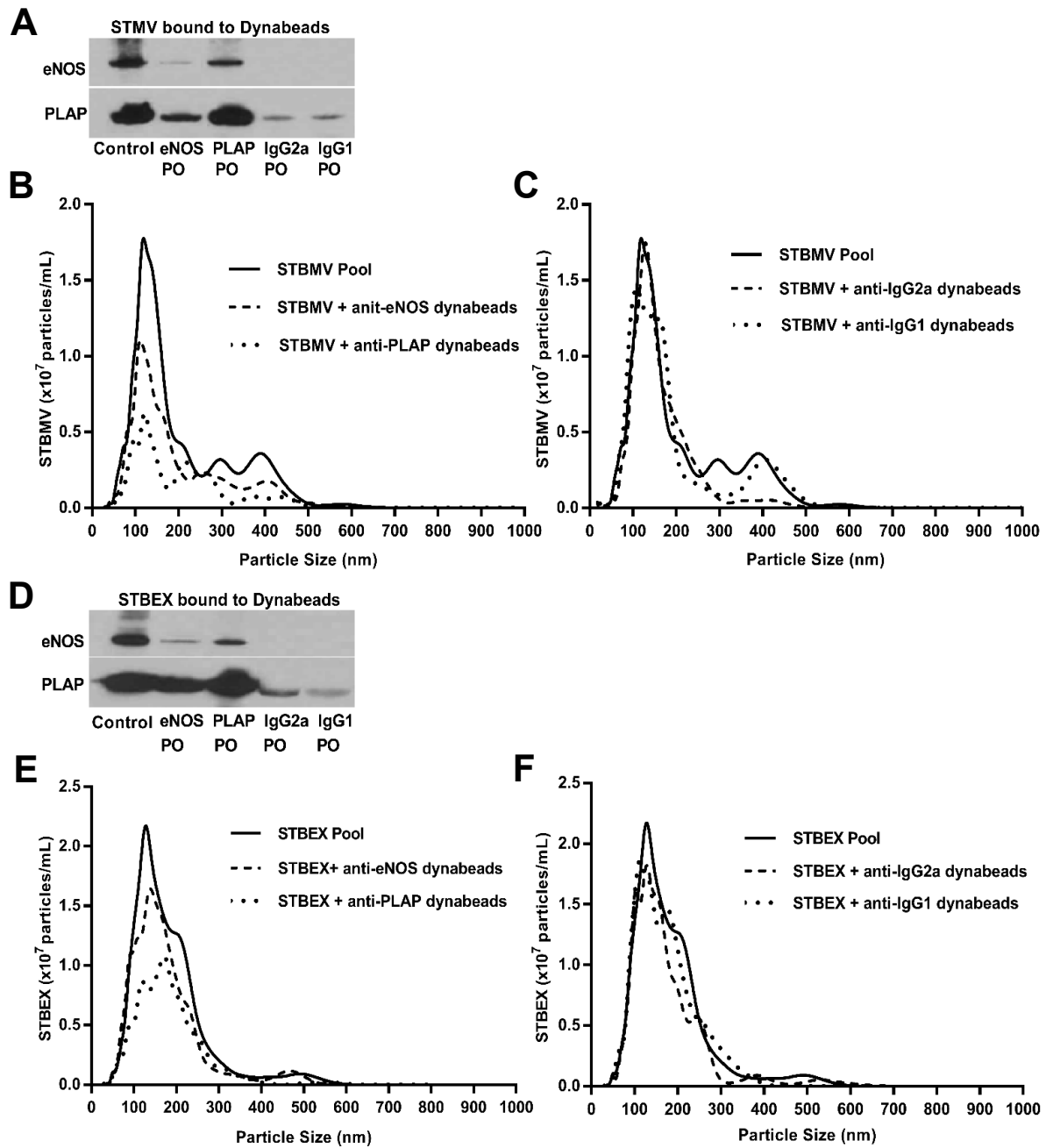
Figure 3. 8. Immunobead depletion and NTA profiles of STBMV and STBEX pools from NP (n=3). A, Representative immunoblot showing eNOS and PLAP co-expression on STBMV pool (Total) as well as STBMV pulled-out (PO) with anti-eNOS Dynabeads, anti-PLAP Dynabeads, anti-IgG2a Dynabeads (isotype control for eNOS) and anti-IgG1 Dynabeads (PLAP isotype positive control). B, Illustrative NTA size vs number profiles of STBMV pool (solid line), the supernatant from post incubation with anti-eNOS Dynabeads (dashed line), and anti-PLAP Dynabeads (dotted line). C, STBMV pool (solid line), the supernatant of post-incubation with anti-IgG2a Dynabeads (dashed line) and anti-IgG1 Dynabeads (dotted line). D, Illustrative immunoblot showing eNOS and PLAP co-expression on STBEX pool (Total), and STBEX PO with anti-eNOS, anti-PLAP, anti-IgG2a and anti-IgG1 Dynabeads. E,

Representative NTA size vs number profiles of STBEX pool alone (solid line), the supernatant from post incubation with anti-eNOS (dashed line) and anti-PLAP (dotted line) Dynabeads. F, STBEX pool (solid line), the supernatant of post-incubation with anti-IgG2a (dashed line) and anti-IgG1 (dotted line) Dynabeads.

3.6.7. Placenta-derived STBEV-eNOS are active and synthesize NO

Separated eNOS dimer (260 kDa) and monomer (140 kDa) were visualized on Western Blot from derived STBMV and STBEX (n=3; **Figure 3.9A**), suggesting STBMV and STBEX bound eNOS are functional. This was demonstrated by increasing dose-dependent NOS activity in terms of nitrite accumulation per hour (n=6 pooled STBEV, ***$p<0.001$ **Figure 3.9B**) as the protein concentration of STBMV and STBEX rose. Nitrite accumulation was decreased in STBMV and STBEX incubated with L-NAME (an eNOS inhibitor) compared to control group (STBMV *$p<0.05$, STBEX * $p<0.05$, n=3; **Figure 3.9C**). STBMV and STBEX treated with iNOS inhibitor 1400W (2µM) showed no change compared to control (both ns, n=3; **Figure 3.9D**).
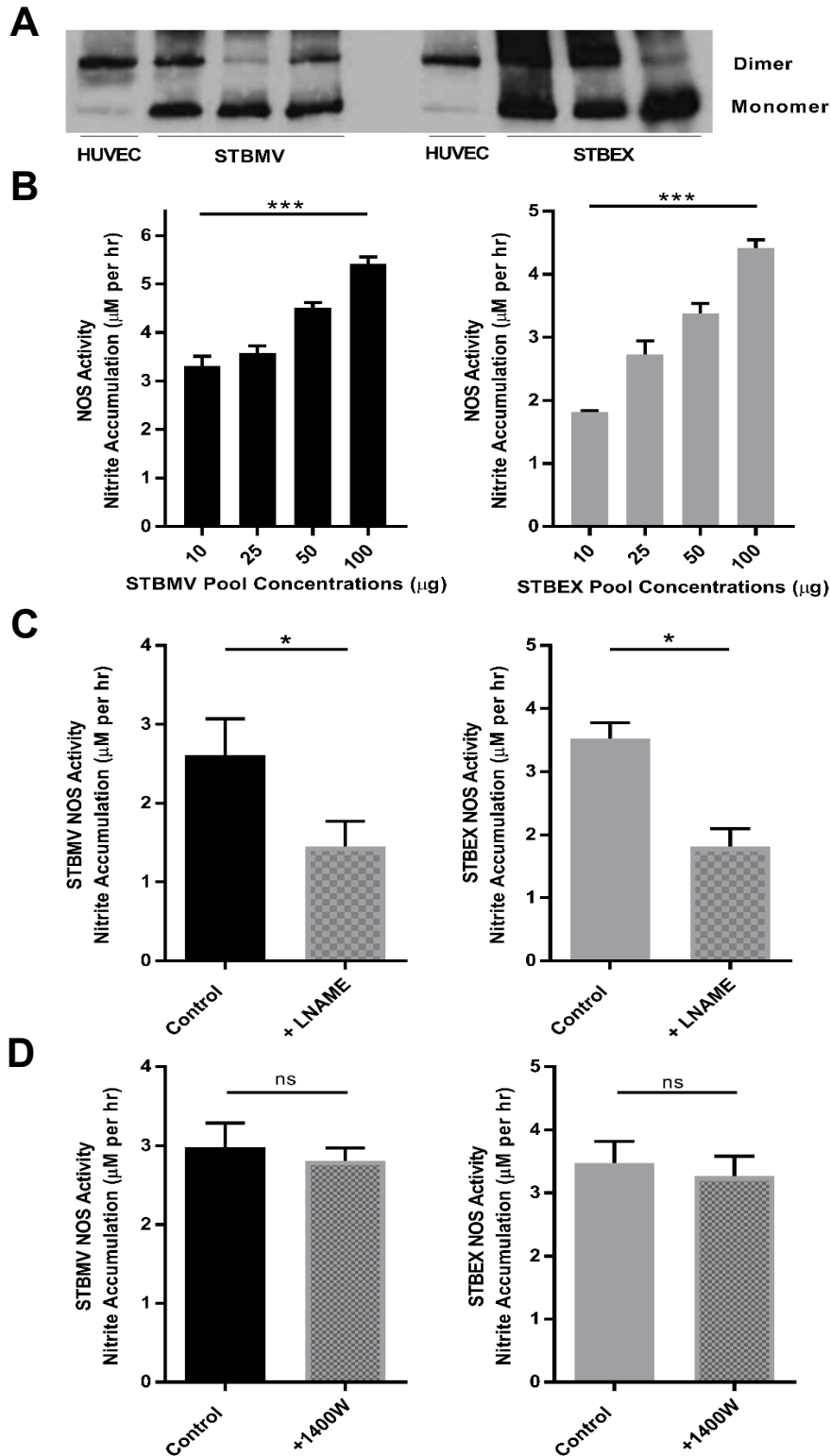
Figure 3. 9. STBMV and STBEX express functional eNOS and produce NO. A, Dimerization of STBEV immunoblot image showing eNOS dimer (260 kDa), and eNOS monomer (140 kDa) expressed in HUVEC, STBMV and STBEX (n=3). B, STBMV (***p<0.001) and STBEX (***p<0.001) pools showed NO synthesis in a dose-dependent conduct (n=6). C, Pool of 25 μg of STBMV and STBEX pre-incubated for

1 hour with 1mM of L-NAME, NOS inhibitor, displayed significant reductions in NO production compared to controls (both *p<0.05; n=3). D, the 25µg pool of STBMV and STBEX pre-incubated for 1 hour with 2 µM 1400W, iNOS specific inhibitor, showed no changes in NO production compared to controls (both ns; n=3).

3.6.8. Placental-derived STBEV-eNOS have reduced activity in PE

NOS activity was assessed between STBEV from NP (n=11) and PE (n=8). For STBMV, the data showed no statistical difference in NOS activity (**Figure 3.7A**). PE patients with a gestational age most comparable to the control group showed a reduction in NOS activity (>34 weeks PE vs <40 weeks NP *p<0.05; **Figure 3.7B**). The earlier gestational ages are more difficult to interpret because of the lack of age-matched NP controls.

The STBEX showed an overall reduction in NOS activity (*p<0.05, **Figure 3.7C**) which persisted when we compared PE samples from patients with a gestational age most similar to controls (**Figure 3.7D**).

Overall, STBMV and STBEX demonstrate a general reduction in NOS activity in PE compared to control.
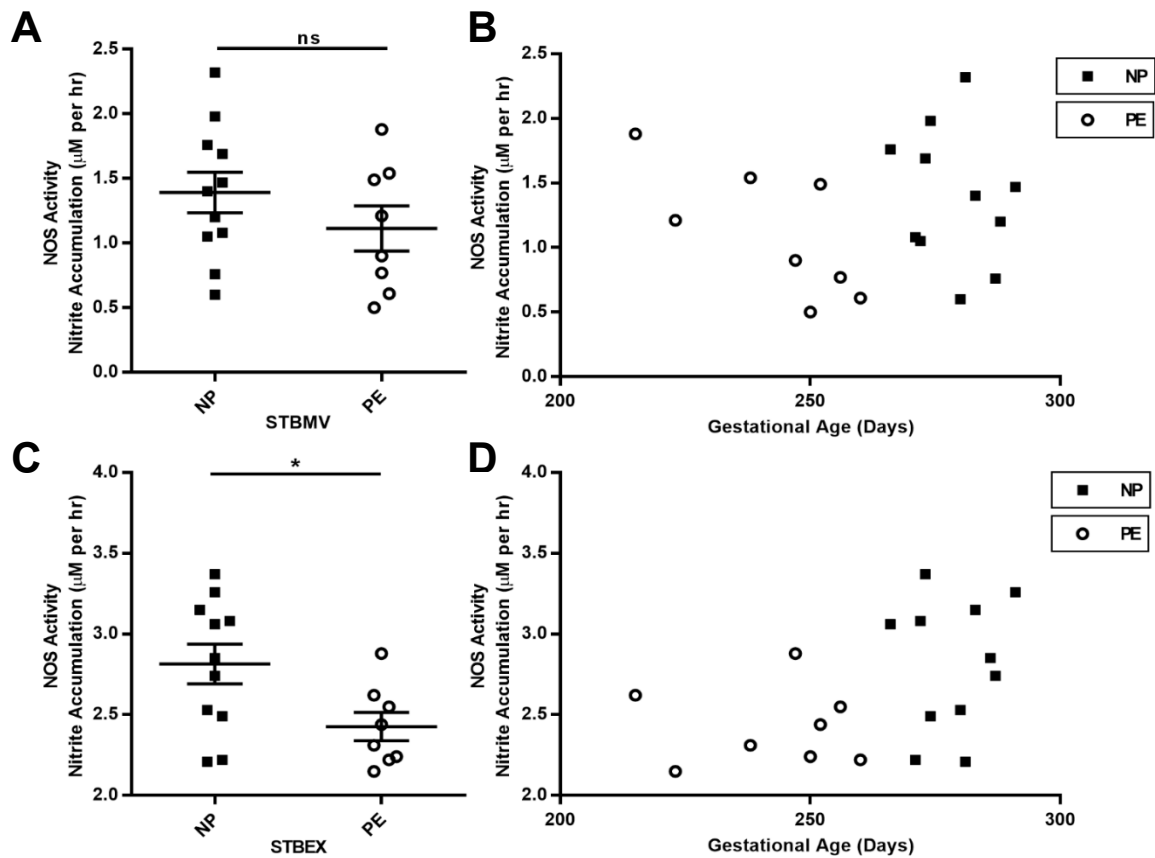
Figure 3. 10. NOS activity of STBMV and STBEX isolated from perfused NP and PE placentae (n=11 and n=8, correspondingly). STBMV (A) from PE patients showed a no overall reduction in NO production compare to NP (ns, p=0.2416). Examination of the same data incorporating the gestational age data of the samples, (B) shows a decrease in NO production in samples closest in gestational age to controls (PE>34 weeks vs NP <40 weeks; *p<0.05). STBEX (C) from PE presented a significant reduction in NO production compared to NP (*p<0.05). This decrease was sustained in samples closest in gestational age to controls (D).

3.7. Discussion

We show, for the first time, that eNOS co-expressed with PLAP on both STBMV and STBEX gathered from *ex vivo* NP placentas via immunoblotting, flow cytometry and paramagnetic immunoprecipitation. *Ex vivo* derived STBMV and STBEX bound eNOS exists as a dimer, a feature required for NOS catalytic activity, and confirmed these are capable of producing NO which can be inhibited by L-NAME (an eNOS inhibitor). In addition, flow cytometry evaluation of circulating STBMV from matched PB, and UV plasma revealed that STBMV-eNOS were released by STB and circulated in the maternal blood.

NO plays an essential role in mediating normal pregnancy vasodilation, while defective endothelial NO synthesis and bioavailability have been associated with PE (Burke *et al.* 2016; Seligman *et al.* 1994). Our study reveals *ex vivo* derived STBMV and STBEX isolated from placental perfused lobes to have a reduced amount of eNOS activity in PE in comparison to healthy controls. Similarly, *in vivo* derived plasma STBMV analysed by flow cytometry showed less STBMV bound eNOS expression in PE to compare to the control group.

We were not able to detect iNOS in healthy STB and its derived EV either by immunoblotting or mass spectrometry. The expression as well as activity of iNOS has been described by few groups in STB and placenta lysate (Conrad & Davis 1995; Kakui *et al.* 2003). Most recently, iNOS differences between normal and hypertensive pregnancies have been reported (Schiessl *et al.* 2005, 2006), whilst others have reported the absence of iNOS in the STB (Lyall 2003; Zarlingo *et al.* 1997), resulting in a debatable relationship between iNOS and PE. Nevertheless, we believe eNOS is the principal isoform bound to STBMV and STBEX.

Several studies corroborate our findings. Smarason *et al.* (Smárason *et al.* 1993b) were first to report that STB microvillous membranes were shed in increased amounts in PE (Knight *et al.* 1998), and that these products affected the growth of endothelial cells *in vitro*. Cockell *et al.* (Cockell *et al.* 1997) reported that perfusion of subcutaneous arteries with STB microvillous membranes resulted in an alteration in the endothelium-dependent behaviour. Most recently, it has been reported that

isolated EV from plasma exert various effects on endothelial and trophoblast cells according to the physiological/pathological state of the pregnant woman (Shomer *et al.* 2013; VanWijk *et al.* 2002). A reduction in the expression and the activity of eNOS bound to circulating non-pregnant EV has also been associated with cardiovascular diseases (Horn *et al.* 2012). Kao *et al.* showed a significant increase in superoxide levels and impaired endothelial dysfunction in rat uterine arteries incubated with human PE plasma (Kao *et al.* 2016). Interestingly, L-NAME abolished this uterine artery vasodilation in both NP- and PE-derived plasma treated vessels, suggesting this effect was due to eNOS. Their findings support our data although "circulating factors" rather than STBEV were described.

We hypothesize that decreased systemic eNOS in the form of circulating STBEV-eNOS may contribute to the reduced bioavailability of NO seen in PE, potentially distressing vascular functions. We are not sure whether eNOS is given to endothelial cells or whether NO is synthesized adjacent to the endothelial cell. Although we show decreased NO production by STBEV-eNOS, there may also be a few other factors that can contribute to the reduction of NO bioavailability. This could include (i) variation in NOS gene expression and activity; (ii) lower substrate L-arginine levels for NOS; (iii) elevated inhibitors of NOS such as ADMA; or (iv) increased breakdown of NO due to ROS *per se* (Myatt & Webster 2009). In addition, altered levels of vasodilatory stimuli such as VEGF or PlGF (Maynard *et al.* 2008), and/or endogenous vasoconstrictors such as endothelin binding to endothelial receptors (ET_B) (Bourque *et al.* 2011), can also dampen NO production in PE.

Diminished NO release would not necessarily be limited by the shedding of fewer STBEV-eNOS from the placenta. Other cell types expressing eNOS, such as platelets (O'Kane *et al.* 2008), endothelial progenitor cells (Heiss *et al.* 2015), or circulating EV derived from endothelial and RBC (Horn *et al.* 2013), may contribute to overall NO bioavailability. In addition, we should take into account factors that impinge eNOS activity and vascular functionality of NO (reviewed in Osol *et al.* 2017). For example, in the absence of BH_4 and L-arginine or due to oxidative stress, the oxygenase domain of eNOS monomer generates superoxide anions instead of NO, a condition referred to as eNOS uncoupling (d'Uscio 2011; Michel & Vanhoutte 2010). Moreover, eNOS

translocation from the plasma membrane to intracellular compartments is essential for eNOS activation and subsequent NO biosynthesis. Coupling of endothelial plasma membrane receptor systems in the caveolar structure, and how eNOS trafficking relates to specific protein-protein interactions are indispensable for eNOS multi-site phosphorylation and signalling (Ramadoss *et al.* 2013). Changes in shear stress and/or its mechanical transduction by endothelium can also contribute to defective NO signalling.

Our study has few limitations. Exosomes cannot be readily examined by routine flow cytometry because of their size. Thus, we were unable to measure STBEX bound eNOS expression as we carried out with STBMV. Nevertheless, we detected decreased levels of NO production in PE-derived STBEX. It is complicated to age match the placental tissue in a disease condition, which characteristically occurs earlier in pregnancy. We have endeavoured to mitigate this by using placentae from patients who developed PE later in pregnancy, but this restriction is common to all PE studies. In addition, despite measuring STBMV bound eNOS expression in plasma, attempts to regulate NO production from plasma-derived STBMV and STBEX were unsuccessful due to the NOS assay limits of detection.

CHAPTER 4

Effect of STBEV isolated from normal and preeclamptic placentae on THP-1 macrophages

4. Effect of STBEV isolated from normal and preeclamptic placentae on THP-1 macrophages

4.1. Abstract

Extracellular vesicles (EV), now recognised as essential carriers of proteins, lipids and nucleic acids, play an important role in feto-maternal communication. Syncytiotrophoblast derived EV (STBEV) from normal pregnancy (NP), comprising microvesicles (STBMV) and exosomes (STBEX), have previously been shown to interact with circulating monocytes/B cells, and induce cytokine release. Early-onset preeclampsia (EOPE) is associated with an exacerbated inflammatory response, yet there is little data regarding late-onset PE (LOPE) and immune function. Here, using a macrophage/monocyte cell line THP-1, we investigated the inflammatory potential of STBEV, isolated from LOPE (n=6) and NP (n=6) placentae via dual-lobe ex-vivo placental perfusion and differential centrifugation. Isolated NP and LOPE STBMV and STBEX were applied to THP-1 macrophages. THP-1 cells bound and internalised both STBMV and STBEX isolated from NP and LOPE placentae, as revealed by flow cytometry, confocal microscopy and ELISA. STBEV-treated THP-1 cells were examined for cytokine gene expression by RT-qPCR and the cell culture media examined for secreted cytokines/chemokines. As has been previously reported, NP STBMV upregulated the transcriptional expression of TNF-α, IL-6, IL-12, IL-8 and TGF-β, while NP STBEX upregulated TNF-α, IL-6, IL-10 and IL-8 gene expression. In contrast, both LOPE STBMV and STBEX did not induce significant inflammatory responses by differentiated THP-1 cells. This decreased effect of LOPE STBEV was echoed in cytokine/chemokine release. LOPE STBEV incubated with THP-1 cells released significantly less macrophage inflammatory protein 1α (MIP-1α) compared to NP STBEV (1,987 pg/mL, LOPE STBMV vs 20,942 pg/ml, NP STBMV: p<0.0001; 2,181 pg/mL, LOPE STBEX vs 6,816 pg/ml, NP STBEX: p=0.0186). This was also true for IL-8 (7,221 pg/mL, LOPE STBMV vs 16,638 pg/ml, NP STBMV; 8,132 pg/mL, LOPE STBEX vs 13,833 pg/ml, NP STBEX: both p<0.0001). Our results appear to suggest that STBEV from LOPE placentae do not have a major immune-modulatory effect on macrophages. In contrast, NP STBEV caused THP-1 cells to release pro-inflammatory cytokines as has been previously described. Our study demonstrates that trophoblast extracellular vesicles from LOPE dampen immune functions of THP-

1 macrophages. This may suggest an alternative mechanism to the pro-inflammatory environment characteristic in LOPE.

4.2. Background

PE is commonly divided into two subgroups: early-onset PE (EOPE), occurring ≤ 34-weeks gestation, and late-onset PE (LOPE), occurring ≥ 34-weeks gestation. The pathophysiology of EOPE is widely believed to lie with the placenta (Redman, Sargent & Staff 2014). Immune imbalance (Vince et al. 1995; Von-Dadelszen et al. 2002; Zhang et al. 2013) and cardiovascular dysfunction (Vaddamani et al. 2017; Valensise et al. 2001) are highly significant in EOPE patients. The late-onset disease is more controversial, with some believing the disease as having a placental origin (Huppertz 2008; Redman, Sargent & Staff 2014) whilst others suggesting the disease is more likely to be a maternal stress response due to an incompatibility between the metabolic demands of the growing fetus close to term and maternal supply (Thilaganathan 2017; Valensise et al. 2008; Von-Dadelszen, Laura A. Magee & Roberts 2003).

STBEV have immunomodulatory roles during pregnancy (Tannetta et al. 2017a; Tong, Abrahams & Chamley 2018; Tong & Chamley 2015). Unseparated STBEV, isolated from NP perfused placentae, have been shown to bind to B cells and monocytes, and enhance the release of pro-inflammatory cytokines by peripheral blood mononuclear cells (PBMCs) and monocytes (Atay, Gercel-Taylor & Taylor 2011; Germain et al. 2007; Messerli et al. 2010; Southcombe et al. 2011). STBMV isolated from PE placenta explants have also been shown to further enhance the secretion of pro-inflammatory cytokines and chemokines in PBMCs, including IL-1β, when compared to NP STBMV (Holder et al. 2012). Similarly, PBMCs, treated with STBMV derived from trophoblast cells grown under hypoxic conditions, release higher levels of IL-6 and TNF-α compared to controls (Mi Lee et al. 2012).

STBEV, as measured by PLAP ELISA, have been shown to circulate in increased levels in maternal peripheral plasma (Knight et al. 1998), especially in early-onset PE (Chen et al. 2012; Goswamia et al. 2006). The different STBEV subtypes (STBMV and STBEX) and their interaction with macrophages have not been studied. Previous studies have (a) used pooled extracellular vesicles (or not differentiated the effects of exosomes from microvesicles); (b) used term placentae taken from a caesarean

section or vaginal delivery (vaginal delivery subjects' placenta to labour stresses (Cindrova-Davies et al. 2007)); or (c) did not clearly define the PE disease state (Germain et al. 2007; Messerli et al. 2010; Southcombe et al. 2011). Taking into account that research has been mostly focused on EOPE placentae, we decided to concentrate our studies on LOPE derived STBEV.

Our hypothesis was that STBEV derived from LOPE placentae would cause an exacerbated inflammatory effect on human THP-1 macrophages compared to controls similar to that seen from EOPE. To investigate this, we examined (1) whether THP-1 cells would internalise STBMV and STBEX derived from NP or LOPE perfused placentae, (2) if there was any difference in the uptake of STBEV derived from NP and LOPE placentae; and (3) whether STBEV isolated from LOPE placentae would induce an altered inflammatory response to THP-1 compared to controls.

4.3. Hypothesis

Our hypothesis was whether STBEV, derived from LOPE placentae, might cause an exacerbated inflammatory effect on THP-1 macrophages compared to controls. To investigate this, we examined (1) whether THP-1 cells would internalise STBMV and STBEX derived from NP or LOPE perfused placentae; (2) if there was any difference in the uptake of STBEV derived NP and PE placentae; and (3) whether STBEV isolated from LOPE placentae would cause an altered inflammatory response to THP-1 compared to controls, as assessed via gene expression and cytokine/chemokine secretion.

4.4. Aims

The work described in this chapter aims to:

- Analyse binding of STBMV derived from NP and PE placentae to cultured THP-1 cells;
- Assess whether specific STB derived vesicles from NP and PE placentae are being uptaken by THP-1 cells differentially;
- Examine whether the STBEV treatment of THP-1 cells triggers pro-inflammatory or anti-inflammatory cytokine response differentially.

- Examine whether the STBEV treatment induces the THP-1 macrophages to release pro- or anti-inflammatory cytokine/chemokines proteins.

4.5. Materials and Methods

4.5.1. Human subjects

Clinical characteristics of normal pregnancy (NP) or preeclamptic pregnancy (PE) women are described in **Table 4.1**.

	Placental STBEV		
	NP (n=6)	**PE** (n=6)	**P value**
Age (years)	37.3 ± 0.7	32.7 ± 4.7	ns
Gestation Age (weeks + days)	38+1 ± 6.5	36+0 ± 5	*
Mean no. of pregnancies	2.3 ± 0.3	0.7 ± 0.3	**
Body Mass Index (kg/m^2)	27.3 ± 2.4	37.1 ± 6.7	ns
Max. Proteinuria qPCR (mg/mmol)	16.1 ± 8.6	256.7 ± 168.7	**
Max. Systolic pressure (mm Hg)	137.3 ± 1.8	181 ± 15.9	**
Max. Diastolic pressure (mm Hg)	81.7 ± 8.7	108.7 ± 6.3	**
New-born weight (g)	4008 ± 137.2	2418 ± 66	**
Smoking History	3/6	2/6	/

Table 4. 1. Clinical data of human subjects. Data presented as Mean ± SEM, significant difference shown as $p<0.01$ (**) or not significant (ns).

4.6. Results

4.6.1. Determination of optimal STBEV particle number for challenging THP-1 cells

It is widely reported that there is the greater shedding of STBEV in LOPE, especially in EOPE (Knight *et al.* 1998). Thus, experiments using similar volumes of plasma means that there are potentially more significant numbers of LOPE vesicles exerting an effect. We were keen to standardise this to ascertain the actual impact of LOPE vesicles. When we analysed equal quantities (50 µg – as reported earlier; Southcombe

et al. 2011) of STBEV from NP and LOPE by NTA, we found that there were a significantly higher number of vesicles in NP compared to LOPE (data not shown). This might mean that the same protein concentration of NP vesicles would target more cells. Therefore, we elected to use the same particle number (1 X 10^9 particles/ml) for subsequent experiments (**Figure 4.1**).
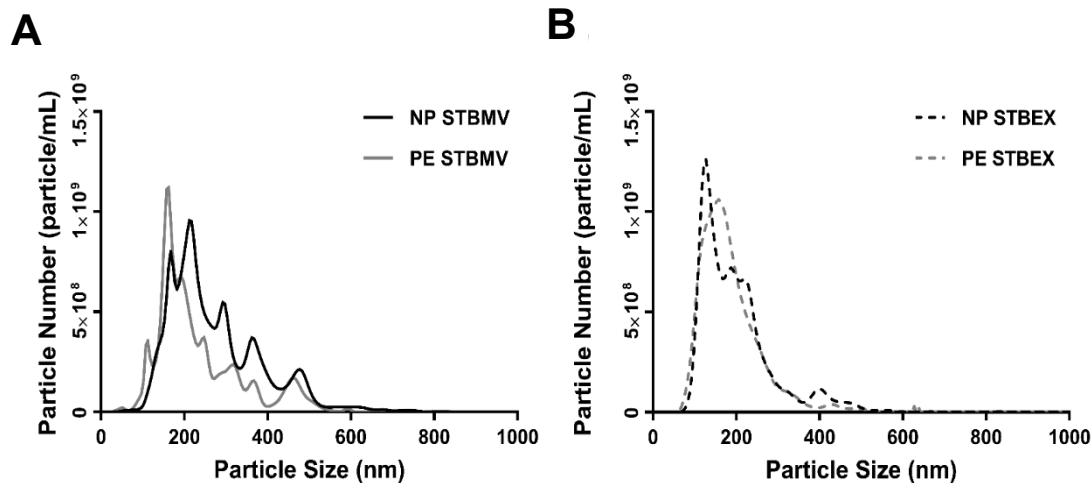
Figure 4. 1. Representative NTA collated graphs demonstrating same particle number and particle size of STBEV. Pools of STBMV (A) and STBEX (B) gathered from NP and PE placentae to treat macrophages.

4.6.2. Flow cytometry optimisation of HLA-ABC antibody using THP-1 cells

First, HLA-ABC antibody was titrated to find the appropriate antibody concentration to stain differentiated THP-1 macrophages (**Figure 4.2**). Cells were stained with an HLA-ABC antibody or its corresponding isotype control (IgG1) at different volumes (10 µL, 5 µL, 2.5 µL, 1.25 µL) as per manufacturer's instructions.

Data was collected using FACSDiva software (BD Biosciences) and plotted using side-scattered light (SSC) and forward-scattered light (FSC) plot (**Figure. 4.2A**), where SSC is an estimation of intracellular granularity, and FCS is an estimation of cell size. Unstained cells were used to assist with the voltage set up and to draw a 'gate' of interest after recording 10,000 events at a low flow rate. Our gate of interest was used as a numerical or graphical boundary to define the characteristics of cells for further analysis. Stained samples were passed through the flow cytometer, and events were

recorded. Histograms plots were used to study fluorescent intensity of labelled cells. Each isotope control sample was used to draw the '1% cut-off gate' (**Figure 4.2B**) to determine the best corresponding eNOS-APC antibody concentration staining (**Figure 4.2C**).

We concluded that 5 µL (0.5 µg/mL) of HLA-ABC-PeCy7 antibody was optimal for subsequent STBEV-treated THP-1 analysis. The optimised HLA-ABC-PeCy7 antibody concentration and its corresponding isotope control (REA-APC) was tested again with STBMV to confirm if the concentration/dilution was adequate.
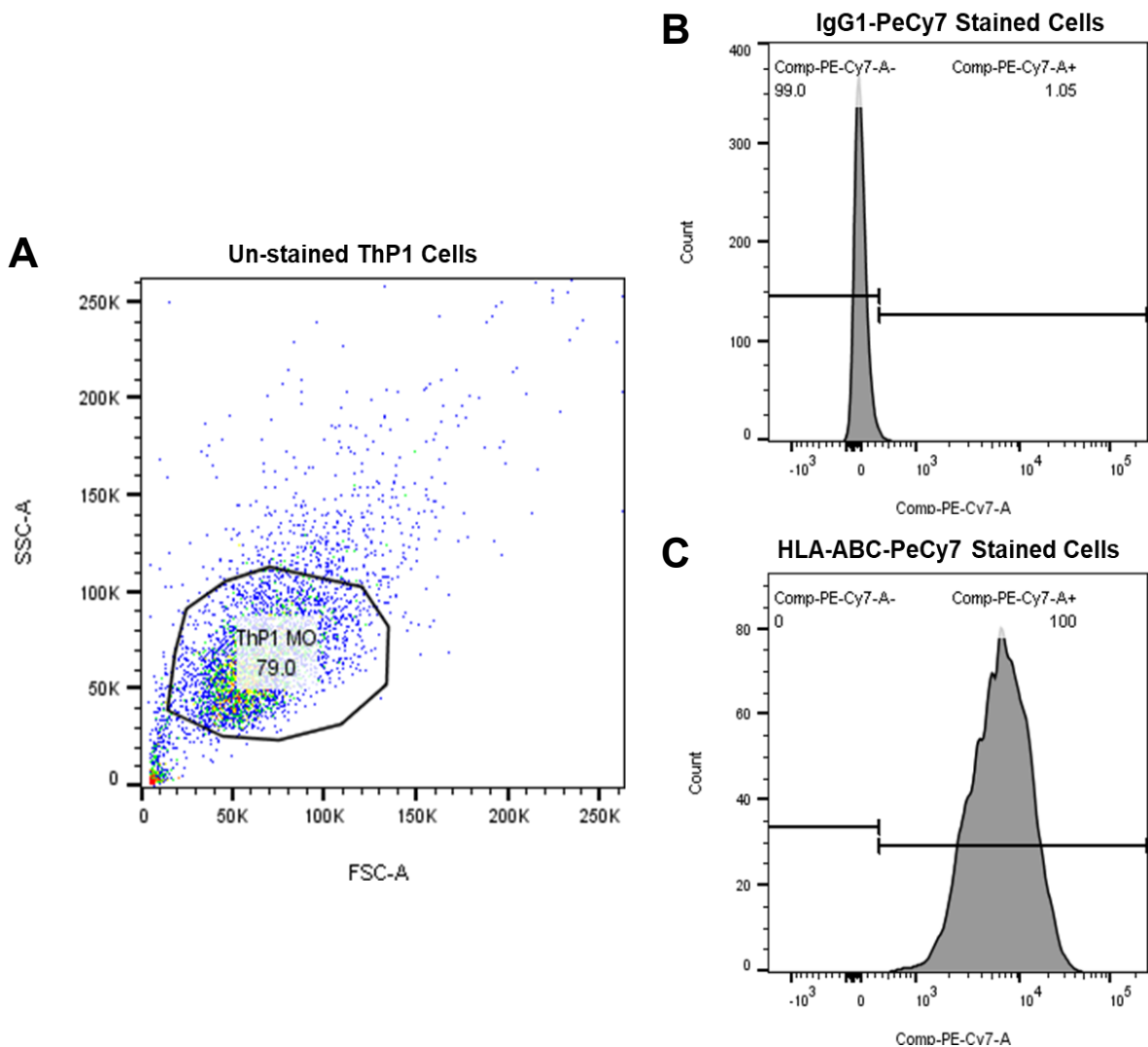
Figure 4. 2. Representative flow cytometry gating strategy used for HLA-ABC-PeCy7 antibody titration analysis using THP-1. A, Side-scattered vs forward-scattered plot showing a gate with chosen THP-1 population (circled). B, Histogram event count vs PeCy7 channel plot from THP-1 population gate showing cells stained with isotype control IgG1-PeCy7. The 1% cut-off gate was set using a vertical line. C, HLA-ABC-PeCy7 stained THP-1 population events depicted from the set-gate histogram (B).

4.6.3. Flow cytometry analysis of STBMV from NP and LOPE are taken up by differentiated THP-1 cells cytometry analysis of the uptake of STBMV derived from NP and LOPE by THP-1 cells

Uptake of NP and LOPE STBMV in differentiated THP-1 cells was investigated by flow cytometry via Bio-maleimide (STBEV membrane marker, FITC) and HLA-ABC (THP-1 cell marker; PeCy7) co-expression (n=3, **Figure 4.3**). Our data revealed that treatment of THP-1 cells with NP and LOPE STBMV showed a double positivity (FITC+PeCy7+) at 2 hours (NP: 70% ± 5.6, PE: 54% ± 8.6) and 6 hours (NP: 75% ± 4.2, PE: 78% ± 6.6), demonstrating uptake of STBMV by THP-1 cells (Quadrant Q2-2; **Figure 4.3.A**). Although uptake of STBMV by THP-1 cells revealed a significant difference in the co-expression of Bio-maleimide and HLA-ABC compared to untreated cells (2hrs: p≤0.01; 6hrs: p≤0.001), it was not significant in the case of STBMV derived from NP and LOPE placentae (p= 0.021; **Figure 4.3.B**), comparable level of phagocytosis.
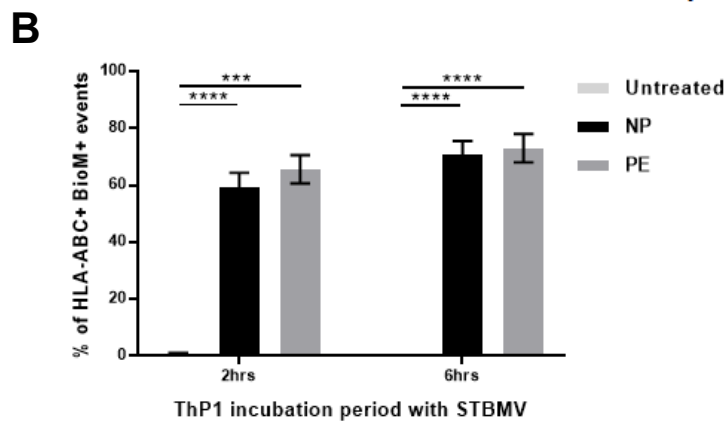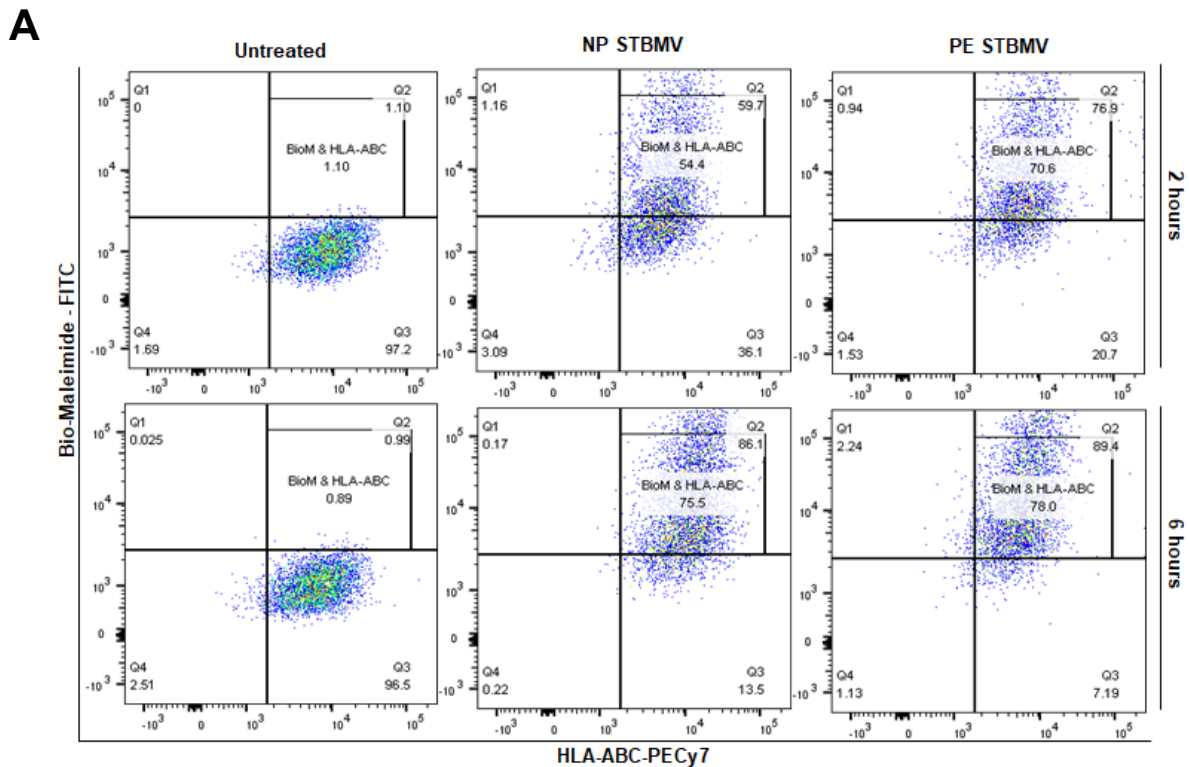
Figure 4. 3. Flow cytometry analysis of uptake of STBMV derived from NP and LOPE placentae into differentiated THP-1 cells (n=3). A, Treatment of Bio-Maleimide stained STBMV to HLA-ABC stained THP-1 macrophages. Representative Bio-Maleimide-FITC vs HLA-ABC-PeCy7 graph at 2 and 6 h treatment showing untreated THP-1, treated THP-1 with STBMV derived from NP and LOPE placentae. B, Bar-graph demonstrating merged results from THP-1 macrophages untreated and treated with NP and LOPE STBMV plotted as HLA-ABC+ Bio-Maleimide+ against incubation period. Data presented as Mean ± SEM, significant difference shown as $p < 0.001$ (***) and $p < 0.0001$ (****).

4.6.4. Confocal microscopy analysis confirmed internalisation of STBEV from NP and LOPE placentae into THP-1 macrophages

Confocal microscopy was used to interrogate whether STBEV (n=3) were being internalised by differentiated THP-1 cells at different time points (2 and 6 hours; **Figure 4.4**). STBEV from each patient group were pre-stained with PKH26 dye (red), the THP-1 cells were labelled with WGA-Alexa 488 (green), and the cell nuclei with Hoechst 33342 (blue). STBMV derived from NP and LOPE STBMV placentae (**Figure 4.4A**), and NP and LOPE STBEX (**Figure 4.4B**) appeared to be internalised by THP-1 cells. THP-1 cells alone were used as the control. We performed a PLAP ELISA in order to quantitate the STBMV that had been internalised (PLAP is a marker of STBMV and is not natively expressed in THP-1 cells).
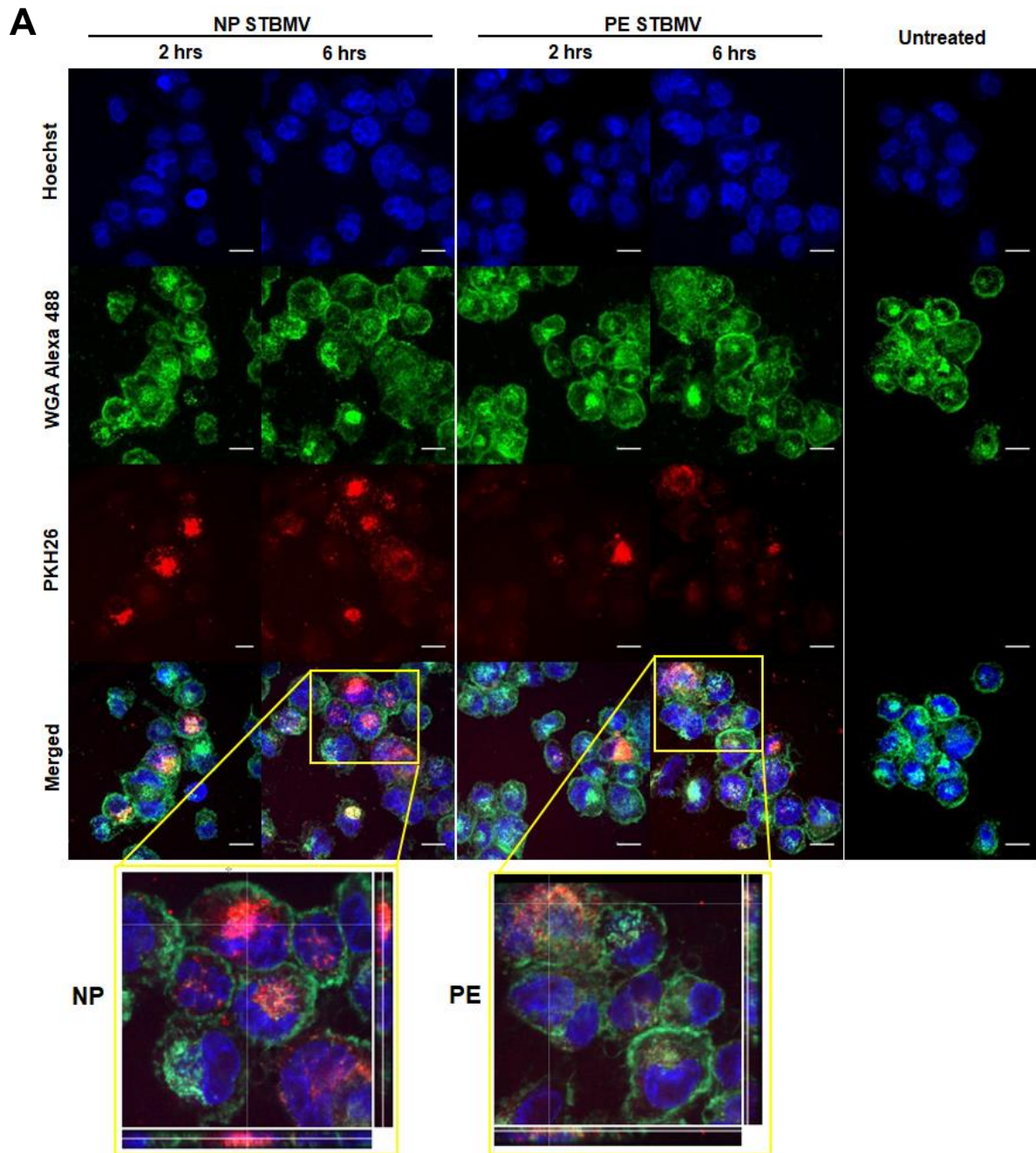
Figure 4. 4. The internalisation of STBEV from NP and LOPE placentae into THP-1 cells by confocal microscopy (n=3). STBMV (A) and STBEX (B) derived from NP and PE patients incubated for 2- and 6-hours incubation with differentiated THP-1 cells. Channels panel show cells' nuclei labelled with Hoechst dye (blue), cells' membrane labelled with WGA Alexa 488 (green), STBEV labelled with PKH26 dye (red) and merged channels. THP-1 only incubated with no STBEV are used as the control. Scale bars, 10 μm.
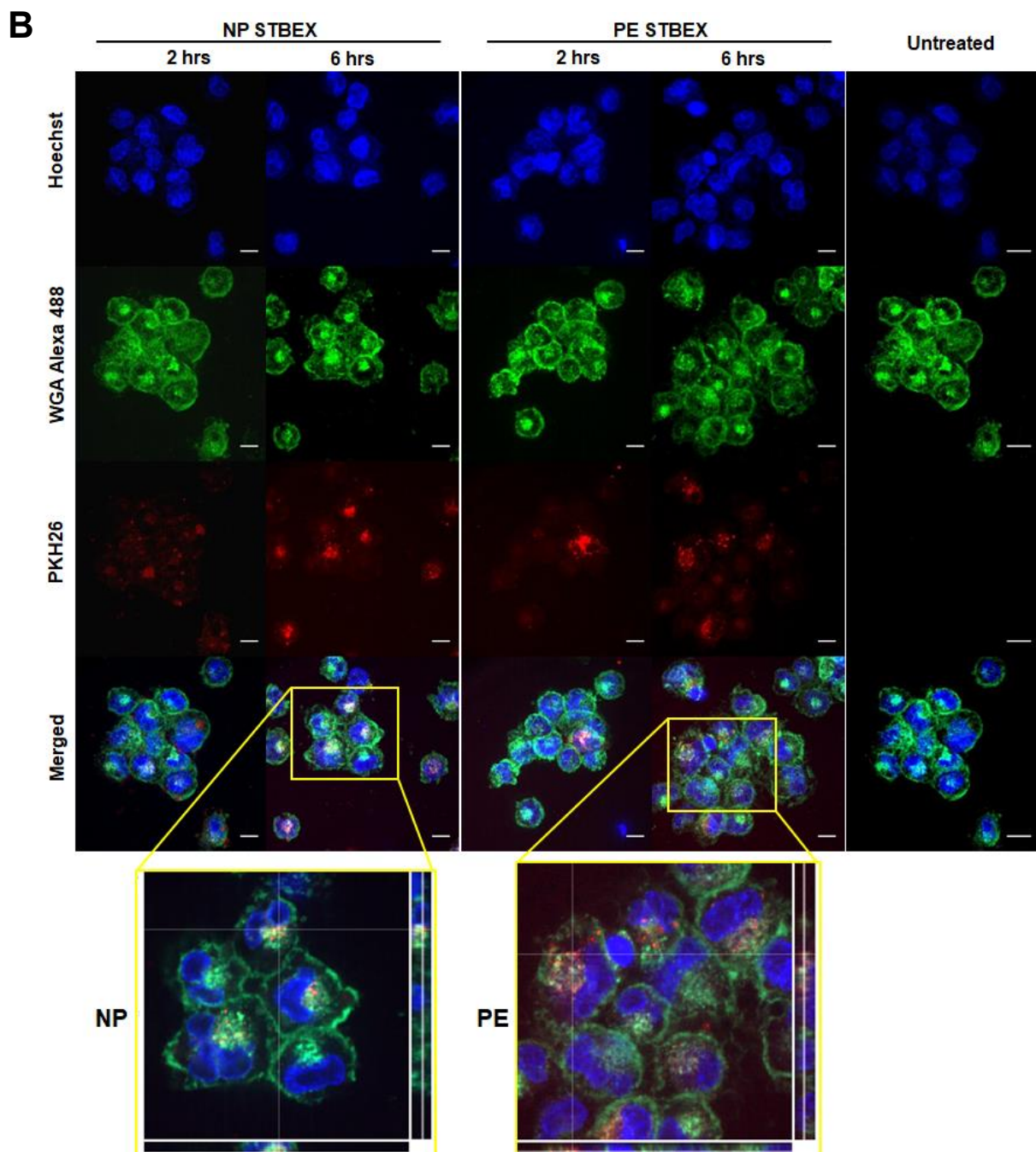
Figure 4. 4. Continuation.

4.6.5. PLAP ELISA confirmed internalisation of STBEV from NP and LOPE patients into THP-1 cells

To quantitate the STBEV vesicles that had been taken up by THP-1, PLAP (a marker of STBEV, thus not natively expressed in THP-1 cells) was measured using an STB specific marker PLAP based ELISA. We confirmed that STBEV were indeed taken up by THP-1 cells (n=3; **Figure 4.5**). This quantification included the internalised STBEV and those bound to the cell membrane of THP-1. STBMV taken up by THP-1 was time-dependent, although there was no significant difference between each group, i.e. NP and LOPE (STBEX uptake showed a significant difference between NP and LOPE at 6-hour time-point (NP < LOPE STBEX: p<0.001). These findings corroborate our confocal microscopy data in regards to STBEX internalisation by THP-1 cells. However, we should take into account that PLAP's expression is reduced in PE derived STBEV (Tannetta et al. 2013b), thus our results might be underestimated. Hence, we can only conclude that both STBMV and STBEX from NP and LOPE are taken up by THP-1 without a significant difference.
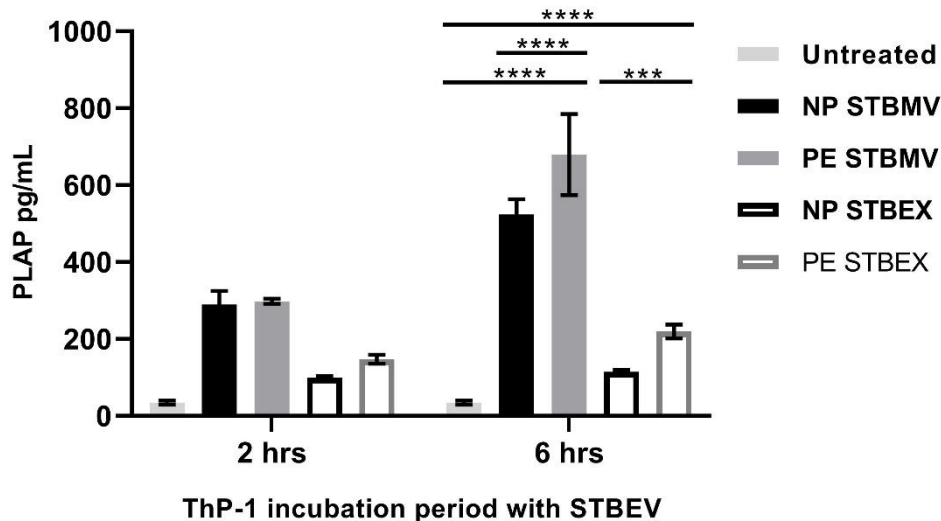
Figure 4. 5. ELISA using STB specific marker, PLAP, on THP-1 macrophages treated with STBEV derived from NP and PE placentae at 2 and 6 hours incubation. Quantification analysis of NP and PE STBMV and STBEX expressing PLAP marker internalised by THP-1 macrophages. Data presented as Mean ± SEM, significant difference shown as p<0.001 (***) and p<0.0001 (****).

4.6.6. NP-STBEV upregulated mRNA expression of pro-inflammatory cytokines in THP-1 macrophages compared to LOPE STBEV

The quantitative real-time RT-qPCR analysis was used to investigate the gene expression of a group of cytokines by differentiated THP-1 cells incubated for 2 and 6 hours with STBEV derived from NP and LOPE placentae (n=3; **Figure 4.6**). TNF-α mRNA was upregulated by log10 1.8 fold following incubation with NP STBMV as well as NP STBEX, in comparison to those derived from LOPE placentae (STBMV: p< 0.0001, STBEX: p< 0.0001, **Figure 4.6A**). LOPE STBMV and STBEX did not induce any changes in TNF-α transcript level. Next, TGF-β was significantly upregulated by log10 1-fold in NP STBMV treated in comparison to LOPE STBMV (p≤ 0.001, **Figure 4.6B**). STBEX from both NP and LOPE did not result in any significant change in mRNA expression of TGF- β. Similarly, IL-6 was highly expressed in THP-1 cells incubated with NP STBMV, and its expression increased significantly over time. NP STBMV brought about a greater change in IL-6 expression compared to LOPE STBMV (p< 0.0001, **Figure 4.6C**). There was a significant difference in the induction of IL-6 in NP compared to LOPE STBEX at 6 hours (P< 0.05, **Figure 4.6C**).

IL-10 mRNA did not show any differences between NP and LOPE STBMV. However, THP-1 cells, incubated with STBEX derived from LOPE, showed a higher expression of IL-10 compared to NP STBEX which was significantly at 2 hours (p≤ 0.01, Figure 4. D); this difference was not noticeable at 6 hours. THP-1 cells, challenged with NP STBMV, showed a higher expression level of IL-12 in comparison to LOPE, especially at 6 hours (p< 0.0001; **Figure 4.6E**). IL-12 did not appear to be affected by STBEX from either NP of LOPE. IL-8 showed a significant response to NP STBMV at both 2 and 6 hours compared to LOPE STBMV (p< 0.0001; **Figure 4.6F**). There was a small induction of IL-8 with STBEX from NP at 2 and 6 hours. The expression of IL-8 at 6 h by NP STBEX was significantly higher compared to LOPE STBEX (p<0.05, **Figure 4.6F**). Overall, THP-1 macrophages challenged with STBMV, especially those derived from NP, showed upregulation of pro-inflammatory cytokines, while STBEX did not induce significant alterations in the cytokine profile consistent with the higher uptake. Surprisingly, LOPE STBEV brought about modest changes in the expression of pro-inflammatory cytokines whilst LOPE STBEX induced upregulation of IL-10 transcripts.

These results appear to suggest that NP-derived STBMV and STBEX induce pro-inflammatory responses, whereas those derived from LOPE placentae (whilst clearly being internalised) do not cause an inflammatory response. The finding of up-regulated IL-10 by LOPE derived STBEX appears to suggest an anti-inflammatory and repair effect.
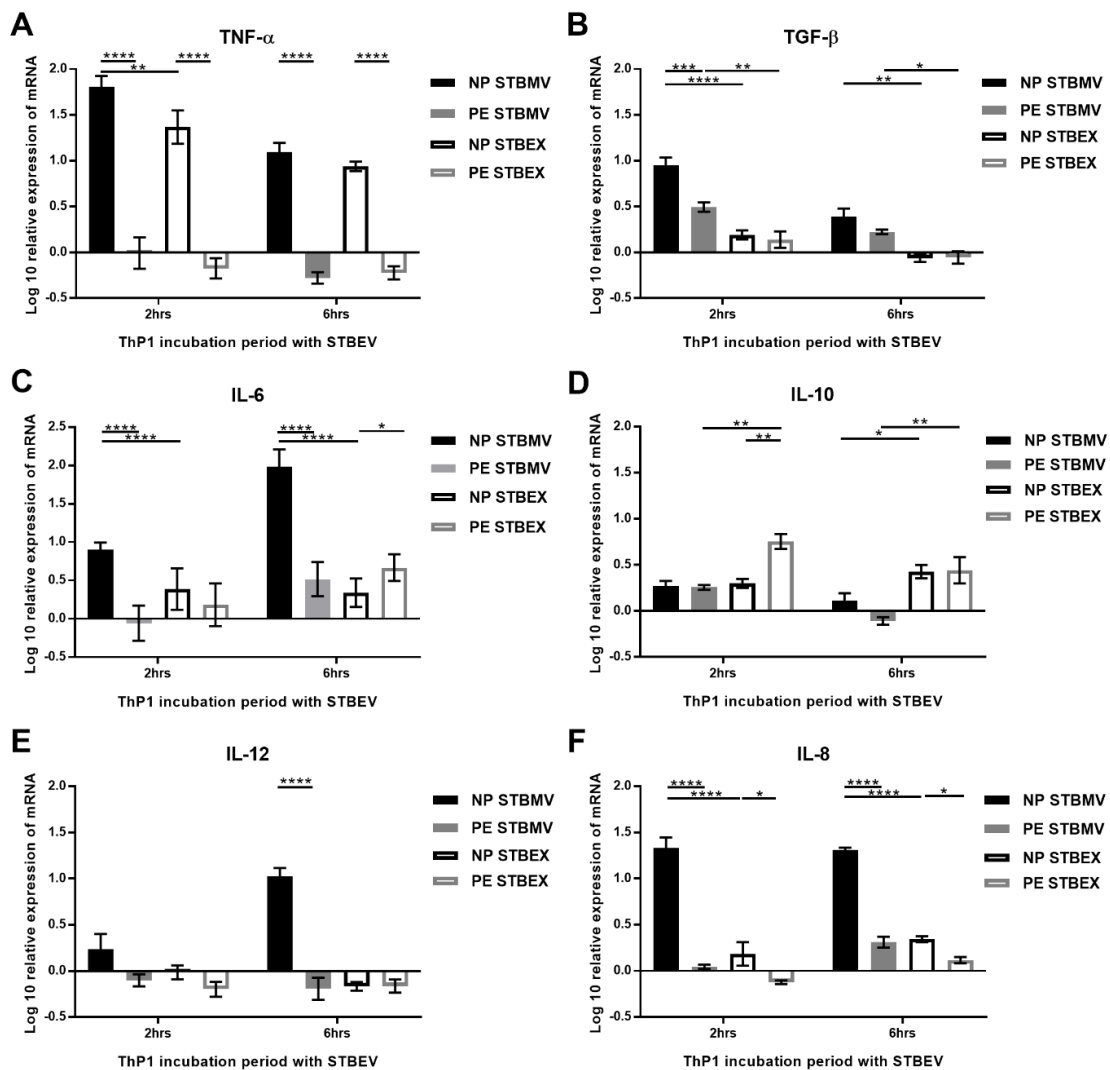
Figure 4. 6. RT-qPCR analysis of the STBEV induced expression of cytokines by differentiated THP-1 cells. Cells were incubated with STBEV from NP and PE placentae at 2 and 6 h' time-points. In control experiments, cells were incubated with filtered PBS at the same time-points. mRNA expression was measured using real-time RT-qPCR for TNF-α (A), TGF-β (B), IL-6 (C), IL-10 (D), IL-12 (E) and IL-8 (F). Data were normalised to 18S rRNA expression that was used as an endogenous control. Values calculated as mean ± SEM of value from cells treated with 50 µg of STBEV minus background cytokine gene expression. To determine significant difference in expression, two-way ANOVA was performed on data: * $p \leq 0.05$, ** $p \leq 0.01$, *** $p \leq 0.001$ and **** $p < 0.0001$.

120

4.6.7. NP-STBEV cause a significant release of MIP-1α and IL-8 from THP-1 cells compared to LOPE STBEV

Multiplex array analysis was used to investigate the secreted levels of a range of cytokines, chemokines, growth factors, and soluble ligands following 12- and 24- hours incubation of differentiated THP-1 cells with STBEV derived from NP and PE placentae (**Figure 4.7**). THP-1 cells challenged with NP STBMV appeared to show a predominantly pro-inflammatory profile, as evident from the significant higher quantities of TNF-α (**A**), IL-6 (**B**), IL-12p40 (**D**), IL-1β (**J**) and GM-CSF (**K**) secretion compared to almost absent secretion by LOPE STBMV treated THP-1 cells at both time points (TNF-α, IL-1β, IL-6, GM-CSF = $p<0.0001$; IL-12p40 = $p<0.001$). Similarly, THP-1 challenged with NP STBEX in comparison to PE STBEX revealed the same trend as STBMV. NP STBMV treated THP-1 cells released around 2-fold higher levels of anti-inflammatory cytokine IL-10 (**C**) compare to LOPE STBMV ($p<0.0001$) at both time points. There was only a significant difference between NP STBEX treated THP-1 release of IL-10 at 12 hours in comparison to LOPE STBEX ($p<0.001$). Though IL-10 transcripts were upregulated in LOPE STBEX, this is not consistent with the protein production by THP-1 after longer incubation with LOPE STBEX.

Chemokines IL-8 (**E**), MIP-1α (**F**), IP-10 (**G**) and MCP-1 (**H**) were also secreted in higher quantities in response to NP STBMV compared to LOPE STBMV, as well as NP STBEX compared to LOPE STBEX. Particularly, NP STBMV released higher quantities of IL-8 compared to LOPE STBMV (12 hours: $p\le 0.0001$, 24 hours: $p\le 0.05$, **Figure 4.7E**). Similarly, IL-8 was significantly secreted when induced with NP STBEX compared to LOPE STBEX (12 hours: $p\le 0.0001$, 24 hours: $p\le 0.05$, **Figure 4.7E**). Both NP STBMV and NP STBEX stimulated the IL-8 release of over 12,500 pg/mL, whilst LOPE STBMV and LOPE STBEX also seemed to increase production of IL-8 but at a lower level (12 hours: < 5,000 pg/mL, 24 hours: > 5,000 pg/mL). Thus, NP STBEV challenged THP-1 cells secreted more IL-8 than LOPE STBEV.

Also, NP STBMV stimulated MIP-1α production that increased over time compared to PE STBMV (12 hours: $p\le 0.01$, 24 hours: $p\le 0.0001$, **Figure 4.7F**). NP STBMV stimulated the production of over 20,000 pg/mL of MIP-1 α in THP-1 cells compared to 2,000 pg/mL for LOPE STBMV at 24 hours. NP STBEX also appeared to induce

more MIP-1α secretion compared to LOPE STBEX (12 hours: p≤ 0.0001, 24 hours: p≤ 0.05, **Figure 4.7F**). Intriguingly, NP STBEX appeared to cause a higher secretion of MIP-1α at 12 hours incubation compared to NP STBMV (p≤ 0.01); this effect was then significantly reduced at 24 hours (p≤ 0.0001). Thus, our results revealed that MIP-1α was released in greater quantities by THP-1 cells when challenged with NP STBEV in comparison to cells challenged with PE STBEV.

Finally, VEGF was secreted in higher quantities by THP-1 challenged with NP STBMV compared to LOPE STBMV (p<0.000.1; **Figure 4.7I**); whilst THP-1 challenged with LOPE STBEX secreted up to 2-fold more quantities of VEGF than NP STBEX (p<0.0001; **Figure 4.7I**).

Overall, our data validate the results of our gene expression analysis by RT-QPCR, corroborating our observations.
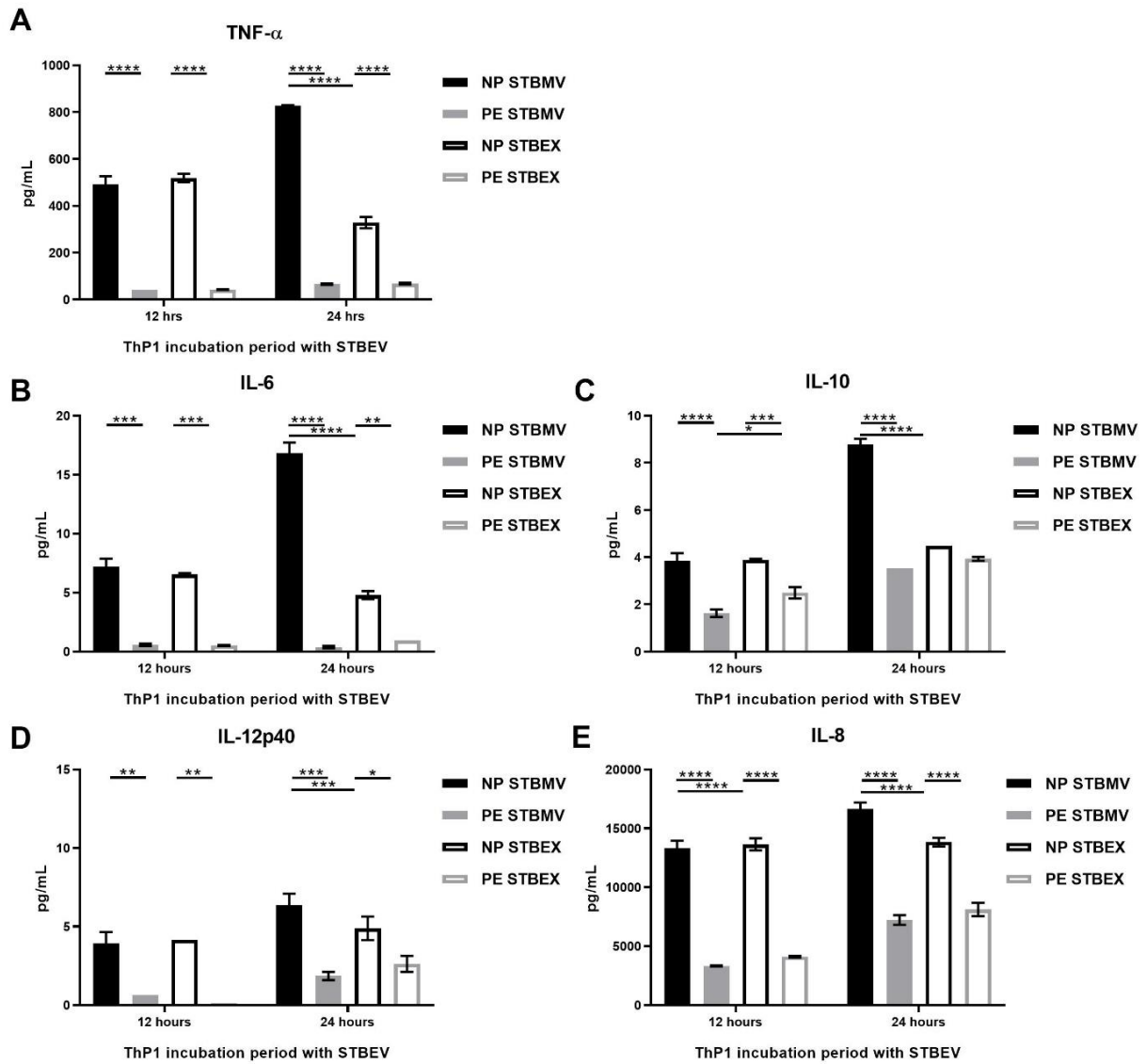
Figure 4. 7. Multiplex array analysis of the supernatants of differentiated THP-1 cells treated with STBEV from NP and PE placentae. Concentrations of TNF-α (A), IL-6 (B), IL-10 (C), IL-12p40 (D), IL-8 (E), MIP-α (F), IP-10 (G), MCP-1 (H), VEGF (I), IL-1β (J) and GM-CSF (K) released by THP-1 cells at 12 and 24 h incubation with STBEV. Values calculated as Mean ± SEM of value from cells treated with 50 μg of STBEV minus background cytokine production. To determine significant difference in production, two-way ANOVA was performed on data: * $p \leq 0.05$, ** $p \leq 0.01$, *** $p \leq 0.001$ and **** $p \leq 0.0001$.
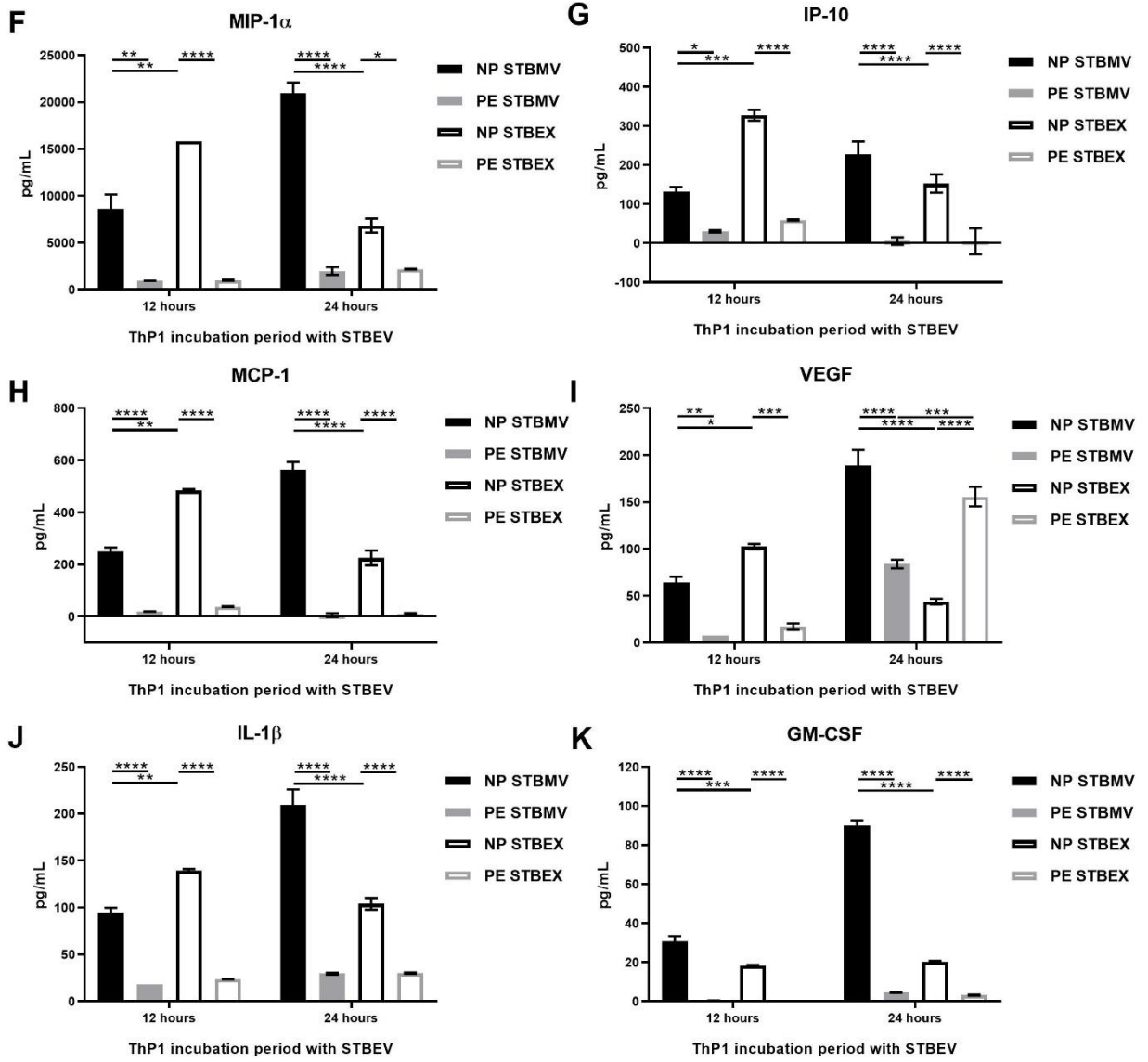
Figure 4. 7. Continuation.

4.6.8. Deep Sequencing Data of STBMV and STBEX from PE and NP pregnancy

Next, we performed deep sequencing analysis on STBMV and STBEX from PE (n=8) and NP (n=6) patients (Tannetta et al. Unpublished data; see Online Data Supplement Figure S1). STBMV (A) and STBEX (B) were specifically interrogated for the presence of target cytokines/chemokines from our previous results. Following normalisation, STBMV revealed expression of IL-8, IL-12B and TGFB1 genes. PE STBMV showed significant higher expression of TGFB1 in comparison to NP STBMV ($p < 0.001$). Similarly, STBEX showed expression for IL-10, IL-12A, IL-12B, IL-8, TNF, IL-6 and TGFB1 genes. PE STBEX revealed a significant expression of IL-6 and TGFB1 in comparison to N STBEX. (IL-6, $p<0.05$; TGFB1, $p<0.01$). These results confirm that our PE STBEV carry a proinflammatory profile cargo in comparison to NP STBEV, yet this cargo had no discernible effect on THP-1 macrophages in our hands.
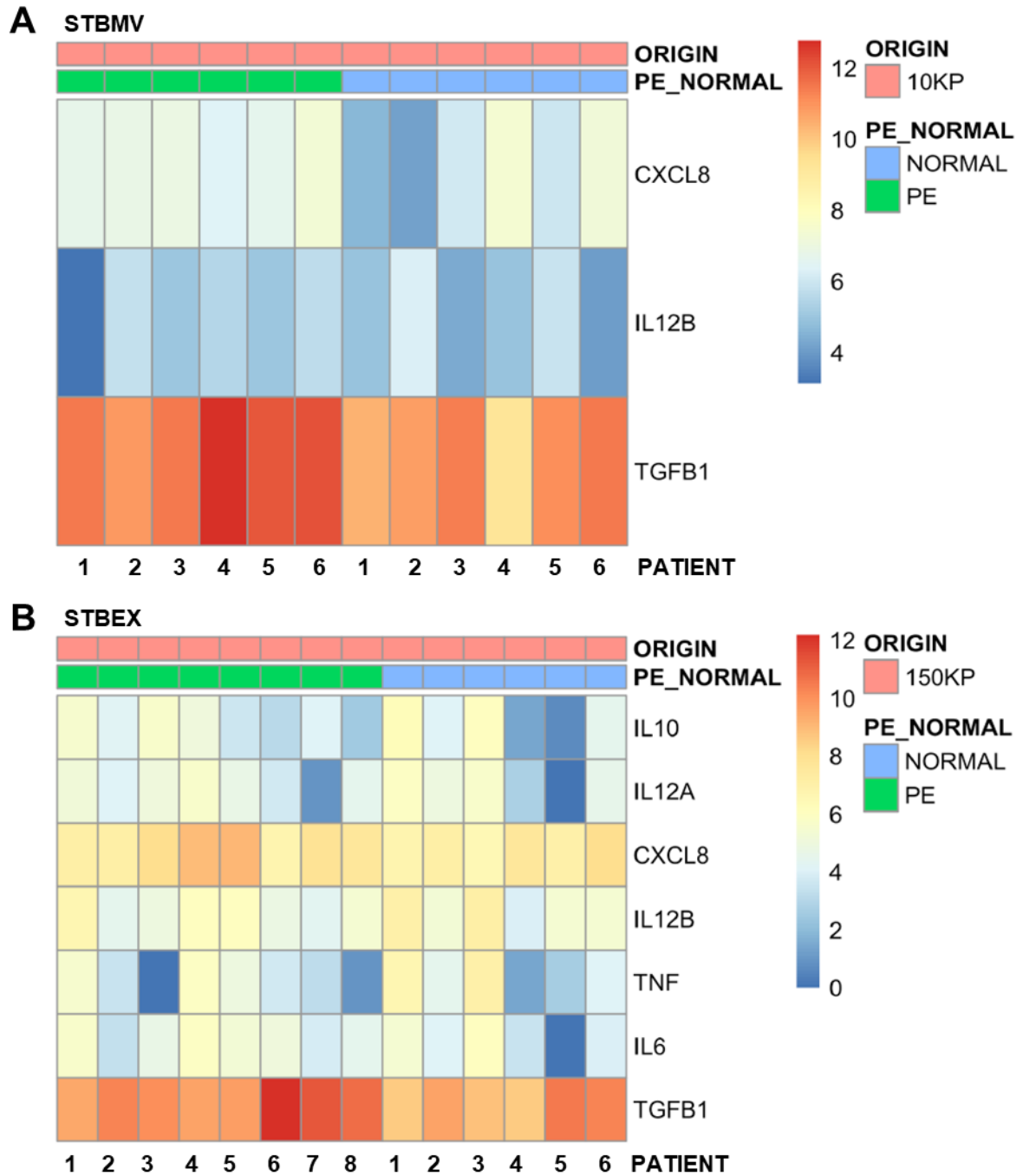
Figure 4.8. Cytokines/chemokines identified by next-generation sequencing. Analysis included STBMV (10K, A) and STBEX (150K, B) samples from NP (n=8) and PE (n=6) patients. Legend uses colour to demonstrate the upregulation of chosen genes: CXCL8 (IL-8), IL-10, IL-12A, IL-12B, TNF, IL-6 and TGFB-1.

4.7. Discussion

PE, most distinctly EOPE, is thought to originate from poor placentation in the first half of pregnancy leading to ineffective remodelling of the uterine spiral arteries. This causes a high-pressure pulsatile flow in the intervillous space, which in turn, causes excess oxidative and hydrostatic stress to the placenta (Redman, Sargent & Staff 2014). Thus, EOPE has been associated with a vigorous maternal systemic inflammatory response to a damaged placenta (C. W G Redman, Sacks & Sargent 1999), major fetal growth restriction, and the increasing amounts of STBEV shedding with different phenotype and cargo compared to a healthy pregnancy (Goswamia et al. 2006; Redman et al. 2012). The late-onset disease is subject to several different theories of pathophysiology with trophoblast villus overcrowding, leading to oxidative stress competing with maladaptation of the maternal cardiovascular system as putative causes. Despite this, a role for the placenta is still evident since delivery brings about an end to PE-associated symptoms in both EOPE as well as LOPE. STBEV (STBMV and STBEX) have been suggested to play different roles in the pathophysiology with STBMV playing a greater role in proinflammatory events compared to STBEX (Tong et al. 2017). We decided to use the THP-1 cell line to standardise the sole effect of STBEV and avoid the implementation of patient-related variances with the use of PBMCs. By using PMA-induced THP-1 cells, we wanted to understand the true effect of STBEV on both circulating monocytes and tissue macrophages. Therefore, we hypothesised that the LOPE placenta would release STBEV, which might have a similar immunomodulatory impact to EOPE, i.e. proinflammatory. However, we observed a significantly weakened inflammatory effect of STBEV isolated from LOPE placentae on THP-1 cells.

Our study shows that both STBEV types (STBMV and STBEX) interact with macrophages and modulate their functions. Flow cytometry revealed co-localisation of STBMV derived from both NP and PE placentae to THP-1 macrophages. Confocal microscopy confirmed this co-localisation was secondary to internalisation of the STBEV. PLAP-based ELISA showing that THP-1 cells internalised placental-derived EV further confirmed this. This is in line with previous work showing mature PBMCs from NP donors phagocytosed SW71 trophoblast cell derived EV (Atay et al. 2011) and STBMV isolated from dual perfusion (Southcombe et al. 2011). When assessing

PLAP levels within the THP-1 cells, we were unable to see any significant difference in the uptake of NP and PE STBEV. We were able to determine enhanced uptake of STBMV compared to STBEX in both NP and LOPE.

Analysis of gene expression via RT-qPCR and cytokine/chemokine secretion via multiplex array revealed that exposure of PE STBEV to THP-1 macrophages had significantly less inflammatory impact compared to NP STBEV. NP-STBEV, especially NP-STBMV, induced a pro-inflammatory response by THP-1 macrophages. Previous studies have shown that NP placental microvesicles induced significant levels of TNF-α, MIP-1α, IL-1α, IL-1β, IL-6 and IL-8 by naïve PBMC (Southcombe et al. 2011; Thibault et al. 1991) and an increased release of IFN-γ, IL-12, IL-18 and TNF-α by PBMCs (Germain et al. 2007). Similarly, NP STBMV derived from in vitro explant cultures from human placentae have been shown to enhance secretion of IL-1β, IL-6 and IL-8 by PBMCs (Messerli et al. 2010). Correspondingly, exosomes derived from SW71 trophoblast cells have been shown to increase monocyte migration and production of IL-1β, IL-6, granulocyte-colony stimulating factor (G-CSF), granulocyte-macrophage colony-stimulating factor (GM-CSF) and TNF-α (Atay et al. 2011).

Collectively, our NP results are consistent with these studies. NP STBMV showed enhanced up-regulation of TNF-α, IL-6, IL-12 and IL-8 mRNA and protein secretion by ThP-1, especially higher levels of MIP-1α and IL-8, implying a proinflammatory phenotype. However, in addition to pro-inflammatory functions, IL-12 also has anti-angiogenic properties (Strasly et al. 2001) which might counteract the pro-angiogenic functions of IL-8 (Strieter et al. 1995). Most surprising, however, was the significantly lower pro-inflammatory effect seen with LOPE STBEV. We expended significant effort to confirm that the STBEV in both conditions were being internalised by the THP-1 cells and having confirmed this in three different ways, felt confident in excluding the possibility that LOPE vesicles were not causing a proinflammatory effect because they were not being internalised.

STBEX have not been extensively studied, but some groups have suggested NP placenta explants derived exosomes to have immunosuppressive roles (Hedlund et al. 2009; Mincheva-Nilsson & Baranov 2014). Our lack of pro-inflammatory phenotype results would, in some part, support this. Our PE STBEX echoes the results that we

obtained from STBMV and did not display the pro-inflammatory response we expected. Our data also provides confirmation by sequencing analysis that our STBEV are not empty and carry genetic material corresponding to our chosen targets. Thus, we interpret our results as LOPE STBEV might not directly impact macrophages but might use an alternative route to induce the proinflammatory state of the disease. This requires further investigation.

Plasma EV derived from PE patients in comparison to those from NP has been shown to affect monocyte functions, such as altered phagocytosis-associated molecular pattern, decreased chemotactic and migratory activity, and increased adhesiveness (Kovács et al. 2018). Unfortunately, this previous study did not focus on STBEV. Hence, we cannot conclude that this effect is directly due to placenta-derived EV. Alternatively, STBEV derived from LOPE might have an impact on other cells in the circulation, apart from immune cells that can stimulate the inflammatory response in PE (Tannetta et al. 2017a). Tannetta et al. provided evidence that STBEV isolated from NP can cause platelet activation, which is augmented by PE STBEV (Tannetta et al. 2015). Increased platelet reactivity due to exposure to STBEV from PE might correlate with the increased thrombotic risk associated with PE, possibly leading to the inflammatory response (Tannetta et al. 2015). STBEV have also been shown to have anti-angiogenic and hypertensive effects preventing endothelial cell monolayer growth in vitro as well as inhibiting relaxation of pre-constricted blood vessels in vivo (a P. Cockell et al. 1997; Gupta et al. 2005; Smárason et al. 1993b). Although these studies have not separated microvesicles and exosomes and differentiated EOPE to LOPE, it is necessary to consider their findings when interpreting our results.

Studies have shown key differences between EOPE and LOPE, supporting the idea that these are separated disease entities. Women with PE show an imbalance between a pro-inflammatory and anti-inflammatory profile in CD4$^+$ T-cell subsets with polarisation to T$_H$17 profiles, predominantly in EOPE (Ribeiro et al. 2017). Notably, this study reported endogenous plasma levels of IL-6, IL-7 and TNF-α to be significantly higher in the EOPE group than in the LOPE and control groups (Ribeiro et al. 2017). Another study found substantially higher concentrations of Hsp70, TNF-α, IL-1β, IL-12, and sTNFRI in patients with EOPE compared to LOPE, as well as

significantly lower IL-10 levels in the EOPE group (Peraçoli et al. 2013). EOPE was, therefore, associated with higher maternal and fetal impairment, highlighting differences in the pathophysiology between EOPE and LOPE (Peraçoli et al. 2013).

Correspondingly, Liang et al. verified 627 genes were differentially expressed in EOPE compared to LOPE's placental tissue, and biological processes including immune response and cell surface receptor linked signal transduction (Liang et al. 2016). Likewise, another study showed 362 genes with $\geq \pm$ 1 fold expression difference in chorionic villous from EOPE compared to LOPE, including genes such as AB13BP, C7, HLA-G and IL2RB (Nevalainen et al. 2017). Similarly, an association between EOPE and upregulated expression of neutrophil TLR2, TLR4 and cryopyrin, increased mRNA expressions of NF-κβ subunits p50 and p65, as well as imbalanced pro-inflammatory and anti-inflammatory cytokine expression in serum has been shown (Xie et al. 2010); reinforcing EOPE to be a particular form of systemic inflammation. Despite these findings, no studies have been performed examining the effects of STBEV from LOPE placenta on immune function. Our data suggest that the differences seen in immune function in EOPE and LOPE may well in part be mediated by the differences in the effects of STBEV from these disease states. In addition, the clear pro-inflammatory phenotype seen in LOPE might not be caused by a direct effect of STBEV on macrophages, but rather an indirect effect on another yet to be determined immune cell or cell type (e.g. platelets).

CHAPTER 5

Characterisation of exosomes released by placental capillary pericytes cultured under normal and hypoxic conditions

5. Characterisation of exosomes released by placental capillary pericytes cultured under normal an hypoxic conditions

5.1. Abstract

Pericyte cells (PC) are multifunctional cells wrapped around the endothelium of small blood vessels which play an essential role in vascular development and blood flow regulation. The role of PC in placental function has not been fully explored. During pregnancy, a short period of low oxygen tension is necessary for appropriate placental development. However, chronic hypoxia may lead to the disruption of trophoblast development, abnormal invasion into maternal decidua, and aberrant remodelling of the spiral arteries. Thus, chronic placental hypoxia is one of main causes of placental damage resulting in obstetric diseases such as fetal growth restriction and preeclampsia. Here, we investigate the role of chronic hypoxia on normal placental PC (PLVP) function. Using PLVP isolated from term human placentae, we aimed to examine the release of cytokines and chemokines, as well as exosomes, from PLVP grown at 20, 8 and 1% O_2 conditions. Both secreted levels of cytokines and chemokines (IL-6, IL-8 and VEGF), as well as exosomes (Alix, Syntenin and CD9-positive) significantly increased in the supernatant as the O_2 levels decreased. Exosomes derived from these PLVP (PLVPex) were subjected to mass spectrometry revealing 640 proteins. Biological pathway analysis suggested VEGF signalling and cell growth and maintenance as being highly regulated by these PLVPex bound proteins. Stimulation of primary human umbilical vein endothelial cells (HUVEC) with PLVPex resulted in a significant increase of HUVEC polygon formation number and tube formation length. We therefore propose that PLVPex act as messengers to stimulate angiogenesis and vessel stabilisation on neighbouring endothelial cells during periods of hypoxia.

5.2. Background

Pericyte cells (PC) are perivascular cells that mainly support microvessels such as capillaries or post-capillary venules. PC are multipotent contractile cells with finger-like projections around the vascular circumference of the endothelium, and these connect functionally and directly to the underlying endothelial cells (EC)(Dore-Duffy & Cleary 2011). PC have significant roles including immunomodulation(Navarro et al. 2016), angiogenesis, vessel stabilisation and maturation(Jain 2003), regulation of blood flow(Hall et al. 2014), and pericyte-endothelial cell signalling via PDGF-BB–PDGFRβ and VEGF-A–VEGFR2, among other pathways(Sweeney, Ayyadurai & Zlokovic 2016). The characteristics and functions of PC are very organ specific, forming a major part of the blood brain barrier(Mathiisen et al. 2010; Sá-Pereira, Brites & Brito 2012), but distributed sparsely in tissues such as the skeletal muscle(Díaz-Flores et al. 2009). PC are also closely related to stromal progenitor cells and they can differentiate into adipocytes, osteoblasts, chondrocytes and vascular muscle cells among other cell types(Hirschi & D'Amore 1996). Therefore, their role in angiogenesis and development is likely to be highly dependent on their functional state and stage of differentiation(Wang & Zhao 2010).

The local conditions of the human placenta allow fetoplacental vasculogenesis and angiogenesis to vary from other human vascular beds, constantly changing through-out gestation to meet the increasing metabolic needs of the growing fetus(Charnock-Jones, Kaufmann & Mayhew 2004). During the first trimester, placentation occurs in a relatively hypoxic environment relative to maternal tissues, which is crucial for appropriate embryonic development(Rodesch et al. 1992). However, during gestation, the oxygen tension in the intervillious space gradually increases. Tissue oxygenation in the placental villi seems to be inversely related to the numerical density of fetal capillaries (Kingdom & Kaufmann 1997). Chronic hypoxia, usually caused by impaired trophoblast invasion and spiral artery modifications, have been shown to be associated with complicated pregnancy disorders such as preeclampsia (PE)(Caniggia et al. 2000; Redman 2005). PE is characterised by endothelial dysfunction and an imbalance of inflammatory mechanisms, primarily affecting the maternal vascular and immune systems,(Christopher W.G. Redman, Sacks & Sargent 1999; Staff, Dechend & Redman 2013) as well as fetal development and health.

Mechanisms by which fetoplacental development becomes altered in PE need to be further explored to understand how abnormal placental function affects the fetus.

Few studies have directly connected altered placental vasculature with placental PC (PLVP) function. Placenta from platelet-derived growth factor receptor β (PDGFRβ) deficient mice, exhibited dilated embryonic blood vessels and a reduced number of both PLVP and trophoblasts(Ohlsson et al. 1999), emphasising the importance of PDGFRβ signalling in murine placental development. Placental capillaries in women from high altitude communities showed an increased vessel profile diameter and a reduced PC association compared to those pregnancies from lowland environments(Zhang et al. 2002), suggesting that reduction of local oxygen tension leads to vascular remodelling. Similarly, semi-quantitative analysis of placental ultrastructural micrographs indicated that PLVP were present in placentae from normal, term pregnancies but increasingly observed in abnormal capillaries such as those from pregnancies complicated by diabetes, post maturity, rhesus incompatibility and PE(Jones & Desoye 2011). While pericyte functions in other organs are now being extensively studied, there are relatively few studies exploring the role of PLVP in prenatal research(Barreto et al. 2019; Gauthier-Fisher, Szaraz & Librach 2019; Jones & Desoye 2011). PLVP are distinctively associated with the fetal circulatory system of the placenta, which can significantly affect the fetus' growth and placental development. There is limited evidence regarding the factors released by the PLVP in response to severe hypoxia and how these can affect neighbouring endothelial cells (EC).

5.3. Hypothesis

Our hypothesis was whether PLVP would secrete any soluble factor or EV with altered number/protein cargo when incubated under different O_2 conditions. We first examined whether supernatant contained any cytokine or chemokine after PLVP incubation in three different states. We also assessed whether the isolated PLVP derived EV had a distinctive exosome phenotype. We wanted to assess whether the PLVPex would enter HUVEC and have a different functional role on HUVEC tube formation when derived from three different O_2 conditions. Finally, we wanted to examine the possible functions of PLVPex on HUVEC and protein cargo.

5.4. Aims

The objectives of the work illustrated in this chapter were as follows:

- To determine the soluble factors secreted by PLVP after 24-hour incubation in EV-free normal and hypoxic media
- To isolate and characterise PLVP derived microvesicles and exosomes from PLVP after a 24-hour incubation in EV-free normal and hypoxic media
- To investigate the non-toxic particle concentration of PLVP exosomes for functional studies
- To examine whether PLVPex bind to surface or enter into HUVEC
- To explore the operational characteristics of PLVPex derived from different O_2 conditions using HUVEC cells
- To confirm and interrogate protein cargo of PLVPex derived from different O_2 conditions

5.5. Results

5.5.1. Hypoxia induces morphological alterations in human placental capillary pericytes

Once PLVP reached 80% confluence in normal conditions, cells were photographed at the start and the end of the 24 hours incubation at 20, 8 and 1% O_2 conditions (n=3, **Figure 5.1**). PLVP incubated in hypoxic conditions (8 and 1% O_2) showed constriction and reduced surface area, revealing an elongated and narrower structure compared to PLVP grown under ambient conditions.
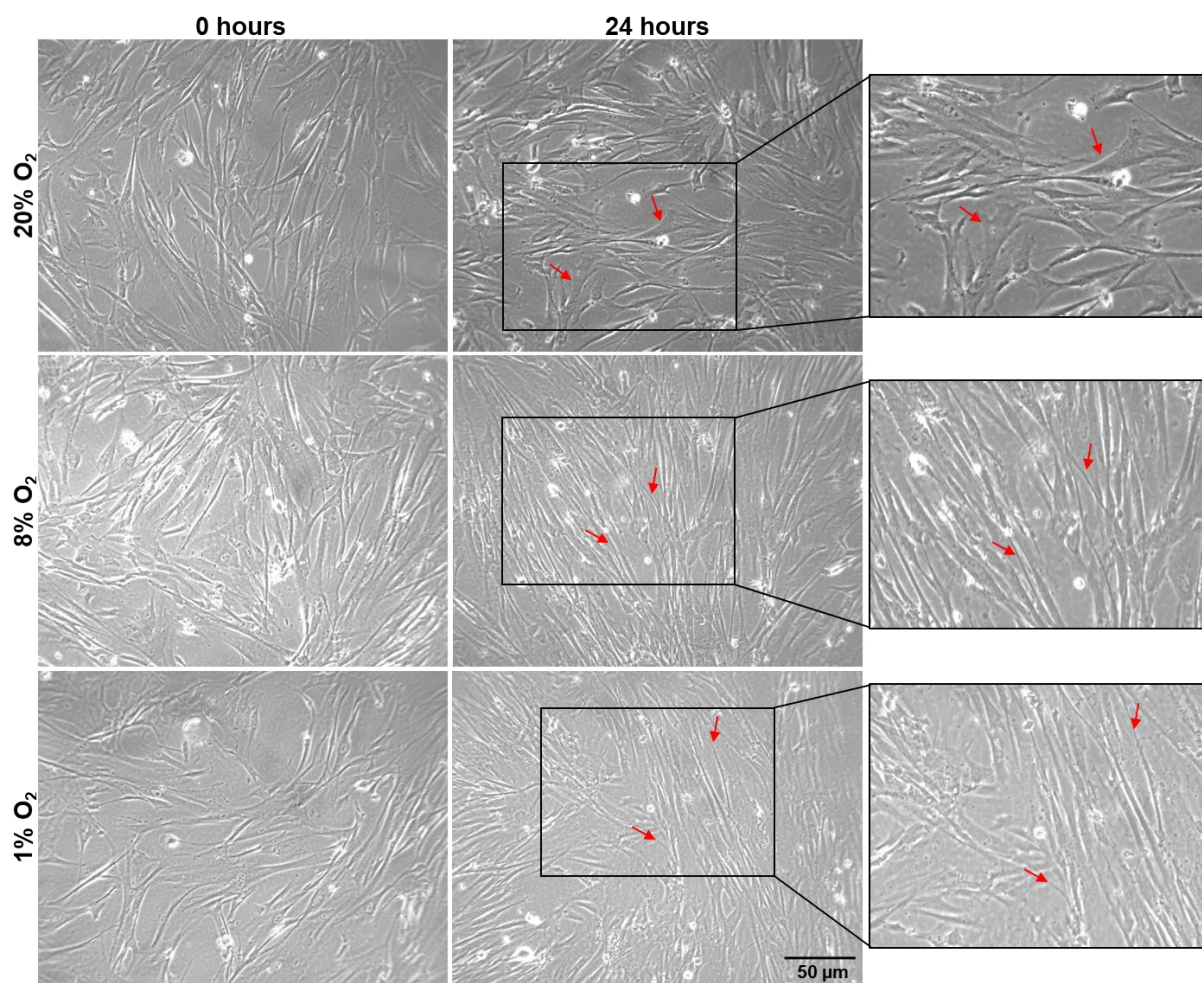
Figure 5. 1. Representative microscopy images of PLVP cells grown at different oxygen percentages (20%, 8% and 1%) at 0 hours and after 24 hours incubation. Red arrows show the diameter differences of PLVP cells in normal and hypoxic conditions. Scale bar indicates 50 µm length.

5.5.2. PLVP release immunomodulatory factors under hypoxic conditions

We assessed PLVP supernatant (after depletion of dead cells and cell debris) from PLVP incubated at different oxygen concentrations using an immunological MILLIPLEX assay (n=3; Figure 1). Several cytokines were released by PLVP when incubated at the three O2 concentrations, however, in relatively low levels (Figure 1.A). PLVP secreted considerably higher concentrations of IL-1α cytokine when incubated at 1% O2 conditions, in comparison to those incubated at both control (20% O2) and 8% O2 concentrations (both non-significant). Most significantly, IL-6 cytokine was the most abundant cytokine produced by PLVP (maximum: 8,756 ± 101 pg/ml). At normal conditions, PLVP released more IL-6 in comparison to those incubated at 8% O2 ($p<0.0001$). However, PLVP incubated at 1% O2 significantly secreted up to 4-fold more IL-6 in comparison to control conditions ($p<0.0001$).

Three chemokines: IL-8, monocyte chemoattractant protein-1 (MCP-1) and growth-regulated oncogene (GRO), were found at greatly elevated levels compared to other chemokines in PLVP supernatant (Figure 1.B). IL-8 was differentially and significantly released from PLVP incubated in 1% O2 at higher levels (15,468 ± 286 pg/ml) compared to 8% O2 ($p<0.0001$), and control ($p<0.0001$); and in lower levels in those incubated at 8% O2 compared to control ($p<0.05$). There seem to be higher levels of secreted interferon gamma-induced protein 10 (IP-10) by PLVP incubated at normal (20% O2) and 8% O2 conditions compared to those incubated under hypoxia (1%O2), though without any significant difference.

Two growth factors: fibroblast growth factor 2 (FGF-2) and vascular endothelial growth factor (VEGF), were identified at high levels in PLVP supernatant (Figure 1.C). FGF-2 levels were significantly higher at 8% O2 (control vs 8%O2, $p<0.001$), but lower at 1% O2 (control vs 1%O2; $p<0.0001$). VEGF levels were significantly higher when PLVP were incubated at 1% O2 conditions (1,064 ± 51 pg/ml) compared to both control and 8% O2 conditions (both $p<0.0001$). At lower quantities, G-CSF and GM-CSF were also secreted in higher levels at 1% O2 conditions in comparison to 20% and 8% O2 conditions (both non-significant). Overall, PLVP released IL-6, IL-8 and VEGF in increasing amounts from 20% O2 to 1% O2.
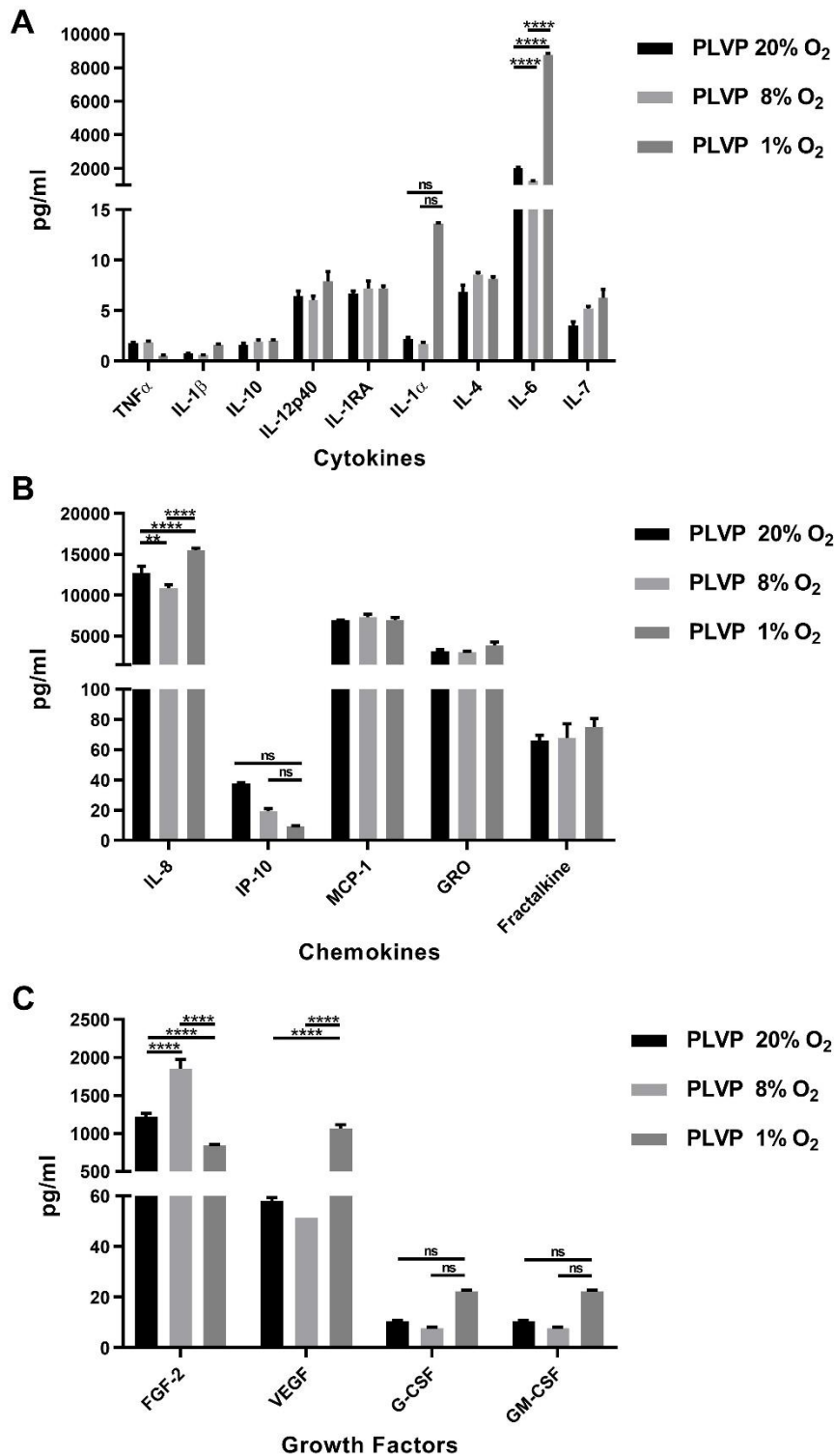
Figure 5. 2. MILLIPLEX assay analysis of PLVP supernatant after a 24-hour incubation in 20, 8 and 1% O_2 conditions (n=3). Cytokine (A) chemokine (B), and growth factors (C) profiles secreted in PLVP supernatant at different growth conditions. Data presented as Mean ± SEM, significant difference shown as p<0.01 (**), p<0.001 (***), p<0.0001 (****) or non-significant (ns).

5.5.3. Isolated PLVP-derived EV confirmed microvesicular and exosomal phenotype and increased in number under hypoxic conditions

PLVP cell lysate and PLVP derived EV (PLVPmv and PLVPex) were collected from PLVP supernatant incubated under 20, 8 and 1% O_2 conditions (n=3; **Figure 5.3**). PLVPex, but not PLVPmv, were shown to express well-known exosomal markers such as Alix, Syntenin and CD9, and loading control Actin (**Figure 5.3A**). Surprisingly, PLVP also expressed Alix and Syntenin, probably due to continuing production of exosomes intracellularly.

NTA was used to ascertain the particle size and number of PLVPmv (**Figure 5.3B**), and PLVPex (**Figure 5.3C**). PLVPmv showed a heterogeneous size distribution (EV ≥200 nm; **Figure 5.3Bi**). PLVPmv were found to be significantly increased in particle number as the O_2 percentage dropped (control vs 1% O_2, $p<0.001$; 8% O_2 vs 1% O_2, $p<0.001$; **Figure 5.3Bii**), while modal size remained unchanged between samples (**Figure 5.3Biii**). PLVPex demonstrated a more homogenous size distribution (EV≤ 200nm; **Figure 5.3Ci**). PLVPex increased significantly in particle number under more hypoxic (control vs 8% O_2: $p<0.05$; control vs 1% O_2: $p<0.0001$; **Figure 5.3Cii**). PLVPex modal size remained unchanged between samples (**Figure 5.3Ciii**).

Since the amount of isolated PLVPmv material was quite limited, we decided to focus on PLVPex.
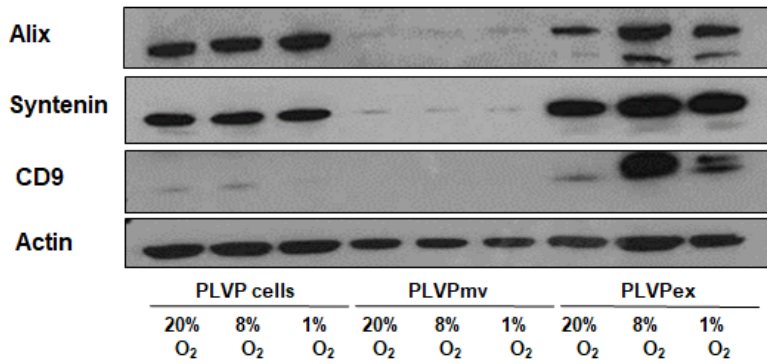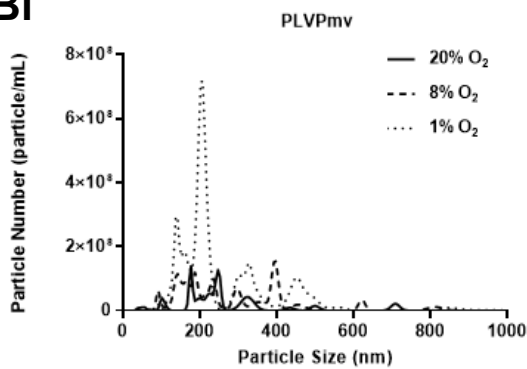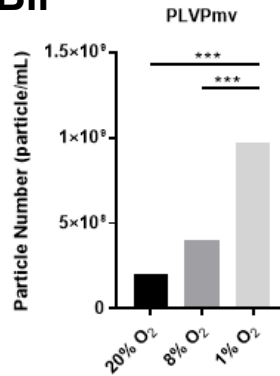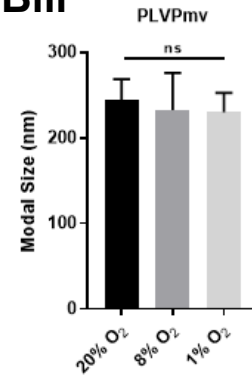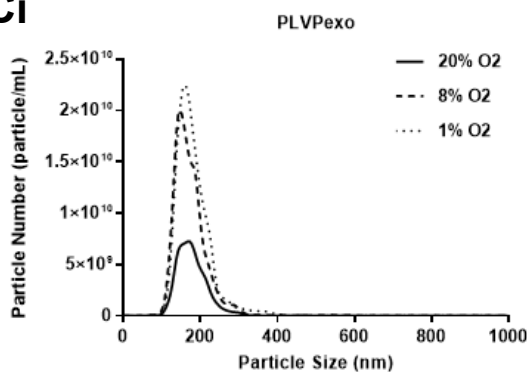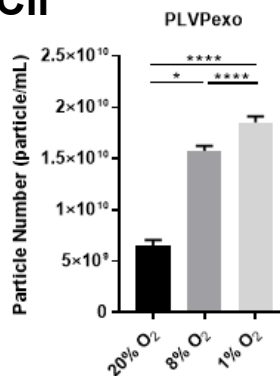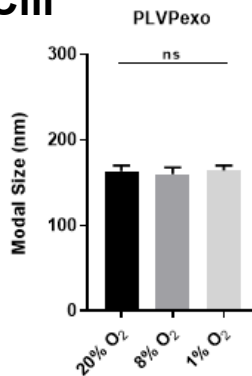
Figure 5. 3. Characterisation and analysis of PLVPev, PLVPmv and PLVPex. A, Representative immunoblot showing enrichment of Actin (42 KDa), the loading control on PLVP cell lysate, PLVPmv and PLVPex; and enrichment of exosomal markers Alix (96 KDa), Syntenin (60 kDa) and CD9 (24 kDa) on mainly PLPVex. B, Representative NTA size and particle number distribution profiles of PLVPmv (Bi), focusing on particle number changes among PLVPmv samples (Bii) and modal size (Biii). C, Representative NTA size and particle number distribution profiles of PLVPex (Ci), focusing on particle number changes among PLVPex samples (Cii) and modal size (Ciii). Data presented as Mean ± SEM, significant difference shown as $p < 0.05$ (*), $p < 0.001$ (***), $p < 0.0001$ (****) or non-significant (ns).

5.5.4. Determining non-toxic PLVPex particle number for functional studies

Before functional studies, we determined the non-toxic particle concentration that could be used to treat HUVEC (n=3; **Figure 5.4**). We used the CellTox^{TM} Green cytotoxicity assay, in which cyanine dye binds DNA released by dead cells following the disruption of the cell membrane. Experiments were set up using three-particle concentrations (1 x 10^8, 1 x 10^9 and 1 x 10^{10} particles/mL) derived from each O_2 condition, each in triplicate. **Figure 5.4A** shows the treatment of PLVPex derived from different O_2 percentage conditions on HUVEC over 21 hours, demonstrating the maximum cytotoxicity (red line), untreated/control (green line) and the three PLVPex particle concentrations. There was not much difference in the fluorescence emitted by cells treated with PLVPex (1 x 10^8 -1 x 10^{10} particles/mL) compared to control. However, the fluorescent intensity seemed to rise as the particle number increased over time, especially HUVEC treated with PLVPex derived from 1% O_2 condition. Thus, we decided that 1 x10^9 particle/mL, the median EV concentration, which showed low cytotoxic effects among the three O_2 conditions (**Figure 5.4B**), would be optimal for subsequent experiments.
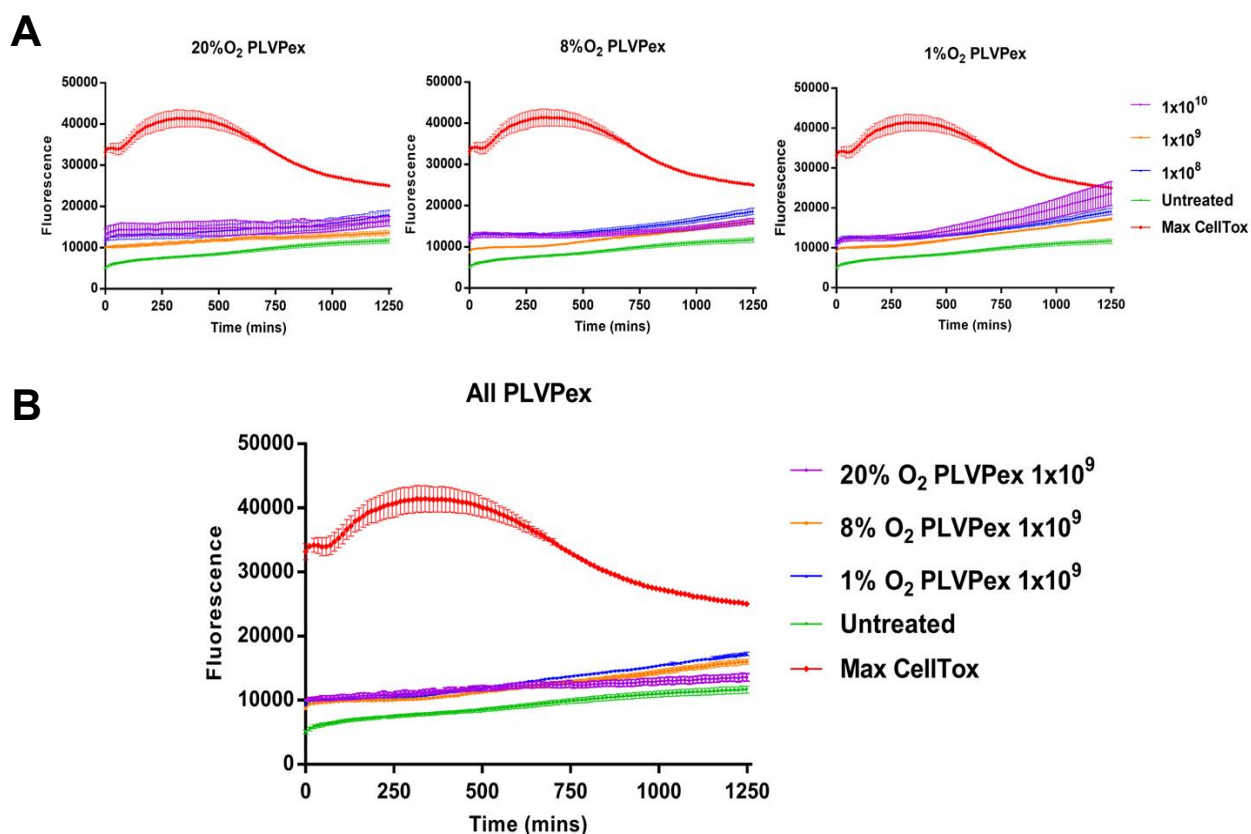
Figure 5. 4. CellToxTM Green cytotoxicity assay to determine non-toxic PLVPex particle concentration on HUVEC. A, Cytotoxicity of PLVPex derived from each O2 conditions at varying particle concentrations and B, cytotoxicity comparison of chosen PLVPex particle concentration (1 x 109 particle/mL) derived from each O2 condition.

5.5.5. Confocal microscopy to assess internalisation of PKH26 stained PLVPex into HUVEC

Confocal microscopy was used to interrogate whether PLVPex derived normal O$_2$ conditions were being internalised by HUVEC at different time points (2 and 6 hours; n=3; **Figure 5.5**). PLVPex from normal O$_2$ conditions (20% O$_2$) were pre-stained with PKH26 dye (red), the HUVEC membrane was labelled with WGA-Alexa 488 (green) and the cell nuclei with Hoechst 33342 (blue). PLVPex derived from normal conditions appeared to be internalised by HUVEC in similar numbers at both incubation time points. Due to the low PLVPex material, we decided to save PLVPex derived from hypoxic conditions for subsequent studies, assuming that these would also be internalised by HUVEC as those derived from normal conditions.
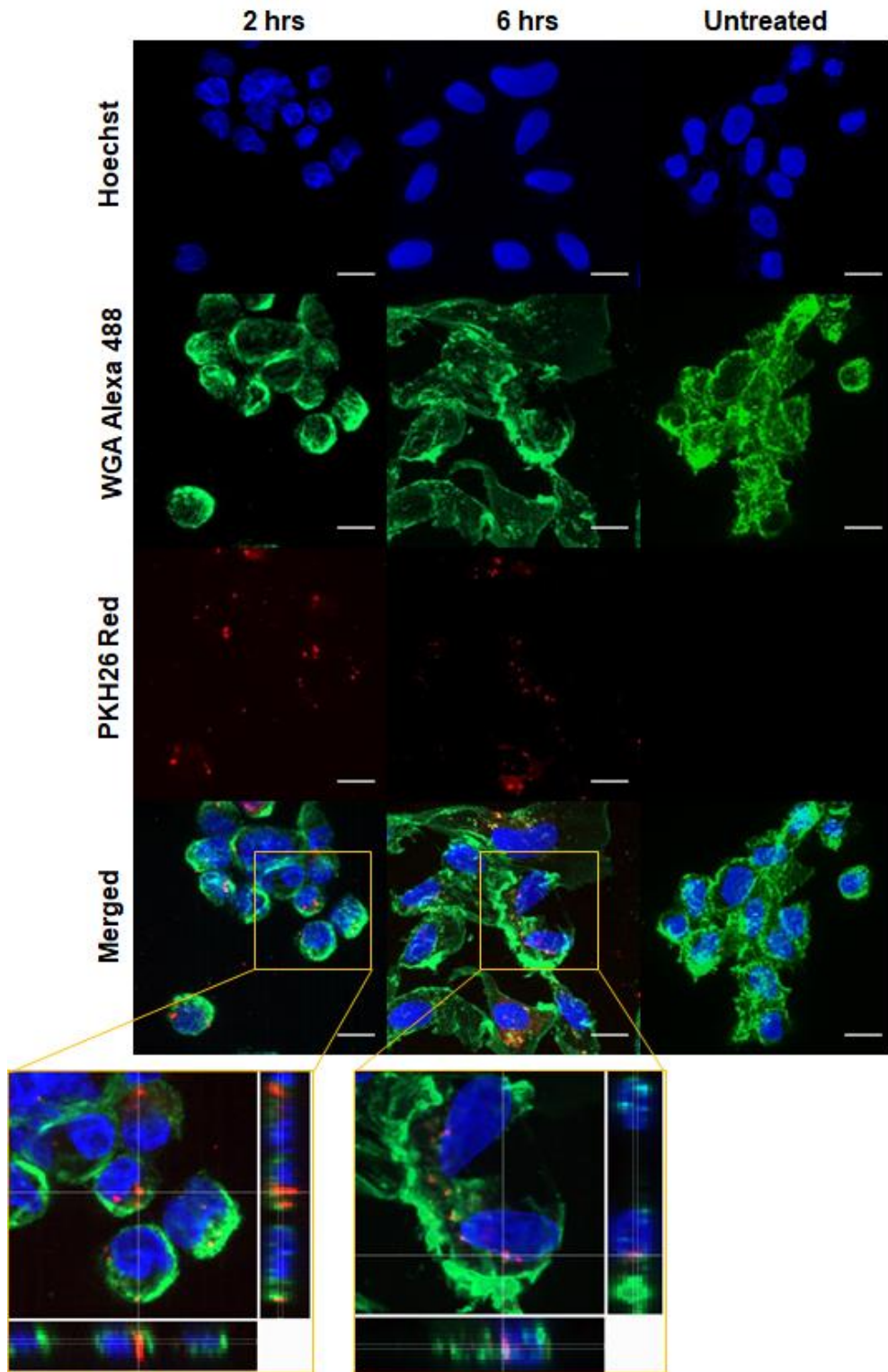
Figure 5. 5. The internalisation of PLVPex derived from normal O_2 conditions (20% O_2) into HUVEC by confocal microscopy (n=3). HUVEC treated with PKH26 stained PLVPex at 1 x10^9 particle/mL at 2- and 6-hours incubation. Channels panel show cells' nuclei labelled with Hoechst dye (blue), cells' membrane labelled with WGA Alexa 488 (green), PLVPex labelled with PKH26 dye (red) and merged channels. HUVEC incubated with no PLVPex were used as the control. Scale bars, 10 μm.

5.5.6. PLVPex stimulates HUVEC tube length and polygon formation

PLVPex and factors derived from PLVP incubated in normal and hypoxic conditions were used to treat HUVEC using a matrigel tube formation assay (n=3; Figure 5.6). Using the same number of particles/ml (1 x109), PLVPex stimulated a significant increase in polygon number on HUVEC compared to untreated HUVEC, regardless of the O2 conditions in which PLVP were cultured (Figure 4.B). There were no significant differences in polygon number between PLVPex derived from cells cultured in 20%, 8% or 1% O2. HUVEC were also treated with EV-free supernatant from PVLP cultured in different O2 conditions. Only HUVEC treated with EV-free supernatant derived from 1% O2 conditions revealed a significantly reduced polygon number when compared to untreated HUVEC ($p<0.05$) and EV-free supernatant from 20% O2 conditions ($p<0.05$).

PLVPex also stimulated a significant increase in HUVEC tube formation length compared to no treatment (under all three O2 conditions) (Figure 4C). Again, there were no significant differences in tube formation length between PLVPex derived from cells cultured in different O2 conditions. Similarly, EV-free supernatant from PLVP cultured under 1% O2 conditions, reduced HUVEC tube formation length compared to untreated HUVEC ($p<0.05$) and EV-free supernatant from 20% O2 ($p<0.05$).

These results suggest that PLVPex at the same particle number stimulate tube formation in HUVEC, irrespective of O2 percentage. Conversely the secreted factors in the EV-free supernatant from PLVP inhibited HUVEC tube formation as the O2 concentration decreased.
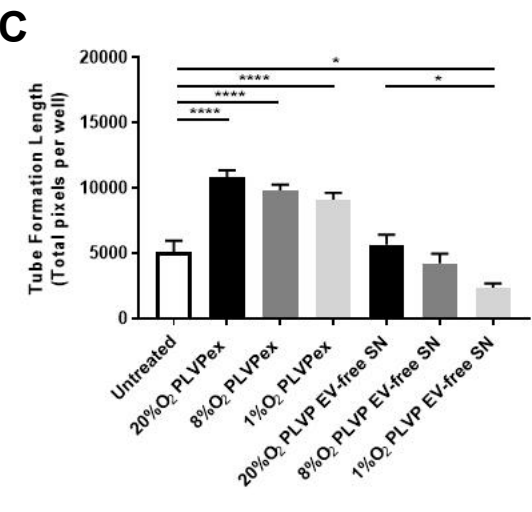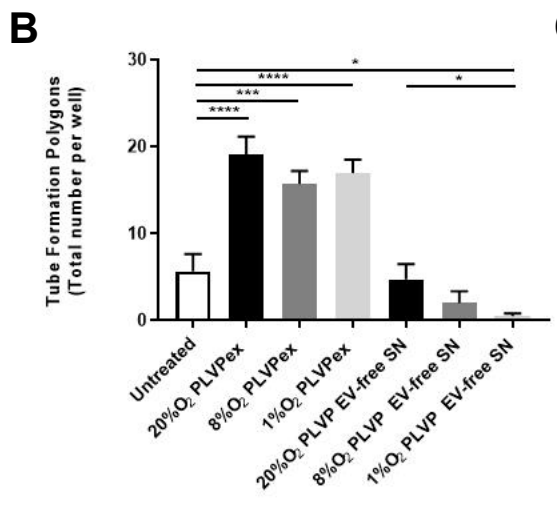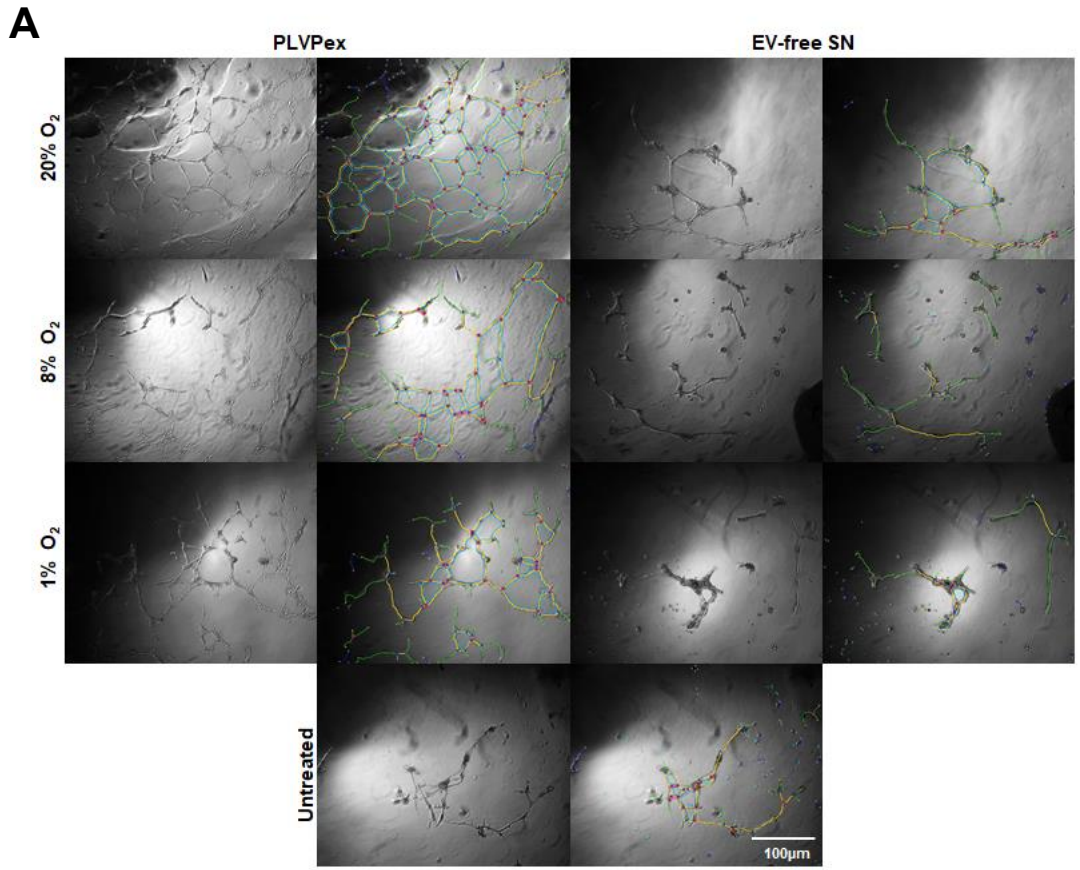
Figure 5. 6. Tube formation analysis of HUVEC treated with PLVPex and EV-free supernatant from normal and hypoxic conditions (n=3). A, Captured images analysed by ImageJ software of HUVEC treated with PLVPex and EV-free SN (EV-free supernatant) derived from 20 %, 8% and 1% O2 conditions and untreated HUVEC. Analysis of HUVEC tube polygon formation (B) and tube length formation (C) when treated with each sample. Data presented as Mean ± SEM, significant difference shown as p<0.05 (*), p<0.01 (**), p<0.001 (***), p<0.0001 (****). Scale bar, 100 µm.

5.5.7. Mass Spectrometry Analysis of PLVPex

To understand fully the likely mechanism of tube formation, we carried out mass spectrometry analysis on PLVPex derived from 20%, 8% and 1% O_2 conditions (pooled of n=3 technical repeats). **Figure 5.7** shows a Venn diagram where 640 proteins were identified from all three PLVPex samples. We were able to locate 366 protein molecules in common among all PLVPex. 93 proteins were shared among 20% O_2 PLVPex and 8% O_2 PLVPex; 62 proteins were shared among 20% O_2 PLVPex and 1% O_2 PLVPex; and 4 proteins were shared among 8% O_2 PLVPex and 1% O_2 PLVPex. Unique peptides were also found per group: 20% O_2 PLVPex (150 proteins), 8% O_2 PLVPex (11 proteins) and 1% O_2 PLVPex (16 proteins).
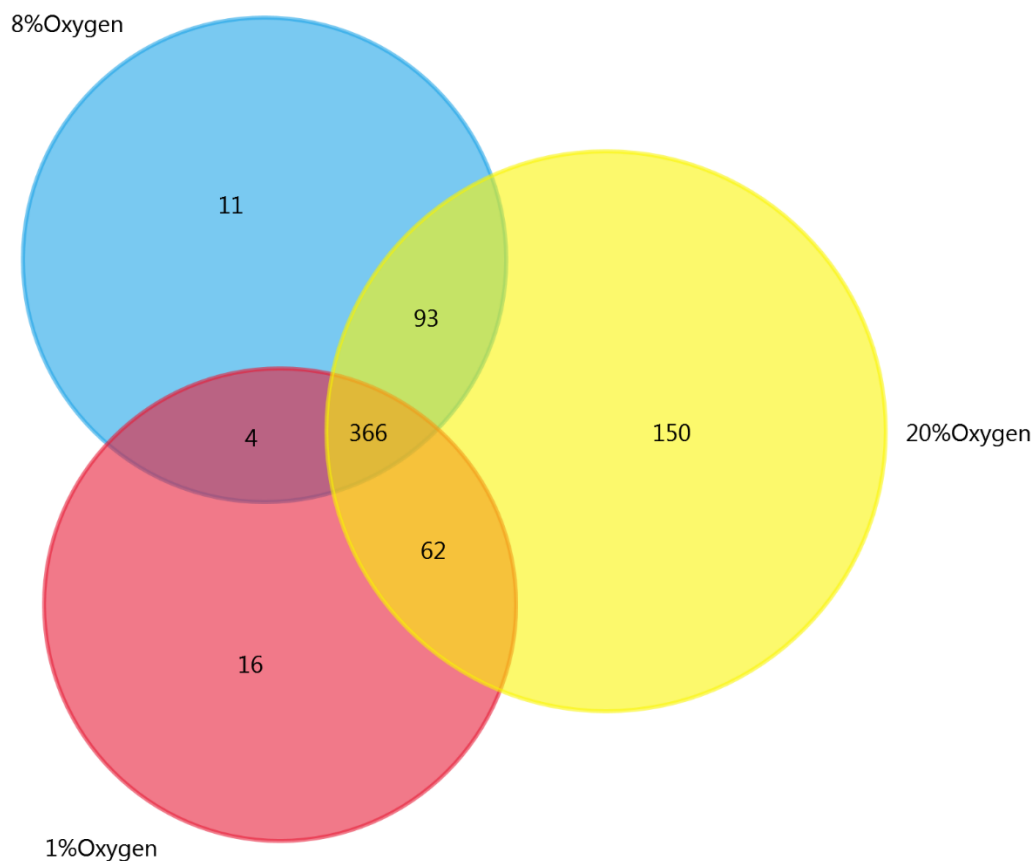
Figure 5. 7. Mass spectrometry analysis of PLVPex derived from 20%, 8% and 1% O_2 conditions.

Top five biological pathways identified from mass spectrometry analysis of PLVPex samples are summarised in a chart in **Figure 5.8**. Top biological pathways included signalling networks such as syndecan-1 mediated, VEGF and VEGFR, proteoglycan

syndecan-mediated, β1-integrin and integrin-family cell surface interactions. The chart demonstrated that PLVPex derived from all O_2 conditions expressed from 34.8 % to 43% of proteins that contribute to these biological pathways.

In particular, proteins contributing to the VEGF and VEGFR signalling network were identified in each PLVPex sample. Lower the O_2 percentage conditions, higher the expression of proteins of this signalling network, although this increase is not significant. PLVPex derived from 20% O_2 conditions expressed 149 out of 420 proteins available in the biological pathway database (35.5%, p<0.001). Similarly, 8% O_2 PLVPex expressed 115 out of 313 proteins (36.74%, p<0.001), while 1% O_2 PLVPex expressed 110 out of 279 proteins (39.3%, p<0.001). Well-known molecules from the VEGF and VEGFR signalling network identified on PLVPex from all O_2 conditions included soluble Flt-1 (FLT1), Neuropilin 1 (NRP1), Endoglin (ENG), TGF beta receptor 2 (TGFβR2) and PDGFRβ among others.

Top five biological processes identified from mass spectrometry analysis of PLVPex samples are summarised in **Figure 5.9**. Top biological processes included cell communication, transport, signal transduction, protein metabolism and cell growth and maintenance. In general, each PLVPex sample expressed similar percentages of proteins contributing to each biological process, without revealing any significant trend. Only the portion of PLVPex derived from 8% O_2 conditions showed a reduction in the cell communication process compared to PLVPex from control and 1% O_2 conditions.

We were interested in the proteins contributing to the cell growth and//or maintenance process. The chart demonstrated that PLVPex derived from all O_2 conditions expressed from 16.2% to 19.7% of proteins that contribute to these biological processes. PLVPex derived from 20% O_2 conditions expressed 106 out of 656 proteins available in the biological process database (16.2 %, p<0.001). Similarly, 8 % O_2 PLVPex expressed 82 out of 462 proteins (17.7 %, p<0.001), while 1% O_2 PLVPex expressed 86 out of 437 proteins (19.7 %, p<0.001). Molecules from the cell growth and maintenance identified on PLVPex from all O_2 conditions included collagen type II alpha chain 1 (COL2A1), Biglycan (BGN), laminin subunit beta 1 (LAMβ1), actinin 4 and vimentin among others.
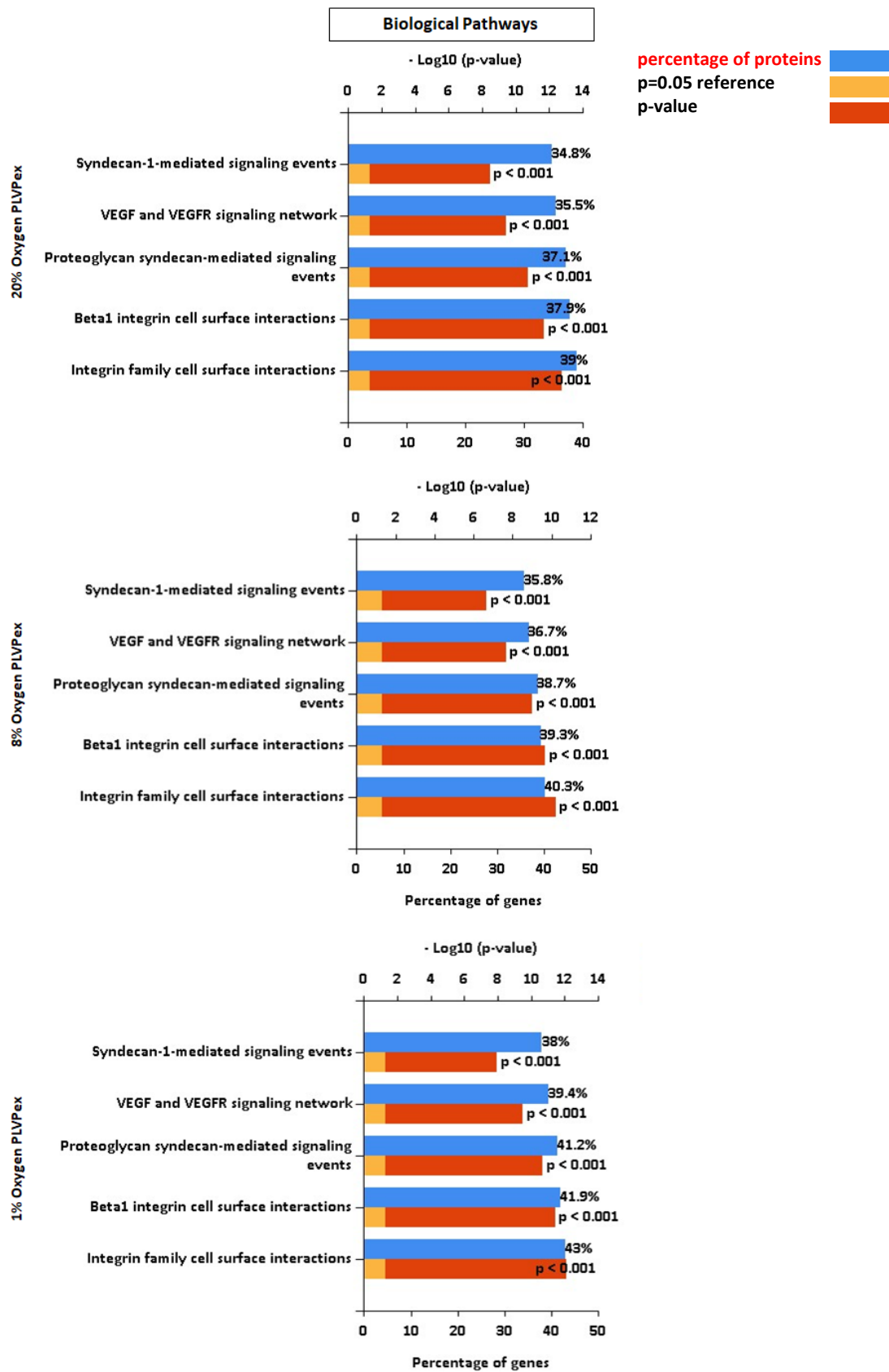
Figure 5. 8. Biological pathways found in mass spectrometry PROGENESIS analysis of PLVPex derived from 20%, 8% and 1% O$_2$ conditions.
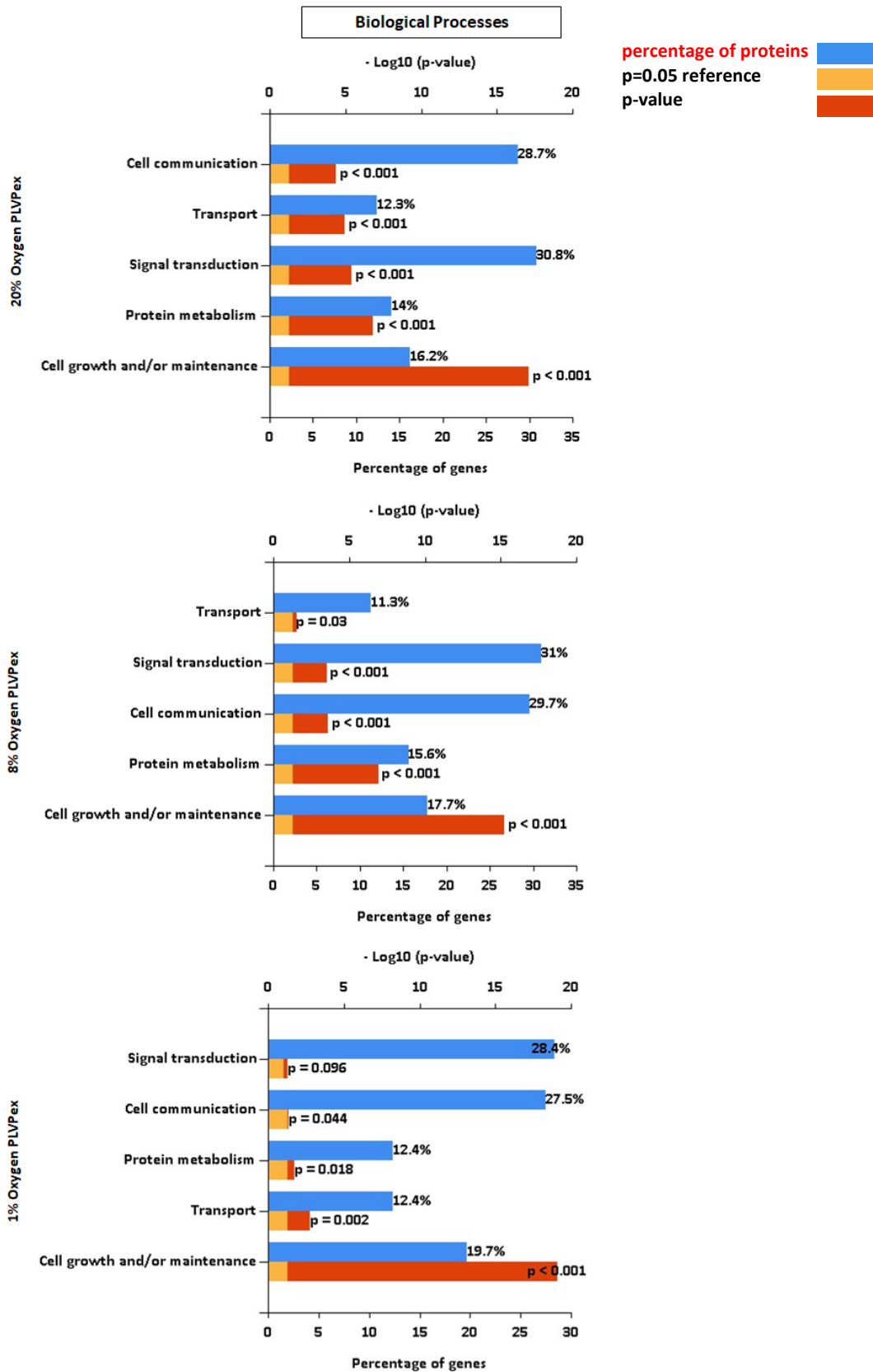
Figure 5. 9. Biological processes found in mass spectrometry PROGENESIS analysis of PLVPex derived from 20%, 8% and 1% O$_2$ conditions.

5.5.8. Mass Spectrometry validation of pro-angiogenic factors carried within PLVPex

We individually interrogated the mass spectrometry analysis for the presence of pro-angiogenic proteins and confirmed exosomal phenotype by the presence of specific exosomal markers (**Table 5.1**). As the starting material gathered for this mass spectrometry analysis was quite low in regards to protein concentration, we decided to focus on most abundant proteins.

We identified some essential pro-angiogenic molecules including NRP1, ENG and PDGFRβ. There was no significant difference between each PLVPex condition. Most significantly, NRP1 was shown to be present via highest number of unique peptides (24) and confidence score (1,263.7) compared to our other chosen proteins.

We were also able to identify exosomal markers CD9 and Syntenin, but not Alix, confirming our PLVPex material possess an exosomal phenotype.

Protein	Unique peptides	Confidence Score	Normalised abundance			Spectral Count		
			1%	8%	20%	1%	8%	20%
NRP1	24	1,263.7	1,638,861	2,907,360	1,707,978	12	9	24
ENG	6	327.8	432,701	604,812	423,217	3	2	6
PDGFRB	3	110.2	46,721	63,250	38,665	1	0	3
CD9	2	140.7	362,130	772,525	451,558	2	1	3
Syntenin	13	721.2	4,517,733	4,283,341	4,494,915	10	8	11

Table 5. 1. Mass spectrometry analysis of PLVPex derived from 20%, 8% and 1% O_2 conditions (n=3). Presence of pro-angiogenic molecules: NRP1, neuropilin 1; ENG endoglin and PDGFRβ, platelet-derived growth factor receptor β. Presence of exosomes markers: CD9 and Syntenin.

Given these findings, we decided to corroborate the expression of these pro-angiogenic proteins connections and validate their presence on PLVPex via Western blotting (**Figure 5.10**). Using the String-Database platform, we were able to analyse the interaction map of our chosen proteins (PDGFRβ, NRP1 an ENG) found in the PLVPex derived from all three O_2 conditions, with no more of 5 interactors on the first shell (**Figure 5.10A**). The String analysis revealed the presence of other key pro-angiogenic molecules such as Flt1 and VEGR2 or KDR, among others. Soluble Flt1 was also shown in our Biological pathway from the PROGENESIS analysis.

Consequently, we decided to validate our MS analysis by Western blotting. Pooled PLVPex (n=3 technical replicates) were run on SS-PAGE and probed for chosen proteins (PDGFRβ, NRP1 and ENG), Actin as our loading control, and VEGFR2 as one of the interactors found in our String analysis (**Figure 5.10B**). Our results demonstrated that PLVPex derived from all three O_2 conditions express PDGFRβ and ENG at their corresponding molecular weights. Interestingly, we were not able to localise the monomer form of NRP1 (130 kDa) on PLVPex, but the dimer form (250 KDa). Furthermore, VEGR2 was expressed on PLVPex. The expression of the dimer form of NRP1 and VEGFR2 on PLVPex reveals that NRP1 is found in its active form on PLVPex, forming a bridge between VEGFR2 and VEGFA$_{165}$ (**Figure 5.10C**; Pellet-Many *et al.* 2008). Further investigations are needed to corroborate this hypothesis and to understand the purpose of this NRP1-VEGR2 bridge on the surface of PLVPex.
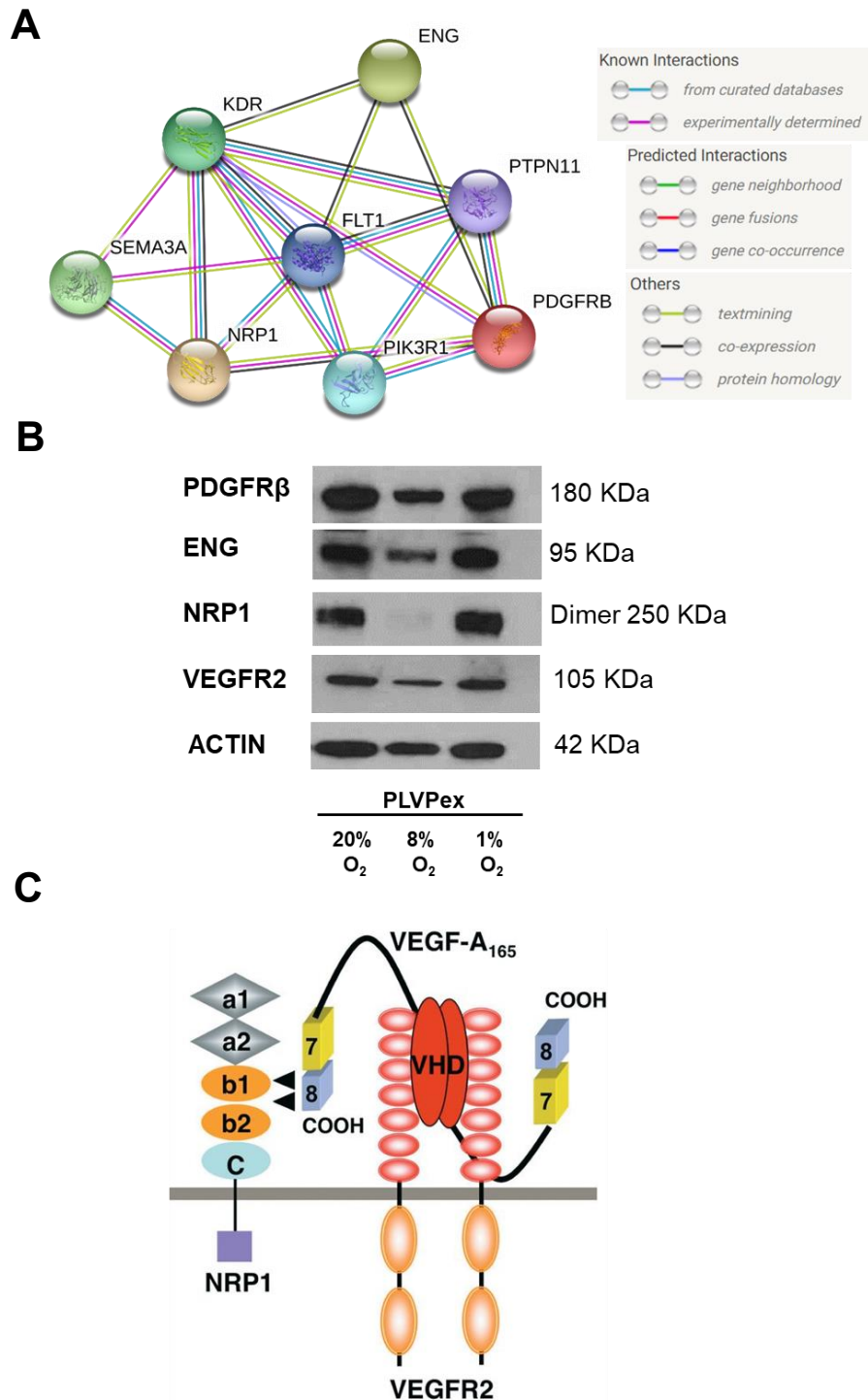
Figure 5. 10. Mass spectrometry analysis validation of pro-angiogenic molecules. A, STRING analysis on PDGFRβ, ENG, NRP1 and interactions with no more of 5 interactors on the first shell. B, Representative western blotting image of PLVPex protein from 20%, 8% and 1% O2 conditions (n=2) expressing PDGFRβ (180 KDa), ENG (95 KDa), as well as VEGFR2 or KDR (105 KDa). The dimer form of NRP1 (250 kDa) was observed but not its monomer form (130Kda). Actin was used as the loading control. C, Mechanism of VEGFA165 binding to NRP1. Image modified from (Pellet-Many *et al.* 2008a). STRING analysis was performed online at www.string-db.org.

5.6. Discussion

In this report, for the first time, we demonstrate in human placental capillary pericytes that severe hypoxia leads to secretion of different interleukins, growth factors, and exosomes (PLVPex). Additionally, we report the distinctive response of PLVP by showing the oxygen-dependent secretion of diverse molecules and PLVPex particle number. Moreover, we provide novel evidence that PLVP derived exosomes are secreted in a stimulus-specific manner by increasing in particle number as the oxygen gets reduced, can be internalised by endothelial cells as well as having a potential pro-angiogenic function by inducing tube formation in primary HUVEC and carrying growth factors in their protein cargo.

As mentioned in the background, pericytes are known to have immunoregulatory functions (Navarro *et al.* 2016). By responding to a series of different stimuli, pericytes have been shown to discharge a heterogenous secretion of pro/anti-inflammatory molecules, pleiotropic cytokines and various stem cell chemokines (Gaceb *et al.* 2018). Only a few papers use hypoxia as a form of stimulus on pericytes. Chen *et al.* showed microvascular pericytes to express high levels of IL-6, leukemia inhibitory factor, cyclooxygenase 2, heme oxygenase 1 (HMOX-1), and HIF-1α, which were sustained under hypoxic conditions (Chen *et al.* 2013). This study also reported pericytes to secrete molecules related to vascular physiology and remodelling; among which VEGFA, PDGFRβ, TGFβ 1 were substantially upregulated under hypoxia, while receptors such as FGF2, were suppressed (Chen *et al.* 2013). Another study revealed pericytes to increase their production of neurotrophins such as NGF, BDNF, NT4-5 (Ishitsuka *et al.* 2012) *in vitro* in response to hypoxia, emphasising a neuroprotective role of pericytes. Our results demonstrated that PLVP secreted IL-6 and VEGF under hypoxic conditions. However, FGF2 was substantially released by PLVP cultured in 8% O_2 hypoxia in comparison to 1% O_2. PLVP might also respond to hypoxia by releasing molecules to protect the vascular physiology and remodelling in the human placenta.

Likewise, pericyte increased NF-kB activation in response to muscle damage has been shown to enhance the proliferation and angiogenesis of co-cultured endothelial cells (LaBarbera *et al.* 2015). Thus, secretion of high levels of IL-8, RANTES and

153

monocyte chemoattractant protein-1 (MCP-1) have been postulated to mediate the cross-talk between pericytes and endothelial cells (LaBarbera *et al.* 2015). Although PLVP in our study secreted MCP-1, yet no difference was found among the O_2 conditions. Likewise, significant quantities of IL-8 in response to 1% O_2 hypoxia stimulus were produced by PLVP. The pro-angiogenic cytokine IL-8 is part of the CXC family, and it signals through CXCRA receptor to directly affect angiogenesis (Strieter *et al.* 1995). We should consider that the factors analysed in our study might be bound to PLVP derived EV, as PLVPex demonstrated tube formation stimulation when co-cultured with primary HUVEC.

PLVP have not been sufficiently explored in regards to their response to a stimulus. PLVP actively participates in the innate immune response. In response to inflammatory mediators, PLVP upregulated their expression of adhesion molecules ICAM-1 and released of chemoattractant MIF, activating leukocytes and 'instructing' them with pattern-recognition and motility programs (Stark *et al.* 2013). In addition, the placental growth factor (PLGF), an angiogenic factor that belongs to the VEGF family, has been found to be secreted by brain pericytes after being treated by PDGF-BB *in vivo* (Gaceb *et al.* 2017). Consequently, PLGF was also demonstrated to exhibit survival-promoting effects on cultured primary cortical neurons under oxygen and glucose deficiency (Du *et al.* 2010); to enhance angiogenesis in cerebral ischemia conditions (Liu *et al.* 2006), and to be upregulated predominately in vessels, neurons and astrocytes (Beck *et al.* 2002). Although we did not investigate these conditions or molecules in our study, it gives us an idea that PLVP might also contribute to the immunosurveillance and survival methods to deprived conditions.

We demonstrate, for the first time, that PLVP secretes EV (both microvesicles and exosomes), and this number increases in an oxygen percentage-dependent manner, possibly as a survival mechanism. Also, we showed PLVP derived exosomes internalisation on primary HUVEC and their stimulation of HUVEC tube formation using the same number of vesicles per O_2 % condition. Though hypoxia did not cause a significant difference in HUVEC tube formation, an excessive amount of exosomes released by PLVP under hypoxia, and the high production of pro-angiogenic molecules such as IL-8, VEGF and FGF-2, which might be bound to exosomes are important

observations to consider further. The EV free culturing conditioned media did not induce a pro-angiogenic function on HUVEC; instead, we observed an inhibitory behaviour especially at hypoxic conditions. This leads us to believe that exosomes exclusively mediated angiogenesis in HUVEC.

Our results align well with other studies on pericytes derived exosomes. Brain pericytes stimulated with $CoCl_2$ have been shown to promote wound healing in cell culture, cord formation in collagen matrices, and microvascular density in spinal cord explants through the secretion of exosomes (Mayo and Bearden, 2015). Similarly, Gaceb et al. demonstrated brain pericytes to secrete pro-regenerative molecules, including the release of microvesicles carrying growth factors, in response to PDGF-BB ligand treatment (Gaceb et al. 2017). This study have also emphasised the importance of extracellular vesicles in the signalling cell-to-cell communication between pericytes and endothelial cells, especially with respect to vessel regeneration and repair (Gaceb et al. 2018).

We are also the first to analyse protein content of exosomes derived from PLVP. We were able to identify several proteins reported to be involved in cell growth and maintenance, cell communication and signal transduction. PLVPex associated ENG, and NRP1 could promote the neighbouring cells' angiogenesis, as well as directly regulate cell communication and signal transduction through control protein PDGFRβ present in the vesicular cargo. Specifically, we found significantly high protein expression of NRP1 in our MS analysis. Interestingly, we showed only the dimer form of NRP1 and the appearance of VEGR2 on PLVPex by immunoblotting, implying the presence of $VEGFA_{165}$ -bridge forming between NRP1 and VEGFR2 (Pellet-Many et al. 2008a). NRP1 facilitates transduction of arterial effects of VEGF and has been shown to have essential roles in vascular and neuronal development (Pellet-Many et al. 2008b; Raimondi & Ruhrberg 2013). NRP1 has been shown to be critical for VEGF-induced sprouting and branching of endothelial cells by demonstrating attenuated angiogenesis and weak association with pericytes when p38MAPK inhibitor $VEGFA_{165}$-containing matrigel plugs were included (Kawamura et al. 2008). Another study showed that vessels from tumours treated with both anti-NRP1 and anti-VEGF lack a close association with pericytes, thus proposing that blocking NRP1 function

155

inhibits vascular remodelling (Pan *et al.* 2007). Hence, the secretion of PLVPex bound to active NRP1 in high amounts under hypoxia might potentially outline a survival mechanism by which PLVP sustain fetoplacental vasculogenesis and angiogenesis in response to reduce oxygen.

We are not the first to imply that the content of EV might have a role in the pericyte-endothelial cross-talk communication (Caporali *et al.* 2017). In response to high glucose culturing conditions, Caporali *et al.* showed the shedding of microparticles bound to miR-503 by endothelial cells, and the integrin-mediated uptake in the recipient pericytes to reduce the expression of ENFB2 and VEGFA, resulting in impaired migration and proliferation (Caporali *et al.* 2015). Another group revealed that stimulation with inflammatory cytokines and endotoxin-induced the shedding of endothelial cell-derived EV loaded with miRs such as miR-328-3p and 1et-7d-3p (Yamamoto *et al.* 2015). Correspondingly, microparticles uptake by pericytes upregulated their VEGF-B mRNA and protein expression which could regulate neovascularisation and vascular leakage after inflammatory stimuli (Yamamoto *et al.* 2015). However, these studies study the pericytes as the recipient target cells while we proposed that pericytes derived exosomes play a role in the regulation of endothelial cells' function.

Our study has some limitations. Hypoxia might not be the only factor implicated in PE, yet we were interested in using the available resources to establish the response of PLVP to reduce oxygen stimulus. Furthermore, our cultured PLVP isolated from one human placenta were purchased commercially. For this study, we were able to determine the pro-angiogenic functions of PLVPex under different oxygen conditions. Further investigation using primary PLVP and its derived EV from different patients from normal and complicated pregnancies is urgently required.

CHAPTER 6

General Discussion and Future Work

6. General discussion

Pregnancy is a fascinating and meaningful period in the lives of the parents-to-be and the rest of the family, but it also accompanies extensive changes in the maternal body systems to create and maintain a pregnancy-promoting environment. Several complications might occur during pregnancy. PE is one of the leading causes of maternal and perinatal morbidity and mortality, affecting 3-8% pregnancies worldwide (World Health Organization 2011). PE can jeopardise both the mother and the unborn fetus. The pathological mechanisms are not fully understood despite considerable research in the field. Both maternal and placental factors are thought to play a part in the development of the disease, including orchestrated communication between cells and tissues.

Recently, the role of EV has generated great interest due to their vital role in cell-to-cell communication. Notably, both microvesicles and exosomes can transfer the intravesicular cargo of proteins and nucleic acids to their target cells in the blood circulation, mediating intercellular communication throughout the entire circulatory system (Yáñez-Mó *et al.* 2015). EV derived from the placenta, specifically STBEV, have been demonstrated to be of great importance in normal and complicated pregnancies (Tannetta *et al.* 2014b, 2017b). In this thesis, we tested the hypothesis that STBEV (isolated from normal and preeclamptic placentae) may affect the maternal vascular and immune systems. Additionally, we investigated human PLVP, a wholly disregarded placental cell type that wraps around the endothelium, and have been postulated to be involved in signalling, angiogenesis and blood flow control (Armulik *et al.* 2011). We tested the hypothesis that PLVP secretes essential factors in response to hypoxia, including extracellular vesicles. Our data advances the current research in elucidating the mechanisms by which PE might occur.

6.1. The potential effect of STBEV on maternal vascular and immune system

Following a systematic approach to identify potential vascular molecules in PE, we encountered eNOS, an enzyme essential for the generation of NO, which it is a potent vasodilator in circulation. We were the first to demonstrate that both STBEV groups, STBMV and STBEX, transport functionally active bound eNOS. We confirmed that

iNOS, another enzyme known to be involved in NO production, was not expressed on either STBMV or STBEX, thus making STBEV-eNOS the first moiety. Furthermore, we established that eNOS co-localised with the specific placental marker, PLAP. This co-expression was also found in the circulating vesicles of both the peripheral and uterine vein blood, higher expression in the plasma derived from a uterine vein, reinforcing STBEV-bound eNOS originating from the placenta.

Most importantly, we interrogated the expression and activity of plasma and placenta-derived STBEV from both healthy and PE pregnancies. We reported STBEV-eNOS expression and activity to be reduced in PE, significantly in STBEX bound eNOS. PE is characterised by endothelial dysfunction, which results from generalised vasoconstriction and reduced blood to multiple organs (Roberts *et al.* 1990). NO synthesis deficiency has been shown to cause vasoconstriction and inadequate perfusion in the feto-maternal unit (Noris, Perico & Remuzzi 2005), partly explaining the pathogenies of PE. Our results suggest that STBEV-eNOS might contribute to the overall decreased NO bioavailability, generally associated with the endothelial dysfunction and overall maternal vascular manifestations seen in PE.

Calcium channel blockers (CCBs) are normally used in pregnancy and lactation to treat hypertension, arrhythmia, PE, and to prevent premature labour and its complications (Alabdulrazzaq & Koren 2012; Jiang et al. 2015). CCBs are direct smooth-muscle dilators that have a negative inotropic effect on the working myocardial cells of the atria and ventricles of the heart (Katz 1986). In vascular smooth muscle cells, entry of Ca^{2+} through the L-type calcium channels lead to activation to myosin light chain kinase which then leads to phosphorylation of light chain myosin, resulting in actin-myosin cross bridging which in turn leads to vasoconstriction. CCBs block the calcium channels resulting in vasodilation, predominantly in arteriolar smooth muscle. Our results resonates and provides understanding to the need of this treatment in PE. We showed that circulating eNOS bound STBMV expression is reduced in PE as well as isolated eNOS-bound STBEV activity in comparison to normal pregnancy derived STBEV. This means that NO synthesis via Ca^{2+} dependent-eNOS is defective in PE

due to low enzyme levels, thus defective vasodilation occurs which might lead to chronic hypertension.

We subsequently found that the NOS activity differed with gestational age, especially in STBMV derived from PE placentae. Although we observed reduced NO production on STBEV in PE, we realised that we should have divided STBEV between early-onset and late-onset PE. STBEV isolated from early-onset and late-onset PE could differ in cargo and function to target cells. Thus, we examined the possible functions of STBEV from normal and late-onset PE placentae to recipient immune cells, specifically a macrophage model, differentiated THP-1 macrophages. We showed that EV derived explicitly from the STB from late-onset PE and normal placentae can be internalised by differentiated THP-1 cells within 2 to 6 hours of treatment.

Interestingly, our data showed that STBEV derived from normal pregnancies caused a pro-inflammatory response by THP-1 cells while those from late-onset PE hardly altered the macrophage cytokine/chemokine profiles. Instead, STBEV from late-onset PE suppressed inflammatory response. Additionally, within the EV groups, we observed that STBMV, not STBEX, predominantly induced an effect on macrophages. The pathophysiology of early-onset and late-onset PE has been previously observed to vary (Von Dadelszen *et al.* 2003; Vatten and Skjaerven, 2004). However, there is not enough evidence suggesting different cargo and functions among these two groups. Thus, our data contribute to the progressively accumulating evidence that early- and late-onset PE are two distinct disease aetiologies of PE. Thus, STBEV could enter and ferry cargo into recipient cells, in this case, immune cells, enhancing or suppressing pro-inflammatory immune response.

6.2. The possible impact of PLVPex on fetal and placental development

Capillary pericytes have been shown to be essential in immunomodulation, vessel stabilisation and maturation, and angiogenesis and vascular homeostasis (Armulik *et al.* 2011; Navarro *et al.* 2016). PLVP have not been examined for their association with PE. Severe hypoxia has been associated with PE, thus, we investigated PLVP response under normal and hypoxic conditions. We found that PLVP released high

quantities of IL-6, IL-8, VEGF an FGF-2 under hypoxia. Furthermore, PLVP released EV, both microvesicles as well as exosomes, in higher quantities under hypoxic conditions.

Using PLVPex, we were also able to show, using the same number of particles, that PLVPex can enter inside and bring out a pro-angiogenic effect on primary HUVEC. Additionally, we indicated that PLVPex carry a cargo of proteins associated with cell growth and maintenance, and cell communication and signal transduction. In particular, we showed PLVPex to express PDGFRβ, a pericyte marker, as well as NRP1, ENG and VEGR2, molecules known to be involved in angiogenesis. Although hypoxia did not alter the pro-angiogenic function of PLVPex on primary HUVEC, reduced oxygen did induce a significant shedding of PLVPex. This might be a survival mechanism by which PLVP responds under hypoxic conditions.

Although few researchers have implicated extracellular vesicles as a signalling mechanism between capillary pericytes and endothelial cells (Caporali *et al.* 2017; Gaceb *et al.* 2018), we are the first to show that PLVP secrete exosomes carrying functional molecules that induce angiogenesis to EC. Hence, our data emphasised the importance of including PLVP in placental biology when investigating pregnancy complications, such as PE, due to its association with vessel formation. In addition, we also explored the idea that the placenta can secrete extracellular vesicles which might also signal to the fetal vasculature since PLVP wraps around the endothelium of capillary vessels.

6.3.   Future work

In Chapter 3, we have demonstrated STBEV carry active bound eNOS and that there is an overall reduced activity in STBEV from PE placentae. Although we have suggested that STBEV-eNOS is the central moiety synthesising low NO production, it would be interesting to confirm eNOS activity using circulating STBEV from plasma. Currently, it is challenging to isolate STBEV from plasma. Still, we have shown the expression of circulating microvesicles that co-express eNOS and PLAP, and display a low expression of eNOS+ PLAP+ levels in STBMV from PE using a method

developed in our laboratory (Zhang *et al. Unpublished*). It would be interesting to optimise this technique further and analyse both microvesicles and exosomes from plasma. Thereby, we could use FACS to sort those STBEV co-expressing eNOS and PLAP and test whether there is an activity difference among patient groups or among gestational trimesters.

Furthermore, microvesicles derived from plasma of PE patients have been shown to affect inflammation, apoptosis, and angiogenesis (Shomer *et al.* 2013). Accordingly, we could use plasma derived STBEV-eNOS from normal and preeclamptic women to treat EC and evaluate their impact on apoptosis, migration and tube formation, and corroborate whether STBEV-eNOS is the cause of endothelial dysfunction. Lastly, in pregnancy, endothelial dysfunction leading to hypertension is a known feature of PE. Thus, it would be remarkable if we could optimise the measurement of vesicular levels of eNOS specifically bound to STBEV in the plasma of healthy pregnancy and PE patients. Techniques such as flow cytometry or ELISA could help determine whether eNOS levels can predict which patients would develop hypertension in pregnancy.

Related to Chapter 4, a study has reported an exacerbated pro-inflammatory impact of EV from the plasma of PE patients to THP-1 macrophages (Kovács *et al.* 2018). However, this group did not consider the different PE groups, either divided microvesicles from exosomes, and used all circulating vesicles, not specifically those derived from the STB. Hence, it would be interesting to analyse whether specific PLAP positive EV from plasma from normal, early-onset, and late-onset patients induce a similar response from THP-1 macrophages. Likewise, it would be interesting to interrogate the protein and RNA content of circulating STBMV and STBEX, and examine whether there are any differences among STBEV and patients' groups. Perhaps, after examinations of these prospective results, we could find a specific marker for early-onset and late-onset PE, and further analyse their functions.

In Chapter 5, we showed that our PLVPex mainly carry the active dimer form of NRP1 and VEGR2, irrespective of oxygen treatment. First, it would be interesting to interrogate whether this complex NRP1-VEGFA$_{165}$-VEGR2 is fully expressed in

PLVPex. Furthermore, whether this complex modulates angiogenesis that have been observed in our PLVPex is unknown to us. We could do use magnetic Dynabeads to deplete our PLVPex from this complex, followed by treatment of these with primary HUVEC using the tube formation assay. It would also be interesting to interrogate if other molecules involved in the VEGF/VEGFR signalling network are also present on PLVPex.

Few protocols have been published about the isolation of capillary pericytes, especially those derived from the human placenta. It would be most exciting to isolate primary PLVP of placentae from normal and complicated pregnancies, such as early-onset PE and intrauterine growth restriction. Next, it would be fascinating to interrogate, using tube formation assays, whether PLVP from complicated pregnancies incubated with EC function differently to those from healthy placentae. Not only it would be remarkable to investigate the content mRNA content of these cells, but also the protein and mRNA cargo of derived extracellular vesicles.

6.4.   Conclusions

In conclusion, PE is a potentially fatal and distressing disorder for both the mother and the fetus. EV hold a potential which could be utilised to understand further the exact mechanisms by which the maternal and fetal manifestations of this disease may occur. Alternatively, EV could be used as diagnostic markers to endothelial dysfunction, or to distinguish between early and late-onset PE. The examination of EV in the unborn fetal plasma has not yet been explored. Here, we propose that the placenta not only sheds vesicles which may affect the maternal body systems as well as the fetoplacental vascularisation and angiogenesis, leading to fetus growth alterations.

REFERENCES

Abrahams, V.M. & Mor, G. 2005, 'Toll-like Receptors and their Role in the Trophoblast', Placenta, vol. 26, no. 7, pp. 540–7, viewed 22 October 2018, <https://www.sciencedirect.com/science/article/pii/S0143400404002243?via%3Dihub>.

Acosta-Sison, H. 1956, 'The relationship of hydatidiform mole to pre-eclampsia and eclampsia: A study of 85 cases', American Journal of Obstetrics and Gynecology, vol. 71, no. 6, pp. 1279–82, viewed 7 July 2018, <https://www.sciencedirect.com/science/article/pii/0002937856904379>.

Agrawal, V. & Hirsch, E. 2012, 'Intrauterine infection and preterm labor.', Seminars in fetal & neonatal medicine, vol. 17, no. 1, pp. 12–9, viewed 20 August 2018, <http://www.ncbi.nlm.nih.gov/pubmed/21944863>.

Al-Hijji, J., Andolf, E., Laurini, R. & Batra, S. 2003, 'Nitric oxide synthase activity in human trophoblast, term placenta and pregnant myometrium.', Reproductive biology and endocrinology : RB&E, vol. 1, p. 51, viewed 26 May 2018, <http://www.ncbi.nlm.nih.gov/pubmed/12875659>.

Alabdulrazzaq, F. & Koren, G. 2012, 'Fetal safety of calcium channel blockers.', Canadian family physician Medecin de famille canadien, vol. 58, no. 7, pp. 746–7, viewed 12 June 2019, <http://www.ncbi.nlm.nih.gov/pubmed/22798461>.

Andrew, P. & Mayer, B. 1999, 'Enzymatic function of nitric oxide synthases', Cardiovascular Research, vol. 43, no. 3, pp. 521–31, viewed 24 May 2018, <https://academic.oup.com/cardiovascres/article-lookup/doi/10.1016/S0008-6363(99)00115-7>.

Apps, R., Murphy, S.P., Fernando, R., Gardner, L., Ahad, T. & Moffett, A. 2009, 'Human leucocyte antigen (HLA) expression of primary trophoblast cells and placental cell lines, determined using single antigen beads to characterize allotype specificities of anti-HLA antibodies', Immunology, vol. 127, no. 1, pp. 26–39, viewed 22 October 2018, <http://doi.wiley.com/10.1111/j.1365-2567.2008.03019.x>.

Arck, P. & Hecher, K. 2013, 'Fetomaternal immune cross-talk and its consequences for maternal and offspring's health', Nature Medicine, vol. 19, no. 5, pp. 548–56, viewed 9 October 2017, <https://www.nature.com/nm/journal/v19/n5/pdf/nm.3160.pdf>.

Armulik, A., Genové, G. & Betsholtz, C. 2011, 'Pericytes: Developmental, Physiological, and Pathological Perspectives, Problems, and Promises', Developmental Cell, vol. 21, no. 2, pp. 193–215, viewed 23 August 2018, <https://www.sciencedirect.com/science/article/pii/S1534580711002693?via%3Dihub>.

Aronoff, D.M., Correa, H., Rogers, L.M., Arav-Boger, R. & Alcendor, D.J. 2017, 'Placental pericytes and cytomegalovirus infectivity: Implications for HCMV placental pathology and congenital disease', American Journal of Reproductive

Immunology, vol. 78, no. 3, p. e12728, viewed 6 December 2017, <http://doi.wiley.com/10.1111/aji.12728>.

Ashworth, J.R., Registrar, S., Chief Technician, A.Y.W., Johnson, I.R. & Baker, P.N. 1998, 'Plasma from pre-eclamptic women and functional change in myometrial resistance arteries', British Journal of Obstetrics and Gynaecology, vol. 105, viewed 26 May 2018, <https://obgyn.onlinelibrary.wiley.com/doi/pdf/10.1111/j.1471-0528.1998.tb10134.x>.

Askelund, K.J. & Chamley, L.W. 2011, 'Trophoblast deportation part I: Review of the evidence demonstrating trophoblast shedding and deportation during human pregnancy', Placenta, vol. 32, no. 10, pp. 716–23, viewed 6 November 2018, <https://www.sciencedirect.com/science/article/pii/S0143400411003390?via%3Dihub>.

Atay, S., Gercel-Taylor, C., Suttles, J., Mor, G. & Taylor, D.D. 2011, 'Trophoblast-Derived Exosomes Mediate Monocyte Recruitment and Differentiation', American Journal of Reproductive Immunology, vol. 65, no. 1, pp. 65–77, viewed 3 May 2018, <http://www.ncbi.nlm.nih.gov/pubmed/20560914>.

Atay, S., Gercel-Taylor, C. & Taylor, D.D. 2011, 'Human Trophoblast-Derived Exosomal Fibronectin Induces Pro-Inflammatory Il-1β Production by Macrophages', American Journal of Reproductive Immunology, vol. 66, no. 4, pp. 259–69, viewed 19 January 2018, <http://doi.wiley.com/10.1111/j.1600-0897.2011.00995.x>.

Attwell, D., Mishra, A., Hall, C.N., O'farrell, F.M. & Dalkara, T. 2016, 'What is a pericyte?', Journal of Cerebral Blood Flow & Metabolism, vol. 36, no. 2, pp. 451–5, viewed 23 August 2018, <http://journals.sagepub.com/doi/pdf/10.1177/0271678X15610340>.

Baban, B., Chandler, P.R., Sharma, M.D., Pihkala, J., Koni, P.A., Munn, D.H. & Mellor, A.L. 2009, 'IDO activates regulatory T cells and blocks their conversion into Th17-like T cells.', Journal of immunology (Baltimore, Md. : 1950), vol. 183, no. 4, pp. 2475–83, viewed 22 August 2018, <http://www.ncbi.nlm.nih.gov/pubmed/19635913>.

Baek, K.J., Thiel, B.A., Lucas, S. & Stuehr, D.J. 1993, 'Macrophage nitric oxide synthase subunits. Purification, characterization, and role of prosthetic groups and substrate in regulating their association into a dimeric enzyme.', The Journal of biological chemistry, vol. 268, no. 28, pp. 21120–9, viewed 24 May 2018, <http://www.ncbi.nlm.nih.gov/pubmed/7691806>.

Baker, P.N., Davidge, S.T. & Roberts, J.M. 1995, 'Plasma from women with preeclampsia increases endothelial cell nitric oxide production.', Hypertension (Dallas, Tex. : 1979), vol. 26, no. 2, pp. 244–8, viewed 26 May 2018, <http://www.ncbi.nlm.nih.gov/pubmed/7543451>.

Balabanov, R., Washington, R., Wagnerova, J. & Dore-Duffy, P. 1996, 'CNS Microvascular Pericytes Express Macrophage-like Function, Cell Surface

Integrin αM, and Macrophage Marker ED-2', Microvascular Research, vol. 52, no. 2, pp. 127–42, viewed 23 August 2018, <https://www.sciencedirect.com/science/article/pii/S0026286296900497?via%3Dihub>.

Barlow, K.D., Sanders, A.M., Soker, S., Ergun, S. & Metheny-Barlow, L.J. 2013, 'Pericytes on the Tumor Vasculature: Jekyll or Hyde?', Cancer Microenvironment, vol. 6, no. 1, pp. 1–17, viewed 23 August 2018, <http://link.springer.com/10.1007/s12307-012-0102-2>.

Barreto, R.S.N., Romagnolli, P., Cereta, A.D., Coimbra-Campos, L.M.C., Birbrair, A. & Miglino, M.A. 2019, 'Pericytes in the Placenta: Role in Placental Development and Homeostasis', Advances in experimental medicine and biology, vol. 1122, pp. 125–51, viewed 8 May 2019, <http://www.ncbi.nlm.nih.gov/pubmed/30937867>.

Beck, H., Acker, T., Püschel, A.W., Fujisawa, H., Carmeliet, P. & Plate, K.H. 2002, 'Cell Type-Specific Expression of Neuropilins in an MCA-Occlusion Model in Mice Suggests a Potential Role in Post-Ischemic Brain Remodeling', Journal of Neuropathology & Experimental Neurology, vol. 61, no. 4, pp. 339–50, viewed 8 November 2018, <https://academic.oup.com/jnen/article-lookup/doi/10.1093/jnen/61.4.339>.

Beltramo, E., Lopatina, T., Berrone, E., Mazzeo, A., Iavello, A., Camussi, G. & Porta, M. 2014, 'Extracellular vesicles derived from mesenchymal stem cells induce features of diabetic retinopathy in vitro', Acta Diabetologica, vol. 51, no. 6, pp. 1055–64, viewed 4 September 2018, <http://link.springer.com/10.1007/s00592-014-0672-1>.

Bergers, G. & Song, S. 2005, 'The role of pericytes in blood-vessel formation and maintenance', Neuro-Oncology, vol. 7, no. 4, pp. 452–64, viewed 23 August 2018, <http://academic.oup.com/neuro-oncology/article/7/4/452/1093750/The-role-of-pericytes-in-bloodvessel-formation-and>.

Bexell, D., Gunnarsson, S., Tormin, A., Darabi, A., Gisselsson, D., Roybon, L., Scheding, S. & Bengzon, J. 2009, 'Bone Marrow Multipotent Mesenchymal Stroma Cells Act as Pericyte-like Migratory Vehicles in Experimental Gliomas', Molecular Therapy, vol. 17, no. 1, pp. 183–90, viewed 23 August 2018, <https://www.sciencedirect.com/science/article/pii/S1525001616314903?via%3Dihub>.

Birbrair, A., Zhang, T., Wang, Z.-M., Messi, M.L., Enikolopov, G.N., Mintz, A. & Delbono, O. 2013, 'Skeletal muscle neural progenitor cells exhibit properties of NG2-glia', Experimental Cell Research, vol. 319, no. 1, pp. 45–63, viewed 4 September 2018, <https://www.sciencedirect.com/science/article/pii/S0014482712004004?via%3Dihub>.

Borzychowski, A.M., Sargent, I.L. & Redman, C.W.G. 2006, 'Inflammation and pre-eclampsia', Seminars in Fetal and Neonatal Medicine, vol. 11, no. 5, pp. 309–16, viewed 24 October 2018,

<https://www.sciencedirect.com/science/article/pii/S1744165X06000436?via%3 Dihub>.

Bouças, A.P., de Souza, B.M., Bauer, A.C. & Crispim, D. 2017, 'Role of Innate Immunity in Preeclampsia: A Systematic Review', Reproductive Sciences, vol. 24, no. 10, pp. 1362–70, viewed 22 August 2018, <http://journals.sagepub.com/doi/10.1177/1933719117691144>.

Bourque, S.L., Davidge, S.T. & Adams, M.A. 2011, 'The interaction between endothelin-1 and nitric oxide in the vasculature: new perspectives', American Journal of Physiology-Regulatory, Integrative and Comparative Physiology, vol. 300, no. 6, pp. R1288–95, viewed 30 May 2018, <http://www.physiology.org/doi/10.1152/ajpregu.00397.2010>.

Le Bouteiller, P. & Sargent, I.L. 2000, 'HLA Class I Molecules in the Placenta: Which ones, Where and What for?—A Workshop Report', Placenta, vol. 21, pp. S93–6, viewed 20 August 2018, <https://www.sciencedirect.com/science/article/pii/S0143400499905301?via%3 Dihub>.

Burke, S.D., Zsengellér, Z.K., Khankin, E. V, Lo, A.S., Rajakumar, A., DuPont, J.J., McCurley, A., Moss, M.E., Zhang, D., Clark, C.D., Wang, A., Seely, E.W., Kang, P.M., Stillman, I.E., Jaffe, I.Z. & Karumanchi, S.A. 2016, 'Soluble fms-like tyrosine kinase 1 promotes angiotensin II sensitivity in preeclampsia.', The Journal of clinical investigation, vol. 126, no. 7, pp. 2561–74, viewed 26 May 2018, <http://www.ncbi.nlm.nih.gov/pubmed/27270170>.

Burton, G.J., Charnock-Jones, D.S. & Jauniaux, E. 2009, 'Regulation of vascular growth and function in the human placenta.', Reproduction (Cambridge, England), vol. 138, no. 6, pp. 895–902, viewed 26 May 2018, <http://www.ncbi.nlm.nih.gov/pubmed/19470597>.

Burton, G.J. & Jones, C.J.P. 2009, 'Syncytial Knots, Sprouts, Apoptosis, and Trophoblast Deportation from the Human Placenta', Taiwanese Journal of Obstetrics and Gynecology, vol. 48, no. 1, pp. 28–37, viewed 6 November 2018, <https://www.sciencedirect.com/science/article/pii/S1028455909600322?via%3 Dihub>.

Caby, M.-P., Lankar, D., Vincendeau-Scherrer, C., Raposo, G. & Bonnerot, C. 2005, 'Exosomal-like vesicles are present in human blood plasma', International Immunology, vol. 17, no. 7, pp. 879–87, viewed 31 October 2018, <http://academic.oup.com/intimm/article/17/7/879/675097/Exosomallike-vesicles-are-present-in-human-blood>.

Cai, S., Khoo, J. & Channon, K.M. 2005, 'Augmented BH4 by gene transfer restores nitric oxide synthase function in hyperglycemic human endothelial cells', Cardiovascular Research, vol. 65, no. 4, pp. 823–31.

Caniggia, I., Winter, J., Lye, S.J. & Post, M. 2000, 'Oxygen and Placental Development During the First Trimester: Implications for the Pathophysiology of Pre-eclampsia', Placenta, vol. 21, pp. S25–30, viewed 7 November 2018,

<https://www.sciencedirect.com/science/article/pii/S0143400499905222?via%3
Dihub>.

Caporali, A., Martello, A., Miscianinov, V., Maselli, D., Vono, R. & Spinetti, G. 2017,
'Contribution of pericyte paracrine regulation of the endothelium to
angiogenesis', Pharmacology & Therapeutics, vol. 171, pp. 56–64, viewed 29
August 2018, <http://linkinghub.elsevier.com/retrieve/pii/S0163725816301796>.

Caporali, A., Meloni, M., Nailor, A., Mitić, T., Shantikumar, S., Riu, F., Sala-Newby,
G.B., Rose, L., Besnier, M., Katare, R., Voellenkle, C., Verkade, P., Martelli, F.,
Madeddu, P. & Emanueli, C. 2015, 'p75NTR-dependent activation of NF-κB
regulates microRNA-503 transcription and pericyte–endothelial crosstalk in
diabetes after limb ischaemia', Nature Communications, vol. 6, no. 1, p. 8024,
viewed 8 November 2018, <http://www.nature.com/articles/ncomms9024>.

Chaiworapongsa, T., Chaemsaithong, P., Yeo, L. & Romero, R. 2014, 'Pre-
eclampsia part 1: current understanding of its pathophysiology', Nature Reviews
Nephrology, vol. 10, no. 8, pp. 466–80, viewed 6 June 2018,
<http://www.nature.com/articles/nrneph.2014.102>.

Chargaff, E. & West, R. 1946, 'The biological significance of the thromboplastic
protein of blood.', The Journal of biological chemistry, vol. 166, no. 1, pp. 189–
97, viewed 31 October 2018, <http://www.ncbi.nlm.nih.gov/pubmed/20273687>.

Charnock-Jones, D.., Kaufmann, P. & Mayhew, T.. 2004, 'Aspects of Human
Fetoplacental Vasculogenesis and Angiogenesis. I. Molecular Regulation',
Placenta, vol. 25, no. 2–3, pp. 103–13, viewed 7 November 2018,
<https://www.sciencedirect.com/science/article/pii/S0143400403002753#BIB36
>.

Chatterjee, P., Weaver, L.E., Chiasson, V.L., Young, K.J. & Mitchell, B.M. 2011, 'Do
double-stranded RNA receptors play a role in preeclampsia?', Placenta, vol. 32,
no. 3, pp. 201–5, viewed 22 August 2018,
<http://www.ncbi.nlm.nih.gov/pubmed/21292321>.

Chatterjee, P., Weaver, L.E., Doersch, K.M., Kopriva, S.E., Chiasson, V.L., Allen,
S.J., Narayanan, A.M., Young, K.J., Jones, K.A., Kuehl, T.J. & Mitchell, B.M.
2012, 'Placental Toll-Like Receptor 3 and Toll-Like Receptor 7/8 Activation
Contributes to Preeclampsia in Humans and Mice', P.B. Szecsi (ed.),PLoS
ONE, vol. 7, no. 7, p. e41884, viewed 25 October 2018,
<https://dx.plos.org/10.1371/journal.pone.0041884>.

Chen, C.-W., Okada, M., Proto, J.D., Gao, X., Sekiya, N., Beckman, S.A., Corselli,
M., Crisan, M., Saparov, A., Tobita, K., Péault, B. & Huard, J. 2013, 'Human
Pericytes for Ischemic Heart Repair', STEM CELLS, vol. 31, no. 2, pp. 305–16,
viewed 7 November 2018, <http://doi.wiley.com/10.1002/stem.1285>.

Chen, Y., Huang, Y., Jiang, R. & Teng, Y. 2012, 'Syncytiotrophoblast-derived
microparticle shedding in early-onset and late-onset severe pre-eclampsia',
International Journal of Gynecology & Obstetrics, vol. 119, no. 3, pp. 234–8,
viewed 5 July 2018, <http://doi.wiley.com/10.1016/j.ijgo.2012.07.010>.

Chesley, L.C. 1972, 'Plasma and red cell volumes during pregnancy', American Journal of Obstetrics and Gynecology, vol. 112, no. 3, pp. 440–50, viewed 8 June 2018, <https://www.sciencedirect.com/science/article/pii/0002937872904930?via%3Dihub>.

Choi, J.W., Im, M.W. & Pai, S.H. 2002, 'Nitric oxide production increases during normal pregnancy and decreases in preeclampsia.', Annals of clinical and laboratory science, vol. 32, no. 3, pp. 257–63, viewed 29 May 2018, <http://www.ncbi.nlm.nih.gov/pubmed/12175088>.

Christiansen, O.B., Nielsen, H.S. & Kolte, A.M. 2006, 'Inflammation and miscarriage', Seminars in Fetal and Neonatal Medicine, vol. 11, no. 5, pp. 302–8, viewed 20 August 2018, <https://www.sciencedirect.com/science/article/pii/S1744165X0600031X?via%3Dihub>.

Cindrova-Davies, T., Yung, H.-W., Johns, J., Spasic-Boskovic, O., Korolchuk, S., Jauniaux, E., Burton, G.J. & Charnock-Jones, D.S. 2007, 'Oxidative Stress, Gene Expression, and Protein Changes Induced in the Human Placenta during Labor', The American Journal of Pathology, vol. 171, no. 4, pp. 1168–79, viewed 6 March 2019, <https://www.sciencedirect.com/science/article/pii/S0002944010623814?via%3Dihub>.

Clark, D.E., Smith, S.K., He, Y., Day, K.A., Licence, D.R., Corps, A.N., Lammoglia, R. & Charnock-Jones, D.S. 1998, 'A Vascular Endothelial Growth Factor Antagonist Is Produced by the Human Placenta and Released into the Maternal Circulation1', Biology of Reproduction, vol. 59, no. 6, pp. 1540–8, viewed 25 October 2018, <https://academic.oup.com/biolreprod/article-lookup/doi/10.1095/biolreprod59.6.1540>.

Cockell, a P., Learmont, J.G., Smárason, a K., Redman, C.W., Sargent, I.L. & Poston, L. 1997, 'Human placental syncytiotrophoblast microvillous membranes impair maternal vascular endothelial function.', British journal of obstetrics and gynaecology, vol. 104, no. 2, pp. 235–40.

Cockell, A.P., Learmont, J.G., Smarason, A.K., Redman, C.W.G., Sargent, I.L. & Poston, L. 1997, 'Human placental syncytiotrophoblast microvillous membranes impair maternal vascular endothelial function', BJOG: An International Journal of Obstetrics and Gynaecology, vol. 104, no. 2, pp. 235–40, viewed 8 March 2018, <http://doi.wiley.com/10.1111/j.1471-0528.1997.tb11052.x>.

Cocucci, E., Racchetti, G. & Meldolesi, J. 2009, 'Shedding microvesicles: artefacts no more', Trends in Cell Biology, pp. 43–51.

Colombo, M., Moita, C., van Niel, G., Kowal, J., Vigneron, J., Benaroch, P., Manel, N., Moita, L.F., Théry, C. & Raposo, G. 2013, 'Analysis of ESCRT functions in exosome biogenesis, composition and secretion highlights the heterogeneity of extracellular vesicles.', Journal of cell science, vol. 126, no. Pt 24, pp. 5553–65, viewed 31 October 2018, <http://www.ncbi.nlm.nih.gov/pubmed/24105262>.

Colombo, M., Raposo, G. & Théry, C. 2014, 'Biogenesis, Secretion, and Intercellular Interactions of Exosomes and Other Extracellular Vesicles', Annual Review of Cell and Developmental Biology, vol. 30, no. 1, pp. 255–89, viewed 31 October 2018, <http://www.annualreviews.org/doi/10.1146/annurev-cellbio-101512-122326>.

del Conde, I., Shrimpton, C.N., Thiagarajan, P. & Ló pez, J.A. 2005, Tissue-factor-bearing microvesicles arise from lipid rafts and fuse with activated platelets to initiate coagulation, viewed 31 October 2018, <www.bloodjournal.org>.

Condon, J.C., Jeyasuria, P., Faust, J.M. & Mendelson, C.R. 2004, 'Surfactant protein secreted by the maturing mouse fetal lung acts as a hormone that signals the initiation of parturition.', Proceedings of the National Academy of Sciences of the United States of America, vol. 101, no. 14, pp. 4978–83, viewed 20 August 2018, <http://www.ncbi.nlm.nih.gov/pubmed/15044702>.

Conrad, K.P. & Davis, A.K. 1995, 'Nitric oxide synthase activity in placentae from women with pre-eclampsia', Placenta, vol. 16, no. 8, pp. 691–9, viewed 26 May 2018, <https://www.sciencedirect.com/science/article/pii/0143400495900136?via%3Dihub>.

Conrad, K.P., Kerchner, L.J. & Mosher, M.D. 1999, 'Plasma and 24-h NO(x) and cGMP during normal pregnancy and preeclampsia in women on a reduced NO(x) diet.', The American journal of physiology, vol. 277, no. 1 Pt 2, pp. F48-57, viewed 26 May 2018, <http://www.ncbi.nlm.nih.gov/pubmed/10409297>.

Conrad, K.P., Vill, M., McGuire, P.G., Dail, W.G. & Davis, A.K. 1993, 'Expression of nitric oxide synthase by syncytiotrophoblast in human placental villi.', FASEB journal : official publication of the Federation of American Societies for Experimental Biology, vol. 7, no. 13, pp. 1269–76, viewed 26 May 2018, <http://www.ncbi.nlm.nih.gov/pubmed/7691671>.

Corselli, M., Crisan, M., Murray, I.R., West, C.C., Scholes, J., Codrea, F., Khan, N. & Péault, B. 2013, 'Identification of perivascular mesenchymal stromal/stem cells by flow cytometry', Cytometry Part A, vol. 83A, no. 8, pp. 714–20, viewed 4 September 2018, <http://doi.wiley.com/10.1002/cyto.a.22313>.

Costello, M.J., Joyce, S.K. & Abrahams, V.M. 2007, 'NOD Protein Expression and Function in First Trimester Trophoblast Cells', American Journal of Reproductive Immunology, vol. 57, no. 1, pp. 67–80, viewed 22 October 2018, <http://doi.wiley.com/10.1111/j.1600-0897.2006.00447.x>.

Crisan, M., Yap, S., Casteilla, L., Chen, C.-W., Corselli, M., Park, T.S., Andriolo, G., Sun, B., Zheng, B., Zhang, L., Norotte, C., Teng, P.-N., Traas, J., Schugar, R., Deasy, B.M., Badylak, S., Bűhring, H.-J., Giacobino, J.-P., Lazzari, L., Huard, J. & Péault, B. 2008, 'A Perivascular Origin for Mesenchymal Stem Cells in Multiple Human Organs', Cell Stem Cell, vol. 3, no. 3, pp. 301–13, viewed 23 August 2018, <https://www.sciencedirect.com/science/article/pii/S1934590908003378?via%3Dihub>.

Cronqvist, T., Tannetta, D., Mörgelin, M., Belting, M., Sargent, I., Familari, M. & Hansson, S.R. 2017, 'Syncytiotrophoblast derived extracellular vesicles transfer functional placental miRNAs to primary human endothelial cells.', Scientific reports, vol. 7, no. 1, p. 4558, viewed 5 July 2018, <http://www.ncbi.nlm.nih.gov/pubmed/28676635>.

d'Uscio, L. V. 2011, 'eNOS uncoupling in pulmonary hypertension', Cardiovascular Research, vol. 92, no. 3, pp. 359–60, viewed 30 May 2018, <https://academic.oup.com/cardiovascres/article-lookup/doi/10.1093/cvr/cvr270>.

Darmochwal-Kolarz, D., Kludka-Sternik, M., Tabarkiewicz, J., Kolarz, B., Rolinski, J., Leszczynska-Gorzelak, B. & Oleszczuk, J. 2012, 'The predominance of Th17 lymphocytes and decreased number and function of Treg cells in preeclampsia', Journal of Reproductive Immunology, vol. 93, no. 2, pp. 75–81, viewed 24 October 2018, <https://www.sciencedirect.com/science/article/pii/S0165037812000290?via%3Dihub>.

Davignon, J. & Ganz, P. 2004, 'Role of endothelial dysfunction in atherosclerosis.', Circulation, vol. 109, no. 23 Suppl 1, pp. III27-32, viewed 25 May 2018, <http://www.ncbi.nlm.nih.gov/pubmed/15198963>.

Davis, E.F., Lazdam, M., Lewandowski, A.J., Worton, S.A., Kelly, B., Kenworthy, Y., Adwani, S., Wilkinson, A.R., McCormick, K., Sargent, I., Redman, C. & Leeson, P. 2012, 'Cardiovascular Risk Factors in Children and Young Adults Born to Preeclamptic Pregnancies: A Systematic Review', Pediatrics, vol. 129, no. 6, pp. e1552–61.

Dekker, G. 2002, 'The partner's role in the etiology of preeclampsia', Journal of Reproductive Immunology, vol. 57, no. 1–2, pp. 203–15, viewed 7 June 2018, <https://www.sciencedirect.com/science/article/pii/S0165037802000396>.

Dekker, G., Robillard, P.Y. & Roberts, C. 2011, 'The etiology of preeclampsia: the role of the father', Journal of Reproductive Immunology, vol. 89, no. 2, pp. 126–32, viewed 7 June 2018, <https://www.sciencedirect.com/science/article/pii/S0165037811000465?via%3Dihub>.

Díaz-Flores, L., Gutiérrez, R., Madrid, J., Varela, H., Valladares, F., Acosta, E., Martín-Vasallo, P. & Díaz-Flores, J.L. 2009, 'Pericytes. Morphofunction, interactions and pathology in a quiescent and activated mesenchymal cell niche.', Histology and histopathology, vol. 24, no. 7, pp. 909–69, viewed 16 May 2019, <http://www.ncbi.nlm.nih.gov/pubmed/19475537>.

Djurisic, S. & Hviid, T.V.F. 2014, 'HLA Class Ib Molecules and Immune Cells in Pregnancy and Preeclampsia', Frontiers in Immunology, vol. 5, p. 652, viewed 22 October 2018, <http://journal.frontiersin.org/article/10.3389/fimmu.2014.00652/abstract>.

Dore-Duffy, P. & Cleary, K. 2011, Morphology and Properties of Pericytes, Humana

Press, pp. 49–68, viewed 23 August 2018,
<http://link.springer.com/10.1007/978-1-60761-938-3_2>.

Dore-Duffy, P., Owen, C., Balabanov, R., Murphy, S., Beaumont, T. & Rafols, J.A. 2000, 'Pericyte Migration from the Vascular Wall in Response to Traumatic Brain Injury', Microvascular Research, vol. 60, no. 1, pp. 55–69, viewed 25 October 2018, <https://www.sciencedirect.com/science/article/pii/S0026286200922441?via%3Dihub>.

Dötsch, J., Hogen, N., Nyúl, Z., Hänze, J., Knerr, I., Kirschbaum, M. & Rascher, W. 2001, 'Increase of endothelial nitric oxide synthase and endothelin-1 mRNA expression in human placenta during gestation.', European journal of obstetrics, gynecology, and reproductive biology, vol. 97, no. 2, pp. 163–7, viewed 29 May 2018, <http://www.ncbi.nlm.nih.gov/pubmed/11451542>.

Dragovic, R.A., Collett, G.P., Hole, P., Ferguson, D.J.P., Redman, C.W., Sargent, I.L. & Tannetta, D.S. 2015, 'Isolation of syncytiotrophoblast microvesicles and exosomes and their characterisation by multicolour flow cytometry and fluorescence Nanoparticle Tracking Analysis.', Methods (San Diego, Calif.), vol. 87, pp. 64–74, viewed 8 November 2017, <http://www.ncbi.nlm.nih.gov/pubmed/25843788>.

Dragovic, R.A., Gardiner, C., Brooks, A.S., Tannetta, D.S., Ferguson, D.J.P., Hole, P., Carr, B., Redman, C.W.G., Harris, A.L., Dobson, P.J., Harrison, P. & Sargent, I.L. 2011, 'Sizing and phenotyping of cellular vesicles using Nanoparticle Tracking Analysis.', Nanomedicine : nanotechnology, biology, and medicine, vol. 7, no. 6, pp. 780–8, viewed 11 June 2019, <http://www.ncbi.nlm.nih.gov/pubmed/21601655>.

Dragovic, R.A., Southcombe, J.H., Tannetta, D.S., Redman, C.W.G. & Sargent, I.L. 2013, 'Multicolor Flow Cytometry and Nanoparticle Tracking Analysis of Extracellular Vesicles in the Plasma of Normal Pregnant and Pre-eclamptic Women1', Biology of Reproduction, vol. 89, no. 6, viewed 7 July 2018, <https://academic.oup.com/biolreprod/article-lookup/doi/10.1095/biolreprod.113.113266>.

Du, H., Li, P., Pan, Y., Li, W., Hou, J., Chen, H., Wang, J. & Tang, H. 2010, 'Vascular endothelial growth factor signaling implicated in neuroprotective effects of placental growth factor in an in vitro ischemic model', Brain Research, vol. 1357, pp. 1–8, viewed 8 November 2018, <https://www.sciencedirect.com/science/article/pii/S0006899310015416>.

Du, R., Petritsch, C., Lu, K., Liu, P., Haller, A., Ganss, R., Song, H., Vandenberg, S. & Bergers, G. 2008, 'Matrix metalloproteinase-2 regulates vascular patterning and growth affecting tumor cell survival and invasion in GBM.', Neuro-oncology, vol. 10, no. 3, pp. 254–64, viewed 25 October 2018, <http://www.ncbi.nlm.nih.gov/pubmed/18359864>.

Duckitt, K. & Harrington, D. 2005, 'Risk factors for pre-eclampsia at antenatal booking: systematic review of controlled studies.', BMJ (Clinical research ed.),

vol. 330, no. 7491, p. 565, viewed 23 May 2018, <http://www.ncbi.nlm.nih.gov/pubmed/15743856>.

Duley, L. 2009, 'The Global Impact of Pre-eclampsia and Eclampsia', Seminars in Perinatology, vol. 33, no. 3, pp. 130–7, viewed 23 May 2018, <https://www.sciencedirect.com/science/article/pii/S0146000509000214?via%3Dihub>.

English, F.A., McCarthy, F.P., McSweeney, C.L., Quon, A.L., Morton, J.S., Sawamura, T., Davidge, S.T. & Kenny, L.C. 2013, 'Inhibition of Lectin-Like Oxidized Low-Density Lipoprotein-1 Receptor Protects Against Plasma-Mediated Vascular Dysfunction Associated With Pre-Eclampsia', American Journal of Hypertension, vol. 26, no. 2, pp. 279–86, viewed 26 May 2018, <https://academic.oup.com/ajh/article-lookup/doi/10.1093/ajh/hps035>.

Faas, M.M. & de Vos, P. 2017, 'Uterine NK cells and macrophages in pregnancy', Placenta, vol. 56, pp. 44–52, viewed 20 August 2018, <https://www.sciencedirect.com/science/article/pii/S0143400417301790>.

Filipe, V., Hawe, A. & Jiskoot, W. 2010, 'Critical evaluation of Nanoparticle Tracking Analysis (NTA) by NanoSight for the measurement of nanoparticles and protein aggregates.', Pharmaceutical research, vol. 27, no. 5, pp. 796–810, viewed 7 August 2018, <http://www.ncbi.nlm.nih.gov/pubmed/20204471>.

Förstermann, U. & Münzel, T. 2006, 'Endothelial nitric oxide synthase in vascular disease: from marvel to menace.', Circulation, vol. 113, no. 13, pp. 1708–14, viewed 25 May 2018, <http://www.ncbi.nlm.nih.gov/pubmed/16585403>.

Gaceb, A., Barbariga, M., Ozen, I.€ & Paul, G. 2018, 'The pericyte secretome: Potential impact on regeneration', Biochimie, viewed 29 August 2018, <https://doi.org/10.1016/j.biochi.2018.04.015>.

Gaceb, A., Ozen, I., Padel, T., Barbariga, M. & Paul, G. 2017, 'Pericytes secrete pro-regenerative molecules in response to platelet-derived growth factor-BB', Journal of Cerebral Blood Flow & Metabolism, vol. 38, no. 1, pp. 45–57, viewed 4 September 2018, <http://journals.sagepub.com/doi/pdf/10.1177/0271678X17719645>.

Gaengel, K., Genové, G., Armulik, A. & Betsholtz, C. 2009, 'Endothelial-Mural Cell Signaling in Vascular Development and Angiogenesis', ATVB In Focus Developmental Biology in the Vasculature, viewed 23 August 2018, <http://ahajournals.org>.

Gardiner, C., Tannetta, D.S., Simms, C.A., Harrison, P., Redman, C.W.G. & Sargent, I.L. 2011, 'Syncytiotrophoblast Microvesicles Released from Pre-Eclampsia Placentae Exhibit Increased Tissue Factor Activity', D.S. Milstone (ed.),PLoS ONE, vol. 6, no. 10, p. e26313, viewed 6 November 2018, <https://dx.plos.org/10.1371/journal.pone.0026313>.

Garvey, E.P., Oplinger, J.A., Furfine, E.S., Kiff, R.J., Laszlo, F., Whittle, B.J. & Knowles, R.G. 1997, '1400W is a slow, tight binding, and highly selective

inhibitor of inducible nitric-oxide synthase in vitro and in vivo', J.Biol.Chem., vol. 272, no. 8, pp. 4959–63.

Gauthier-Fisher, A., Szaraz, P. & Librach, C.L. 2019, Pericytes in the Umbilical Cord, Springer, Cham, pp. 211–33, viewed 8 May 2019, <http://link.springer.com/10.1007/978-3-030-11093-2_12>.

Genbacev, O., Joslin, R., Damsky, C.H., Polliotti, B.M. & Fisher, S.J. 1996, 'Hypoxia alters early gestation human cytotrophoblast differentiation/invasion in vitro and models the placental defects that occur in preeclampsia.', The Journal of clinical investigation, vol. 97, no. 2, pp. 540–50, viewed 8 June 2018, <http://www.ncbi.nlm.nih.gov/pubmed/8567979>.

Germain, S.J., Sacks, G.P., Sooranna, S.R., Soorana, S.R., Sargent, I.L. & Redman, C.W. 2007, 'Systemic inflammatory priming in normal pregnancy and preeclampsia: the role of circulating syncytiotrophoblast microparticles.', Journal of immunology (Baltimore, Md. : 1950), vol. 178, no. 9, pp. 5949–56, viewed 14 December 2017, <http://www.ncbi.nlm.nih.gov/pubmed/17442979>.

Gervasi, M.-T., Chaiworapongsa, T., Pacora, P., Naccasha, N., Yoon, B.H., Maymon, E. & Romero, R. 2001, 'Phenotypic and metabolic characteristics of monocytes and granulocytes in preeclampsia', American Journal of Obstetrics and Gynecology, vol. 185, no. 4, pp. 792–7, viewed 18 October 2018, <https://www.sciencedirect.com/science/article/pii/S0002937801440464?via%3 Dihub>.

Gnainsky, Y., Granot, I., Aldo, P., Barash, A., Or, Y., Mor, G. & Dekel, N. 2015, 'Biopsy-induced inflammatory conditions improve endometrial receptivity: the mechanism of action.', Reproduction (Cambridge, England), vol. 149, no. 1, pp. 75–85, viewed 20 August 2018, <http://www.ncbi.nlm.nih.gov/pubmed/25349438>.

Godo, S., Sawada, A., Saito, H., Ikeda, S., Enkhjargal, B., Suzuki, K., Tanaka, S. & Shimokawa, H. 2016, 'Disruption of Physiological Balance Between Nitric Oxide and Endothelium-Dependent Hyperpolarization Impairs Cardiovascular Homeostasis in Mice.', Arteriosclerosis, thrombosis, and vascular biology, vol. 36, no. 1, pp. 97–107, viewed 26 May 2018, <http://www.ncbi.nlm.nih.gov/pubmed/26543099>.

Goswami, D., Tannetta, D.S., Magee, L.A., Fuchisawa, A., Redman, C.W.G., Sargent, I.L. & von Dadelszen, P. 2006, 'Excess syncytiotrophoblast microparticle shedding is a feature of early-onset pre-eclampsia, but not normotensive intrauterine growth restriction', Placenta, vol. 27, no. 1, pp. 56–61, viewed 5 July 2018, <https://www.sciencedirect.com/science/article/pii/S0143400404002930?via%3 Dihub>.

Goswamia, D., Tannetta, D.S., Magee, L.A., Fuchisawa, A., Redman, C.W.G., Sargent, I.L. & von Dadelszen, P. 2006, 'Excess syncytiotrophoblast microparticle shedding is a feature of early-onset pre-eclampsia, but not normotensive intrauterine growth restriction', Placenta, vol. 27, no. 1, pp. 56–61.

Goumans, M.-J., Valdimarsdottir, G., Itoh, S., Rosendahl, A., Sideras, P. & ten Dijke, P. 2002, 'Balancing the activation state of the endothelium via two distinct TGF-beta type I receptors.', The EMBO journal, vol. 21, no. 7, pp. 1743–53, viewed 30 October 2018, <http://www.ncbi.nlm.nih.gov/pubmed/11927558>.

Guller, S., Tang, Z., Ma, Y.Y., Di Santo, S., Sager, R. & Schneider, H. 2011, 'Protein composition of microparticles shed from human placenta during placental perfusion: Potential role in angiogenesis and fibrinolysis in preeclampsia.', Placenta, vol. 32, no. 1, pp. 63–9, viewed 6 November 2018, <http://www.ncbi.nlm.nih.gov/pubmed/21074265>.

Gupta, A.K., Rusterholz, C., Huppertz, B., Malek, A., Schneider, H., Holzgreve, W. & Hahn, S. 2005, A Comparative Study of the Effect of Three Different Syncytiotrophoblast Micro-particles Preparations on Endothelial Cells, viewed 14 March 2018, <http://www.placentajournal.org/article/S0143-4004(04)00108-0/pdf>.

Hailu, F.G., Yihunie, G.T., Essa, A.A. & Tsega, W.K. 2017, 'Advanced abdominal pregnancy, with live fetus and severe preeclampsia, case report.', BMC pregnancy and childbirth, vol. 17, no. 1, p. 243, viewed 7 July 2018, <http://www.ncbi.nlm.nih.gov/pubmed/28747162>.

Hall, C.N., Reynell, C., Gesslein, B., Hamilton, N.B., Mishra, A., Sutherland, B.A., O'Farrell, F.M., Buchan, A.M., Lauritzen, M. & Attwell, D. 2014, 'Capillary pericytes regulate cerebral blood flow in health and disease', Nature, vol. 508, no. 7494, pp. 55–60, viewed 20 March 2018, <http://www.nature.com/articles/nature13165>.

Hamilton, N.B., Attwell, D. & Hall, C.N. 2010, 'Pericyte-mediated regulation of capillary diameter: a component of neurovascular coupling in health and disease', Frontiers in Neuroenergetics, vol. 2, p. 5, viewed 25 October 2018, <http://journal.frontiersin.org/article/10.3389/fnene.2010.00005/abstract>.

Hanna, J., Goldman-Wohl, D., Hamani, Y., Avraham, I., Greenfield, C., Natanson-Yaron, S., Prus, D., Cohen-Daniel, L., Arnon, T.I., Manaster, I., Gazit, R., Yutkin, V., Benharroch, D., Porgador, A., Keshet, E., Yagel, S. & Mandelboim, O. 2006, 'Decidual NK cells regulate key developmental processes at the human fetal-maternal interface', Nature Medicine, vol. 12, no. 9, pp. 1065–74, viewed 22 October 2018, <http://www.nature.com/articles/nm1452>.

Hansen, A.R., Barnés, C.M., Folkman, J. & McElrath, T.F. 2010, 'Maternal Preeclampsia Predicts the Development of Bronchopulmonary Dysplasia', The Journal of Pediatrics, vol. 156, no. 4, pp. 532–6, viewed 23 May 2018, <http://www.ncbi.nlm.nih.gov/pubmed/20004912>.

Harrison, P., Gardiner, C. & Sargent, I.L. 2014, Extracellular vesicles in health and disease, Pan Stanford.

Hayashi, T., Yamada, K., Esaki, T., Kuzuya, M., Satake, S., Ishikawa, T., Hidaka, H. & Iguchi, A. 1995, 'Estrogen Increases Endothelial Nitric Oxide by a Receptor Mediated System', Biochemical and Biophysical Research Communications, vol.

214, no. 3, pp. 847–55, viewed 24 May 2018, <https://www.sciencedirect.com/science/article/pii/S0006291X85723649>.

Hayden, M.R., Sowers, J.R. & Tyagi, S.C. 2005, 'The central role of vascular extracellular matrix and basement membrane remodeling in metabolic syndrome and type 2 diabetes: the matrix preloaded.', Cardiovascular diabetology, vol. 4, p. 9, viewed 25 October 2018, <http://www.ncbi.nlm.nih.gov/pubmed/15985157>.

Hayman, R., Warren, A., Johnson, I. & Baker, P. 2001, 'Inducible change in the behavior of resistance arteries from circulating factor in preeclampsia: An effect specific to myometrial vessels from pregnant women', American Journal of Obstetrics and Gynecology, vol. 184, no. 3, pp. 420–6, viewed 26 May 2018, <http://linkinghub.elsevier.com/retrieve/pii/S0002937801549030>.

Hedlund, M., Stenqvist, A.-C., Nagaeva, O., Kjellberg, L., Wulff, M., Baranov, V. & Mincheva-Nilsson, L. 2009, 'Human placenta expresses and secretes NKG2D ligands via exosomes that down-modulate the cognate receptor expression: evidence for immunosuppressive function.', Journal of immunology (Baltimore, Md. : 1950), vol. 183, no. 1, pp. 340–51, viewed 21 March 2019, <http://www.ncbi.nlm.nih.gov/pubmed/19542445>.

Heiss, C., Rodriguez-Mateos, A. & Kelm, M. 2015, 'Central Role of eNOS in the Maintenance of Endothelial Homeostasis', Antioxidants & Redox Signaling, vol. 22, no. 14, pp. 1230–42.

Hirschi, K.K. & D'Amore, P.A. 1996, 'Pericytes in the microvasculature.', Cardiovascular research, vol. 32, no. 4, pp. 687–98, viewed 26 March 2019, <http://www.ncbi.nlm.nih.gov/pubmed/8915187>.

Hoch, R. V, Soriano, Philippe, Kalén, M., Karlsson, L., Pekny, M., Pekna, M., Soriano, P & Betsholtz, C. 2003, 'Roles of PDGF in animal development.', Development (Cambridge, England), vol. 130, no. 20, pp. 4769–84, viewed 30 October 2018, <http://www.ncbi.nlm.nih.gov/pubmed/9693135>.

Holder, B.S., Tower, C.L., Jones, C.J.P., Aplin, J.D. & Abrahams, V.M. 2012, 'Heightened Pro-Inflammatory Effect of Preeclamptic Placental Microvesicles on Peripheral Blood Immune Cells in Humans1', Biology of Reproduction, vol. 86, no. 4, viewed 13 December 2017, <https://academic.oup.com/biolreprod/article-lookup/doi/10.1095/biolreprod.111.097014>.

Horn, P., Cortese-Krott, M.M., Amabile, N., Hundsdörfer, C., Kröncke, K.-D., Kelm, M. & Heiss, C. 2012, 'Circulating microparticles carry a functional endothelial nitric oxide synthase that is decreased in patients with endothelial dysfunction.', Journal of the American Heart Association, vol. 2, no. 1, p. e003764, viewed 26 May 2018, <http://www.ncbi.nlm.nih.gov/pubmed/23525410>.

Horn, P., Cortese-Krott, M.M., Amabile, N., Hundsdörfer, C., Kröncke, K.D., Kelm, M. & Heiss, C. 2013, 'Circulating microparticles carry a functional endothelial nitric oxide synthase that is decreased in patients with endothelial dysfunction.', Journal of the American Heart Association, vol. 2, no. 1, pp. 1–12.

Houser, B.L., Tilburgs, T., Hill, J., Nicotra, M.L. & Strominger, J.L. 2011, 'Two unique human decidual macrophage populations.', Journal of immunology (Baltimore, Md. : 1950), vol. 186, no. 4, pp. 2633–42, viewed 22 October 2018, <http://www.ncbi.nlm.nih.gov/pubmed/21257965>.

Hughes, S.-J., Wall, N., Scholfield, C.N., McGeown, J.G., Gardiner, T.A., Stitt, A.W. & Curtis, T.M. 2004, 'Advanced glycation endproduct modified basement membrane attenuates endothelin-1 induced [Ca2+]i signalling and contraction in retinal microvascular pericytes.', Molecular vision, vol. 10, pp. 996–1004, viewed 25 October 2018, <http://www.ncbi.nlm.nih.gov/pubmed/15635291>.

Hung, T.-H. & Burton, G.J. 2006, 'Hypoxia and Reoxygenation: a Possible Mechanism for Placental Oxidative Stress in Preeclampsia', Taiwanese Journal of Obstetrics and Gynecology, vol. 45, no. 3, pp. 189–200, viewed 10 October 2018, <https://www.sciencedirect.com/science/article/pii/S1028455909602242?via%3Dihub>.

Hung, T.-H., Skepper, J.N. & Burton, G.J. 2001, 'In Vitro Ischemia-Reperfusion Injury in Term Human Placenta as a Model for Oxidative Stress in Pathological Pregnancies', The American Journal of Pathology, vol. 159, no. 3, pp. 1031–43, viewed 10 October 2018, <https://www.sciencedirect.com/science/article/pii/S0002944010617786?via%3Dihub>.

Huppertz, B. 2008, 'Placental Origins of Preeclampsia', Hypertension, vol. 51, no. 4, pp. 970–5, viewed 13 March 2019, <https://www.ahajournals.org/doi/10.1161/HYPERTENSIONAHA.107.107607>.

Hutchinson, E.S., Brownbill, P., Jones, N.W., Abrahams, V.M., Baker, P.N., Sibley, C.P. & Crocker, I.P. 2009, 'Utero-Placental Haemodynamics in the Pathogenesis of Pre-Eclampsia', Placenta, vol. 30, no. 7, pp. 634–41, viewed 10 October 2018, <https://www.sciencedirect.com/science/article/pii/S014340040900143X?via%3Dihub>.

Ignarro, L.J. 1990, 'Nitric oxide. A novel signal transduction mechanism for transcellular communication.', Hypertension (Dallas, Tex. : 1979), vol. 16, no. 5, pp. 477–83, viewed 24 May 2018, <http://www.ncbi.nlm.nih.gov/pubmed/1977698>.

Inglis, H.C., Danesh, A., Shah, A., Lacroix, J., Spinella, P.C. & Norris, P.J. 2016, 'Techniques to improve detection and analysis of extracellular vesicles using flow cytometry', Cytometry Part A, vol. 87, no. 11, pp. 1052–63.

Ishitsuka, K., Ago, T., Arimura, K., Nakamura, K., Tokami, H., Makihara, N., Kuroda, J., Kamouchi, M. & Kitazono, T. 2012, 'Neurotrophin production in brain pericytes during hypoxia: A role of pericytes for neuroprotection', Microvascular Research, vol. 83, no. 3, pp. 352–9, viewed 8 November 2018, <https://www.sciencedirect.com/science/article/pii/S0026286212000519>.

Jain, R.K. 2003, 'Molecular regulation of vessel maturation', Nature Medicine, vol. 9, no. 6, pp. 685–93, viewed 23 August 2018, <http://www.nature.com/articles/nm0603-685>.

Jauniaux, E., Watson, A. & Burton, G. 2001, 'Evaluation of respiratory gases and acid-base gradients in human fetal fluids and uteroplacental tissue between 7 and 16 weeks' gestation', American Journal of Obstetrics and Gynecology, vol. 184, no. 5, pp. 998–1003, viewed 6 June 2018, <http://linkinghub.elsevier.com/retrieve/pii/S0002937801989768>.

Jiang, N., Liu, Q., Liu, L., Yang, W.W. & Zeng, Y. 2015, 'The effect of calcium channel blockers on prevention of preeclampsia in pregnant women with chronic hypertension.', Clinical and experimental obstetrics & gynecology, vol. 42, no. 1, pp. 79–81, viewed 12 June 2019, <http://www.ncbi.nlm.nih.gov/pubmed/25864288>.

Johansen, M., Redman, C.W.., Wilkins, T. & Sargent, I.. 1999, 'Trophoblast Deportation in Human Pregnancy—its Relevance for Pre-eclampsia', Placenta, vol. 20, no. 7, pp. 531–9, viewed 6 November 2018, <https://www.sciencedirect.com/science/article/pii/S0143400499904228?via%3Dihub>.

Jones, C.J.P. & Desoye, G. 2011, 'A new possible function for placental pericytes.', Cells, tissues, organs, vol. 194, no. 1, pp. 76–84, viewed 6 December 2017, <http://www.ncbi.nlm.nih.gov/pubmed/21196697>.

K Buttery, L.D., McCARTHYb, A., SPRINGALLupd, D.R., F SULLIVANb, M.H., Elder, M.G., Michel, T. & Polak, J.M. 1994, 'Endothelial Nitric Oxide Synthase in the Human Placenta: Regional Distribution and Proposed Regulatory Role at the Feto- Maternal Interface', Placenta, vol. 15, no. 15, pp. 257–65, viewed 26 May 2018, <https://ac.els-cdn.com/0143400494900175/1-s2.0-0143400494900175-main.pdf?_tid=831e5168-d4bd-4e77-84cc-c44824c445f2&acdnat=1527347193_9581cba0c300a223cf4d2c6553fd0999>.

Kakui, K., Sagawa, N., Itoh, H., Yura, S., Korita, D., Takemura, M., Nuamah, M. a & Fujii, S. 2003, 'Expression of nitric oxide synthase isoforms in the human placenta is not altered by labor.', Endocrine journal, vol. 50, no. 5, pp. 535–44.

Kao, C.K., Morton, Jude S, Quon, Anita L, Reyes, Laura M, Lopez-Jaramillo, P., Davidge, Sandra T, Cunningham, F.G., Leveno, K.J., Bloom, S.L., Hauth, J.C., Rouse, D.J., Spong, C.Y., Vandenbosche, R., Kirchner, J., Karumanchi, S.A., Lim, K.-H., August, P., Ashworth, J.R., Warren, A.Y., Johnson, I.R., Baker, P.N., Hayman, R., Warren, A., Brockelsby, J., Johnson, I., Baker, P., Hayman, R., Warren, A., Johnson, I., Baker, P., English, F.A., McCarthy, F.P., McSweeney, C.L., Quon, A.L., Morton, J.S., Sawamura, T., Davidge, S.T., Kenny, L.C., Wijk, M.J. van, Svedas, E., Boer, K., Nieuwland, R., VanBavel, E., Kublickiene, K.R., Amaral, L.M., Pinheiro, L.C., Guimaraes, D.A., Palei, A.C.T., Sertório, J.T., Portella, R.L., Tanus-Santos, J.E., Lekontseva, O., Jiang, Y., Schleppe, C., Davidge, S.T., Bird, I.M., Zhang, L., Magness, R.R., Khalil, A., Hardman, L., O'Brien, P., Krause, B.J., Hanson, M.A., Casanello, P., Poston, L., McCarthy,

A.L., Ritter, J.M., Majed, B.H., Khalil, R.A., Reyes, L.M., García, R.G., Ruiz, S.L., Camacho, P.A., Ospina, M.B., Aroca, G., Accini, J.L., López-Jaramillo, P., Kenny, L., Baker, P., Kendall, D., Randall, M., Dunn, W., Walsh, S.K., English, F.A., Johns, E.J., Kenny, L.C., Garvey, E., Oplinger, J., Furfine, E., Kiff, R., Laszlo, F., Whittle, B., Knowles, R., Sankaralingam, S., Xu, Y., Sawamura, T., Davidge, S.T., Shimokawa, H., Oyama, J. -i., Okatani, Y., Watanabe, K., Sagara, Y., Aris, A., Benali, S., Ouellet, A., Moutquin, J.M., Leblanc, S., Kharfi, A., Giguère, Y., Grandpré, P. De, Moutquin, J.-M., Forest, J.-C., Cederbaum, S.D., Yu, H., Grody, W.W., Kern, R.M., Yoo, P., Iyer, R.K., Osol, G., Moore, L.G., Sankaralingam, S., Arenas, I.A., Lalu, M.M., Davidge, S.T., Greer, I., Lyall, F., Perera, T., Boswell, F., Macara, L., Oliveira-Paula, G., Lacchini, R., Tanus-Santos, J.E., Faxen, M., Nisell, H., Kublickiene, K.R., Matsubara, K., Matsubara, Y., Hyodo, S., Katayama, T., Ito, M., Boisrame-Helms, J., Meziani, F., Sananes, N., Boisrame, T., Langer, B., Schneider, F., Ragot, T., Andriantsitohaina, R., Tesse, A., Wang, X., Athayde, N., Trudinger, B., Mayeux, P.R., Kadowitz, P.J., McNamara, D.B., Magee, L.A., Pels, A., Helewa, M., Rey, E., Dadelszen, P. von, Audibert, F., Bujold, E., Cote, A.-M., Douglas, M.J., Eastabrook, G., Mandalà, M., Gokina, N., Barron, C., Osol, G., Giles, T.D., Sander, G.E., Nossaman, B.D., Kadowitz, P.J., Goulopoulou, S. & Davidge, S.T. 2016, 'Mechanism of vascular dysfunction due to circulating factors in women with pre-eclampsia.', Clinical science (London, England : 1979), vol. 130, no. 7, pp. 539–49.

Katz, A.M. 1986, 'Pharmacology and mechanisms of action of calcium-channel blockers.', Journal of clinical hypertension, vol. 2, no. 3 Suppl, pp. 28S-37S, viewed 12 June 2019, <http://www.ncbi.nlm.nih.gov/pubmed/3540226>.

Kawamura, H., Li, X., Goishi, K., van Meeteren, L.A., Jakobsson, L., Cébe-Suarez, S., Shimizu, A., Edholm, D., Ballmer-Hofer, K., Kjellén, L., Klagsbrun, M. & Claesson-Welsh, L. 2008, 'Neuropilin-1 in regulation of VEGF-induced activation of p38MAPK and endothelial cell organization.', Blood, vol. 112, no. 9, pp. 3638–49, viewed 8 November 2018, <http://www.ncbi.nlm.nih.gov/pubmed/18664627>.

Keller, S., Ridinger, J., Rupp, A.-K., Janssen, J.W. & Altevogt, P. 2011, 'Body fluid derived exosomes as a novel template for clinical diagnostics', Journal of Translational Medicine, vol. 9, no. 1, p. 86, viewed 31 October 2018, <http://translational-medicine.biomedcentral.com/articles/10.1186/1479-5876-9-86>.

Kenny, L., Baker, P.N. & Cunningham, F.G. 2009, Chapter 18 - Platelets, Coagulation, and the Liver. Chesley's hypertensive disorders in pregnancy, M.D. Lindheimer, J.M. Roberts & F.G. Cunningham (eds), Academic Press/Elsevier.

Khalil, A., Hardman, L. & O´Brien, P. 2015, 'The role of arginine, homoarginine and nitric oxide in pregnancy', Amino Acids, vol. 47, no. 9, pp. 1715–27, viewed 26 October 2018, <http://link.springer.com/10.1007/s00726-015-2014-1>.

Kingdom, J.C.P. & Kaufmann, P. 1997, 'Oxygen and placental villous development: Origins of fetal hypoxia', Placenta, vol. 18, no. 8, pp. 613–21, viewed 7

November 2018,
<https://www.sciencedirect.com/science/article/pii/S014340049790000X>.

Klatt, P., Pfeiffer, S., List, B.M., Lehner, D., Glatter, O., Bächinger, H.P., Werner, E.R., Schmidt, K. & Mayer, B. 1996, 'Characterization of heme-deficient neuronal nitric-oxide synthase reveals a role for heme in subunit dimerization and binding of the amino acid substrate and tetrahydrobiopterin.', The Journal of biological chemistry, vol. 271, no. 13, pp. 7336–42, viewed 24 May 2018, <http://www.ncbi.nlm.nih.gov/pubmed/8631754>.

Knight, M., Redman, C.W.G., Linton, E.A. & Sargent, I.L. 1998, 'Shedding of syncytiotrophoblast microvilli into the maternal circulation in pre-eclamptic pregnancies', BJOG: An International Journal of Obstetrics and Gynaecology, vol. 105, no. 6, pp. 632–40, viewed 30 May 2018, <http://doi.wiley.com/10.1111/j.1471-0528.1998.tb10178.x>.

Koga, K. & Mor, G. 2010, 'Toll-like receptors at the maternal-fetal interface in normal pregnancy and pregnancy disorders.', American journal of reproductive immunology (New York, N.Y. : 1989), vol. 63, no. 6, pp. 587–600, viewed 22 August 2018, <http://www.ncbi.nlm.nih.gov/pubmed/20367625>.

Kovács, Á.F., Láng, O., Turiák, L., Ács, A., Kőhidai, L., Fekete, N., Alasztics, B., Mészáros, T., Buzás, E.I., Rigó, J. & Pállinger, É. 2018, The impact of circulating preeclampsia-associated extracellular vesicles on the migratory activity and phenotype of THP-1 monocytic cells.

Krause, B.J., Hanson, M.A. & Casanello, P. 2011, 'Role of nitric oxide in placental vascular development and function', Placenta, vol. 32, no. 11, pp. 797–805.

Kučera, T., Vyletěl, I., Moravcová, M., Krejčí, V., Žižka, Z. & Jirkovská, M. 2010, 'Pericyte coverage of fetoplacental vessels in pregnancies complicated by Type 1 diabetes mellitus', Placenta, vol. 31, no. 12, pp. 1120–2, viewed 30 October 2018, <https://www.sciencedirect.com/science/article/pii/S0143400410003590?via%3Dihub>.

LaBarbera, K.E., Hyldahl, R.D., O, K.S., Clarkson, P.M., Witkowski, S., Katherine LaBarbera, C.E., Bld, T. & Ln, E. 2015, 'Pericyte NF-jB activation enhances endothelial cell proliferation and proangiogenic cytokine secretion in vitro', Physiol Rep, vol. 3, no. 4, viewed 4 September 2018, <https://www.ncbi.nlm.nih.gov/pmc/articles/PMC4425949/pdf/phy20003-e12309.pdf>.

Laresgoiti-Servitje, E. 2013, 'A leading role for the immune system in the pathophysiology of preeclampsia', Journal of Leukocyte Biology, vol. 94, no. 2, pp. 247–57, viewed 24 October 2018, <http://doi.wiley.com/10.1189/jlb.1112603>.

Lawson, C., Vicencio, J.M., Yellon, D.M. & Davidson, S.M. 2016, 'Microvesicles and exosomes: new players in metabolic and cardiovascular disease', Journal of Endocrinology, vol. 228, no. 2, pp. R57–71, viewed 19 November 2018,

<http://www.ncbi.nlm.nih.gov/pubmed/26743452>.

Liang, M., Niu, J., Zhang, L., Deng, H., Ma, J., Zhou, W., Duan, D., Zhou, Y., Xu, H. & Chen, L. 2016, 'Gene expression profiling reveals different molecular patterns in G-protein coupled receptor signaling pathways between early- and late-onset preeclampsia', Placenta, vol. 40, pp. 52–9, viewed 5 September 2018, <http://dx.doi.org/10.1016/j.placenta.2016.02.015>.

Lindström, T.M. & Bennett, P.R. 2005, 'The role of nuclear factor kappa B in human labour.', Reproduction (Cambridge, England), vol. 130, no. 5, pp. 569–81, viewed 20 August 2018, <http://www.ncbi.nlm.nih.gov/pubmed/16264088>.

Liu, H., Honmou, O., Harada, K., Nakamura, K., Houkin, K., Hamada, H. & Kocsis, J.D. 2006, 'Neuroprotection by PlGF gene-modified human mesenchymal stem cells after cerebral ischaemia', Brain, vol. 129, no. 10, pp. 2734–45, viewed 8 November 2018, <https://academic.oup.com/brain/article-lookup/doi/10.1093/brain/awl207>.

Lyall, F. 2003, 'Development of the utero-placental circulation: The role of carbon monoxide and nitric oxide in trophoblast invasion and spiral artery transformation', Microscopy Research and Technique, vol. 60, no. 4, pp. 402–11.

Lyall, F., Simpson, H., Nicola Bulmer, J., Barber, A. & Courtenay Robson, S. 2001, 'Transforming Growth Factor-β Expression in Human Placenta and Placental Bed in Third Trimester Normal Pregnancy, Preeclampsia, and Fetal Growth Restriction', The American Journal of Pathology, vol. 159, no. 5, pp. 1827–38, viewed 6 June 2018, <https://www.sciencedirect.com/science/article/pii/S0002944010630295>.

Maier, Cheryl L, Shepherd, B.R., Yi, T. & Pober, J.S. 2010, 'Explant outgrowth, propagation and characterization of human pericytes.', Microcirculation (New York, N.Y. : 1994), vol. 17, no. 5, pp. 367–80, viewed 20 March 2018, <http://www.ncbi.nlm.nih.gov/pubmed/20618694>.

Maier, Cheryl L., Shepherd, B.R., Yi, T. & Pober, J.S. 2010, 'Explant Outgrowth, Propagation and Characterization of Human Pericytes', Microcirculation, vol. 17, no. 5, p. no-no, viewed 4 September 2018, <http://doi.wiley.com/10.1111/j.1549-8719.2010.00038.x>.

Maisonpierre, P.C., Suri, C., Jones, P.F., Bartunkova, S., Wiegand, S.J., Radziejewski, C., Compton, D., McClain, J., Aldrich, T.H., Papadopoulos, N., Daly, T.J., Davis, S., Sato, T.N. & Yancopoulos, G.D. 1997, 'Angiopoietin-2, a natural antagonist for Tie2 that disrupts in vivo angiogenesis.', Science (New York, N.Y.), vol. 277, no. 5322, pp. 55–60, viewed 30 October 2018, <http://www.ncbi.nlm.nih.gov/pubmed/9204896>.

Manaster, I., Mizrahi, S., Goldman-Wohl, D., Sela, H.Y., Stern-Ginossar, N., Lankry, D., Gruda, R., Hurwitz, A., Bdolah, Y., Haimov-Kochman, R., Yagel, S. & Mandelboim, O. 2008, 'Endometrial NK cells are special immature cells that await pregnancy.', Journal of immunology (Baltimore, Md. : 1950), vol. 181, no.

3, pp. 1869–76, viewed 22 October 2018,
<http://www.ncbi.nlm.nih.gov/pubmed/18641324>.

Marinoni, E., Di Iorio, R., Lucchini, C., Di Netta, T., Letizia, C. & Cosmi, E. V 2004, 'Adrenomedullin and nitric oxide synthase at the maternal-decidual interface in early spontaneous abortion.', The Journal of reproductive medicine, vol. 49, no. 3, pp. 153–61, viewed 26 May 2018,
<http://www.ncbi.nlm.nih.gov/pubmed/15098884>.

Mathiisen, T.M., Lehre, K.P., Danbolt, N.C. & Ottersen, O.P. 2010, 'The perivascular astroglial sheath provides a complete covering of the brain microvessels: An electron microscopic 3D reconstruction', Glia, vol. 58, no. 9, pp. 1094–103, viewed 16 May 2019, <http://doi.wiley.com/10.1002/glia.20990>.

Mathivanan, S., Lim, J.W.E., Tauro, B.J., Ji, H., Moritz, R.L. & Simpson, R.J. 2010, 'Proteomics analysis of A33 immunoaffinity-purified exosomes released from the human colon tumor cell line LIM1215 reveals a tissue-specific protein signature.', Molecular & cellular proteomics : MCP, vol. 9, no. 2, pp. 197–208, viewed 31 October 2018, <http://www.ncbi.nlm.nih.gov/pubmed/19837982>.

Matsubara, K., Higaki, T., Matsubara, Y. & Nawa, A. 2015, 'Nitric oxide and reactive oxygen species in the pathogenesis of preeclampsia', International Journal of Molecular Sciences, vol. 16, no. 3, pp. 4600–14.

Matsubara, K., Matsubara, Y., Hyodo, S., Katayama, T. & Ito, M. 2010, 'Role of nitric oxide and reactive oxygen species in the pathogenesis of preeclampsia', Journal of Obstetrics and Gynaecology Research, vol. 36, no. 2, pp. 239–47, viewed 18 October 2018, <http://doi.wiley.com/10.1111/j.1447-0756.2009.01128.x>.

Maynard, S., Epstein, F.H. & Karumanchi, S.A. 2008, 'Preeclampsia and Angiogenic Imbalance', Annual Review of Medicine, vol. 59, no. 1, pp. 61–78, viewed 30 May 2018,
<http://www.annualreviews.org/doi/10.1146/annurev.med.59.110106.214058>.

Maynard, S.E., Min, J.-Y., Merchan, J., Lim, K.-H., Li, J., Mondal, S., Libermann, T.A., Morgan, J.P., Sellke, F.W., Stillman, I.E., Epstein, F.H., Sukhatme, V.P. & Karumanchi, S.A. 2003, 'Excess placental soluble fms-like tyrosine kinase 1 (sFlt1) may contribute to endothelial dysfunction, hypertension, and proteinuria in preeclampsia.', The Journal of clinical investigation, vol. 111, no. 5, pp. 649–58, viewed 25 October 2018, <http://www.ncbi.nlm.nih.gov/pubmed/12618519>.

Mayo, Jamie N & Bearden, S.E. 2015, 'Driving the Hypoxia-Inducible Pathway in Human Pericytes Promotes Vascular Density in an Exosome-Dependent Manner.', Microcirculation (New York, N.Y. : 1994), vol. 22, no. 8, pp. 711–23, viewed 6 November 2018, <http://www.ncbi.nlm.nih.gov/pubmed/26243428>.

Mayo, Jamie N. & Bearden, S.E. 2015, 'Driving the Hypoxia-Inducible Pathway in Human Pericytes Promotes Vascular Density in an Exosome-Dependent Manner', Microcirculation, vol. 22, no. 8, pp. 711–23, viewed 29 August 2018, <http://doi.wiley.com/10.1111/micc.12227>.

Medawar, P.B. 1961, Immunologieal Tolerance The phenomenon of tolerance provides a testing ground for theories of the immune response, viewed 22 August 2018, <https://about.jstor.org/terms>.

Messerli, M., May, K., Hansson, S.R., Schneider, H., Holzgreve, W., Hahn, S. & Rusterholz, C. 2010, 'Feto-maternal interactions in pregnancies: Placental microparticles activate peripheral blood monocytes', Placenta, vol. 31, no. 2, pp. 106–12, viewed 14 December 2017, <http://www.sciencedirect.com/science/article/pii/S0143400409003749?via%3Di hub>.

Mi Lee, S., Romero, R., Jeong Lee, Y., Sook Park, I., Park, C.-W., Hyun Yoon, B. & to, C. 2012, 'Systemic inflammatory stimulation by microparticles derived from hypoxic trophoblast as a model for inflammatory response in preeclampsia', Am J Obstet Gynecol, vol. 207, no. 4, pp. 337–1, viewed 27 April 2018, <https://www.ncbi.nlm.nih.gov/pmc/articles/PMC4161024/pdf/nihms587306.pdf> .

Michel, T. & Vanhoutte, P.M. 2010, 'Cellular signaling and NO production', Pflügers Archiv - European Journal of Physiology, vol. 459, no. 6, pp. 807–16, viewed 30 May 2018, <http://link.springer.com/10.1007/s00424-009-0765-9>.

Miko, E., Szereday, L., Barakonyi, A., Jarkovich, A., Varga, P. & Szekeres-Bartho, J. 2009, 'Immunoactivation in preeclampsia: Vδ2+ and regulatory T cells during the inflammatory stage of disease', Journal of Reproductive Immunology, vol. 80, no. 1–2, pp. 100–8, viewed 24 October 2018, <https://www.sciencedirect.com/science/article/pii/S0165037809000497?via%3 Dihub>.

Mills, C.D., Kincaid, K., Alt, J.M., Heilman, M.J. & Hill, A.M. 2000, 'M-1/M-2 macrophages and the Th1/Th2 paradigm.', Journal of immunology (Baltimore, Md. : 1950), vol. 164, no. 12, pp. 6166–73, viewed 20 August 2018, <http://www.ncbi.nlm.nih.gov/pubmed/10843666>.

Mincheva-Nilsson, L. & Baranov, V. 2014, 'Placenta-Derived Exosomes and Syncytiotrophoblast Microparticles and their Role in Human Reproduction: Immune Modulation for Pregnancy Success', American Journal of Reproductive Immunology, vol. 72, no. 5, pp. 440–57, viewed 17 August 2018, <http://doi.wiley.com/10.1111/aji.12311>.

Mishra, N., Nugent, W.H., Mahavadi, S. & Walsh, S.W. 2011, 'Mechanisms of Enhanced Vascular Reactivity in Preeclampsia', Hypertension, vol. 58, no. 5, pp. 867–73, viewed 24 October 2018, <https://www.ahajournals.org/doi/10.1161/HYPERTENSIONAHA.111.176602>.

Mol, B.W.J., Roberts, C.T., Thangaratinam, S., Magee, L.A., De Groot, C.J.M. & Hofmeyr, G.J. 2016, 'Pre-eclampsia', The Lancet, vol. 387, no. 10022, pp. 999–1011.

Mor, G., Aldo, P. & Alvero, Ayesha B. 2017, 'The unique immunological and microbial aspects of pregnancy', Nature Reviews Immunology, vol. 17, no. 8, pp.

469–82, viewed 13 December 2017,
<http://www.nature.com/doifinder/10.1038/nri.2017.64>.

Mor, G., Aldo, P. & Alvero, Ayesha B 2017, The unique immunological and microbial aspects of pregnancy, viewed 13 October 2017, <https://www.nature.com/nri/journal/v17/n8/pdf/nri.2017.64.pdf>.

Mutlu-Türkoglu, U., Aykaç-Toker, G., Ibrahimoglu, L., Ademoglu, E. & Uysal, M. 1999, 'Plasma nitric oxide metabolites and lipid peroxide levels in preeclamptic pregnant women before and after delivery.', Gynecologic and obstetric investigation, vol. 48, no. 4, pp. 247–50, viewed 26 May 2018, <http://www.ncbi.nlm.nih.gov/pubmed/10592426>.

Myatt, L., Brockman, D.E., Eis, A.L.W. & Pollock, J.S. 1993a, 'Immunohistochemical localization of nitric oxide synthase in the human placenta', Placenta, vol. 14, no. 5, pp. 487–95.

Myatt, L., Brockman, D.E., Eis, A.L.W. & Pollock, J.S. 1993b, 'Immunohistochemical localization of nitric oxide synthase in the human placenta', Placenta, vol. 14, no. 5, pp. 487–95, viewed 26 May 2018, <https://www.sciencedirect.com/science/article/pii/S0143400405802024?via%3Dihub>.

Myatt, L., Eis, a L., Brockman, D.E., Greer, I. a & Lyall, F. 1997, 'Endothelial nitric oxide synthase in placental villous tissue from normal, pre-eclamptic and intrauterine growth restricted pregnancies.', Human reproduction (Oxford, England), vol. 12, no. 1, pp. 167–72.

Myatt, L. & Webster, R.P. 2009, 'Vascular biology of preeclampsia', Journal of Thrombosis and Haemostasis, vol. 7, no. 3, pp. 375–84, viewed 26 May 2018, <http://doi.wiley.com/10.1111/j.1538-7836.2008.03259.x>.

National Institute for Health and Clinical Excellence 2011, 'Hypertension in pregnancy : the management of hypertensive disorders during pregnancy the management of hypertensive disorders', Royal College of Obstetricians and Gynaecologists, vol. 107, no. August, p. 47.

Navarro, R., Compte, M., Álvarez-Vallina, L. & Sanz, L. 2016, 'Immune Regulation by Pericytes: Modulating Innate and Adaptive Immunity.', Frontiers in immunology, vol. 7, p. 480, viewed 23 August 2018, <http://www.ncbi.nlm.nih.gov/pubmed/27867386>.

Nevalainen, J., Skarp, S., Savolainen, E.-R., Ryynänen, M. & Järvenpää, J. 2017, 'Intrauterine growth restriction and placental gene expression in severe preeclampsia, comparing early-onset and late-onset forms', Journal of Perinatal Medicine, vol. 45, no. 7, pp. 869–77, viewed 5 September 2018, <http://www.degruyter.com/view/j/jpme.2017.45.issue-7/jpm-2016-0406/jpm-2016-0406.xml>.

Noris, M., Perico, N. & Remuzzi, G. 2005, 'Mechanisms of Disease: pre-eclampsia', Nature Clinical Practice Nephrology, vol. 1, no. 2, pp. 98–114, viewed 26 May

2018, <http://www.nature.com/articles/ncpneph0035>.

Novaro, V., Colman-Lerner, A., Ortega, F.V., Jawerbaum, A., Paz, D., Nostro, F. Lo, Pustovrh, C., Gimeno, M.F. & González, E. 2001, 'Regulation of metalloproteinases by nitric oxide in human trophoblast cells in culture', Reproduction, Fertility and Development, vol. 13, no. 6, p. 411, viewed 26 May 2018, <http://www.publish.csiro.au/journals/abstractHTML.cfm?J=RD&V=13&I=6&F=RD01036abs.XML>.

O'Kane, P.D., Jackson, G. & Ferro, A. 2008, 'Whole body nitric oxide production is not decreased in patients with coronary atherosclerosis but is inversely related to plasma homocysteine.', Atherosclerosis, vol. 196, no. 2, pp. 574–9, viewed 26 May 2018, <http://www.ncbi.nlm.nih.gov/pubmed/17662292>.

Oettel, A., Lorenz, M., Stangl, V., Costa, S.-D., Zenclussen, A.C. & Schumacher, A. 2016, 'Human Umbilical Vein Endothelial Cells foster conversion of CD4+CD25−Foxp3− T cells into CD4+Foxp3+ Regulatory T Cells via Transforming Growth Factor-β', Scientific Reports, vol. 6, no. 1, p. 23278, viewed 22 October 2018, <http://www.nature.com/articles/srep23278>.

Ogge, G., Chaiworapongsa, T., Romero, R., Hussein, Y., Kusanovic, J.P., Yeo, L., Kim, C.J. & Hassan, S.S. 2011, 'Placental lesions associated with maternal underperfusion are more frequent in early-onset than in late-onset preeclampsia.', Journal of perinatal medicine, vol. 39, no. 6, pp. 641–52, viewed 18 October 2018, <http://www.ncbi.nlm.nih.gov/pubmed/21848483>.

Ohlsson, R., Falck, P., Hellström, M., Lindahl, P., Boström, H., Franklin, G., Ährlund-Richter, L., Pollard, J., Soriano, P. & Betsholtz, C. 1999, 'PDGFB Regulates the Development of the Labyrinthine Layer of the Mouse Fetal Placenta', Developmental Biology, vol. 212, no. 1, pp. 124–36, viewed 30 October 2018, <https://www.sciencedirect.com/science/article/pii/S0012160699993065?via%3Dihub>.

Osol, G., Ko, N.L. & Mandalà, M. 2017, 'Altered Endothelial Nitric Oxide Signaling as a Paradigm for Maternal Vascular Maladaptation in Preeclampsia', Current Hypertension Reports, vol. 19, no. 10, p. 82, viewed 28 May 2018, <http://link.springer.com/10.1007/s11906-017-0774-6>.

Ozerdem, U. & Stallcup, W.B. 2003, 'Early Contribution of Pericytes to Angiogenic Sprouting and Tube Formation', Angiogenesis, vol. 6, no. 3, pp. 241–9, viewed 23 August 2018, <http://link.springer.com/10.1023/B:AGEN.0000021401.58039.a9>.

Palmer, R.M.J., Ashton, D.S. & Moncada, S. 1988, 'Vascular endothelial cells synthesize nitric oxide from L-arginine', Nature, vol. 333, no. 6174, pp. 664–6, viewed 24 May 2018, <http://www.nature.com/doifinder/10.1038/333664a0>.

Pan, Q., Chanthery, Y., Liang, W.-C., Stawicki, S., Mak, J., Rathore, N., Tong, R.K., Kowalski, J., Yee, S.F., Pacheco, G., Ross, S., Cheng, Z., Le Couter, J., Plowman, G., Peale, F., Koch, A.W., Wu, Y., Bagri, A., Tessier-Lavigne, M. &

Watts, R.J. 2007, 'Blocking Neuropilin-1 Function Has an Additive Effect with Anti-VEGF to Inhibit Tumor Growth', Cancer Cell, vol. 11, no. 1, pp. 53–67, viewed 8 November 2018, <https://www.sciencedirect.com/science/article/pii/S1535610806003679?via%3Dihub>.

Papapetropoulos, A., García-Cardeña, G., Madri, J.A. & Sessa, W.C. 1997, 'Nitric Oxide Production Contributes to the Angiogenic Properties of Vascular Endothelial Growth Factor in Human Endothelial Cells', J. Clin. Invest, vol. 100, no. 12, pp. 3131–9, viewed 26 May 2018, <http://www.jci.org>.

Pasquet, J.-M., Dachary-Prigent, J. & Nurden, A.T. 1996, 'Calcium Influx is a Determining Factor of Calpain Activation and Microparticle Formation in Platelets', European Journal of Biochemistry, vol. 239, no. 3, pp. 647–54, viewed 31 October 2018, <http://doi.wiley.com/10.1111/j.1432-1033.1996.0647u.x>.

Pathak, N., Sawhney, H., Vasishta, K. & Majumdar, S. 1999, 'Estimation of Oxidative Products of Nitric Oxide (nitrates, nitrites) in Preeclampsia', The Australian and New Zealand Journal of Obstetrics and Gynaecology, vol. 39, no. 4, pp. 484–7, viewed 29 May 2018, <http://doi.wiley.com/10.1111/j.1479-828X.1999.tb03139.x>.

Pellet-Many, C., Frankel, P., Jia, H. & Zachary, I. 2008a, 'Neuropilins: structure, function and role in disease.', The Biochemical journal, vol. 411, no. 2, pp. 211–26, viewed 3 August 2018, <http://www.ncbi.nlm.nih.gov/pubmed/18363553>.

Pellet-Many, C., Frankel, P., Jia, H. & Zachary, I. 2008b, 'Neuropilins: structure, function and role in disease.', The Biochemical journal, vol. 411, no. 2, pp. 211–26, viewed 24 August 2018, <http://www.ncbi.nlm.nih.gov/pubmed/18363553>.

Peraçoli, J.C., Bannwart-Castro, C.F., Romao, M., Weel, I.C., Ribeiro, V.R., Borges, V.T.M., Rudge, M. V., Witkin, S.S. & Peraçoli, M.T. 2013, 'High levels of heat shock protein 70 are associated with pro-inflammatory cytokines and may differentiate early- from late-onset preeclampsia', Journal of Reproductive Immunology, vol. 100, no. 2, pp. 129–34, viewed 7 November 2018, <https://www.sciencedirect.com/science/article/pii/S0165037813001034?via%3Dihub>.

Pineda, A., Verdin-Terán, S.L., Camacho, A. & Moreno-Fierros, L. 2011, 'Expression of Toll-like Receptor TLR-2, TLR-3, TLR-4 and TLR-9 Is Increased in Placentas from Patients with Preeclampsia', Archives of Medical Research, vol. 42, no. 5, pp. 382–91, viewed 25 October 2018, <https://www.sciencedirect.com/science/article/pii/S0188440911001652?via%3Dihub>.

Pisitkun, T., Shen, R.-F. & Knepper, M.A. 2004, 'Identification and proteomic profiling of exosomes in human urine.', Proceedings of the National Academy of Sciences of the United States of America, vol. 101, no. 36, pp. 13368–73, viewed 31 October 2018, <http://www.ncbi.nlm.nih.gov/pubmed/15326289>.

Plaks, V., Birnberg, T., Berkutzki, T., Sela, S., BenYashar, A., Kalchenko, V., Mor, G., Keshet, E., Dekel, N., Neeman, M. & Jung, S. 2008, 'Uterine DCs are crucial for decidua formation during embryo implantation in mice.', The Journal of clinical investigation, vol. 118, no. 12, pp. 3954–65, viewed 20 August 2018, <http://www.ncbi.nlm.nih.gov/pubmed/19033665>.

Plazyo, O., Romero, R., Unkel, R., Balancio, A., Mial, T.N., Xu, Y., Dong, Z., Hassan, S.S. & Gomez-Lopez, N. 2016, 'HMGB1 Induces an Inflammatory Response in the Chorioamniotic Membranes That Is Partially Mediated by the Inflammasome.', Biology of reproduction, vol. 95, no. 6, p. 130, viewed 20 August 2018, <http://www.ncbi.nlm.nih.gov/pubmed/27806943>.

Poloski, E., Oettel, A., Ehrentraut, S., Luley, L., Costa, S.-D., Zenclussen, A.C. & Schumacher, A. 2016, 'JEG-3 Trophoblast Cells Producing Human Chorionic Gonadotropin Promote Conversion of Human CD4+FOXP3− T Cells into CD4+FOXP3+ Regulatory T Cells and Foster T Cell Suppressive Activity1', Biology of Reproduction, vol. 94, no. 5, viewed 22 October 2018, <https://academic.oup.com/biolreprod/article-lookup/doi/10.1095/biolreprod.115.135541>.

Possomato-Vieira, J.S. & Khalil, R.A. 2016, 'Mechanisms of Endothelial Dysfunction in Hypertensive Pregnancy and Preeclampsia.', Advances in pharmacology (San Diego, Calif.), vol. 77, pp. 361–431, viewed 8 June 2018, <http://www.ncbi.nlm.nih.gov/pubmed/27451103>.

Potente, M., Gerhardt, H. & Carmeliet, P. 2011, 'Basic and Therapeutic Aspects of Angiogenesis', Cell, vol. 146, no. 6, pp. 873–87, viewed 23 August 2018, <https://www.sciencedirect.com/science/article/pii/S0092867411010099?via%3Dihub>.

Pritchard, J.A. 1965, 'Changes in the Blood Volume During Pregnancy and Delivery', Anesthesiology: The Journal of the American Society of Anesthesiologists, vol. 26, [American Society of Anesthesiologists, etc.], pp. 393–9, viewed 24 May 2018, <http://anesthesiology.pubs.asahq.org/article.aspx?articleid=1966343>.

Raimondi, C. & Ruhrberg, C. 2013, 'Neuropilin signalling in vessels, neurons and tumours', Seminars in Cell & Developmental Biology, vol. 24, no. 3, pp. 172–8, viewed 8 November 2018, <https://www.sciencedirect.com/science/article/pii/S1084952113000025?via%3Dihub>.

Rajakumar, A., Cerdeira, A.S., Rana, S., Zsengeller, Z., Edmunds, L., Jeyabalan, A., Hubel, C.A., Stillman, I.E., Parikh, S.M. & Karumanchi, S.A. 2012, 'Transcriptionally active syncytial aggregates in the maternal circulation may contribute to circulating soluble fms-like tyrosine kinase 1 in preeclampsia.', Hypertension (Dallas, Tex. : 1979), vol. 59, no. 2, pp. 256–64, viewed 6 November 2018, <http://www.ncbi.nlm.nih.gov/pubmed/22215706>.

Ramadoss, J., Pastore, M.B. & Magness, R.R. 2013, 'Endothelial Caveolar Subcellular Domain Regulation of Endothelial Nitric Oxide Synthase', Clin Exp Pharmacol Physiol, vol. 40, no. 11, pp. 753–64, viewed 30 May 2018,

<https://www.ncbi.nlm.nih.gov/pmc/articles/PMC4287270/pdf/nihms489552.pdf>
.

Ramhorst, R., Fraccaroli, L., Aldo, P., Alvero, A.B., Cardenas, I., Leirós, C.P. & Mor, G. 2012, 'Modulation and Recruitment of Inducible Regulatory T Cells by First Trimester Trophoblast Cells', American Journal of Reproductive Immunology, vol. 67, no. 1, pp. 17–27, viewed 20 August 2018, <http://doi.wiley.com/10.1111/j.1600-0897.2011.01056.x>.

Raposo, G., Nijman, H.W., Stoorvogel, W., Liejendekker, R., Harding, C. V, Melief, C.J. & Geuze, H.J. 1996a, 'B lymphocytes secrete antigen-presenting vesicles.', The Journal of experimental medicine, vol. 183, no. 3, pp. 1161–72, viewed 31 October 2018, <http://www.ncbi.nlm.nih.gov/pubmed/8642258>.

Raposo, G., Nijman, H.W., Stoorvogel, W., Liejendekker, R., Harding, C. V, Melief, C.J. & Geuze, H.J. 1996b, 'B lymphocytes secrete antigen-presenting vesicles.', The Journal of experimental medicine, vol. 183, no. 3, pp. 1161–72, viewed 6 November 2018, <http://www.ncbi.nlm.nih.gov/pubmed/8642258>.

Raposo, G. & Stoorvogel, W. 2013, 'Extracellular vesicles: exosomes, microvesicles, and friends.', The Journal of cell biology, vol. 200, no. 4, pp. 373–83, viewed 10 October 2018, <http://www.ncbi.nlm.nih.gov/pubmed/23420871>.

Ratajczak, J., Miekus, K., Kucia, M., Zhang, J., Reca, R., Dvorak, P. & Ratajczak, M.Z. 2006, 'Embryonic stem cell-derived microvesicles reprogram hematopoietic progenitors: evidence for horizontal transfer of mRNA and protein delivery', Leukemia, vol. 20, no. 5, pp. 847–56, viewed 31 October 2018, <http://www.nature.com/articles/2404132>.

Reddy, A., Zhong, X.Y., Rusterholz, C., Hahn, S., Holzgreve, W., Redman, C.W.G. & Sargent, I.L. 2008, 'The Effect of Labour and Placental Separation on the Shedding of Syncytiotrophoblast Microparticles, Cell-free DNA and mRNA in Normal Pregnancy and Pre-eclampsia', Placenta, vol. 29, no. 11, pp. 942–9, viewed 5 July 2018, <https://www.sciencedirect.com/science/article/pii/S0143400408002634?via%3Dihub>.

Redman, C.W. 2005, 'Latest Advances in Understanding Preeclampsia', Science, vol. 308, no. 5728, pp. 1592–4.

Redman, C.W. & Sargent, I.L. 2005, 'Latest advances in understanding preeclampsia.', Science (New York, N.Y.), vol. 308, no. 5728, pp. 1592–4, viewed 6 June 2018, <http://www.ncbi.nlm.nih.gov/pubmed/15947178>.

Redman, C.W., Sargent, I.L. & Staff, A.C. 2014, 'IFPA Senior Award Lecture: Making sense of pre-eclampsia – Two placental causes of preeclampsia?', Placenta, vol. 35, pp. S20–5, viewed 6 March 2019, <https://www.sciencedirect.com/science/article/pii/S0143400413008680?via%3Dihub#fig1>.

Redman, C.W.G. 1991, 'Pre-eclampsia and the placenta', Placenta, vol. 12, no. 4,

pp. 301–8, viewed 6 June 2018, <https://www.sciencedirect.com/science/article/pii/014340049190339H?via%3Dihub>.

Redman, C. W G, Sacks, G.P. & Sargent, I.L. 1999, 'Preeclampsia: An excessive maternal inflammatory response to pregnancy', American Journal of Obstetrics and Gynecology, vol. 180, no. 2 I, pp. 499–506.

Redman, Christopher W.G., Sacks, G.P. & Sargent, I.L. 1999, 'Preeclampsia: An excessive maternal inflammatory response to pregnancy', American Journal of Obstetrics and Gynecology, vol. 180, no. 2, pp. 499–506, viewed 14 March 2018, <https://www.sciencedirect.com/science/article/pii/S0002937899702395?via%3Dihub>.

Redman, C.W.G. & Sargent, I.L. 2007, 'Microparticles and immunomodulation in pregnancy and pre-eclampsia', Journal of Reproductive Immunology, vol. 76, no. 1–2, pp. 61–7, viewed 24 October 2018, <https://www.sciencedirect.com/science/article/pii/S0165037807000733?via%3Dihub>.

Redman, C. W.G. & Sargent, I.L. 2007, 'Microparticles and immunomodulation in pregnancy and pre-eclampsia', Journal of Reproductive Immunology, vol. 76, no. 1–2, pp. 61–7.

Redman, C.W.G. & Sargent, I.L. 2008, 'Circulating Microparticles in Normal Pregnancy and Pre-Eclampsia', Placenta, vol. 29, no. SUPPL., pp. 73–7.

Redman, C.W.G. & Sargent, I.L. 2010a, 'Immunology of Pre-Eclampsia', American Journal of Reproductive Immunology, vol. 63, no. 6, pp. 534–43, viewed 14 December 2017, <http://doi.wiley.com/10.1111/j.1600-0897.2010.00831.x>.

Redman, C.W.G. & Sargent, I.L. 2010b, 'Immunology of Pre-Eclampsia', American Journal of Reproductive Immunology, vol. 63, no. 6, pp. 534–43, viewed 7 June 2018, <http://doi.wiley.com/10.1111/j.1600-0897.2010.00831.x>.

Redman, C.W.G. & Sargent, I.L. 2010c, 'Immunology of Pre-Eclampsia', American Journal of Reproductive Immunology, vol. 63, no. 6, pp. 534–43, viewed 9 October 2017, <http://www.ncbi.nlm.nih.gov/pubmed/20331588>.

Redman, C.W.G., Tannetta, D.S., Dragovic, R.A., Gardiner, C., Southcombe, J.H., Collett, G.P. & Sargent, I.L. 2012, 'Review: Does size matter? Placental debris and the pathophysiology of pre-eclampsia', Placenta, vol. 33, pp. S48–54, viewed 9 October 2017, <https://ac.els-cdn.com/S0143400411005868/1-s2.0-S0143400411005868-main.pdf?_tid=ef87b6ec-ad08-11e7-bca7-00000aab0f27&acdnat=1507564136_21cceee0edfa5de35364d1016a7e6da2>.

Ribeiro, A.L. & Okamoto, O.K. 2015, 'Combined Effects of Pericytes in the Tumor Microenvironment', Stem Cells International, vol. 2015, pp. 1–8, viewed 23 August 2018, <http://www.hindawi.com/journals/sci/2015/868475/>.

Ribeiro, V.R., Romao-Veiga, M., Romagnoli, G.G., Matias, M.L., Nunes, P.R., Borges, V.T.M., Peracoli, J.C. & Peracoli, M.T.S. 2017, 'Association between cytokine profile and transcription factors produced by T-cell subsets in early- and late-onset pre-eclampsia', Immunology, vol. 152, no. 1, pp. 163–73, viewed 7 November 2018, <http://doi.wiley.com/10.1111/imm.12757>.

Roberts, J.. & Redman, C.W.. 1993, 'Pre-eclampsia: more than pregnancy-induced hypertension', The Lancet, vol. 341, no. 8858, pp. 1447–51, viewed 26 October 2018, <https://www.sciencedirect.com/science/article/pii/014067369390889O?via%3Di hub>.

Roberts, J.M., Edep, M.E., Goldfien, A. & Taylor, R.N. 1992, 'Sera from preeclamptic women specifically activate human umbilical vein endothelial cells in vitro: morphological and biochemical evidence.', American Journal of Reproductive Immunology, vol. 27, no. 3–4, pp. 101–8, viewed 18 October 2018, <http://www.ncbi.nlm.nih.gov/pubmed/1418401>.

Roberts, J.M., Taylor, R.N., Musci, T.J., Rodgers, G.M., Hubel, C.A. & McLaughlin, M.K. 1990, 'Preeclampsia: An endothelial cell disorder', International Journal of Gynecology & Obstetrics, vol. 32, no. 3, pp. 299–299, viewed 7 June 2018, <http://doi.wiley.com/10.1016/0020-7292%2890%2990402-7>.

Roberts, J.M. & Von Versen-Hoeynck, F. 2007, 'Maternal Fetal/Placental Interactions and Abnormal Pregnancy Outcomes', Hypertension, vol. 49, no. 1, pp. 15–6, viewed 18 October 2018, <https://www.ahajournals.org/doi/10.1161/01.HYP.0000251523.44824.02>.

Robson, S.C., Hunter, S., Boys, R.J. & Dunlop, W. 1989, 'Serial study of factors influencing changes in cardiac output during human pregnancy.', The American journal of physiology, vol. 256, no. 4 Pt 2, pp. H1060-5, viewed 24 May 2018, <http://www.ncbi.nlm.nih.gov/pubmed/2705548>.

Rodesch, F., Simon, P., Donner, C. & Jauniaux, E. 1992, 'Oxygen measurements in endometrial and trophoblastic tissues during early pregnancy.', Obstetrics and gynecology, vol. 80, no. 2, pp. 283–5, viewed 7 November 2018, <http://www.ncbi.nlm.nih.gov/pubmed/1635745>.

Rodgers, G.M., Taylor, R.N. & Roberts, J.M. 1988, 'Preeclampsia is associated with a serum factor cytotoxic to human endothelial cells', American Journal of Obstetrics and Gynecology, vol. 159, no. 4, pp. 908–14, viewed 18 October 2018, <https://www.sciencedirect.com/science/article/pii/S0002937888801698?via%3 Dihub>.

Romero, R., Espinoza, J., Kusanovic, J., Gotsch, F., Hassan, S., Erez, O., Chaiworapongsa, T. & Mazor, M. 2006, 'The preterm parturition syndrome', BJOG: An International Journal of Obstetrics & Gynaecology, vol. 113, pp. 17–42, viewed 20 August 2018, <http://doi.wiley.com/10.1111/j.1471-0528.2006.01120.x>.

Romero, R., Lockwood, C., Oyarzun, E. & Hobbins, J.C. 1988, 'Toxemia: new concepts in an old disease.', Seminars in perinatology, vol. 12, no. 4, pp. 302–23, viewed 7 June 2018, <http://www.ncbi.nlm.nih.gov/pubmed/3065943>.

Roos, N., Kieler, H., Sahlin, L., Ekman-Ordeberg, G., Falconer, H. & Stephansson, O. 2011, 'Risk of adverse pregnancy outcomes in women with polycystic ovary syndrome: population based cohort study.', BMJ (Clinical research ed.), vol. 343, p. d6309, viewed 6 June 2018, <http://www.ncbi.nlm.nih.gov/pubmed/21998337>.

Rossmanith, W.G., Hoffmeister, U., Wolfahrt, S., Kleine, B., McLean, M., Jacobs, R.A. & Grossman, A.B. 1999, 'Expression and functional analysis of endothelial nitric oxide synthase (eNOS) in human placenta.', Molecular human reproduction, vol. 5, no. 5, pp. 487–94, viewed 29 May 2018, <http://www.ncbi.nlm.nih.gov/pubmed/10338373>.

Rouget, C. 1874, 'Note sur le developpement de la tunique contractile des vaisseaux', Compt Rend Acad Sci, vol. 59, pp. 559–62.

Sá-Pereira, I., Brites, D. & Brito, M.A. 2012, 'Neurovascular Unit: a Focus on Pericytes', Molecular Neurobiology, vol. 45, no. 2, pp. 327–47, viewed 16 May 2019, <http://link.springer.com/10.1007/s12035-012-8244-2>.

Sacks, G.P., Studena, K., Sargent, I.L. & Redman, C.W.G. 1998, 'Normal pregnancy and preeclampsia both produce inflammatory changes in peripheral blood leukocytes akin to those of sepsis', American Journal of Obstetrics and Gynecology, vol. 179, no. 1, pp. 80–6, viewed 18 October 2018, <https://www.sciencedirect.com/science/article/pii/S0002937898702546?via%3Dihub>.

Saito, S., Nakashima, A., Shima, T. & Ito, M. 2010, 'Th1/Th2/Th17 and Regulatory T-Cell Paradigm in Pregnancy', American Journal of Reproductive Immunology, vol. 63, no. 6, pp. 601–10, viewed 18 August 2018, <http://doi.wiley.com/10.1111/j.1600-0897.2010.00852.x>.

Saito, S. & Sakai, M. 2003, 'Th1/Th2 balance in preeclampsia', Journal of Reproductive Immunology, vol. 59, no. 2, pp. 161–73, viewed 24 October 2018, <https://www.sciencedirect.com/science/article/pii/S0165037803000457?via%3Dihub>.

Saito, S., Shiozaki, A., Nakashima, A., Sakai, M. & Sasaki, Y. 2007, 'The role of the immune system in preeclampsia', Molecular Aspects of Medicine, vol. 28, no. 2, pp. 192–209, viewed 24 October 2018, <https://www.sciencedirect.com/science/article/pii/S0098299707000301?via%3Dihub>.

Salomon, C., Torres, M.J., Kobayashi, M., Scholz-Romero, K., Sobrevia, L., Dobierzewska, A., Illanes, S.E., Mitchell, M.D. & Rice, G.E. 2014, 'A Gestational Profile of Placental Exosomes in Maternal Plasma and Their Effects on Endothelial Cell Migration', C. Oudejans (ed.),PLoS ONE, vol. 9, no. 6, p. e98667, viewed 14 December 2017,

<http://dx.plos.org/10.1371/journal.pone.0098667>.

Santillan, M.K., Pelham, C.J., Ketsawatsomkron, P., Santillan, D.A., Davis, D.R., Devor, E.J., Gibson-Corley, K.N., Scroggins, S.M., Grobe, J.L., Yang, B., Hunter, S.K. & Sigmund, C.D. 2015, 'Pregnant mice lacking indoleamine 2,3-dioxygenase exhibit preeclampsia phenotypes.', Physiological reports, vol. 3, no. 1, viewed 22 August 2018, <http://www.ncbi.nlm.nih.gov/pubmed/25602015>.

Santner-Nanan, B., Peek, M.J., Khanam, R., Richarts, L., Zhu, E., Fazekas de St Groth, B. & Nanan, R. 2009, 'Systemic increase in the ratio between Foxp3+ and IL-17-producing CD4+ T cells in healthy pregnancy but not in preeclampsia.', Journal of immunology (Baltimore, Md. : 1950), vol. 183, no. 11, pp. 7023–30, viewed 24 October 2018, <http://www.ncbi.nlm.nih.gov/pubmed/19915051>.

Sato, T.N., Tozawa, Y., Deutsch, U., Wolburg-Buchholz, K., Fujiwara, Y., Gendron-Maguire, M., Gridley, T., Wolburg, H., Risau, W. & Qin, Y. 1995, 'Distinct roles of the receptor tyrosine kinases Tie-1 and Tie-2 in blood vessel formation', Nature, vol. 376, no. 6535, pp. 70–4, viewed 30 October 2018, <http://www.nature.com/doifinder/10.1038/376070a0>.

Schiessl, B. 2007, 'Inflammatory response in preeclampsia', Molecular Aspects of Medicine, vol. 28, no. 2, pp. 210–9, viewed 24 October 2018, <https://www.sciencedirect.com/science/article/pii/S0098299707000349?via%3Dihub>.

Schiessl, B., Mylonas, I., Hantschmann, P., Kuhn, C., Schulze, S., Kunze, S., Friese, K. & Jeschke, U. 2005, 'Expression of endothelial NO synthase, inducible NO synthase, and estrogen receptors alpha and beta in placental tissue of normal, preeclamptic, and intrauterine growth-restricted pregnancies.', The journal of histochemistry and cytochemistry : official journal of the Histochemistry Society, vol. 53, no. 12, pp. 1441–9, viewed 26 May 2018, <http://www.ncbi.nlm.nih.gov/pubmed/15983116>.

Schiessl, B., Mylonas, I., Kuhn, C., Kunze, S., Schulze, S., Friese, K. & Jeschke, U. 2006, 'Expression of Estrogen Receptor-α, Estrogen Receptor-β and Placental Endothelial and Inducible NO Synthase in Intrauterine Growth-Restricted and Normal Placentas', Archives of Medical Research, vol. 37, no. 8, pp. 967–75, viewed 26 May 2018, <https://www.sciencedirect.com/science/article/pii/S0188440906002141?via%3Dihub>.

Seligman, S.P., Buyon, J.P., Clancy, R.M., Young, B.K. & Abramson, S.B. 1994, 'The role of nitric oxide in the pathogenesis of preeclampsia.', American journal of obstetrics and gynecology, vol. 171, no. 4, pp. 944–8, viewed 26 May 2018, <http://www.ncbi.nlm.nih.gov/pubmed/7943106>.

Shah, D.A. & Khalil, R.A. 2015, 'Bioactive factors in uteroplacental and systemic circulation link placental ischemia to generalized vascular dysfunction in hypertensive pregnancy and preeclampsia', Biochemical Pharmacology, vol. 95,

no. 4, pp. 211–26, viewed 26 May 2018, <https://www.sciencedirect.com/science/article/pii/S0006295215002178?via%3Dihub>.

Shomer, E., Katzenell, S., Zipori, Y., Sammour, R.N., Isermann, B., Brenner, B. & Aharon, A. 2013, 'Microvesicles of women with gestational hypertension and preeclampsia affect human trophoblast fate and endothelial function.', Hypertension (Dallas, Tex. : 1979), vol. 62, no. 5, pp. 893–8, viewed 26 May 2018, <http://www.ncbi.nlm.nih.gov/pubmed/24082057>.

Sibai, B.M. & Frangieh, A. 1995, 'Maternal adaptation to pregnancy.', Current opinion in obstetrics & gynecology, vol. 7, no. 6, pp. 420–6, viewed 8 June 2018, <http://www.ncbi.nlm.nih.gov/pubmed/8620073>.

Silver, R.K., Kupferminc, M.J., Russell, T.L., Adler, L., Mullen, T.A. & Caplan, M.S. 1996, 'Evaluation of nitric oxide as a mediator of severe preeclampsia', American Journal of Obstetrics and Gynecology, vol. 175, no. 4, pp. 1013–7, viewed 29 May 2018, <http://linkinghub.elsevier.com/retrieve/pii/S0002937896800445>.

Simpson, R.J., Jensen, S.S. & Lim, J.W.E. 2008, 'Proteomic profiling of exosomes: Current perspectives', PROTEOMICS, vol. 8, no. 19, pp. 4083–99, viewed 31 October 2018, <http://doi.wiley.com/10.1002/pmic.200800109>.

Sladek, S.M., Magness, R.R. & Conrad, K.P. 1997, 'Nitric oxide and pregnancy', Am. J. PhysioZ.Regzdatory Integrative Comp. PhysioZ, vol. 272, no. 41, viewed 24 May 2018, <https://www.physiology.org/doi/pdf/10.1152/ajpregu.1997.272.2.R441>.

Smárason, A.K., Sargent, I.L., Starkey, P.M. & Redman, C.W. 1993a, 'The effect of placental syncytiotrophoblast microvillous membranes from normal and pre-eclamptic women on the growth of endothelial cells in vitro.', British journal of obstetrics and gynaecology, vol. 100, no. 10, pp. 943–9, viewed 6 November 2018, <http://www.ncbi.nlm.nih.gov/pubmed/8217980>.

Smárason, A.K., Sargent, I.L., Starkey, P.M. & Redman, C.W. 1993b, 'The effect of placental syncytiotrophoblast microvillous membranes from normal and pre-eclamptic women on the growth of endothelial cells in vitro.', British journal of obstetrics and gynaecology, vol. 100, no. 10, pp. 943–9, viewed 30 May 2018, <http://www.ncbi.nlm.nih.gov/pubmed/8217980>.

SoRelle, R. 1998, 'Nobel prize awarded to scientists for nitric oxide discoveries.', Circulation, vol. 98, no. 22, pp. 2365–6, viewed 26 May 2018, <http://www.ncbi.nlm.nih.gov/pubmed/9832478>.

Southcombe, J., Tannetta, D., Redman, C. & Sargent, I. 2011, 'The immunomodulatory role of syncytiotrophoblast microvesicles', PLoS ONE, vol. 6, no. 5.

Souza, J.P., Gülmezoglu, A.M., Vogel, J., Carroli, G., Lumbiganon, P., Qureshi, Z., Costa, M.J., Fawole, B., Mugerwa, Y., Nafiou, I., Neves, I., Wolomby-Molondo,

J.-J., Bang, H.T., Cheang, K., Chuyun, K., Jayaratne, K., Jayathilaka, C.A., Mazhar, S.B., Mori, R., Mustafa, M.L., Pathak, L.R., Perera, D., Rathavy, T., Recidoro, Z., Roy, M., Ruyan, P., Shrestha, N., Taneepanichsku, S., Tien, N.V., Ganchimeg, T., Wehbe, M., Yadamsuren, B., Yan, W., Yunis, K., Bataglia, V., Cecatti, J.G., Hernandez-Prado, B., Nardin, J.M., Narváez, A., Ortiz-Panozo, E., Pérez-Cuevas, R., Valladares, E., Zavaleta, N., Armson, A., Crowther, C., Hogue, C., Lindmark, G., Mittal, S., Pattinson, R., Stanton, M.E., Campodonico, L., Cuesta, C., Giordano, D., Intarut, N., Laopaiboon, M., Bahl, R., Martines, J., Mathai, M., Merialdi, M. & Say, L. 2013, 'Moving beyond essential interventions for reduction of maternal mortality (the WHO Multicountry Survey on Maternal and Newborn Health): a cross-sectional study.', Lancet (London, England), vol. 381, no. 9879, pp. 1747–55, viewed 23 May 2018, <http://www.ncbi.nlm.nih.gov/pubmed/23683641>.

Stadtman, E.R. & Levine, R.L. 2006, 'Protein Oxidation', Annals of the New York Academy of Sciences, vol. 899, no. 1, pp. 191–208, viewed 31 October 2018, <http://doi.wiley.com/10.1111/j.1749-6632.2000.tb06187.x>.

Staff, A.C., Dechend, R. & Redman, C.W.G. 2013, 'Review: Preeclampsia, acute atherosis of the spiral arteries and future cardiovascular disease: Two new hypotheses', Placenta, vol. 34, no. SUPPL, pp. S73–8.

Stark, K., Eckart, A., Haidari, S., Tirniceriu, A., Lorenz, M., von Brühl, M.-L., Gärtner, F., Khandoga, A.G., Legate, K.R., Pless, R., Hepper, I., Lauber, K., Walzog, B. & Massberg, S. 2013, 'Capillary and arteriolar pericytes attract innate leukocytes exiting through venules and "instruct" them with pattern-recognition and motility programs', Nature Immunology, vol. 14, no. 1, pp. 41–51, viewed 12 September 2018, <http://www.nature.com/articles/ni.2477>.

Steegers, E.A., Von-Dadelszen, P., Duvekot, J.J. & Pijnenborg, R. 2010, 'Pre-eclampsia', The Lancet, vol. 376, no. 9741, pp. 631–44, viewed 23 May 2018, <https://www.sciencedirect.com/science/article/pii/S0140673610602796?via%3Dihub>.

Stillman, I.E. & Karumanchi, S.A. 2007, 'The glomerular injury of preeclampsia.', Journal of the American Society of Nephrology : JASN, vol. 18, no. 8, pp. 2281–4, viewed 8 June 2018, <http://www.ncbi.nlm.nih.gov/pubmed/17634433>.

Strand, K.M., Heimstad, R., Iversen, A.-C., Austgulen, R., Lydersen, S., Andersen, G.L., Irgens, L.M. & Vik, T. 2013, 'Mediators of the association between pre-eclampsia and cerebral palsy: population based cohort study.', BMJ (Clinical research ed.), vol. 347, p. f4089, viewed 23 May 2018, <http://www.ncbi.nlm.nih.gov/pubmed/23838554>.

Strasly, M., Cavallo, F., Geuna, M., Mitola, S., Colombo, M.P., Forni, G. & Bussolino, F. 2001, 'IL-12 inhibition of endothelial cell functions and angiogenesis depends on lymphocyte-endothelial cell cross-talk.', Journal of immunology (Baltimore, Md. : 1950), vol. 166, no. 6, pp. 3890–9, viewed 6 June 2019, <http://www.ncbi.nlm.nih.gov/pubmed/9469420>.

Strieter, R.M., Polverini, P.J., Arenberg, D.A., Walz, A., Opdenakker, G., Van

Damme, J. & Kunkel, S.L. 1995, 'Role of C-X-C chemokines as regulators of angiogenesis in lung cancer', Journal of Leukocyte Biology, vol. 57, no. 5, pp. 752–62, viewed 8 November 2018, <http://doi.wiley.com/10.1002/jlb.57.5.752>.

Stuehr, D.J. 1997, 'STRUCTURE-FUNCTION ASPECTS IN THE NITRIC OXIDE SYNTHASES', Annual Review of Pharmacology and Toxicology, vol. 37, no. 1, pp. 339–59, viewed 24 May 2018, <http://www.annualreviews.org/doi/10.1146/annurev.pharmtox.37.1.339>.

Stuehr, D.J. 1999, 'Mammalian nitric oxide synthases.', Biochimica et biophysica acta, vol. 1411, no. 2–3, pp. 217–30, viewed 26 May 2018, <http://www.ncbi.nlm.nih.gov/pubmed/10320659>.

Sweeney, M.D., Ayyadurai, S. & Zlokovic, B. V 2016, 'Pericytes of the neurovascular unit: key functions and signaling pathways', Nature Neuroscience, vol. 19, no. 6, pp. 771–83, viewed 23 August 2018, <http://www.nature.com/articles/nn.4288>.

Takeuchi, O. & Akira, S. 2010, 'Pattern Recognition Receptors and Inflammation', Cell, vol. 140, no. 6, pp. 805–20, viewed 25 October 2018, <https://www.sciencedirect.com/science/article/pii/S0092867410000231?via%3Dihub>.

Tannetta, D., Dragovic, R., Alyahyaei, Z. & Southcombe, J. 2014a, 'Extracellular vesicles and reproduction–promotion of successful pregnancy', Cellular and Molecular Immunology, vol. 11, no. 6, pp. 548–63, viewed 13 December 2017, <http://www.nature.com/doifinder/10.1038/cmi.2014.42>.

Tannetta, D., Dragovic, R., Alyahyaei, Z. & Southcombe, J. 2014b, 'Extracellular vesicles and reproduction–promotion of successful pregnancy', Cellular & Molecular Immunology, vol. 11, no. 6, pp. 548–63, viewed 7 July 2018, <http://www.nature.com/articles/cmi201442>.

Tannetta, D., Masliukaite, I., Vatish, M., Redman, C. & Sargent, I. 2017a, 'Update of syncytiotrophoblast derived extracellular vesicles in normal pregnancy and preeclampsia', Journal of Reproductive Immunology, vol. 119, pp. 98–106, viewed 9 October 2017, <https://ac.els-cdn.com/S0165037816303886/1-s2.0-S0165037816303886-main.pdf?_tid=063971aa-ad09-11e7-89f9-00000aacb35e&acdnat=1507564173_cdc0fa7db15535525a8edd62df089674>.

Tannetta, D., Masliukaite, I., Vatish, M., Redman, C. & Sargent, I. 2017b, 'Update of syncytiotrophoblast derived extracellular vesicles in normal pregnancy and preeclampsia', Journal of Reproductive Immunology, vol. 119, pp. 98–106, viewed 13 December 2017, <http://www.sciencedirect.com/science/article/pii/S0165037816303886?via%3Dihub>.

Tannetta, D.S., Dragovic, R.A., Gardiner, C., Redman, C.W. & Sargent, I.L. 2013a, 'Characterisation of Syncytiotrophoblast Vesicles in Normal Pregnancy and Pre-Eclampsia: Expression of Flt-1 and Endoglin', PLoS ONE, vol. 8, no. 2.

Tannetta, D.S., Dragovic, R.A., Gardiner, C., Redman, C.W. & Sargent, I.L. 2013b,

‘Characterisation of Syncytiotrophoblast Vesicles in Normal Pregnancy and Pre-Eclampsia: Expression of Flt-1 and Endoglin’, Y.-L. Wang (ed.),PLoS ONE, vol. 8, no. 2, p. e56754, viewed 3 May 2019, <http://dx.plos.org/10.1371/journal.pone.0056754>.

Tannetta, D.S., Hunt, K., Jones, C.I., Davidson, N., Coxon, C.H., Ferguson, D., Redman, C.W., Gibbins, J.M., Sargent, I.L. & Tucker, K.L. 2015, ‘Syncytiotrophoblast Extracellular Vesicles from Pre-Eclampsia Placentas Differentially Affect Platelet Function’, C. Oudejans (ed.),PLOS ONE, vol. 10, no. 11, p. e0142538, viewed 18 January 2018, <http://dx.plos.org/10.1371/journal.pone.0142538>.

Théry, C., Amigorena, S., Raposo, G. & Clayton, A. 2006, ‘Isolation and Characterization of Exosomes from Cell Culture Supernatants and Biological Fluids’, Current Protocols in Cell Biology, vol. 30, no. 1, pp. 3.22.1-3.22.29, viewed 6 November 2018, <http://doi.wiley.com/10.1002/0471143030.cb0322s30>.

Thibault, G., Degenne, D., Girard, A.C., Guillaumin, J.M., Lacord, M. & Bardos, P. 1991, ‘The inhibitory effect of human syncytiotrophoblast plasma membrane vesicles on in vitro lymphocyte proliferation is associated with reduced interleukin 2 receptor expression’, Cellular Immunology, vol. 138, no. 1, pp. 165–74, viewed 3 May 2018, <https://www.sciencedirect.com/science/article/pii/000887499190141W?via%3Dihub>.

Thilaganathan, B. 2017, ‘Placental syndromes: getting to the heart of the matter’, Ultrasound in Obstetrics & Gynecology, vol. 49, no. 1, pp. 7–9, viewed 13 March 2019, <http://doi.wiley.com/10.1002/uog.17378>.

Thornton, C., Dahlen, H., Korda, A. & Hennessy, A. 2013, ‘The incidence of preeclampsia and eclampsia and associated maternal mortality in Australia from population-linked datasets: 2000-2008’, American Journal of Obstetrics and Gynecology, vol. 208, no. 6, pp. 476.e1-476.e5, viewed 7 June 2018, <https://www.sciencedirect.com/science/article/pii/S0002937813002378?via%3Dihub>.

Tian, X., Brookes, O. & Battaglia, G. 2017, ‘Pericytes from Mesenchymal Stem Cells as a model for the blood-brain barrier’, Scientific Reports, vol. 7, no. 1, p. 39676, viewed 23 August 2018, <http://www.nature.com/articles/srep39676>.

Tong, M., Abrahams, V.M. & Chamley, L.W. 2018, ‘Immunological effects of placental extracellular vesicles’, Immunology and Cell Biology, viewed 27 April 2018, <http://doi.wiley.com/10.1111/imcb.12049>.

Tong, M. & Chamley, L.W. 2015, ‘Placental Extracellular Vesicles and Feto-Maternal Communication’, Cold Spring Harbor perspectives in medicine, viewed 25 April 2018, <https://www.ncbi.nlm.nih.gov/pmc/articles/PMC4355256/pdf/cshperspectmed-RPM-a023028.pdf>.

Tong, M., Chen, Q., James, J.L., Stone, P.R. & Chamley, L.W. 2017, 'Micro- and Nano-vesicles from First Trimester Human Placentae Carry Flt-1 and Levels Are Increased in Severe Preeclampsia', Frontiers in Endocrinology, vol. 8, p. 174, viewed 27 February 2018, <http://journal.frontiersin.org/article/10.3389/fendo.2017.00174/full>.

Tong, M., Kleffmann, T., Pradhan, S., Johansson, C.L., DeSousa, J., Stone, P.R., James, J.L., Chen, Q. & Chamley, L.W. 2016, 'Proteomic characterization of macro-, micro- and nano-extracellular vesicles derived from the same first trimester placenta: relevance for feto-maternal communication', Human Reproduction, vol. 31, no. 4, pp. 687–99, viewed 23 February 2018, <https://academic.oup.com/humrep/article-lookup/doi/10.1093/humrep/dew004>.

Tousoulis, D., Kampoli, A.-M., Tentolouris, C., Papageorgiou, N. & Stefanadis, C. 2012, 'The role of nitric oxide on endothelial function.', Current vascular pharmacology, vol. 10, no. 1, pp. 4–18.

Tranquilli, A., Dekker, G., Magee, L., Roberts, J., Sibai, B., Steyn, W., Zeeman, G. & Brown, M. 2014, 'The classification, diagnosis and management of the hypertensive disorders of pregnancy: A revised statement from the ISSHP', Pregnancy Hypertension: An International Journal of Women's Cardiovascular Health, vol. 4, pp. 97–104, viewed 23 May 2018, <http://isshp.org/wp-content/uploads/2011/08/Revised-statement-ISSHP-2014.pdf>.

Tu, Z., Li, Y., Smith, D.S., Sheibani, N., Huang, S., Kern, T. & Lin, F. 2011, 'Retinal Pericytes Inhibit Activated T Cell Proliferation', Investigative Opthalmology & Visual Science, vol. 52, no. 12, p. 9005, viewed 23 August 2018, <http://iovs.arvojournals.org/article.aspx?doi=10.1167/iovs.11-8008>.

Vaddamani, S., Keepanasseril, A., Pillai, A.A. & Kumar, B. 2017, 'Maternal cardiovascular dysfunction in women with early onset preeclampsia and late onset preeclampsia: A cross-sectional study', Pregnancy Hypertension, vol. 10, pp. 247–50, viewed 9 July 2018, <https://www.sciencedirect.com/science/article/pii/S2210778917302994?via%3Dihub>.

Valadi, H., Ekström, K., Bossios, A., Sjöstrand, M., Lee, J.J. & Lötvall, J.O. 2007, 'Exosome-mediated transfer of mRNAs and microRNAs is a novel mechanism of genetic exchange between cells', Nature Cell Biology, vol. 9, no. 6, pp. 654–9, viewed 26 April 2018, <http://www.nature.com/articles/ncb1596>.

Valensise, H., Novelli, G.P., Vasapollo, B., Di Ruzza, G., Romanini, M.E., Marchei, M., Larciprete, G., Manfellotto, D., Romanini, C. & Galante, A. 2001, 'Maternal diastolic dysfunction and left ventricular geometry in gestational hypertension.', Hypertension (Dallas, Tex. : 1979), vol. 37, no. 5, pp. 1209–15, viewed 9 July 2018, <http://www.ncbi.nlm.nih.gov/pubmed/11358930>.

Valensise, H., Vasapollo, B., Gagliardi, G. & Novelli, G.P. 2008, 'Early and Late Preeclampsia', Hypertension, vol. 52, no. 5, pp. 873–80, viewed 6 March 2019, <https://www.ahajournals.org/doi/10.1161/HYPERTENSIONAHA.108.117358>.

Vanhoutte, P.. 2000, 'Say NO to ET', Journal of the Autonomic Nervous System, vol. 81, no. 1–3, pp. 271–7, viewed 26 May 2018, <https://www.sciencedirect.com/science/article/pii/S0165183800001260?via%3 Dihub>.

Vanhoutte, P.M., Zhao, Y., Xu, A. & Leung, S.W.S. 2016, 'Thirty Years of Saying NO: Sources, Fate, Actions, and Misfortunes of the Endothelium-Derived Vasodilator Mediator.', Circulation research, vol. 119, no. 2, pp. 375–96, viewed 25 May 2018, <http://www.ncbi.nlm.nih.gov/pubmed/27390338>.

VanWijk, M.J., Svedas, E., Boer, K., Nieuwland, R., VanBavel, E. & Kublickiene, K.R. 2002, 'Isolated microparticles, but not whole plasma, from women with preeclampsia impair endothelium-dependent relaxation in isolated myometrial arteries from healthy pregnant women', American Journal of Obstetrics and Gynecology, vol. 187, no. 6, pp. 1686–93, viewed 26 May 2018, <https://www.sciencedirect.com/science/article/pii/S000293780200491X?via%3 Dihub>.

Vatten, L.J. & Skjaerven, R. 2004, 'Is pre-eclampsia more than one disease?', BJOG: An International Journal of Obstetrics and Gynaecology, vol. 111, no. 4, pp. 298–302, viewed 7 July 2018, <http://doi.wiley.com/10.1111/j.1471-0528.2004.00071.x>.

Vince, G.S., Starkey, P.M., Austgulen, R., Kwiatkowski, D. & Redman, C.W.G. 1995, 'Interleukin-6, turnour necrosis factor and soluble turnour necrosis factor receptors in women with pre-eclampsia', BJOG: An International Journal of Obstetrics and Gynaecology, vol. 102, no. 1, pp. 20–5, viewed 7 July 2018, <http://doi.wiley.com/10.1111/j.1471-0528.1995.tb09020.x>.

Von-Dadelszen, P., Hurst, G. & Redman, C.W. 1999, 'Supernatants from co-cultured endothelial cells and syncytiotrophoblast microvillous membranes activate peripheral blood leukocytes in vitro.', Human reproduction (Oxford, England), vol. 14, no. 4, pp. 919–24, viewed 6 November 2018, <http://www.ncbi.nlm.nih.gov/pubmed/10221219>.

Von-Dadelszen, P., Magee, L.A., Lee, S.K., Stewart, S.D., Simone, C., Koren, G., Walley, K.R. & Russell, J.A. 2002, Activated protein C in normal human pregnancy and pregnancies complicated by severe preeclampsia: A therapeutic opportunity?*, viewed 7 July 2018, <https://insights.ovid.com/pubmed?pmid=12163810>.

Von-Dadelszen, P., Magee, Laura A & Roberts, J.M. 2003, 'Hypertension in Pregnancy Subclassification of Preeclampsia', Hypertension in Pregnancy, vol. 22, no. 2, pp. 143–8, viewed 23 May 2018, <http://www.tandfonline.com/action/journalInformation?journalCode=ihip20>.

Von-Dadelszen, P., Magee, Laura A. & Roberts, J.M. 2003, 'Subclassification of Preeclampsia', Hypertension in Pregnancy, vol. 22, no. 2, pp. 143–8, viewed 23 May 2018, <http://www.tandfonline.com/doi/full/10.1081/PRG-120021060>.

Wang, Y. & Zhao, S. 2010, Cell Types of the Placenta, viewed 26 March 2019,

<https://www.ncbi.nlm.nih.gov/books/NBK53245/?report=reader>.

Weiss, G., Goldsmith, L.T., Taylor, R.N., Bellet, D. & Taylor, H.S. 2009, 'Inflammation in Reproductive Disorders', Reproductive Sciences, vol. 16, no. 2, pp. 216–29, viewed 24 October 2018, <http://journals.sagepub.com/doi/10.1177/1933719108330087>.

Wiley, L.A., Rupp, G.R. & Steinle, J.J. 2005, 'Sympathetic Innervation Regulates Basement Membrane Thickening and Pericyte Number in Rat Retina', Investigative Opthalmology & Visual Science, vol. 46, no. 2, p. 744, viewed 25 October 2018, <http://iovs.arvojournals.org/article.aspx?doi=10.1167/iovs.04-1023>.

Winyard, P.G., Ryan, B., Eggleton, P., Nissim, A., Taylor, E., Lo Faro, M.L., Burkholz, T., Szabó-Taylor, K.E., Fox, B., Viner, N., Haigh, R.C., Benjamin, N., Jones, A.M. & Whiteman, M. 2011, 'Measurement and meaning of markers of reactive species of oxygen, nitrogen and sulfur in healthy human subjects and patients with inflammatory joint disease.', Biochemical Society transactions, vol. 39, no. 5, pp. 1226–32, viewed 31 October 2018, <http://www.ncbi.nlm.nih.gov/pubmed/21936794>.

Witwer, K.W., Buzás, E.I., Bemis, L.T., Bora, A., Lässer, C., Lötvall, J., Nolte-'t Hoen, E.N., Piper, M.G., Sivaraman, S., Skog, J., Théry, C., Wauben, M.H. & Hochberg, F. 2013, 'Standardization of sample collection, isolation and analysis methods in extracellular vesicle research', Journal of Extracellular Vesicles, vol. 2, no. 1, p. 20360, viewed 6 November 2018, <https://www.tandfonline.com/doi/full/10.3402/jev.v2i0.20360>.

Wolf, P. 1967, 'The Nature and Significance of Platelet Products in Human Plasma', British Journal of Haematology, vol. 13, no. 3, pp. 269–88, viewed 31 October 2018, <https://onlinelibrary.wiley.com/doi/abs/10.1111/j.1365-2141.1967.tb08741.x>.

World Health Organization 2011, 'WHO recommendations for prevention and treatment of pre-eclampsia and eclampsia', Geneva: World Health Organization.

Xie, F., Hu, Y., Turvey, S., Magee, L., Brunham, R., Choi, K.-C., Krajden, M., Leung, P., Money, D., Patrick, D., Thomas, E. & von Dadelszen, P. 2010, 'Toll-like receptors 2 and 4 and the cryopyrin inflammasome in normal pregnancy and pre-eclampsia', BJOG: An International Journal of Obstetrics & Gynaecology, vol. 117, no. 1, pp. 99–108, viewed 5 September 2018, <http://doi.wiley.com/10.1111/j.1471-0528.2009.02428.x>.

Xu, R., Greening, D.W., Zhu, H.-J., Takahashi, N. & Simpson, R.J. 2016, 'Extracellular vesicle isolation and characterization: toward clinical application.', The Journal of clinical investigation, vol. 126, no. 4, pp. 1152–62, viewed 6 November 2018, <http://www.ncbi.nlm.nih.gov/pubmed/27035807>.

Yamamoto, S., Niida, S., Azuma, E., Yanagibashi, T., Muramatsu, M., Huang, T.T., Sagara, H., Higaki, S., Ikutani, M., Nagai, Y., Takatsu, K., Miyazaki, K., Hamashima, T., Mori, H., Matsuda, N., Ishii, Y. & Sasahara, M. 2015,

'Inflammation-induced endothelial cell-derived extracellular vesicles modulate the cellular status of pericytes', Scientific Reports, vol. 5, no. 1, p. 8505, viewed 4 September 2018, <http://www.nature.com/articles/srep08505>.

Yáñez-Mó, M., R-M Siljander, P., Andreu, Z., Bedina Zavec, A., Borràs, F.E., Buzas, E.I., Buzas, K., Casal, E., Cappello, F., Carvalho, J., Colás, E., Cordeiro-da Silva, A., Fais, S., Falcon-Perez, J.M., Ghobrial, I.M., Giebel, B., Gimona, M., Graner, M., Gursel, I., Gursel, M., H Heegaard, N.H., Hendrix, A., Kierulf, P., Kokubun, K., Kosanovic, M., Kralj-Iglic, V., Krämer-Albers, E.-M., Laitinen, S., Lässer, C., Lener, T., Ligeti, E., Linē, A., Lipps, G., Llorente, A., Lötvall, J., Manček-Keber, M., Marcilla, A., Mittelbrunn, M., Nazarenko, I., Nolte-, E.N., Nyman, T.A., Olivan, M., Oliveira, C., Pállinger, É., del Portillo, H.A., Reventós, J., Rigau, M., Rohde, E., Sammar, M., Sánchez-Madrid, F., Santarém, N., Schallmoser, K., Stampe Ostenfeld, M., Stoorvogel, W., Stukelj, R., Van der Grein, S.G., Helena Vasconcelos, M., M Wauben, M.H. & De Wever, O. 2015, 'Biological properties of extracellular vesicles and their physiological functions', Journal of Extracellular Vesicles, viewed 31 October 2018, <https://doi.org/10.3402/jev.v4.27066>.

Yoshinaga, K. 2012, 'Two Concepts on the Immunological Aspect of Blastocyst Implantation', Journal of Reproduction and Development, vol. 58, no. 2, pp. 196–203, viewed 24 October 2018, <http://japanlinkcenter.org/DN/JST.JSTAGE/jrd/2011-027?from=CrossRef&type=abstract>.

Zarlingo, T.J., Eis, A.L., Brockman, D.E., Kossenjans, W. & Myatt, L. 1997, 'Comparative localization of endothelial and inducible nitric oxide synthase isoforms in haemochorial and epitheliochorial placentae.', Placenta, vol. 18, no. 7, pp. 511–20, viewed 26 May 2018, <http://www.ncbi.nlm.nih.gov/pubmed/9290145>.

Zenclussen, A.C. & Hämmerling, G.J. 2015, 'Cellular Regulation of the Uterine Microenvironment That Enables Embryo Implantation', Frontiers in Immunology, vol. 6, p. 321, viewed 20 August 2018, <http://journal.frontiersin.org/Article/10.3389/fimmu.2015.00321/abstract>.

Zeringer, E., Barta, T., Li, M. & Vlassov, A. V 2015, 'Strategies for isolation of exosomes.', Cold Spring Harbor protocols, vol. 2015, no. 4, pp. 319–23, viewed 6 November 2018, <http://www.ncbi.nlm.nih.gov/pubmed/25834266>.

Zhang, E.G., Burton, G.J., Smith, S.K. & Charnock-Jones, D.S. 2002, 'Placental Vessel Adaptation During Gestation and to High Altitude: Changes in Diameter and Perivascular Cell Coverage', Placenta, vol. 23, no. 10, pp. 751–62, viewed 30 October 2018, <https://www.sciencedirect.com/science/article/pii/S0143400402908568>.

Zhang, J., Chen, Z., Smith, G.N. & Croy, B.A. 2011, 'Natural killer cell-triggered vascular transformation: maternal care before birth?', Cellular & Molecular Immunology, vol. 8, no. 1, pp. 1–11, viewed 22 October 2018, <http://www.nature.com/articles/cmi201038>.

Zhang, Z., Gao, Y., Zhang, Linlin, Jia, L., Wang, P., Zhang, Lin & Li, H. 2013, 'Alterations of IL-6, IL-6R and gp130 in early and late onset severe preeclampsia', Hypertension in Pregnancy, vol. 32, no. 3, pp. 270–80, viewed 9 July 2018, <http://www.tandfonline.com/doi/full/10.3109/10641955.2013.798332>.

Zimmermann, K.W. 1923, 'Der Ieinere Bau der Bluteapillaren.', Aus Dem Anatomischen Institut Der Universitat Bern, vol. 68, no. 1, pp. 29–109, viewed 23 August 2018, <https://link.springer.com/content/pdf/10.1007/BF02593544.pdf>.